UNIVERSIDAD PÚBLICA DE NAVARRA

E.T.S Ingenieros Agrónomos

Departamento de Agronomía, Biotecnología y Alimentación

Papel de las tiorredoxinas plastidiales en la regulación del metabolismo del cloroplasto

The role of plastid thioredoxins in the regulation of chloroplast metabolism

Memoria de la Tesis Doctoral para optar al título de Doctor presentada por:

María Ancín Rípodas

Directora: Dra. Inmaculada Farran Blanch

Profesora Contratada Doctora

Departamento de Agronomía, Biotecnología y Alimentación

Universidad Pública de Navarra

Pamplona, 2018

La **Dra. Inmaculada Farran Blanch**, Profesora Contratada Doctora de Producción Vegetal del Departamento de Agronomía, Biotecnología y Alimentación de la Universidad Pública de Navarra,

INFORMA,

Que la presente memoria de Tesis Doctoral “Papel de las tiorredoxinas plastidiales en la regulación del metabolismo del cloroplasto” elaborada por **María Ancín Rípodas** ha sido realizada bajo su dirección, y que cumple las condiciones exigidas por la legislación vigente para optar al grado de Doctor.

Y para que así conste, firma la presente en Pamplona/Iruñea a, X de Enero de 2018.

Fdo. Dra. Inmaculada Farran Blanch

La realización de esta Tesis Doctoral por parte de María Ancín Rípodas ha sido posible gracias al disfrute de una ayuda para la Formación del Profesorado Universitario (FPU) con referencia FPU13/01675, y a la ayuda de Movilidad para Estancias Breves para beneficiarios de este subprograma (EST15/00101), ambas concedidas por el Ministerio de Ciencia, Innovación y Universidades. La estancia se realizó en la Universidad de Tennessee (Knoxville), en el Departamento de Bioquímica y Biología Celular y Molecular, por un periodo de tres meses bajo la dirección de la Dra. Tessa Burch-Smith. Durante la Tesis Doctoral también se realizó otra estancia de un mes, financiada por el propio grupo de investigación, en el Instituto Nacional de Investigación Agronómica (INRA) de Burdeos, bajo la dirección del Dr. Yves Gibon.

La financiación para la realización de esta Tesis Doctoral ha sido posible gracias a los proyectos “Ingeniería genética en cultivos energéticos alternativos para su utilización en la producción de bioetanol” del Ministerio de Ciencia e Innovación (AGL2010-15107) y “Papel de las tiorredoxinas plastidiales en la regulación del metabolismo del almidón en plantas” de la Fundación Caja Navarra.

La Tesis doctoral comprendida en este volumen está organizada según el modelo contemplado por las Normas Reguladoras del Doctorado en la Universidad Pública de Navarra, según la resolución 2307/2017, de 15 de diciembre, del Rector de la Universidad Pública de Navarra, publicado en el BON del 12 de febrero de 2018. De esta manera, los resultados obtenidos durante la realización de la misma se agrupan en capítulos, que corresponden con los artículos científicos a los que ha dado, o se prevé que de lugar, el desarrollo de los objetivos planteados. Así, cada capítulo contiene una introducción específica, la descripción de materiales y métodos utilizados, los resultados obtenidos y la discusión de los mismos. Por lo tanto, cada capítulo agrupa la información necesaria relacionada al tema que en él se desarrolla, permitiendo su lectura de manera independiente del resto de capítulos. Este documento incluye, además, un resumen, una introducción general que describe de manera más amplia la regulación redox del metabolismo del carbono y el nitrógeno en el cloroplasto mediada por las tiorredoxinas plastidiales, los objetivos perseguidos durante la elaboración de la Tesis Doctoral, un apartado de perspectivas futuras en el que se sugieren futuras líneas de investigación, las conclusiones obtenidas durante el presente trabajo de investigación y, por último, la bibliografía generada en la elaboración del documento.

AGRADECIMIENTOS

Me gustaría que estas líneas sirvieran para agradecer de corazón a todas las personas que, de un modo u otro, me han ayudado durante esta etapa.

Imma, de tu mano entré en este loco mundo de la ciencia hace ya unos cuantos años, y gracias a ti he aprendido a disfrutar y a sufrir con ella. Gracias por todo tu apoyo, tanto académico como personal. Te considero una muy buena investigadora y para mí eres un ejemplo de trabajo, constancia y optimismo. Junto a ti, a todo el L3: Jon, Alicia, Luis, JonGon y todas las personas que ha pasado por el laboratorio en estos años. Sin vosotras esto no hubiera sido igual y habéis sido el mejor apoyo que podría tener.

Iker, Yves y Tessa, tres grandes investigadores que me han inspirado y enseñado muchas cosas. Además, mis estancias en vuestros centros me han servido para ver que hay muchas maneras de hacer investigación y lo importante es enriquecerse con todas ellas. Mila esker! Merci beaucoup! Thank you!

Jokin y Enrique de Navarra Biomed, gracias por haberme introducido en el mundo de la proteómica, por vuestra paciencia y enseñanzas.

Cómo olvidarme de mis compis del IdAB, gracias por animarme, por alegrarme el día a día en el instituto, por los raticos de café, escapes y salidas varias...gracias por vuestra amistad.

Victor y Mari Jose, siempre atentos, pendientes de ayudarme en lo que fuera, ya sea con una plaga o arreglando cualquier desaguisado. Solo puedo agradecer vuestros consejos y vuestro cariño.

Por otro lado, a toda la gente ajena al mundo de la investigación, que habéis conseguido apoyarme aun sin saber muy bien, en la mayoría de casos, que es lo que estaba haciendo con unas plantas de tabaco en un laboratorio...

A toda mi familia, en especial a mis padres. Amatxo, aitatxo, por vuestro apoyo, porque siempre habéis confiado en mí y habéis sido un ejemplo de cómo conseguir tus objetivos trabajando duro, sin importar tus orígenes.

A ti maitia, mi compañero de viaje. A pesar de no pertenecer al mundo científico has sabido comprenderme, apoyarme, animarme y también criticarme o ponerme las pilas cuando lo he necesitado. Gracias por estar siempre ahí.

Por último, pero no menos importante, a todas mis amigas y amigos. No os nombro a todas porque me faltaría papel. Cuadri, bildukristianos, zutarris, betikoak, agrónomas de bata y bota, Jess, Nate... Gracias por ayudarme a desconectar, por animarme, por vuestra alegría y cariño tan sincero.

Aunque ha sido un camino en el que he tropezado más de una vez, con vuestro impulso he aprendido a levantarme y seguir caminando con más fuerza.

ÍNDICE

ÍNDICE DE FIGURAS

INTRODUCCIÓN GENERAL

CAPÍTULO I

CAPÍTULO II

CAPÍTULO III

CAPÍTULO IV

ÍNDICE DE TABLAS

INTRODUCCIÓN

CAPÍTULO I

CAPÍTULO II

CAPÍTULO III

CAPÍTULO IV

ABREVIATURAS

2OG 2-oxoglutarato; *2-oxoglutarate*
ACHT ..... *Atypical Cys/His-rich thioredoxin*
ADPG..... Adenosín difosfato-glucosa; *Adenosin diphosphate-glucose*
AGPase ..... ADPG pirofosforilasa; *ADPG pyrophosphorylase*
AGPB..... Subunidad pequeña de la AGPase; *AGPase small subunit*
AMY ..... α-amilasa; *α-amilase*
A_N..... Tasa neta de asimilación de CO_2; *Net rate of CO_2 assimilation*
APR ..... 5' adenilsulfato reductasa; *5' adenylsulphate reductase*
ATPase ..... ATP sintasa; *ATP synthase*
BAM ..... β-amilasa; *β-amilase*
BE ..... .Enzima ramificadora de almidón; *Starch branching enzyme*
BIFC..... Complementación bimolecular de fluorescencia; *Bimolecular fluorescence complementation*
C ..... Carbono; Carbon
CBC ..... Ciclo de Calvin-Benson; *Calvin-Benson cycle*
CDSP32..... *Chloroplastic drought-induced stress protein*
CEF..... Flujo cíclico de transporte de electrones; *Cyclic electron transport flow*
Chl ..... Clorofila; *Chlorophyll*
C_i..... Concentración de CO_2 subestomática; *Sub-stomatal CO_2 concentration*
CURT1..... *Curvature thylakoid protein 1*
Cys..... Cisteína; Cysteine
Cyt ..... Citocromo; *Cytochrome*
DiT1 ..... Transportador de 2OG/Mal; *2OG/Mal translocator*
DiT2 ..... Transportador de Glu/Mal; *Glu/Mal translocator*
DBE ..... Enzima desramificadora de almidón; *Starch debranching enzyme*
DPE ..... 4-α-glucanotransferasa; *Disproportionating enzyme*
DSP4 ..... Fosfoglucano fosfatasa (SEX4); Phosphoglucan phosphatase s*tarch excess 4* (SEX4)
ETR..... Tasa de transporte electrónico; *Electron transport rate*
E ..... Tasa de transpiración; *Transpiration rate*
FBPase ..... Fructosa 1,6-bifosfatasa; *Fructosa 1,6-bisphosphatase*
Fd..... Ferredoxina; *Ferredoxin*
FNR ..... Fd-NADP reductasa; *Fd-NADP reductase*
FR ..... Rojo lejano; *Far red*
FTR..... Fd-Trx reductasa; *Fd-Trx reductase*
G6PDH ..... Glucosa-6-fosfato deshidrogenasa; *Glucose-6-phosphate dehydrogenase*
GAPDH ..... Gliceraldehído-3-fosfato deshidrogenasa; *Gliceraldehyde-3-phosphate dehydrogenase*

GBSS .....Almidón sintasa unida al gránulo; *Ganule bound starch synthase*
GDH .....Glutamato deshidrogenasa; *Glutamate dehydrogenase*
Gln.....Glutamina; *Glutamine*
Glu.....Glutamato; *Glutamate*
Gly.....Glicina; *Glycine*
Fd-GOGAT .....Glutamato sintasa dependiente de Fd; Fd-dependent g*lutamate synthase*
Grx .....Glutarredoxina; *Glutaredoxin*
g_S.....Conductancia estomática; *Stomatal conductance*
GS2 .....Glutamina sintetasa cloroplástica; Chloroplastic g*lutamine synthetase*
GSH.....Glutatión reducido; *Reduced glutathione*
GWD.....α-glucano H_2O diquinasa; α*-glucan water dikinase*
HCF164 .....del inglés *High chlorophyll fluorescent 164 protein*
HL.....Alta intesidad de luz; High light
ISA .....Isoamilasa; *Isoamylase*
J_{max}.....Tasa máxima de transporte electrónico que contribuye a la regeneración de RuBP; Maximum electron transport rate contributing to RuBP regeneration
LDA .....Limit-dextrinasa/pululanasa; *Limit dextrinase/pullulanase*
LHCI .....Complejo antena asociado al PSI; *Light harvesting complexI*
LHCII .....Complejo antena asociado al PSII; *Light harvesting complexII*
LL .....Baja intensidad de luz; Low light
LSF2.....Fosfoglucano fosfatasa tipo SEX4; *Phosphoglucan phosphatase like-SEX4*
LTO1 .....*Lumenal thiol oxidoreductase 1*
Mal .....Malato; *Malate*
MDH .....Malato deshidrogenasa; *Malate dehydrogenase*
MS.....Espectrometría de masas; *Mass spectrometry*
MSR .....Metionina sulfóxido reductasa; *Methionine sulphoxide reductase*
N.....Nitrógeno; *Nitrogen*
NiR .....Nitrito reductasa; *Nitrite reductase*
NPQ.....Disipación no fotoquímica; *Non photoquemical quenching*
NR .....Nitrato reductasa; *Nitrate reductase*
NTR.....TR dependiente de NADPH; *NADPH dependent TR*
NTRC .....*TR tipo C dependiente de NADPH; C-type NADPH dependent TR*
OJIP .....*Fast Chl a fluorescence transient*
OPPP .....Ciclo oxidativo de las pentosas fosfato; *Oxidative pentose phosphate pathway*
PEP .....Fosfo*enol*piruvato; *Phosphoenolpyruvate*
PEPC.....PEP carboxilasa; *PEP carboxylase*
PetC .....Proteína de Rieske; *Rieske iron-sulfur protein*
PGK.....Fosfoglicerato kinasa; *Phosphoglycerate kinase*

Phe ..... Fenilalanina; *Phenylalanine*
PHS ..... α-glucano fosforilasa; *α-glucan phosphorylasae*
PPFD ..... Densidad del flujo de fotones; *Photosynthetic photon flux density*
PQ..... Plastoquinona; *Plastoquinone*
PRK ..... Fosforribuloquinasa; *Phosphoribulokinase*
Prx ..... Peroxirredoxina; *Peroxiredoxin*
PSI ..... Fotosistema I, *Photosystem I*
PSII ..... Fotosistema II, *Photosystem II*
PWD ..... Fosfoglucano H_2O diquinasa; *Phosphoglucan water dikinase*
ROS ..... Especies reactivas del oxígeno; *Oxygen reactive species*
Rubisco ..... RuBP carboxilasa oxigenasa; *RuBP carboxylase-oxy*genase
RuBP Ribulosa-1,5-bifosfato; *Ribulose-1,5-bisphosphate*
Ser ..... Serina; *Serine*
SBPase Sedoheptulosa-1,7-bifosfatasa; *Sedoheptulose-1,7-bisphosphatase*
SOQ1 ..... *Suppressor of quenching*
SS ..... Almidón sintasa; *Starch synthase*
TCA..... Ácidos tricarboxílicos; *Tricarboxylic acids*
TEM ..... Microscopio electrónico de transmisión; *Transmission electron microscopy*
TP ..... Triosas fosfato; *Triose phosphate*
TPI ..... Triosafosfato isomerasa; *Triosephosphate isomerase*
TPU..... Tasa de utilización de TP; *TP utilization rate*
TR ..... Tiorredoxina reductasa; *Thioredoxin reductase*
Trx..... Tiorredoxina; Thioredoxin
Vc_{max} ..... Velocidad máxima de carboxilación de la Rubisco; *Maximum carboxylation velocity of Rubisco*
VIGS ..... Silenciamiento génico inducido por virus; *Virus-induced gene silencing*
Wt ..... Genotipo silvestre; Wild type
YFP..... Yellow fluorescent protein

RESUMEN

El carbono (C) y el nitrógeno (N) son dos nutrientes esenciales para el crecimiento y desarrollo de la planta. Los metabolismos de estos dos elementos se encuentran estrechamente coordinados y sometidos a una compleja regulación dentro de la célula. En este sentido, el estado redox cellular constituye uno de los principales integradores del metabolismo, incluyendo modificaciones post-traduccionales sobre enzimas diana mediante intercambios ditiol/disulfuro llevados a cabo por las tiorredoxinas (Trxs). En los cloroplastos actúan dos sistemas Trx en paralelo: (i) el sistema ferredoxina (Fd)-Trx en el que la Fd reducida durante la fotosíntesis transmite los electrones a la Fd-Trx reductasa, que a su vez reduce a las Trxs; (ii) el sistema formado por la Trx reductasa tipo C dependiente de NADPH (NTRC), que contiene en un mismo polipéptido un dominio Trx reductasa y un dominio Trx. NTRC es reducida tanto por el NADPH proveniente de las reacciones dependientes de la luz, como por el generado en la ruta oxidativa de las pentosas fosfato en oscuridad. Esta tesis doctoral se ha centrado en el papel regulador ejercido por las Trxs plastidiales f, m y NTRC en el metabolismo del cloroplasto.

En el Capítulo I se estudia el papel de las Trxs f y m en la regulación de la kinasa STN7, involucrada en la fosforilación del complejo antena del fotosistema II (LHCII), que a su vez regula los estados de transición. Los resultados obtenidos mostraron que solo la sobreexpresión de Trx m se asociaba con una completa desfosforilación de los LHCII, y que esta no se correlacionaba con una disminución en la cantidad de STN7. Esta ausencia de fosforilación impedía la migración de los LHCII desde el fotosistema II (PSII) al PSI, y por tanto la formación del complejo PSI-LHCII. Consecuentemente, la ultraestructura de los tilacoides se encontraba alterada en las plantas que sobreexpresan Trx m, con una reducción en el grado de apilamiento de los grana. Además, la tasa de transporte electrónico se vio afectada negativamente, causando un impacto en los procesos de demanda energética como la capacidad máxima de carboxilación de la ribulose-1,5-bifosfato carboxilasa/oxigenasa o la tasa de regeneración de ribulose-1,5-bifosfato. Este hecho causó una fuerte disminución en la capacidad fotosintética de estas plantas. Finalmente, se observó que plantas de tabaco con sobreexpresión del mutante redox de Trx m, carente del sitio activo, presentaban un fenotipo similar a las plantas control, indicando que la actividad oxidorreductasa de la Trx m resulta clave para la desactiva la kinasa STN7.

El Capítulo II estudia el papel específico de Trx f y NTRC en el metabolismo del almidón en plantas. Con este propósito se analizaron plantas de tabaco con sobreexpresión de NTRC o Trx f desde el genoma plastidial, así como plantas de *Nicotiana benthamiana* en las que se silenciaron individualmente ambas proteínas. Tanto la sobreexpresión de NTRC como Trx f produjeron un aumento en la

acumulación de almidón en hojas, sin embargo, los mecanismo que dieron lugar a este fenotipo parecen ser distintos. El aumento de almidón en plantas con sobreexpresión de NTRC respondía a una disminución de la tasa neta de degradación de almidón por la noche. Este fenotipo podría estar relacionado con el aumento en el estado de reducción de la ADP-glucosa pirofosforilasa y/o con una desactivación redox dependiente de una putativa enzima desramificadora de almidón. Por otro lado, el aumento de almidón en plantas que sobreexpresan Trx f se relacionó con un aumento en la capacidad de las enzimas almidón sintasas durante el periodo de luz. En conjunto, se demuestra que NTRC y el sistema Fd-Trx son relevantes en el metabolism del almidón, si bien ejercen papeles diferentes en los mecanismo de regulación de su síntesis y degradación.

El capítulo III describe la influencia de Trx m en la partición del carbono (C) y el nitrógeno (N) en plantas de tabaco. La sobreexpresión de Trx m mostró una alteración en el metabolismo del C (menos almidón y azúcares solubles en hoja) y del N (mayor cantidad de aminoácidos y proteína soluble), lo que sugiere una activación del metabolismo del N a expensas de los carbohidratos. Además, un análisis metabolómico y de actividades enzimáticas apuntaban a una activación de la ruta glutamina sintetasa-glutamato sintasa. Plantas de tabaco con elevados niveles de Trx m mostraron un aumento específico en la actividad y estabilidad de la glutamina sintetasa, por lo que se propone una posible regulación redox de esta enzima mediada por la Trx m a través de un mecanismo que podría involucrar una interacción entre ambas proteínas. Además, estas plantas presentaron una elevada tasa de fotorrespiración y una acumulación de nitrato, sugiriendo que la sobreexpresión de Trx m favorece el ciclo fotorrespiratorio del N en lugar de la asimilación primaria de nitrato. En general, se concluye que la Trx m ejerce un papel importante en la regulación redox del metabolism del N en cloroplastos.

En el Capítulo IV se presenta un nueva nueva estrategia para la identificación *in vivo* de proteínas diana aplicado a las Trxs plastidiales f, m y NTRC. Para ello, las formas mutadas de estas Trxs, en las que la cisteína resolutiva del centro activo se sustituye por serina, se sobreexpresaron en hojas de *N. benthamiana*. Los mutantes monocisteínicos unidos covalentemente con sus dianas, fueron capturados en columnas de afinidad, y las dianas se eluyeron con DTT y se identificaron mediante espectrometría de masas. Con esta estrategia se logró la identificación de 30 nuevas proteínas como posibles dianas de Trx f, m, y NTRC, con cisteínas conservadas y que actúan en diferentes procesos dentro del cloroplasto. Aunque la especificad obtenida entre Trx f y m fue baja, sí se consiguió mantener una mayor especificidad para las dianas de NTRC.

ABSTRACT

Carbon (C) and nitrogen (N) are two essential nutrients required for plant growth and development. The cellular metabolism of both elements is tightly coordinated and subjected to a complex regulation. In this regard, the redox status operates as a major integrator of cellular metabolism, involving post-translational modifications of target enzymes by thiol-disulfide exchanges exerted by thioredoxins (Trxs). In plant chloroplasts two Trx systems function in parallel: (i) the ferredoxin (Fd)-Trx system that depends on photosynthetically reduced Fd to supply electrons to the Fd-Trx reductase, which in turn reduces Trxs; (ii) the NADPH dependent Trx reductase type C (NTRC) that contains both a Trx-reductase and a Trx domain in a single polypeptide. NTRC is reduced by NADPH, which in addition to the light reactions, is also produced in the oxidative pentose phosphate pathway in darkness. This PhD thesis has been focused on the regulatory role of plastid Trx f, m and NTRC in chloroplast metabolism.

Chapter I presents the role of Trx f and m in the regulation of the protein kinase STN7, involved in the phosphorylation of the light-harvesting complex II (LHCII) proteins, which in turn regulates state transitions. Tobacco plants overexpressing Trx f or m showed that only Trx m overexpression was associated with a complete loss of LHCII phosphorylation that did not correlate with decreased STN7 levels. The absence of phosphorylation impeded migration of LHCII from photosystem II (PSII) to PSI, with the concomitant loss of PSI-LHCII complex formation. Consequently, the thylakoid ultrastructure was altered in Trx m overexpressing plants, showing reduced grana stacking. Moreover, the electron transport rate was negatively affected, showing an impact on energy demanding processes such as the ribulose-1,5-bisphosphate carboxylase/oxygenase maximum carboxylation capacity and ribulose-1,5-bisphosphate regeneration rate values, which caused a strong depletion in net photosynthetic rate. Finally, tobacco plants overexpressing a Trx m mutant lacking the reactive redox site, showed equivalent physiological performance to control plants, indicating that the oxidoreductase activity of Trx m is a key factor in the STN7 kinase deactivation.

Chapter II focuses on the specific role of Trx f and NTRC in plant starch metabolism. To address this point, tobacco plants overexpressing NTRC and Trx f from the chloroplast genome, as well as *Nicotiana benthamiana* plants with reduced levels of these proteins, were analysed. Both NTRC and Trx f overexpression induced enhanced starch accumulation in tobacco leaves, however, the mechanisms that generated this phenotype seems to differ between both Trxs. NTRC overexpression was associated with an increase in the accumulation of transitory leaf starch, at least in part, as a consequence of a diminished starch turnover during the dark period due to a significantly increase of ADP-glucose pyrophosphorylase reduction and/or a redox

deactivation of a putative debranching enzyme. On the other hand, increased starch content in Trx f overexpressing plants was related with an increase in the capacity of soluble starch synthases during the light period. Taken together, these results indicate the relevance of both NTRC and the Fd/Trx system on starch metabolism, although they play distinct roles in starch turnover.

Chapter III describes the influence of Trx m on carbon (C) and nitrogen (N) partitioning in tobacco plants. Trx m overexpression showed altered metabolism of C (lower leaf starch and soluble sugar accumulation) and N (higher amounts of amino acids and soluble protein), which pointed to an activation of N metabolism at the expense of carbohydrates. Moreover, metabolomic and enzymatic analysis indicated an up-regulation of the glutamine synthetase-glutamate synthase pathway. Trx m-overexpressing plants specifically displayed increased activity/stability of the chloroplastic glutamine synthetase, suggesting a putative redox modulation of this enzyme exerted by Trx m in a mechanism that possibly involves a direct interaction between both enzymes. Additionally, higher rates of photorespiration and nitrate accumulation were determined in these plants, suggesting that overexpression of Trx m favors the photorespiratory N cycle rather than primary nitrate assimilation. Taken together, the combined results reveal the importance of Trx m as a key molecular mediator of N metabolism in plant chloroplasts.

Chapter IV presents a new strategy for the *in vivo* identification of target proteins applied to chloroplastic Trx f, m and NTRC. For this purpose, mutated variants of these Trxs with the buried cysteine of the active disulfide replaced by serine, were overexpressed on *N. benthamiana* leaves. The monocysteinic mutants, together with their covalently linked proteins, were trapped on affinity columns, eluted with DTT and identified by mass spectrometry. This approach led to the identification of 30 potential new targets for Trx f, m and NTRC with conserved cysteines that function in different chloroplast processes. Although target specificity between Trx f and m remains to be investigated, our results achieved a higher specificity for NTRC targets.

INTRODUCCIÓN GENERAL

1. Metabolismo del carbono en cloroplastos

1.1 Fotosíntesis

Las plantas, algas y cianobacterias utilizan la energía lumínica para convertir el CO_2 atmosférico en energía química, proceso denominado fotosíntesis oxigénica. Este mecanismo celular, que ocurre en los cloroplastos, consta de dos fases: i) reacciones de captación de luz, y ii) reacciones de fijación del CO_2, que almacenan la energía capturada en azúcares fosfato. Los productos finales de la fotosíntesis son utilizados para proporcionar energía al metabolismo celular y promover el crecimiento de la planta.

La primera fase tiene lugar en los tilacoides, una compleja red de membranas en el interior de los cloroplastos, donde la energía lumínica es captada por los fotosistemas I y II (PSI y PSII), y posteriormente los electrones excitados pasan a una cadena de transporte dando lugar, finalmente, a la síntesis de ATP y NADPH. Los dos fotosistemas presentan dos partes funcionalmente diferentes: el núcleo, que contiene el centro de reacción donde se dan las reacciones fotoquímicas, y un complejo antena periférico que capta y transfiere la energía de excitación de la luz a los centros de reacción de los fotosistemas [1]. El núcleo del PSII está formado por 25-30 subunidades cuya función solo se conoce parcialmente y parecen estar involucradas en el ensamblaje, reparación y regulación del PSII [2,3]. Las cuatro subunidades principales son las proteínas de membrana D1 (PsbA), D2 (PsbD), CP43 (PsbC) y CP47 (PsbB). El complejo D1-D2 junto al citocromo (Cyt) 559 se considera el centro de reacción del PSII ya que se une a la mayoría de cofactores necesarios para la actividad foto-catalítica. CP43 y CP47 también se unen a este complejo y, a su vez, otras proteínas se asocian en la periferia del lado lumenal encargadas de la oxidación del agua o de la optimización del proceso, conocidas como *oxygen-evolving enhancer protein*s [4]. Por otro lado, el núcleo del PSI está formado por menos subunidades, donde PsaA y PsaB forman un hetero dímero que se une a la mayoría de cofactores necesarios para la captación de la luz y la transferencia de electrones (Figura. 1).

Los complejos antena de los PSI y PSII (LHCI y LHCII respectivamente) se asocian con moléculas de clorofila (Chl) *a*, *b* y carotenoides. Existen cuatro proteínas diferentes asociadas al PSI (Lhca1-4) y seis asociadas al PSII (Lhcb1-6), cada una en una posición específica del fotosistema (Figura 1). Las proteínas Lhcb1-3 se organizan en forma de trímeros conectados al núcleo del PSII a través de monómeros de CP26 (Lhcb5) y CP29 (Lhcb4), además de CP24 (Lhcb6) que conecta con CP29. En función de la fuerza de unión de los trímeros al núcleo del PSII, éstos se denominan S (del inglés *strong*), M (del inglés *moderate*) o L (del inglés *loose*). También existen diferencias en su composición: los trímeros M están formados principalmente por Lhcb1 y Lhcb3, mientras que los S y L están más enriquecidos en Lhcb2 en

comparación a los M [5]. Se ha observado que, en plantas, el PSII se asocia con dos trímeros S y dos M para formar un supercomplejo $C_2S_2M_2$ *in vivo* [6]. Sin embargo, la posición de los trímeros L no está definida claramente. Por otro lado, en el PSI se ha encontrado una única capa de proteínas Lhca unidas a una de las caras del núcleo (Figura 1). Cabe destacar que el complejo antena periférico del PSII es mucho más flexible y dinámico que el del PSI, ya que aumenta o disminuye de tamaño para adaptarse a las condiciones ambientales.

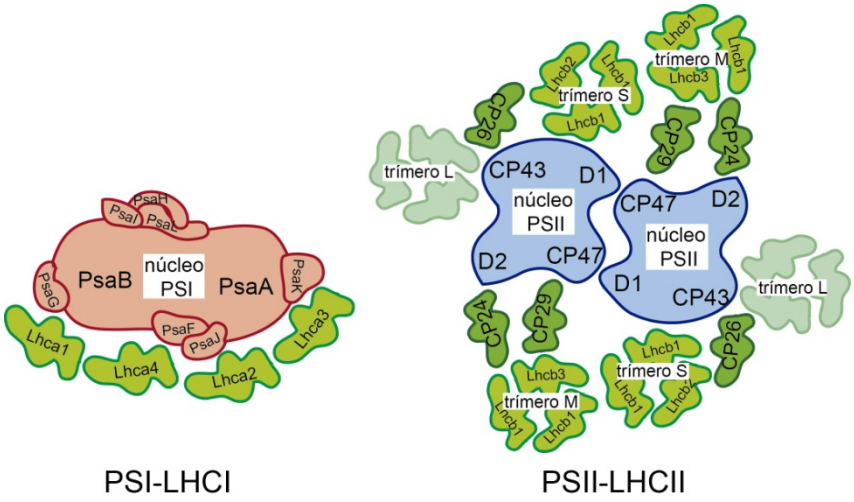

Figura 1. Estructura de los fotosistemas de plantas superiores. Representación simplificada de los fotosistemas I y II asociados a sus complejos antena (PSI-LHCI y PSII-LHCII) basada en imágenes de microscopia electrónica y cristalografía [6–8].

Por tanto, durante la primera fase de la fotosíntesis (Figura 2) la clorofila P680 del PSII es excitada por la luz, oxidándose al liberar un electrón que asciende a un nivel superior de energía. El PSII recupera los electrones que ha perdido a partir de la descomposición del agua en oxígeno y protones por acción de la luz (fotólisis del agua). De esta manera, se desencadena una cascada de electrones en el interior de la membrana tilacoidal acoplada a la formación de un gradiente de pH transtilacoidal. El electrón pasará a lo largo de la cadena transportadora de electrones, formada por la plastoquinona (PQ), el complejo asociado a la membrana Cytb_6f, y la plastocianina localizada en el lumen. Esta última, cederá finalmente el electrón a la clorofila P700 del PSI. Los protones generados por la fotólisis del agua, junto con los que se bombean al lumen en el paso de los electrones por la cadena de transporte, pasan a través de la ATP sintasa (ATPase) originando moléculas de ATP. En el PSI la luz produce el mismo efecto sobre la clorofila P700, de modo que algún electrón adquiere un nivel energético superior, abandona la molécula y es finalmente recogido por otro aceptor de

electrones, la ferredoxina (Fd), que a través de la ferredoxina-NADP reductasa (FNR) genera NADPH (Figura 2).

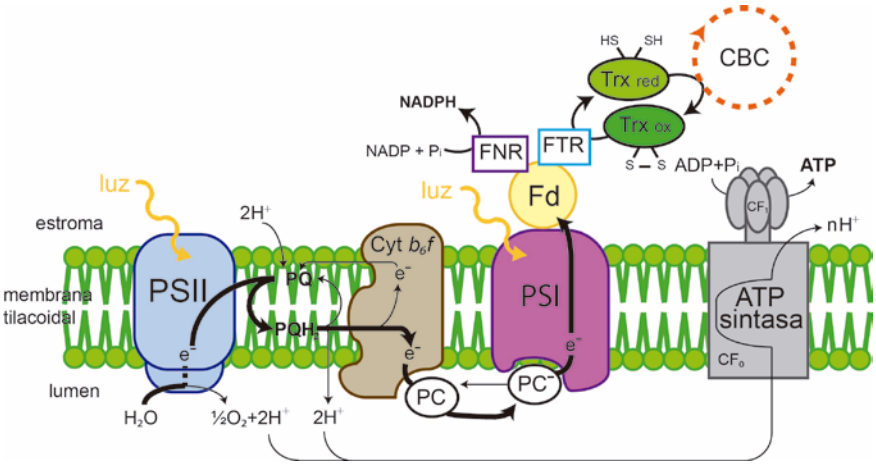

Figura 2. Fase de asimilación de luz de la fotosíntesis en relación al sistema ferredoxina/tiorredoxina. En la primera fase de la fotosíntesis se generan ATP y NADPH, además de producirse la reducción dependiente de la luz de las tiorredoxinas (Trxs) cloroplásticas que regulan posteriormente enzimas del Ciclo Calvin-Benson (CBC), entre otras, a través de intercambios ditiol/disulfuro. PSI y PSII, fotosistema I y II; Cytb_6f, citocromo b_6f; PC, plastocianina; Fd, ferredoxina; FNR, ferredoxina-NADPH reductasa; FTR, ferredoxina-tiorredoxina reductasa.

La segunda fase de la fotosíntesis, que se produce en el estroma, se conoce como Ciclo de Calvin-Benson (CBC). Aquí se utilizan los productos generados en la fase anterior, ATP y NADPH, para fijar el CO_2 atmosférico en esqueletos de carbono [9]. Este ciclo consta de 11 enzimas diferentes, que catalizan 13 reacciones y se inicia por la enzima ribulosa-1,5-bifosfato carboxilasa/oxigenasa (Rubisco) que cataliza la carboxilación de la molécula aceptora de CO_2, la ribulosa-1,5-bisfosfato (RuBP). El 3-fosfoglicerato formado en esta reacción es utilizado posteriormente para generar triosas fosfato (TP), gliceraldehido-3-fosfato y dihidroxiacetona fosfato, mediante dos reacciones que consumen ATP y NADPH. En la fase regenerativa del CBC la mayor parte de las TP formadas son utilizadas para regenerar la RuBP, sin embargo, las TP restantes son finalmente utilizadas para proveer intermediarios a otros procesos metabólicos del cloroplasto, como la biosíntesis de carbohidratos, la ruta del sikimato para la biosíntesis de aminoácidos y lignina, la biosíntesis de isoprenoides o precursores para el metabolismo de los nucleótidos y la síntesis de la pared celular [10]. Las TP generadas en el CBC también se exportan fuera del cloroplasto para promover la síntesis de sacarosa en el citosol [11].

Tradicionalmente, las dos fases del proceso fotosintético habían sido denominadas como “fase luminosa” y “fase oscura”. Sin embargo, durante los años 1960-70 varios estudios cuestionaron esta separación inicial, revelando que, lejos de ser independiente de la luz, la fase de fijación del carbono (C) requiere de la luz para la activación de enzimas específicas del CBC. Dicha activación se produce por reducción de los puentes disulfuro de las enzimas mediante el sistema Fd/tiorredoxina (Trx) [12] (Figura 2). Así, las plantas pueden satisfacer sus requerimientos energéticos mediante la fotosíntesis bajo un estricto control dependiente de la luz [13–15].

Durante el crecimiento de las plantas las condiciones de luz son cambiantes, por lo que estas se ven forzadas a ajustar su metabolismo y mantener la homeostasis redox dentro del cloroplasto [16]. La optimización de la fotosíntesis a distintas intensidades de luz se logra mediante distintos mecanismos que actúan tanto a largo como a corto plazo. Los mecanismos a largo plazo se basan en regular la estequiometría de los LHCs y así el ratio PSII/PSI [17]. Por otro lado, los mecanismos a corto plazo más estudiados son la disipación no fotoquímica (NPQ) que permite a las plantas protegerse frente al daño fotooxidativo en condiciones de alta irradiación [18], y los estados de transición, que permiten optimizar la fotosíntesis en condiciones de baja irradiación [19–21].

Los estados de transición conforman un mecanismo de adaptación a los cambios de luz en el que los dos fotosistemas modifican el tamaño de sus complejos antena para redistribuir la energía entre ellos [22]. Cuando hay un desequilibrio en la absorción entre los dos fotosistemas en favor del PSII, una pequeña parte (20-25%) de los LHCII, asociados al PSII, se fosforilan de manera reversible, desplazándose hacia el PSI (estado 2) [23]. Parece que son principalmente los trímeros L asociados al PSII los que estarían involucrados en este proceso [5]. Esta migración hace que disminuya la energía absorbida por el PSII y aumente la probabilidad de absorber energía por el PSI al aumentar el tamaño de su complejo antena. Por el contrario, cuando se excita preferencialmente el PSI, los LHCII se desfosforilan por acción de una fosfatasa (TAP38/PPH1) y vuelven a migrar hacia el PSII (estado 1) (Figura 3).

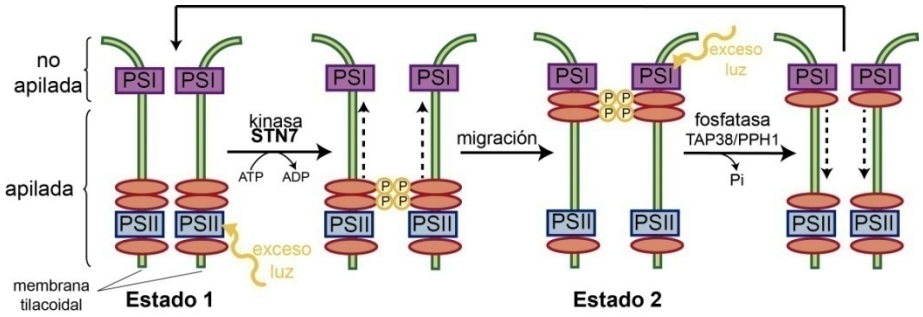

Figura 3. Los estados de transición conforman un mecanismo de control de la distribución de la energía entre los fotosistemas regulando el transporte no cíclico de electrones. Un exceso de energía en el fotosistema II (PSII) desencadena un proceso de fosforilación de sus complejos antena (LHCII, representados en rojo) mediado por la kinasa STN7 que permite su migración hacia el PSI (estado 2), favoreciendo la absorción de luz del PSI. Un exceso de activación del PSI resulta en la activación de la fosfatasa TAP38/PPH1 que desfosforila los LHCII favoreciendo su migración hacia el PSII (estado 1).

La proteína que regula la fosforilación de los LHCII en plantas es la kinasa STN7, la cual está sometida a regulación redox [24]. La STN7 es una proteína transmembrana que se activa cuando el pool de PQ está muy reducido (cuando el PSII recibe mucha más luz que el PSI), fosforilando los LHCII y haciendo que migren del PSII al PSI. Parece que su activación está relacionada con la unión de la PQ reducida al sitio Q_0 del complejo Cytb_6f [25,26], que parece implicar una interacción directa con la proteína Rieske (PetC) que forma parte de este complejo [27]. Pero además de este mecanismo, se ha visto que en condiciones de alta irradiación, cuando la formación de poder reductor excede al necesario, la actividad de STN7 se ve fuertemente inhibida [28], probablemente por mediación del sistema Fd/Trx [29]. Así, las Trxs estromáticas reducidas serían capaces de reducir un puente disulfuro localizado en el lado estromático de la kinasa STN7, inactivándola [29,30], por lo que la fosforilacion de los LHCII queda inhibida y la distribución de energía entre ambos fotosistemas ya no se produce [31]. Sin embargo, estas cisteínas (Cys), aunque sí se encuentran conservadas en plantas, no lo están en algas verdes unicelulares. Además, parecen no ser requeridas para la actividad kinasa de STN7 [27]. Por tanto, la regulación de este mecanismo continúa actualmente en debate.

1.2 Metabolismo del almidón

El almidón es la forma principal de almacenamiento de carbohidratos en plantas vasculares. Este se puede clasificar en dos tipos según su función biológica, almidón transitorio y almidón de reserva. El primero se sintetiza en las células del mesófilo de la hoja directamente a partir del 40-50% de los fotoasimilados producidos durante el día, y se degrada por la noche para mantener el metabolismo celular en ausencia de fotosíntesis. Sin embargo, y aunque existe controversia al respecto, se han encontrado evidencias de degradación de almidón también durante el día [32,33]. También se ha descrito la existencia de degradación diurna bajo diferentes tipos de estrés [34–36] o en células guarda para controlar la apertura estomática [34,37]. Por otro lado, el almidón de reserva es acumulado en tejidos no fotosintéticos como semillas o tubérculos por periodos de tiempo más largos. La removilización de este almidón tiene lugar bajo estímulos concretos, durante la germinación, brotación o cuando la demanda de energía y esqueletos carbonados supera a la aportada por la fotosíntesis [38].

El almidón se sintetiza en los plastidios en forma de gránulos semicristalinos insolubles, compuestos por dos polímeros de glucosa: amilosa y amilopectina [39]. Ambos están formados por cadenas lineales de glucosa (unidas mediante enlaces glucosídicos α-1,4) intercaladas con regiones ramificadas donde las moléculas de glucosa se unen mediante enlaces glucosídicos α-1,6. En el caso de la amilosa, el polímero apenas presenta ramificaciones. Sin embargo, la amilopectina se caracteriza por presentar ramificaciones muy frecuentes y además, es el componente mayoritario del almidón ya que puede suponer más del 75% del gránulo [38].

La síntesis del almidón en los cloroplastos comienza con la producción de ADP-glucosa (ADPG) a partir de glucosa 1-fosfato gracias a la enzima ADP-glucosa pirofosforilasa (AGPase) (Figura 4). Este paso se ha considerado clave en la síntesis de almidón, y hay evidencias de su regulación tanto a nivel transcripcional como traduccional [40]. Sin embargo, existe otro modelo en el que a partir de las TP en el citosol se produce ADPG por la enzima sacarosa sintasa [32,41], que después entra al cloroplasto [42] para participar directamente en la síntesis de almidón. En la síntesis del gránulo de almidón intervienen básicamente tres enzimas de manera simultánea e interdependiente, las almidón sintasas (SS), las enzimas ramificadoras del almidón (BE) y las enzimas desramificadoras (DBE) [43]. Las SS catalizan la adición de moléculas de ADPG al almidón en formación [44]. En plantas superiores existen cinco isoformas: GBSS, SSI, SSII, SSIII y SSIV. Las GBSS (Figura 4) se encuentran fuertemente unidas al gránulo de almidón y parecen ser responsables exclusivas de la síntesis de amilosa en diferentes especies [45–47]. Las otras SS (Figura 4) generan las cadenas de amilopectina y se encuentran de forma soluble en el estroma, o una

parte soluble y otra parte asociada al gránulo [38]. La contribución de cada clase de SS en la síntesis de amilopectina varía según los tejidos y las especies.

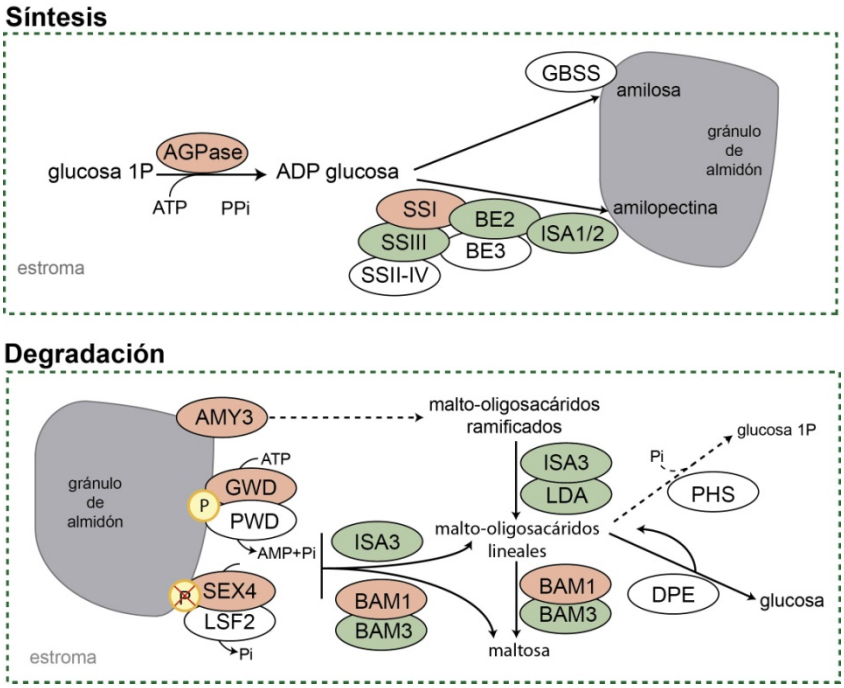

Figura 4. Esquema general de las enzimas implicadas en las rutas de síntesis y degradación del almidón y su regulación redox. En la síntesis, la ADP-glucosa pirofosforilasa (AGPase) produce ADP-glucosa como substrato para las almidón sintasas (SS). Las almidón sintasas unidas al gránulo (GBSS) sintetizan amilosa mientras que las SS solubles, las enzimas ramificadoras de almidón (BE) y el complejo isoamilasa 1/2 (ISA1/2) conjuntamente sintetizan amilopectina. En el proceso de degradación intervienen las fosforilasas α-glucano H_2O diquinasa (GWD) y fosfoglucano H_2O diquinasa (PWD) y las fosfatasas SEX4 y LSF2 sobre la superfcie del gránulo, permitiendo que las β-amilasas (BAM) e ISA3 produzcan maltosa y malto-oligosacáridos lineales. La α-amilasa 3 (AMY3) también participa en el proceso generando malto-oligosacáridos ramificados que son transformados en lineales por ISA3 y pululanasa/limit dextrinasa (LDA). Las enzimas representadas en rojo son aquellas en las que se ha descrito una activación específica por Trxs; las de color verde son aquellas sensibles a cambios en las condiciones redox; y para las de color blanco no se ha descrito ningún tipo de regulación redox (discutido en el apartado 4.1.2). Las líneas discontínuas representan rutas minoritarias. Adaptado de [48].

Por otro lado, las enzimas BE (Figura 4) se encargan de ramificar la cadena de glicanos con enlaces glucosídicos α-1,6. En plantas superiores existen dos isoformas, BEI y BEII, siendo las primeras las que transfieren preferentemente cadenas más largas [49]. Posteriormente, por homología de secuencias, fue descubierta una tercera

isoforma BEIII [50–52] pero aún no se ha definido su actividad catalítica ni su función biológica. Además, se ha demostrado que la eliminación de algunas de estas ramificaciones, catalizada por las enzimas DBE, es también importante para la biosíntesis de almidón [53]. En plantas hay dos tipos de enzimas DBE: las isoamilasas (ISA), representadas por tres isoformas ISA1, ISA2 e ISA3 [54] y las pululanasas o limit-dextrinasas (LDA). Ambos tipos son capaces de hidrolizar enlaces α-1,6. ISA1 e ISA2 forman un complejo que está implicado en la síntesis de amilopectina [55], mientras que ISA3 y LDA parecen tener un papel más relevante en la degradación del almidón [56,57]. En conjunto, el proceso de biosíntesis de amilopectina es complejo ya que existe un solapamiento funcional entre las enzimas [58], interferencias entre las enzimas de síntesis y degradación [53, 55,59] e incluso formación de complejos entre las diferentes enzimas [60–64].

En cuanto a la degradación del almidón, este proceso difiere entre órganos. En las hojas, el almidón transitorio se degrada por hidrólisis dando maltosa y glucosa, que pueden ser exportadas fuera del cloroplasto y metabolizadas en el citosol [65,66]. La degradación del almidón está regulada por un proceso de fosforilación reversible de glucanos, el cual altera la superficie del gránulo de almidón facilitando así el inicio de su degradación [67]. En el proceso de fosforilación intervienen dos enzimas, primero la α-glucano H_20 diquinasa (GWD) que fosforila los residuos glucosídicos en la posición C6 y posteriormente la fosfoglucano H_20 diquinasa (PWD) que fosforila las cadenas pre-fosforiladas en la posición C3 [68–71]. Las fosfoglucano fosfatasas (SEX4 y LSF2) son capaces de desfosforilar los grupos previamente añadidos por las fosforilasas [72–74], proceso también necesario para la degradación del almidón (Figura 4).

En el proceso de degradación propiamente dicho intervienen diversas enzimas hidrolíticas que degradan los enlaces α-1,4 y α-1,6. Entre ellas está la familia de las β-amilasas (BAM), que son exo-amilasas que hidrolizan cadenas lineales de glucanos liberando maltosa (Figura 4). En plantas superiores están codificadas por muchos genes, por nueve concretamente en Arabidopsis (*Arabidopsis thaliana*) [75]. También están las α-amilasas (AMY) que son endo-amilasas que hidrolizan enlaces α-1,4 internos (Figura 4). En plantas superiores se han identificado tres isoformas (AMY1-3) [76], siendo AMY3 la única localizada en el cloroplasto con función conocida en Arabidopsis. Además, como se ha indicado antes, algunas enzimas DBE (ISA3 y LDA) intervienen en la degradación del almidón hidrolizando los enlaces α-1,6 de las cadenas ramificadas formando cadenas lineales (Figura 4). Otras enzimas que también intervienen en el proceso de degradación son las α-glucano fosforilasas (PHS), que catalizan la fosforolisis reversible de la glucosa del extremo no reductor de la cadena de glucanos generando glucosa 1-fosfato [39], y las 4-α-glucanotransferasas (DPE) que metabolizan cadenas cortas de oligosacáridos (Figura 4) [77].

La síntesis y degradación del almidón trasitorio están estrechamente y recíprocamente coordinadas, y a la vez integradas con otras rutas del metabolismo central. Ambas dependen tanto de los ciclos de luz-oscuridad como de su reloj biológico [78].

2. Metabolismo del nitrógeno en cloroplastos y su relación con el carbono

2.1 Metabolismo del nitrógeno

La asimilación del nitrógeno (N) inorgánico es un proceso vital en las plantas, que comienza con la absorción del N de la rizosfera en forma de nitrato preferentemente, a través de dos sistemas de transporte, uno no saturable de baja afinidad y otro de alta afinidad pero saturable [79]. Una vez absorbido, el N puede metabolizarse directamente en el citosol de las células de la raíz, acumularse en la vacuola o bien ser transportado pasivamente por el xilema hasta la parte aérea. En las hojas, el primer paso de la reducción del nitrato ocurre en el citosol gracias a la enzima nitrato reductasa (NR) que lo transforma en nitrito. Después es importado al cloroplasto donde es reducido a amonio por la enzima nitrito reductasa (NiR) (Figura 5). Estos dos pasos involucrados en la reducción del nitrato son energéticamente costosos (necesitan NADPH y Fd reducida) y están estrictamente regulados [80].

Dentro del cloroplasto el amonio, bien absorbido directamente del suelo o bien obtenido de la reducción del nitrato, es incorporado a esqueletos carbonados para la síntesis de aminoácidos mediante la acción de dos enzimas, la glutamina sintetasa y la glutamato sintasa. Estas dos enzimas constituyen el denominado sistema GS/GOGAT que es la principal ruta de asimilación del amonio en las plantas [81]. En un primer paso, la isoforma de GS localizada en cloroplastos (GS2) incorpora amonio al glutamato (Glu) para sintetizar glutamina (Gln) en una reacción dependiente de ATP. A su vez la GOGAT dependiente de Fd (Fd-GOGAT), utilizando la Gln y 2-oxoglutarato (2OG) como fuente de C, da lugar a dos moléculas de Glu, de las cuales, una de ellas es reciclada y la otra se utiliza para la síntesis de los restantes aminoácidos (Figura 5). Además, el sistema GS/GOGAT no solo asimila el amonio generado en la reducción del nitrato, sino que es el responsable de la reasimilación del amonio proveniente de la fotorrespiración en tejidos fotosintéticos, que puede ser hasta 10 veces superior al proveniente de la asimilación primaria [82]. Dicho amonio es rápidamente reasimilado para evitar su acumulación en la célula, ya que resultaría tóxico [83].

Se ha observado que las tres enzimas cloroplásticas involucradas en la asimilación primaria del nitrógeno (NiR, GS2 y Fd-GOGAT) forman complejos proteicos. Las variaciones tanto en tamaño como en la localización de estos complejos sugieren que tienen un papel en la regulación de la función de estas enzimas [84]. Además, se ha observado que GS presenta complejos proteicos específicos de órgano en *Medicago truncatula* [85], lo que sugiere una modificación post-traduccional diferente en cada órgano bajo condiciones fisiológicas distintas.

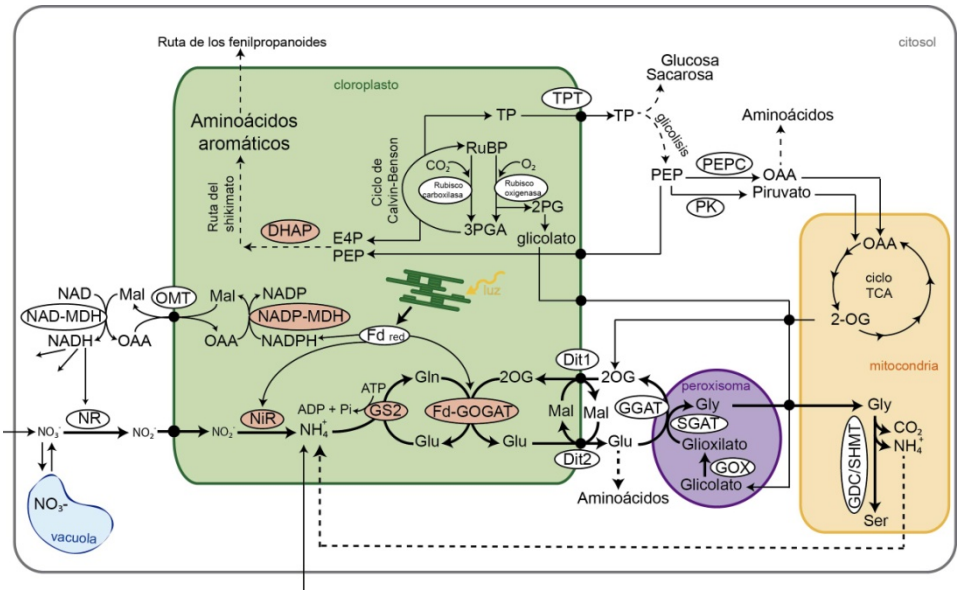

Figura 5. Representación simplificada de la ruta de asimilación del nitrógeno y su regulación redox en relación con la fotosíntesis y la fotorrespiración. NR, nitrato reductasa; NiR, nitrito reductasa; GS2, glutamina sintetasa cloroplástica; Fd-GOGAT, glutamato sintasa dependiente de ferredoxina; DiT1, trasportador de 2-oxoglutarato/malato; DiT2, transportador de glutamato/malato; GGAT, glutamato:glioxilato aminotransferasa; SGAT, serina:glioxilato aminotransferasa; GOX, glicolato oxidasa; GDC/SHMT, glicina descarboxilasa/serina hidroximetiltransferasa; PEPC, fosfo*enol*piruvato carboxilasa; PK, piruvato kinasa; TPT, transportador de triosas fosfato; DHAP,deoxy-D-arabino-heptulosonato 7-fosfato; NADPH-MDH, malato deshidrogenasa dependiente de NADPH; OMT (=DiT1), trasportador de 2-oxoglutarato/malato; Fd red, ferredoxina reducida; Gln, glutamina; Glu, glutamato; 2OG, 2-oxoglutarato; Mal, malato; Gly, glicina; Ser, serina; OAA, oxaloacetato; PEP, fosofo*enol*piruvato; TP, triosas fosofato; RuBP, ribulosa -1,5-bifosfato; 3PGA, 3-fosfoglicerato; 2PG, 2-fosfoglicolato; E4P, eritrosa-4-fosfato. Adapatado de [86]. Las enzimas susceptibles a regulación redox se indican en rojo (discutido en el apartado 4.2). Las líneas discontínuas indican rutas en las que interviene más de una enzima.

En plantas superiores existe también una isoforma citosólica de GS (GS1), pero su función se ha relacionado más con la reasimilación del amonio proveniente de la degradación de proteínas durante la senescencia foliar y germinación de las semillas [87,88]. Cuando los aminoácidos son hidrolizados y convertidos en Glu, que es desaminado por acción de la glutamato deshidrogenasa (NADH-GDH), se produce amonio y 2OG para proveer al ciclo de Krebs o ciclo de los ácidos tricarboxílicos (TCA) [89]. En cuanto a la GOGAT, también existe otra forma dependiente de NADH (NADH-GOGAT) más abundante en tejidos no fotosintéticos como la raíz, donde interviene en la asimilación de amonio [90].

Para que el sistema GS/GOGAT funcione es necesario importar 2OG al cloroplasto y exportar Glu, proceso en el que intervienen dos transportadores (DiT1 y DiT2) involucrados en el paso de los ácidos dicarboxílicos a través de la membrana plastidial [91,92]. DiT1 importa 2OG y exporta malato (Mal), mientras que DiT2 exporta Glu a expensas de Mal (Figura 5). Plantas de tabaco deficientes en DiT1 mostraron un fenotipo fotorrespiratorio típico: menor capacidad de transportar 2OG, síntesis de aminoácidos afectada, menor cantidad de proteína y azúcares en hoja, así como una menor capacidad fotosintética [93]. A su vez, se demostró que este transportador (llamado también OMT) actúa también intercambiando oxaloacetato y Mal en la vávula de Mal [94] (Figura 5). Respecto al otro transportador, mutantes deficientes en el gen *DiT2.1* de Arabidopsis mostraron también un fenotipo fotorrespiratorio, identificando por primera vez su relevancia en el transporte de Glu y Mal [95].

2.2 Interacción entre el carbono y el nitrógeno

Los metabolismos del C y del N en cloroplastos están estrechamente unidos e interregulados [96,97]. La asimilación de N no solo está integrada con la fotosíntesis, sino también con la fotorrespiración y la respiración. La partición del C asimilado entre la síntesis de ácidos orgánicos, almidón y azúcares se ve afectada por la disponibilidad de N, sugiriendo la existencia de mecanismos de regulación en respuesta al N tanto a nivel transcripcional como post-transcripcional [98–102].

La fotosíntesis tiene un papel importante en la asimilación de N, ya que aporta el poder reductor, el ATP y los esqueletos carbonados necesarios para la biosíntesis de aminoácidos. A su vez, se invierten grandes cantidades de N en construir y mantener el aparato fotosintético, principalmente en forma de Rubisco y LHC [103]. Claras evidencias de esta integración son la correlación positiva que existe entre la actividad de la NR y el contenido de carbohidratos en hojas [104], o la mayor tasa de asimilación de N inorgánico en luz que oscuridad [105,106] debido a su activación dependiente de la luz [107].

La fotorrespiración también tiene una gran implicación en el metabolismo del N, abarcando reacciones en diferentes compartimentos celulares: cloroplastos, peroxisomas, mitocondrias y citosol. La fotorrespiración ocurre cuando la Rubisco, en presencia de luz, fija O_2 en lugar de CO_2 formando 3-fosfoglicerato y 2-fosfoglicolato. Este último puede resultar tóxico si se acumula en grandes cantidades, por eso es rápidamente metabolizado, convirtiéndose en glicolato. El glicolato es transportado a los peroxisomas donde se convierte en glioxilato y finalmente en glicina, que es nuevamente conducida a las mitocondrias donde se convierte en serina (Figura 5). En este último proceso se libera CO_2 y amonio en la mitocondria, que debe ser reasimilado rápidamente para evitar toxicidad. Como se ha mencionado antes, esta reasimilación se da gracias al sistema GS/GOGAT en el cloroplasto, proceso que se

conoce como ciclo fotorrespiratorio del N [108]. De hecho, se estima que el 90% del amonio que se consume en el ciclo GS/GOGAT proviene de la fotorrespiración [109–111], indicando la importancia de su función.

La respiración es el tercer proceso del metabolismo energético en plantas que interacciona con la asimilación del N. La respiración, y en concreto la actividad del ciclo del TCA, es indispensable para suministrar los esqueletos de C y el poder reductor para la asimilación del N [112]. Parece que durante el día, el ciclo del TCA provee, al menos en parte, el 2OG necesario para la producción de Glu y Gln [113–116] (Figura 5). Este proceso va acompañado de la actividad anaplerótica de la enzima fosfo*enol*piruvato carboxilasa (PEPC) que produce oxaloacetato. Este puede, o bien entrar al ciclo del TCA, o ser transaminado a aspartato [117], punto a partir del que se sintetizan otros aminoácidos (Figura 5). Además se ha observado que el fosfo*enol*piruvato (PEP), producido en la glicolisis, junto con la eritrosa-4-fosfato tienen influencia en la tasa de síntesis de aminoácidos aromáticos por la vía del sikimato [118,119] (Figura 5).

El metabolismo del N presenta una regulación compleja, donde actúan distintos mecanismos en respuesta a metabolitos o al propio nivel del N en la planta, modulando la expresión tanto de sistemas de transporte como la actividad de algunas enzimas. Hace ya décadas se sugirió que los pools de aminoácidos podrían ser indicativos del nivel de N en la planta, produciendo una señal que puede regular la absorción y la asimilación de N [112]. El propio nitrato actúa también como una potente señal de regulación [120–122]. La disponibilidad de NADH también parece ser crítica para la asimilación de nitrato y amonio [123]. En definitiva, existen una serie de componentes que constituyen un complejo sistema de señalización capaz de regular el metabolismo del nitrógeno [112].

3. Regulación redox en cloroplastos

Para lograr el mantenimiento de la homóstasis redox, en la célula actúan una serie de mecanismos que constituyen un sistema realmente complejo [124]. Entre ellos, las especies reactivas, las modificaciones redox y las proteínas con actividad oxidorreductasa actúan de forma conjuna transmitiendo una señal que informa a la célula de las condiciones ambientales, y le permite reaccionar fisiológicamente respondiendo ante situaciones de estrés. Dentro de los mecanismos de regulación post-traduccional, la regulación redox tiene gran importancia en el cloroplasto.

3.1 Tiorredoxinas

3.1.1 Tiorredoxinas: qué son y cómo actúan

Las Trxs conforman una superfamilia de proteínas que desarrollan una actividad disulfuro oxidorreductasa, que engloba también a las glutarredoxinas (Grxs), a las glutatión-S-transferasas y a las proteínas disulfuro isomerasas, estas últimas con funciones disulfuro oxidorreductasa y/o disulfuro isomerasa [125]. Dentro de esta superfamilia, las Trxs clásicas se caracterizan por tener un motivo estructural común, altamente conservado, denominado plegamiento tipo Trx, formado por 4 hélices α rodeando a una lámina β de 5 hebras con un grupo ditiol/disulfuro en el sitio activo [126,127]. Además, contienen el sitio activo canónico WC(G/P)PC, donde las dos Cys reactivas están separadas generalmente por los residuos glicina y prolina. En esta conformación, las Cys se encuentran accesibles para la interacción con sus proteínas diana desde uno de los lados de la molécula [128].

El mecanismo de acción de las Trxs consiste en reducir los puentes disulfuro expuestos de sus proteínas diana [126]. La proteína diana oxidada puede ser un monómero con un puente disulfuro intramolecular, como por ejemplo la fructosa 1,6-bifosfatasa (FBPase), pero también un homo o heterodímero que forme un puente disulfuro intermolecular, como es el caso de la malato deshidrogenasa (MDH) [129,130]. Esta reacción tiene lugar en dos pasos (Figura 6). Primero, el grupo tiol de la Cys N-terminal del sitio activo (Cys nucleofílica) de la Trx reducida transfiere un electrón a una de las Cys del puente disulfuro de la proteína diana oxidada, formando un puente disulfuro con la otra Cys de la proteína diana. En segundo lugar, el complejo intermedio formado es reducido por el grupo tiol C-terminal de la segunda Cys de la Trx (Cys resolutiva), liberándose así la proteína diana reducida y la Trx oxidada. Las Trxs, una vez oxidadas, son de nuevo reducidas específicamente, salvo alguna excepción, por Trx-reductasas (TR).

Mediante estos intercambios ditiol/disulfuro las Trxs producen un tipo de regulación post-traduccional que afecta a la conformación y función de sus proteínas diana. De

esta forma, las Trxs modulan la actividad de un amplio número de proteínas, activándolas o desactivándolas, y controlando así importantes procesos celulares [125]. Por otro lado, también se han atribuido a las Trxs otros mecanismos de regulación idependientes a su actividad oxidorreductasa, como la actividad chaperona [131]. Esto les permite mejorar el plegamiento de otras proteínas e incluso de otras chaperonas, promoviendo de esta manera la regulación de otros procesos en la célula [132–134].

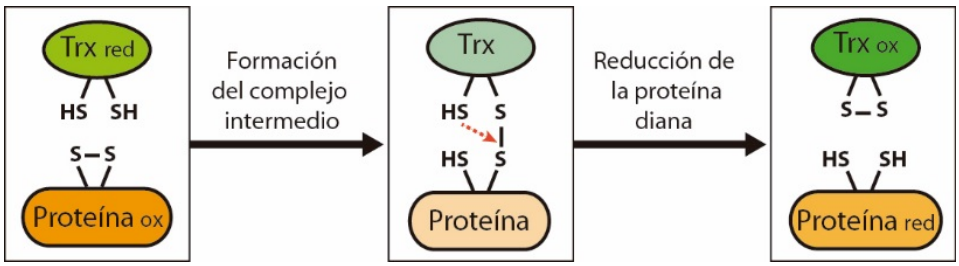

Figura 6. Mecanismo de acción de las tiorredoxinas. El grupo tiol N-terminal del motivo CXXC de la tiorredoxina (Trx) ataca al puente disulfuro de la proteína diana, liberándose un grupo tiol y formando un puente disulfuro con la segunda cisteína de la proteína diana. Después, el grupo tiol C-terminal de la Trx rompe este puente disulfuro intermolecular dando lugar a la proteína diana reducida y quedándose la Trx oxidada.

Los fundamentos del campo de estudio de la biología redox (reducción/oxidación) se remontan a 1964, cuando Peter Reichard y colaboradores descubrieron y acuñaron el nombre de “tiorredoxina” (review histórico en [135]). En un inicio este término hacía referencia a una proteína que en *Escherichia coli* presentaba la capacidad de ceder electrones a enzimas como la ribonucleótido reductasa y la metionina sulfóxido reductasa (MSR) [136]. Más adelante, en cloroplastos, se demostró la activación de algunas enzimas del metabolismo del C por reducción, con la identificación de la Fd como activadora no directa de las mismas [137]. Se propuso por tanto la existencia de dos proteínas adicionales necesarias en este mecanismo de regulación: la Trx [138,139] y la Fd-Trx reductasa (FTR) [140]. De esta manera se identificó el conocido como sistema Fd/Trx, formado por Fd, FTR y las Trxs, dando lugar a un mecanismo de regulación del CBC, de la síntesis de ATP y de la exportación de poder reductor fuera del cloroplasto en respuesta a la luz (Buchanan, 1980). Las Trxs cloroplásticas f y m fueron las primeras Trxs descubiertas en plantas [141]. Recibieron sus nombres por la selectividad mostrada por ciertas enzimas: Trx f por la activación de la FBPase, y Trx m por la MDH.

3.1.2 Tipos de tiorredoxinas en plantas

El sistema Trx en plantas es especialmente complejo, a diferencia de lo que ocurre en animales y bacterias. La secuenciación del genoma de Arabidopsis ha revelado una gran multiplicidad de genes que codifican alrededor de 40 Trxs [125]. Las Trxs pueden clasificarse en diferentes grupos y subgrupos, según su secuencia primaria y su localización subcelular. En cuanto a la similitud de su secuencia aminoacídica se clasifican en 15 subgrupos [142]. Dentro de esta clasificación se encuentran las ya mencionadas Trxs clásicas. En Arabidopsis se han identificado hasta 20 isoformas diferentes de Trxs clásicas localizadas en distintos compartimentos subcelulares. Pero además existen muchas proteínas tipo Trx o Trxs atípicas que contienen sitios activos no canónicos, múltiples dominios Trx o en las que los motivos Trx se asocian con otros dominios no Trx [142].

3.1.2.1 Tiorredoxinas extraplastidiales

Algunas isoformas de Trxs identificadas en Arabidopsis se ubican fuera de los plastidios, en compartimentos celulares como citosol, núcleo o mitocondrias [142,143].

En el citosol se encuentran mayoritariamente las Trxs de tipo h, codificadas por 10 genes en Arabidopsis. Estas se dividen en tres subtipos, siendo las Trxs del subtipo I mayoritariamente citosólicas y reducidas por una TR dependiente de NADPH (NTR) [144]. Sin embargo también hay Trxs tipo h que se localizan en el núcleo, retículo endoplásmico o mitocondrias [145,146] o que pueden ser reducidas por el sistema glutatión (GSH)/Grx [147]. Las Trxs tipo h se han relacionado con funciones en el desarrollo de la planta [148], con procesos de germinación [149], con mecanismos de respuesta a patógenos [150,151], al estrés oxidativo [152] o termotolerancia [153].

El grupo de las Trxs tipo o está formado por dos miembros en Arabidopsis, uno de ellos (Trxo1) localizado en mitocondrias y el otro (Trxo2) sin una ubicación clara [154]. Trx o1 también se ha localizado en el núcleo en otras especies [155]. Estas Trxs se relacionan principalmente con la defensa frente a especies reactivas de oxígeno (ROS) en las mitocondrias [156,157], con la regulación del ciclo del TCA [158] o con la defensa frente a condiciones de estrés como la salinidad o la sequía [159,160].

Además de estas Trxs clásicas, también se han identificado varias Trxs atípicas con diferente localización extraplastidial, como las nucleorredoxinas, presentes en núcleo y citosol y compuestas por hasta tres módulos tipo Trx [161,162]; la tetratricorredoxina, localizada en el citosol y en el núcleo que contiene un dominio Trx en la región C-terminal y la repetición de tres tetratricopéptidos en la N-terminal [163]; dos Trxs de tipo h monocisteínicas, que muestran gran actividad disulfuro isomerasa en presencia de GSH [164]; una Trx tipo h citosólica en maíz en la que las Cys del centro activo se sustituyen por asparagina y serina, con una función de defensa frente al virus del mosaico de la caña de azúcar [165]; o dos isoformas con un sitio activo

atípico denominadas Trx s1 y s2, localizadas en el retículo endoplásmico de las leguminosas que parecen estar involucradas en la asociación simbiótica de la planta con bacterias fijadoras de nitrógeno [166].

3.1.2.2 Tiorredoxinas cloroplásticas

Más de la mitad de las Trxs presentes en la célula vegetal se encuentran en los cloroplastos, y estas se subdividen a su vez en 11 tipos que se localizan mayoritariamente en el estroma [142], englobando tanto Trxs clásicas como Trxs atípicas.

Tiorredoxinas cloroplásticas clásicas

Además de las Trxs f y m, se identificaron otras Trxs clásicas en el cloroplasto, denominadas y, x, z [167–169]. Presentan funciones que no son siempre coincidentes, e incluso los patrones de expresión en los diferentes tejidos también difieren para cada isoforma en Arabidopsis [170,171]. Mientras que Trx f1, m1, m2, m4, y x presentan un alto nivel de expresión en tejidos verdes, Trx m3, y1, y z apenas se detectan. En comparación con las hojas, la expresión en raíces parece ser mucho menor para todas las isoformasen general.

Las Trxs f y m, al ser las primeras Trxs descubiertas en plantas, han sido también las más estudiadas. Ambas difieren en su origen filogenético [172,173]. La Trx f tiene origen eucariota por lo que está presente solo en organismos fotosintéticos eucariotas, mientras que Trx m es de origen procariota y está presente tanto en organismos fotosintéticos eucariotas como procariotas [173]. Ambas Trxs pueden ser reducidas indistintamente por la FTR y pueden distinguirse claramente por su estructura primaria, que solo presenta un 30% de identidad. Se sabe que la Trx m de espinaca es más similar a la Trx de *E. coli* que la Trx f, tanto en su secuencia, en su especificidad enzimática [174], y también a nivel estructural [175]. Según la secuenciación del genoma, se han encontrado dos isoformas de Trx f (f1 y f2) en Arabidopsis [143] y en *Chlamydomonas* [176]. Mientras que el grupo de las Trxs de tipo m presenta una mayor multiplicidad, con cuatro genes que codifican Trx m (m1, m2, m3 y m4) [143], aunque solo se ha identificado un gen en *Chlamydomonas* [176].

En cuanto a su función, no siempre es fácil realizar una distinción funcional entre ambas proteínas, seguramente debido a las condiciones *in vitro* utilizadas en los ensayos de activación de proteínas diana [177,178]. Sin embargo, mediante el uso de técnicas de genética reversa, se han conseguido avances importantes en este aspecto. Así, Trx f está principalmente involucrada en la regulación redox de procesos como el CBC, el metabolismo del almidón, la síntesis de lípidos, la válvula de Mal, el ciclo oxidativo de las pentosas fosfato (OPPP) y la síntesis de clorofila o de ATP en el cloroplasto [179,180]. La Trx m se ha relacionado igualmente con estos procesos, pero también más específicamente con otros como la asimilación de N o mecanismos de

defensa antioxidante, ya que se demostrado que es capaz de regular específicamente la activación de MSR *in vivo* [181,182]. Cabe destacar que la Trx m3 de Arabidopsis presenta diferencias respecto al resto de isoformas y parece estar presente en menor cantidad respecto al resto [170,183]. Se ha demostrado que tiene un papel en el movimiento de proteínas a través de los plasmodesmos, específicamente en desde el floema a las células del meristemo apical de la raíz [184].

Por otro lado, las Trxs x, y o z parecen jugar un papel más importante en la regulación de proteínas relacionadas con la defensa frente al estrés oxidativo [141, 143, 177,180]. En concreto, la Trx x se ha relacionado específicamente con la regulación de la 2-Cys peroxirredoxina (Prx) [177]. Por su parte la Trx y ha mostrado ser un regulador eficaz de proteínas antioxidantes, como la Prx Q [185], la glutatión peroxidasa [186] y las MSRs [187,188]. Más recientemente, se ha propuesto que la Trx z tiene influencia en la expresión de genes en el plastidio, ya que es capaz de modular la actividad de una enzima que a su vez es necesaria para activar la RNA polimerasa plastidial [189,190].

Tiorredoxinas cloroplásticas atípicas

Dentro del cloroplasto existe una gran variedad de Trxs atípicas. Entre ellas destaca la tiorredoxina reductasa tipo C dependiente de NADPH (NTRC), que fue descubierta no sólo en cloroplastos [191] sino también en plastidios de tejidos no fotosintéticos [192]. NTRC presenta en el mismo polipétido un dominio Trx y un dominio NTR [191]. Esta enzima puede reducir eficientemente a la 2-Cys Prx, por lo que se le atribuye una función antioxidante frente a ROS [193–195]. La caracterización en Arabidopsis de líneas *knockout* de *ntrc* indican que también tiene un papel importante en la regulación redox de otros procesos dentro de los plastidios, como el metabolismo del almidón [196,197], la biogénesis de los cloroplastos, la biosíntesis de tetrapirroles [198,199] o la defensa frente otros tipos de estrés, como alta salinidad y sequia [191] u oscuridad prolongada [200]. Recientemente, se ha propuesto que NTRC actúa coordinadamente con el sistema Fd/Trx regulando el balance redox de la 2-Cys Prx en cloroplastos [201] o para mantener la fotosíntesis en cotiledones [202]. Estos últimos trabajos sugieren que NTRC actuaría de forma indirecta en la regulación redox de los procesos dependientes de las Trxs en el cloroplasto.

Respecto al resto de Trxs atípicas, la CDSP32 (del inglés, *chloroplastic drought-induced stress protein*) es una proteína de 32 kDa con dos dominios Trx, pero solo uno con actividad oxidoreductasa [203], y parece estar involucrada en la respuesta al estrés oxidativo [204–206]. Las APRs (5'adenilsulfato reductasas), codificadas por tres genes, contienen un dominio APR fusionado a un dominio Trx, por lo que están implicadas en la asimilación de sulfato [207] y son reducidas por GSH [208]. Y por último los miembros de las familias ACHT (del inglés, *atypical Cys/His-rich Trx*) y WCRKC, con 6 y 2 isoformas respectivamente [142,143,209]. En el caso de WCRKC,

se ha descubierto recientemente su implicación en la regulación por oxidación de proteínas en oscuridad como la Rubisco activasa, FBPase o sedoheptulosa-1,7-bifosfatasa (SBPase) [210].

Además de estas Trx solubles, los cloroplastos contienen Trxs atípicas asociadas a la membrana de los tilacoides, de forma que pueden regular el estado redox de proteínas del lumen [211]. Una de ellas es la proteína transmembrana HCF164 (del inglés, *high chlorophyll fluorescent 164 protein*), que según el modelo propuesto, es reducida por la proteína CcdA, reducida a su vez por la Trx m, de forma que es capaz de reducir a sus proteínas diana en el lumen gracias a que contiene un sitio redox activo atípico en la región lumenal [212]. También se han identificado otras dos Trx atípicas con su centro activo en la cara lumenal de los tilacoides denominadas SOQ1 (del inglés, *suppressor of quenching*) y LTO1 (del inglés, *lumen thiol oxidoreductase 1*) [213,214], relacionadas con la eficiencia en la captación de luz por los LHC y el ensamblaje del PSII respectivamente.

3.2 Sistemas de reducción de las tiorredoxinas en plantas

Las plantas superiores presentan múltiples sistemas de reducción de las Trxs. En los compartimentos extraplastidiales (citosol y mitocondrias) el poder reductor necesario proviene del NADPH, y la reducción de las Trxs se lleva a cabo por una TR dependiente de NADPH, denominada NTR, conformando el sistema NADPH/Trx (Figura 7) [154,215]. En cambio, las Trxs cloroplásticas son reducidas por otro tipo de TR, la FTR, presente en cloroplastos, cianobacterias y posteriormente descubierta en amiloplastos [216] y plastidios de tejidos no fotosintéticos [217]. La FTR recibe el poder reductor de la Fd, conformando lo que se conoce como el sistema Fd/Trx (Figura 7). Este sistema es capaz de detectar los cambios en el potencial redox que ocurren en el estroma debidos a los cambios de iluminación y traducirlos en señales que activan y desactivan distintas rutas catabólicas [15]. De esta manera, en presencia de luz, la Fd transmite el flujo de electrones, procedente del PSI, a la FTR, quien finalmente reduce a las Trxs. Sin embargo, en condiciones de oscuridad o en plastidios heterotróficos, como los amiloplastos, es la FNR quien reduce a la Fd gracias al NADPH producido en el OPPP [218,219] (Figura 7).

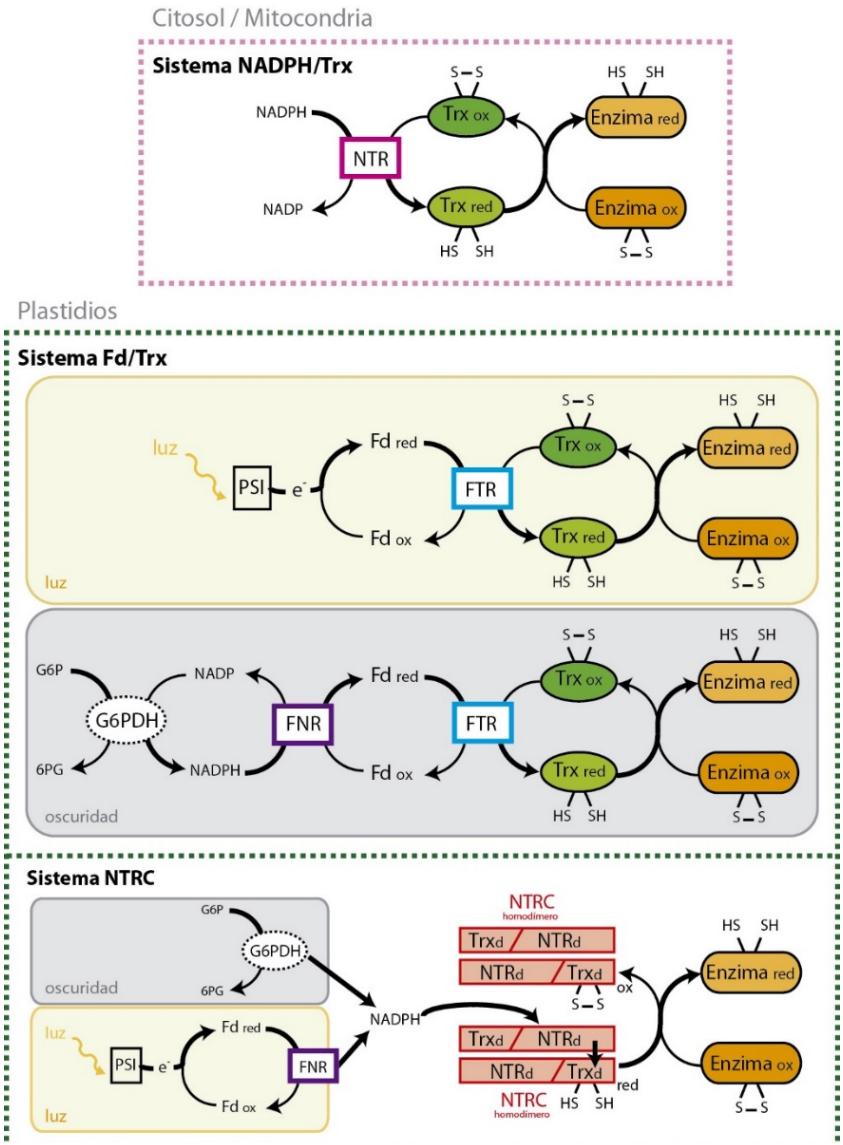

Figura 7. Sistemas de reducción de las tiorredoxinas en plantas. Las tiorredoxinas (Trxs) citoplásmicas y mitocodriales son reducidas por el sistema NADPH/Trx, catalizado por la enzima NADPH-Trx reductasa (NTR) utilizando el NADPH como fuente de poder reductor. En los plastidios, las Trx son reducidas por el sistema ferredoxina/Trx (Fd/Trx), donde la Fd puede ser reducida por la cadena transportadora de electrones en presencia de luz o a través del NADPH obtenido en el ciclo oxidativo de las pentosas fosfato en oscuridad. También en los plastidios, la Trx reductasa tipo C dependiente de NADPH (NTRC), proteína que consta de un dominio NTR (NTRd) seguido de otro Trx (TRXd), conforma un sistema Trx dependiente de NADPH (producido a partir de la Fd-NADP reductasa FNR en luz o del OPPP en osuridad). PSI, fotosistema I; G6P, Glucosa 6-fosfato; 6PG, 6-fosfogluconato; G6PDH, glucosa 6-fosfato deshidrogenasa.

Además, la Trx atípica NTRC es la única NTR que por sí sola conforma un sistema Trx dependiente de NADPH completo en el cloroplasto, ya que, como se ha dicho anteriormente, además del dominio NTR en el extremo N-terminal, contiene un dominio Trx en el extremo C-terminal [191,200]. En Arabidopsis un solo gen codifica esta enzima, que según el modelo propuesto, funciona en forma de homodímero [196,220]. Así, el sitio activo del dominio NTR de una subunidad reduce el puente disulfuro del dominio Trx de la segunda subunidad, que subsecuentemente reduce a sus proteínas diana. También se ha visto que NTRC es capaz de interaccionar con la Trx f *in vivo* mediante su dominio NTR [221], aunque estudios *in vitro* sugieren lo contrario [170,222]. NTRC utiliza el NADPH como fuente de poder reductor, bien generado por la cadena transportadora de electrones, vía Fd y FNR en presencia de luz, o bien proveniente del OPPP en oscuridad (Figura 7). Parece que este sistema podría tener funciones regulatorias distintas a las del sistema Fd/Trx [222], pero actuarían también de forma coordinada y en algunos casos con funciones coincidentes en la regulación de la fotosíntesis o en el crecimiento de la planta [202,223].

Finalmente, indicar que si bien FTR es el transmisor del poder reductor a las Trxs clásicas f, m, x e y [12], sobre Trx z hay resultados contradictorios. Mientras que por un lado se observó que Trx z solo podía ser reducida por FTR [224], por otro lado se defendió que FTR y NTRC eran incapaces de reducirla [170], pero Trx f, m, x e y sí podían activarla. Más adelante se ha postulado que NTRC es el principal reductor de Trz z *in vitro* [222].

3.3 Identificación de proteínas diana de tiorredoxinas

En los 25 años siguientes al descubrimiento del sistema Fd/Trx, se identificaron diferentes proteínas diana mediante métodos bioquímicos [225]. Aunque se sabía que quedaban dianas por descubrir, no fue hasta el desarrollo de las técnicas de análisis proteómico cuando se empezaron a identificar nuevas proteínas diana de manera sistemática. Estás técnicas se desarrollaron de forma exitosa a partir de 2001, aunque se siguen aplicando ajustes para mejorar sus resultados. La identificación de las proteínas diana, tanto en cloroplastos como posteriormente en otros compartimentos celulares, ha supuesto un gran avance en el conocimiento de sus funciones en plantas, algas (*Chlamydomonas*) y cianobacterias (*Synechocystis*) [226]. Además, algunas de las dianas ya identificadas se han confirmando mediante estudios genéticos *in vivo*, bien por mutagénesis o sobreexpresión de Trxs. Esta estrategia también ha permitido identificar algunas dianas nuevas [180].

3.3.1 Métodos bioquímicos

Diez años antes de la identificación en 1977 del sistema Fd/Trx en cloroplastos, FBPase fue la primera enzima que dio lugar al descubrimiento de la regulación redox

en proteínas [137]. Más adelante, se observó que la Trx f podía activar la FBPase específicamente *in vitro* [177,227,228], pero que Trx m era incapaz de hacerlo. Los experimentos iniciales estaban basados en los cambios de actividad de las proteínas tras su reducción, generalmente con DTT. Desde estos inicios hasta la actualidad se ha realizado un amplio estudio de activación/desactivación *in vitro* de proteínas diana con Trxs purificadas o recombinantes [142,180]. En la Tabla 1 se recogen las principales enzimas diana de Trxs f, m y NTRC que han sido identificadas por métodos bioquímicos, mediante ensayos *in vitro*.

3.3.2 La era de la proteómica

Con la aparición y el desarrollo de las técnicas de análisis proteómico el número identificado de dianas potenciales de las Trxs aumentó mucho, y junto a ello lo hicieron también los procesos de regulación con los que se las relaciona, entre los que se incluyen el metabolismo del carbono, la asimilación de nitrógeno, la traducción, el plegamiento de proteínas, la síntesis de aminoácidos, el metabolismo de lípidos o la síntesis de hormonas [226]. A lo largo de estos años se han desarrollado dos estrategias para mejorar la identificación de proteínas poco abundantes en la célula, permitiendo así el análisis a gran escala y con un alto rendimiento de posibles proteínas diana, demostrando así la complementariedad de ambas en varios trabajos [229–232].

La primera de ellas se basa en el marcaje de proteínas diana con sondas tiol específicas. La metodología consiste en reducir los puentes disulfuro de un extracto de proteínas utilizando sistemas NTR/Trx (NADPH, NTR y Trx) reconstituidos *in vitro,* y finalmente marcar los grupos sulfidrilo generados con sondas específicas. Al mismo tiempo, la muestra control, sin reducción previa, también se incuba con la sonda y así la comparación entre ambas permite distinguir las proteínas que han sido reducidas por el sistema NTR/Trx de las que no. Como sonda se ha utilizado tanto monobromobimane, que fluoresce después de unirse covalentemente a los grupos sulfidrilo [149,233–236], como cianina 5 maleimida, que es igualmente fluorescente pero más sensible [237]. Posteriormente se introdujo el uso de una nueva sonda marcada con ^{14}C para visualizar las proteínas reducidas por Trxs en extractos de hojas de Arabidopsis [238]. Utilizando esta sonda, se bloquean los grupos sulfidrilo libres de la muestra con iodoacetamida, previamente a la reducción. Esto permitió la identificación de 19 dianas nuevas y la confirmación de 21 dianas previamente identificadas. Más recientemente se ha aplicado una nueva estrategia, similar a la anterior, basada en el método ICAT (del inglés, *isotope-coded affinity tag*) [232,239]. En este caso, se utilizan dos sondas marcadas radiactivamente (^{12}C y ^{13}C) unidas a biotina (Figura 8). Además, esta técnica permite aislar los péptidos marcados mediante cromatografía de afinidad en columna de avidina, que tras analizarse por espectrometría de masas permite su cuantificación. Finalmente, se ha descrito una

nueva adaptación de este método utilizando como sonda de marcaje cysTMT (del inglés, *cysteine reactive tandem mass tag*), que consiste en seis tags con diferente peso molecular que se unen específicamente a los grupos sulfidrilo [240]. Al igual que la técnica de CysTMT, presenta la ventaja de permitir la cuantificación de los péptidos marcados.

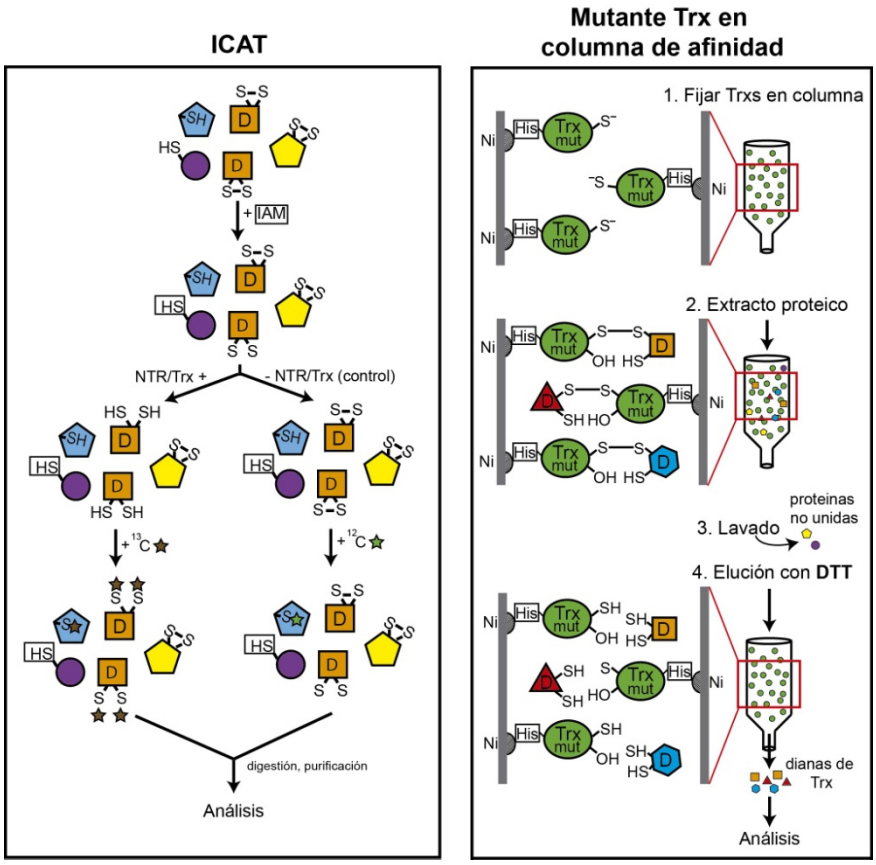

Figura 8. Estrategias para la identificación de proteínas diana de Trxs. Destacan dos tipos de estrategias: (i) el uso de sondas específicas para el marcaje de los grupos tiol como *isotope-coded affinity tag* (ICAT); (ii) la cromatografía de afinidad con mutantes de tiorredoxina (Trx), basada en la formación de un complejo heterodisulfuro intermedio estable entre la diana y la Trx monocisteínica. D, diana; IAM, iodoacetamida; NTR, NADPH-Trx reductasa; Ni, níquel; His, cola de histidinas. Adaptado de [226,232].

La segunda estrategia está basada en el mecanismo de reducción de las Trxs y consiste en atrapar las posibles dianas con mutantes de Trxs en columnas de afinidad. De manera que cuando la segunda Cys del centro activo (Cys resolutiva) es sustituida por serina o alanina, el complejo heterodisulfuro intermedio que se forma entre la Trx y

la diana queda estabilizado covalentemente [241,242]. Esta unión puede romperse posteriormente con la presencia de DTT, permitiendo así recuperar las proteínas diana (Figura 8). Este método fue empleado por primera vez *in vivo* [243] expresando la Trx monocisteínica de *E. coli* en levaduras. Posteriormente, esta técnica ha sido ampliamente utilizada, inmovilizando diferentes tipos de Trxs monocisteínicas recombinantes (Trx f, m, h, o) en columnas de afinidad, haciendo pasar por ellas un extracto proteico y finalmente eluyendo con DTT las dianas unidas a Trx para su identificación por diferentes técnicas [157,244–248]. Cuando se han utilizado las Trx f y m para analizar extractos estromáticos, se ha observado una pérdida de especificidad por sus dianas [244,245].

Además, esta técnica se ha utilizado para la identificación de dianas de Trxs atípicas como CDSP32 [249] y HCF164 [211], y no solo se ha empleado en plantas sino también en cianobacterias [250], algas verdes [232,251] y protozoos [252]. Teniendo en cuenta la gran cantidad de dianas identificadas mediante estas técnicas, a modo de resumen, en la Tabla 1, se recogen las enzimas pertenecientes a las rutas metabólicas más importantes en el cloroplasto identificadas como dianas de Trx f, Trx m y NTRC.

3.3.3 Identificación *in vivo*

En los últimos años se han llevado a cabo estudios genéticos, utilizando mutantes *knockout* o plantas con sobreexpresión de los distintos tipos de Trxs, para identificar sus roles específicos *in vivo* [179,180]. Por un lado, mediante técnicas de genética reversa se han obtenido líneas de Arabidopsis con mutaciones en los diferentes tipos e isoformas de Trxs, tanto cloroplásticas como mitocondriales o citosólicas. Como ejemplo, mutantes *ntrc* permitieron identificar el papel de NTRC en la regulación de la proteína glutamyl-transfer RNA reductasa 1, involucrada en la ruta de biosíntesis de tetrapirroles [253]. El complejo NADH tipo deshidrogenasa (NDH), que interviene en una de las rutas de reducción de PQ que regulan el transporte cíclico de electrones, se identificó como diana de Trx m *in vivo,* gracias al estudio de mutantes de Trx m4 en Arabidopsis y plantas de tabaco con sobreexpresión de su gen ortólogo [254].

Existen numerosos estudios de este tipo, por lo que en la Tabla 1 se recogen las principales proteínas diana de Trxs f, m y NTRC que han sido identificadas *in vivo*.

Tabla 1. Proteínas diana plastidiales y su especificidad por las diferentes isoformas: Trx f, Trx m y NTRC. Las Trxs de la lista provienen de *Arabidopsis thaliana* o de otras especies cuando se añaden las siguientes iniciales: As, Anabaena sp.; Hv, *Hordeum vulgare*; Nt, *Nicotiana tabacum*; Os, *Oryza sativa*; Ps, *Pisum sativum*; Pt, *Populus trichocarpa*; So, *Spinacia oleracea*; Zm, *Zea mays*.

Proteínas	Regulación *in vitro*	Referencias	Regulación *in vivo*	Referencias	Métodos proteómicos[1]	Referencias
Biogénesis del fotosistema II						
Proteína PsbB del fotosistema II (CP47)			Trx m1+m2+m4[2]	[259]		
Transporte cíclico de electrones						
Complejo NADH tipo dehydrogenase (NDH)			**Trx m4, NtTrx m[3]**	[254]		
Complejo de regulación del gradiente de protones (PGR)	Trx m /(f)[4], **Trx m4, NtTrx m**	[254,270]	**NtTrx m**	[254]		
Ciclo de Calvin-Benson						
CP12	**Trx f1/m1/m2**	[277,525]			Trx h3	[238]
Fructosa -1,6-bisfosfatasa (FBPase)	Trx f1/f2, SoTrx f	[177,178,222,228]	Trx f1, Trxf1+f2, NTRC, NTRC+Trx f1, Trx m1+m2+m4	[183,221,223,228,278]		
Gliceraldehído-3-fosfate deshidrogenase (GAPDH)	Trx f1, SoTrx f	[277,526,527]			Trx m/f, Trx h3	[238,244,245]
Fosforibuloquinasa (PRK)	Trx f1/m1/m2, SoTrx f	[277,282,528]	NTRC	[221]	Trx h3, Trx f/m	[238,245]
Rubisco activasa	SoTrx f	[282]	Trx f1, Trx f1+f2	[278]	Trx m/f	[244,245,470]
Sedoheptulosa-1,7-bifosfatasa (SBPase)	Trx f1/f2/m2/m4, SoTrx f	[222,228,529,530]	NTRC, Trx m1+m2+m4	[183,222]	Trx m/f, Trx h3	[238,244,245]
Rubisco (subunidad pequeña -RBCS)					Trx m/f	[244,245,470]
Rubisco (subunidad grande -RBCL)					Trx A, Trx m	[231,287,470]
Triosa-fosfato isomerasa (TPI)					Trx m/f, Trx h3	[238,245]
Transcetolasa					Trx f/m, Trx h3	[238,245,311]
Fosfoglicerato quinasa (PGK)	SoTrx m	[531]			Trx h3	[238]
Fructosa -1,6-bisfosfato aldolasa					Trx h	[470]
Síntesis de ATP						
CF1-ATPasa	So Trx f/(m), NTRC	[266,268,532]	NTRC, Trx m1+m2+m4	[183,221,222,267,268]	Trx h	[470]
Válvula de malato						
NADP-malato deshidrogenasa (NADP-MDH)	Trx f1/f2/m1/m2/m4, SoTrx m/f	[177,222,228,533,534]	Trx m1+2, Trx m1+m2+m4	[183,285]	Trx f/m, Trx h3	[238,245]
Metabolismo del almidón						
ADP-glucosa pirofosforilasa (AGPase)	Trx f1/m1, SoTrx f/m, OsNTRC	[302,303,304]	Trx f1, NTRC, Trx f1+NTRC, SlTrx f	[197,223,304,306,422]	Trx m	[216]
Almidón sintasa 1 (SS1)	Trx f1/m4, NTRC	[308]	SlTrx f	[422]		
α-Amilasa 3 (AMY3)	Trx f1/m1/m2/(m4/m3)	[318]				
β- amilasa 1 (BAM1)	Trx f1/(m1/m2/m4), NTRC	[34,317]			Trx f	[245]
α-Glucano H_2O diquinasa (GWD)	SoTrx f/m	[313]				
Fosfoglucano fosfatasa (DSP4 o SEX4)	Trx f1/m4/m1	[316]				
α 1,4-glucano fosforilasa					Trx m	[311]
Enzima ramificante IIa (SBEIIa)					Trx m	[311]
Brittle-1 (Transportador plastidial de ADPg)					Trx m	[311]
Síntesis de lípidos						
Acetil-CoA carboxilasa (ACCase)	SoTrx f/m	[535]			Trx f/m	[245,311]
Monogalactosil diacilglicerol (MGDG) sintasa	Trx f/m	[467]				

Tabla 1. Proteínas diana plastidiales y su especificidad por las diferentes isoformas: Trx f, Trx m y NTRC (continuación).

Metabolismo de la clorofila						
Magnesio protoporfirin metiltransferasa (CHLM)	NTRC	[253]	NTRC	[253]		
Glutamil-transfer RNA reductasa (GluTR)			NTRC	[253]		
Magnesio quelatasa (CHLI)	NTRC, Trx m2/(f1), PsTrx f, SoTrx f	[199,222,257,258]	NTRC, PsTrx f+m	[199,222,258]	Trx f/m	[245]
Feoforbide a oxigenasa (PAO)	HvTrx f/m	[468]				
Ciclo oxidativo de las pentosas fosfato						
Glucosa 6-fosfato deshidrogenasa (G6PDH)	**Trx f1/m1/m4/(m3), SoTrx m/f, (PtTrx z)**	[534,536,537]			Trx m Trx m/f; Trx h3	[311] [238,244,245,322]
Metabolismo del nitrógeno						
3-deoxi-D-arabinoheptulosonato-7-fosfato sintasa (DAHPS)	SoTrx f	[329]				
Ferredoxina:glutamato sintasa (Fd-GOGAT)	SoTrx m	[181]				
Glutamina sintetasa (GS)			Trx m1+m2+m4	[256]		
Ciclo de las xantofilas						
Zeaxantin epoxidasa (ZE)	NTRC	[268]			Trx m/f Trx h3 Trx m, Trx A	[244,245,311] [238] [244,287]
Detoxificación						
2-Cys peroxirredoxina (2-Cys Prx)	NTRC, OsNTRC, Trx f1/m2/(m1), SoTrx f/m	[177,222,364]	NTRC, Trx f, OsNTRC	[200,201,221,222,280]		
Metionina sulfóxido reductasa B (MSRB)	Trx m1/(f2/m2/m4)	[188]	NtTrx m	[182]		
Peroxirredoxina Q (PrxQ)	Trx f1/f2/m2/m4, NTRC	[222,228]				
Transporte de proteínas						
Translocon precursor NADPH:protoclorofílide oxidoreductasa (PTC52)	HvTrx f/m	[468]				
Proteína 55 del translocon de la membrana interna cloroplástica (TIC55)	HvTrx f/m	[468]				
Proteína 110 del translocon de la membrana interna cloroplástica (TIC110)	PsTrx f/m	[538]				
Transcripción y traducción						
Factor de estabilización del RNA (Nac2-RBP40)	**AsNTRC**	[469]				
Plastid redox insensitive 2 (PRIN2)	TrxF1	[189]				
Proteína de unión a RNA 60kDa (RB60)	Trx m	[539]			Trx f/m	[245]
Proteína ribosomal S30					Trx f/m	[245]
Ribonucleoproteína 28kDa					Trx f/m	[245]
Factor de elongación Tu						
Plegamiento/Ensamblaje de proteínas						
Ciclofilina	SoTrx m	[540]			Trx m, Trx h3	[244,238,311]
Proteína disulfuro isomerasa (PDI)					Trx m, Trx h3	[238,311]
Proteína de unión a Rubisco α y β (CPN60-α y β)					Trx m/f	[216,245]
Proteína de choque térmico 70kDa (Hsp70)					Trx m/f	[245,311]

Tabla 1. Proteínas diana plastidiales y su especificidad por las diferentes isoformas: Trx f, Trx m y NTRC (continuación)**.**

Proteínas	Regulación *in vitro*	Referencias	Regulación *in vivo*	Referencias	Métodos proteómicos[3]	Referencias
Fotosíntesis						
Proteína extrínseca del fotosistema II PsbO1 (OEE 1)					Trx h3, Trx A	[238,287,470]
Proteína extrínseca del fotosistema II PsbO2 (OEE 2)					Trx A	[287,470]
Ferredoxina					Trx h3	[238]
Plastocianina (PC)					Trx h	[470]
Centro de reacción del fotosistema I, subunidad psaK					Trx h	[470]
Centro de reacción del fotosistema I, subunidad psaN					Trx A, Trx h	[287,470]
Proteína de unión a clorofila a/b (LHCIIb)					Trx h	[470]
Equilibrio $HCO3^-/CO_2$						
Anhidrasa carbónica					Trx m/f, Trx h3	[238,245]
Degradación de proteínas						
Clp proteasa-ATP dependiente					Trx m/f	[216,245]
Kinasas						
STN7	Trx f	[345]				

1. Indica qué Trx se ha utilizado a para la caza de proteínas diana mediante métodos proteómicos.
2. Si las funciones *in vivo* de las Trxs han sido documentadas utilizando dobles/triples/cuadruples mutantes, las Trxs se unen añadiendo un "+".
3. Las Trxs con función de desactivación se indican en negrita.
4. Las Trxs que presentan menor eficiencia en en la regulación redox de sus proteínas diana se indican entre parentesis.

4. Regulación redox del metabolismo del carbono y el nitrógeno

Tanto el metabolismo del C como del N presentan una regulación muy compleja en la que intervienen desde factores ambientales, como la luz, hasta procesos específicos de regulación a nivel transcripcional o post-transcripcional. En plantas, las modificaciones post-traduccionales constituyen un elemento de regulación de gran importancia. Concretamente, en los cloroplastos destaca la regulación por oxido-reducción de muchas enzimas involucradas tanto en el metabolismo del C como del N. En este tipo de control, las Trxs desempeñan un papel relevante.

4.1 Papel de las tiorredoxinas en el metabolismo del carbono

4.1.1 Fotosíntesis

Como se ha mencionado anteriormente, estudios sobre la fotosíntesis, especialmente en la regulación de CBC, dieron lugar al descubrimiento de las Trxs en organismos fotosintéticos. Desde entonces las Trxs han sido propuestas como responsables de la regulación, directa o indirecta, de muchos de los mecanismos que afectan a la eficiencia fotosintética en los cloroplastos.

Comenzando con la propia biogénesis de los cloroplastos, se ha observado que las Trxs pueden regular la ruta de los tetrapirroles encargada de sintetizar la clorofila [255]. Existen evidencias de que tanto Trx f y m [256–258] como NTRC [199,253] ejercen una regulación redox en enzimas de esta ruta, como la subunidad CHLI de la magnesio quelatasa o la magnesio-protoporfirin IX metiltransferasa. Por otro lado, se ha sugerido que la Trx m tiene un papel importante en la biogénesis del PSII [259], regulando el ensamblaje de las proteínas CP47 que forman el núcleo. También se ha observado en *Chlamydomonas* que las Trxs están involucradas en la regulación de la traducción de la proteína D1 del PSII gracias a la interacción con una proteína disulfuro isomerasa denominada RB60 [260,261].

Además se ha establecido que un componente de la cadena transportadora de electrones, concretamente la subunidad ɣ de la ATPase, es susceptible de ser rápidamente reducida por la luz y oxidada en oscuridad, regulándose así la producción de ATP en el cloroplasto [262]. Se observó que el sistema Fd/Trx intervenía en esta reducción y que las Trxs podían reducir esta enzima en plantas superiores y así modular su actividad [13,263]. El elemento estructural que permite esta regulación redox es un motivo en la subunidad ɣ con dos Cys que forman un puente disulfuro, pero la interacción entre las subunidades ε y ɣ también resulta importante en este tipo de regulación, porque el puente disulfuro de la subunidad ɣ es protegido frente a la reducción por parte del extremo C terminal de la subunidad ε [264]. Los primeros

experimentos demostraron que tanto la Trx f, como m y la Trx de *E.coli* eran capaces de activar la ATPase en luz [265], pero más adelante se confirmó que Trx f era claramente la más eficiente [266]. Resultados más recientes han aportado evidencias de que NTRC también es un regulador clave de la ATPase, con un papel no redundante en la reducción de la subunidad ɣ en condiciones de baja irradiación [221,267,268]. Hasta la fecha no se conoce la existencia de regulación mediada por Trxs de otros componentes primarios de la cadena transportadora de electrones fotosintética. Sin embargo, el mecanismo que controla la captura y la distribución de la energía de la luz entre los fotosistemas también parece estar regulado por las Trxs. Como se ha comentado anteriormente, la STN7 kinasa es inactivada por las Trxs, evitando la fosforilación de los LHCII de forma que se interrumpen los estados de transición en las plantas que son sometidas a condiciones de alta irradiación [29,269]. Por otro lado, también se ha relacionado a las Trxs, principalmente Trx m y NTRC, con la regulación del transporte cíclico de electrones [254,270,271]. Finalmente se ha visto que Trx m, así como la Trx atípica unida a tilacoide SOQ1 y NTRC, tienen un papel en la fotoprotección mediante la regulación del NPQ [213, 256,268].

En los cloroplastos, la acción mejor caracterizada de las Trxs cloroplásticas es la activación inducida por la luz de las enzimas del CBC. El sistema Trx activa varias enzimas de este ciclo en las transiciones entre luz y oscuridad mediante la reducción de sus Cys redox activas. La FBPase es una de las enzimas clásicas reguladas por la luz. La forma cloroplástica, a diferencia de la citosólica, contiene una inserción en la mitad de su estructura primaria que constituye el sitio activo con las Cys que participan en el mecanismo de regulación mediado por las Trxs [15]. La SBPase también es una enzima regulada por Trxs, específicamente por Trx f. Presenta un motivo CXXXXC con las dos Cys involucradas en su regulación redox, comprobado por mutagénesis dirigida [272]. La gliceraldehído-3-fosfato deshidrogenasa (GAPDH), presenta dos isoformas en cloroplastos de plantas terrestres (GapA y GapB). La isoforma más grande forma un heterotetrámero (A2B2) de forma que puede ser regulado por la Trx f [273] ya que GapB contiene una región C terminal adicional que incluye dos Cys muy conservadas en diferentes especies de plantas. La fosforribuloquinasa (PRK) es otra de las enzimas clásicas regulada por el sistema Fd/Trx y, aunque en un primer momento parecía ser activada por la Trx f [13], más tarde se comprobó que también lo hacía la Trx m [274]. Esta enzima presenta dos Cys en la región N terminal que forman el puente disulfuro susceptible de ser redox regulado [275]. Además PRK agrega en oscuridad formando complejos inactivos de alto peso molecular con GAPDH y CP12 [276]. Estos complejos se disocian cuando los cloroplastos son iluminados y se ha visto que la Trx f preferentemente es capaz de disociar los complejos GAPDH/PRK/CP12 y activar completamente PRK [277]. La especificidad de las diferentes isoformas de Trxs en la regulación de la fijación del C ha sido discutida más recientemente analizando líneas de Arabidopsis con una expresión reducida de una o varias Trxs, lo que permite tener

evidencias *in vivo* del papel que ejercen *in planta*. El doble mutante Trxf1+f2 [228,278] y el triple Trxm1+m2+m4 [183] apoyan las observaciones *in vitro* originales que dicen que tanto las isoformas de Trx f como de Trx m están involucradas en las regulación de las enzimas del CBC. También NTRC parece estar implicada en la regulación del CBC. Así, se ha demostrado que NTRC interacciona con PRK y FBPase en ensayos de complementación bimolecular de fluorescencia y los niveles de activación de estas enzimas son más altos en hojas iluminadas de plantas de Arabidopsis que sobreexpresan NTRC [221]. Por otro lado, la activación redox dependiente de la luz de la FBPase se ve más afectada en el doble mutante ntrc+trxf1 que en el mutante simple de cualquiera de estos genes [223]. Estas observaciones sugieren que NTRC también regula la actividad de estas enzimas del CBC, bien directamente o bien a través de la activación de Trx f. Sin embargo, las conclusiones obtenidas a partir de las plantas *knockout* de Trxs hay que tomarlas con precaución, ya que además del efecto directo de la falta del gen, el estado redox general del cloroplasto puede estar alterado en estos mutantes debido al aumento de estrés oxidativo, generando efectos que no están directamente relacionados con el papel de las Trxs [259,279,280].

La Rubisco también parece estar regulada de manera indirecta por las Trxs mediante la Rubisco activasa. Esta enzima facilita la activación de la Rubisco por eliminación de los azúcares fosfato de su sitio activo [281]. La enzima presenta dos isoformas, de las cuales la más grande contiene dos Cys en la región C terminal que están reguladas por Trx f *in vitro* [282] y posiblemente *in vivo* [278], permitiendo, por tanto, la regulación de la Rubisco en respuesta a la intensidad de luz [283]. Sin embargo, esta isoforma no está presente en algunas especies como tabaco. De la misma manera, se identificó otra proteína susceptible de ser regulada por Trxs que es un inhibidor nocturno de la Rubisco. Se trata de la carboxiarabinitol-1-fosfato fosfatasa, involucrada en la hidrolisis de carboxiarabinitol-1-fosfato, que es activada tanto por Trxs reducidas como por GSH [284].

Más recientemente se han realizado estudios que reflejan la importancia de las Trxs en la regulación de algunas enzimas en condiciones de luz fluctuante. Así, gracias al estudio de mutantes de Arabidopsis, se demostró que la Trx f tiene un papel relevante en la activación en luz de la fijación y acumulación del C en los primeros minutos del día. Mecanismo que permite prevenir la inhibición de la cadena de transporte electrónico cuando se produce un aumento rápido en la intensidad de la luz [278]. En el caso de Trx m, plantas de Arabidopsis deficientes en las dos isoformas más abundantes (Trx m1+m2) mostraron una menor eficiencia fotosintética en los picos de alta intensidad de luz debido a su menor capacidad para activar de forma rápida la enzima NADP-MDH que exporta el poder reductor que está en exceso en el cloroplasto [285]. Por lo tanto, la activación redox de enzimas mediada por las Trxs f y m en Arabidopsis juega un papel crucial en la sincronización de la activación de las enzimas estromáticas con la tasa de transporte electrónico para regular de manera

dinámica la eficiencia fotosintética en condiciones de luz fluctuante. Pero no solo esto, sino que hace unos meses se ha evidenciado la oxidación de proteínas del CBC en oscuridad, como la FBPase, mediante un mecanismo en el que participan las Trxs junto con la 2-Cys Prx. Por lo que también en oscuridad las Trxs podrían intervenir en la regulación de enzimas en el cloroplasto [286].

Por último cabe destacar que, aunque no se han identificado Trxs solubles en el lumen, sí se han identificado varias proteínas con localización lumenal como posibles dianas de las Trxs estromáticas [287]. De hecho, más del 40% de las proteínas localizadas en el lumen pueden formar puentes disulfuro, por lo que la actividad de muchas de ellas podría estar redox regulada [288]. Cada vez existen más evidencias que apuntan a que el poder reductor se transfiere desde el estroma hacia el lumen a través de la membrana tilacoidal [212,289,290]. Se ha propuesto un mecanismo en el que intervienen además de la Trx m, la proteína transmembrana CcdA y la Trx atípica anclada a la cara lumenal de la membrana tilacoidal HCF164 [211,212] funcionando como un transmisor de poder reductor del estroma al lumen. Se ha visto que HCF164 es capaz de reducir los puentes disulfuro de la subunidad N del PSI y también se han identificado al Cyt f y la proteína PetC (componentes del Cytb_6f) como sus posibles dianas [211]. También se ha relacionado a NTRC con este sistema, ya que se especuló sobre si la transferencia de poder reductor a las proteínas del lumen podría estar restringido a los periodos de oscuridad [287], donde este sistema transtilacoidal sería iniciado desde el estroma por acción de NTRC.

Otra Trx atípica identificada en la membrana del tilacoide, SOQ1, parece encargada de preservar la eficiencia en la captación de luz en condiciones de alta irradiación así como de mantener a las proteínas diana en un estado reducido en el ambiente oxidante del lumen [213,291]. Hasta la fecha se desconoce si SOQ1 recibe el poder reductor de la CcdA o directamente de las Trxs estromáticas. Más tarde se identificó otra Trx atípica anclada a la membrana tilacoidal, LTO1, que parece interactuar con la subunidad PsbO del PSII, siendo responsable de su correcto plegamiento y su unión estable al PSII [214]. Otras posibles dianas de LTO1 en el lumen son HCF164 y la violaxantina de-epoxidasa [292]. Finalmente, otra proteína localizada en el lumen del cloroplasto, perteneciente al grupo de las inmunofilinas y denominada FKBP13 en Arabidopsis, contiene un par único de puentes disulfuro que son susceptibles de ser reducidos por Trx m y la Trx de *E. coli* [293], haciendo que la enzima pierda su actividad peptidil-prolil isomerasa. Se ha propuesto que esta enzima, sintetizada en el citosol, es reducida por las Trxs a su paso por el estroma, inactivándose, y cuando llega al lumen se activa por oxidación donde interviene en la formación del complejo Cytb_6f [293,294]. La regulación redox de la actividad peptidil-prolil isomerasa de otras inmunofilinas en el lumen parece tener un papel importante en el ensamblaje y funcionamiento de los fotosistemas, pero su regulación por Trxs no está del todo confirmada [295–297].

4.1.2 Metabolismo del almidón

Algunas de las enzimas directamente implicadas en el metabolismo del almidón están reguladas por cambios en su estado redox (Figura 4), permitiendo así ajustar el metabolismo del almidón al estado fisiológico de la planta y a las variaciones del entorno [40, 48,77].

Hace décadas se propuso concretamente que los cambios producidos por la luz en los grupos sulfidrilo de la enzima AGPase de Arabidopsis estaban involucrados en su regulación [298]. La AGPase es una enzima heterotetramérica que contiene dos subunidades grandes y dos subunidades pequeñas [299,300]. La regulación redox de esta enzima está mediada por la formación de un puente disulfuro intermolecular entre las dos subunidades pequeñas. En estado reducido, AGPase se activa y aumenta su afinidad por el sustrato [301]. Estudios *in vitro* demuestran que tanto Trx f como m son igualmente eficientes en la reducción de AGPase en tubérculos de patata [302] y en cloroplastos de espinaca [303]. Sin embargo, parece que solo Trx f tiene un papel importante en su regulación redox *in vivo*, ya que tanto el estado de activación de la AGPase como la acumulación de almidón se vieron reducidos en mutantes deficientes en la Trx f1 de Arabidopsis [223,304]. Si bien, la sobreexpresión de Trx f desde el genoma plastidial de tabaco no alteró la activación redox de esta enzima [305] a pesar de la elevada acumulación de almidón alcanzada. Por otro lado, NTRC también parece ser un reductor eficiente de AGPase tanto en cloroplastos como en amiloplastos, por lo que se le atribuye un papel coordinador entre la síntesis de sacarosa en hojas y su almacenamiento en forma de almidón en tejidos no fotosintéticos [197, 223,306]. Más recientemente, también se ha observado que la Trx atípica ACHT4 es capaz de desactivar la AGPase por oxidación de las Cys de la subunidad pequeña en condiciones de baja iluminación [279].

Por otro lado, se dispone de poca información relativa a la regulación de otras enzimas involucradas en la síntesis de almidón. Un estudio en Arabidopsis sugiere que SS1, SS3, BE2 y el complejo ISA1/ISA2 podrían estar sujetas a regulación redox [307]. Pero solo se ha demostrado mediante ensayos bioquímicos que la SS1 puede ser activada *in vitro* por Trx f1, Trx m4 y NTRC, identificando también las Cys que intervienen en la formación del puente disulfuro [308]. Además, la sobreexpresión de Trx f de maíz y soja en Arabidopsis dio lugar a plantas con una mayor acumulación de almidón y un aumento en la expresión y actividad de las diferentes isoformas de SS y GBSS [309,310], indicando una posible regulación *in vivo* de estas enzimas por parte de la Trx f. Estudios proteómicos realizados a partir de endospermo de trigo ya identificaban a BE2 como posible diana de Trxs [311]. Estos autores también apuntan al transportador de ADPG, Brittle-1 y a PHS como posibles dianas de Trxs en amiloplastos. En el caso de Brittel-1, estudios fisiológicos posteriores han confirmado esta regulación redox [312].

Asimismo, se ha demostrado la regulación redox de enzimas involucradas en la degradación del almidón. Se ha visto que la Trx f es capaz de activar la GWD *in vitro* en tubérculos de patata de forma más eficiente que Trx m [313] reduciendo un puente disulfuro intramolecular. Así, el estado redox de GWD afectaría a su unión reversible a los gránulos de almidón, de forma que en oscuridad la enzima estaría oxidada e inactiva unida a los gánulos, pero en presencia de luz la enzima se reduciría solubilizándose y volviendo a su estado activo. Esto sería contradictorio con su papel en la degradación de almidón durante la noche, ya que no estaría activa. Además, se ha observado que esta función no sería esencial *in vivo*, ya que la sobreexpresión de una GWD permanentemente activa no dio lugar a cambios en la degradación del almidón es estas plantas [314]. Tampoco la sobreexpresión o la reducción de los niveles de esta proteína en Arabidopsis dieron lugar a cambios importantes en la degradación durante la noche. Si bien, sí se observaron cambios en la síntesis de almidón durante el día [314].

De la misma manera se identificó la regulación redox medida por Trxs de la enzima SEX4 [315,316], que se activa *in vitro* por acción de las Trxs cloroplásticas, principalmente por Trx f. Otra enzima que participa en el proceso de degradación, BAM, se identificó como posible diana de Trxs mediante un estudio proteómico [245]. Entre las diferentes BAMs, solo BAM1 se ha relacionado con una regulación redox por parte de las Trxs *in vitro* [34,317], siendo Trx f el reductor más eficiente. En el caso de BAM3 no hay evidencias experimentales de su posible regulación redox, pero [307] se postuló, a partir de estudios *in vitro* [307], que BAM3 podría estar también sometida a regulación redox en Arabidopsis. En este mismo estudio se observó que AMY3 cloroplástica era sensible a los cambios redox y se activaba por reducción. Más tarde se identificaron las Cys involucradas en la formación del puente disulfuro y se comprobó que esta isoforma podía ser reactivada *in vitro* por Trxs, más eficientemente por Trx f [318]. Por tanto, BAM1 y AMY3 deberían ser activas durante el día cuando el sistema de reducción de las Trxs está activo, sin embargo, la removilización del almidón transitorio ocurre principalmente durante la noche. Esto ha llevado a sugerir que podrían estar involucradas en el proceso de degradación de almidón durante el día en respuesta al estrés [37]. Otra posible explicación sería que NTRC fuera la responsable de su activación por la noche. De hecho, se ha visto que BAM1 puede ser reactivada por NTRC *in vitro* [34], aunque menos eficientemente que por Trx f, por lo que sería interesante hacer esta comprobación para AMY3.

Finalmente, las enzimas desramificadoras ISA3 y LDA parecen mostrar sensibilidad a los cambios en las condiciones redox [307,319,320], pero en ningún caso se ha descrito una activación específica por Trxs.

4.2 Papel de las tiorredoxinas en el metabolismo del nitrógeno

Mientras que la función de las Trxs en la regulación de la fijación de CO_2 y el almacenamiento de carbohidratos en cloroplastos ha sido ampliamente estudiado y está más asentado, su papel en la asimilación del nitrato y posterior conversión a aminoácidos resulta más controvertido. Sin embargo, sí existen algunas evidencias al respecto.

En los primeros pasos de la ruta de asimilación del N participa la enzima NiR (Figura 5), que cataliza la reducción del nitrito a amonio utilizando a la Fd reducida como fuente de electrones [321]. Aunque esta enzima presenta una regulación redox, las Trxs no parecen estar involucradas. Por otro lado, existen evidencias *in vitro* de que las dos enzimas responsables de la asimilación del amonio en el cloroplasto, GS2 y Fd-GOGAT, pueden estar reguladas por Trxs. En cuanto a GS2, en un inicio se vio que podía ser activada eficientemente por las Trxs en algas verdes [322–324] y cianobacterias [325]. Más adelante se demostró en plantas que el DTT podía activar la forma cloroplástica en *Canavalia lineata* y que la mutación de dos Cys, no presentes en la isoforma citosólica, evitaba esa activación [326]. Se demostró que estas Cys se encuentran muy conservadas en plantas (angiospermas) y que la actividad de GS2 aumenta considerablemente al pasar las plantas de condiciones de oscuridad a luz [327]. Otra evidencia de su posible regulación redox es que esta proteína se ha identificado como posible diana de Trx utilizando columnas de afinidad con diferentes Trxs, tanto en extractos de espinaca como Arabidopsis [238,244,245].

Por otro lado, se ha visto que la Fd-GOGAT aislada de cloroplastos de espinaca y soja puede ser activada por DTT o Trxs, pero no por GSH. Entre las Trxs ensayadas parece que Trx m la reduce más eficientemente que Trx f, aumentando su afinidad por el 2OG [181]. Esta enzima utiliza la Fd directamente como substrato pero también indirectamente como regulador, por lo que su regulación se encuentra asociada al estado de iluminación del plastidio.

Por lo tanto, parece que la relevancia de estos indicios necesita una confirmación *in vivo*. De hecho, sí existe una evidencia *in planta* de la activación por reducción del ciclo GS/GOGAT producida por la presencia de DTT en hojas de Arabidopsis [328].

Además de estas dos enzimas involucradas en la asimilación del N, se han propuesto como posibles dianas de Trxs otras enzimas que intervienen en la biosíntesis de aminoácidos. Entre ellas está la deoxy-D-arabino-heptulosonato 7-fosfato, que es la primera enzima de la ruta del shikimato, que da lugar a la síntesis de corismato, el precursor de los aminoácidos ramificados fenilalanina, triptófano y tirosina además de varios metabolitos secundarios (Figura 5). La actividad de esta enzima parece estar redox regulada [329], siendo la Trx f el reductor más eficiente. También se sugirió que la enzima fenilalanina amonio-liasa, que convierte la fenilalanina en ácido transcinámico y amonio iniciando la ruta de los fenilpropanoides, podría tener

una regulación dependiente de Trxs [330]. Por otro lado, la enzima fosfoglicerato deshidrogenasa, que cataliza el primer paso de la biosíntesis de serina en cloroplastos por la ruta fosforilativa, fue identificada como posible diana de Trx m en un ensayo proteómico de captura de dianas *in vitro* [245]. Un estudio en amiloplastos apunta a otras siete enzimas involucradas en la síntesis de aminoácidos como posibles dianas de Trxs [216]: la acetilornitina aminotransferasa, ornitina carbamoiltransferasa y argininosuccinato liasa, implicadas en la síntesis de arginina; la dihidroxi ácido deshidratasa en la biosíntesis de valina e isoleucina; la imidazol glicerol fosfato sintasa involucrada en la síntesis de histidina; y la subunidad β de la triptófano sintasa que participa en la síntesis de triptófano.

.

OBJETIVOS

OBJETIVOS

El objetivo principal de esta tesis es ahondar en el estudio del papel de las Trxs plastidiales en el metabollismo del cloroplasto, y más concretamente, en el metabolismo del carbono y del nitrógeno. Para ello, se plantean los siguientes objetivos específicos:

1. Estudiar el posible papel de las Trxs plastidiales f y m en la fosforilación de los complejos antenna del PSII y su implicación en la actividad fotosintética.

2. Investigar el modo de acción de las Trx f y NTRC en la regulación de los mecanismos de síntesis y degradación de almidón en hojas de tabaco.

3. Analizar la regulación del metabolismo del nitrógeno ejercida por la Trx m en cloroplastos de tabaco y su interacción con el metabolismo del carbono.

4. Caracterizar el interactoma de las Trxs plastidiales f, m y NTRC mediante una nueva estrategia *in vivo* con el objeto de ganar especificidad en la identificación de las proteínas diana entre los diferentes tipos de Trxs.

CAPÍTULO I

Thioredoxin m overexpression in tobacco chloroplasts inhibits the protein kinase STN7 and alters photosynthetic performance

Este capítulo ha sido publicado como**:** Ancín, M.; Fernández-San Millán, A.; Larraya, L.; Morales, F.; Veramendi, J.; Aranjuelo, I. and Farran, I. 2018. *Thioredoxin m overexpression in tobacco chloroplasts inhibits the protein kinase STN7 and alters photosynthetic performance*. J. Exp. Botany., doi: 10.1093/jxb/ery415. (Accepted manuscript).

1.1 Introduction

The gathering of light energy and its later transformation into chemical energy is a central process for the proper functioning of photosynthetic machinery and plant performance. In photosynthetic organisms, light energy is captured by a set of light-harvesting complexes (LHC) that constitute, together with their associated reaction centers and electron donors/acceptors, the PSI and PSII photosystems. Both photosystems are connected in series by a cytochrome (Cyt) b_6f complex. This connection allows the transport of electrons generated from the splitting of water in PSII towards the final electron acceptor of PSI, ferredoxin (Fd), all of which comprise the photosynthetic electron transport chain. Likewise, Fd provides electrons to key enzymes of the Calvin-Benson cycle (CBC) for CO_2 fixation via the Fd-thioredoxin (Trx) system, which carefully coordinates the light and carbon reactions of photosynthesis [15]. As part of this system, chloroplast Trxs catalyze the reduction of disulfide bonds in target proteins, modulating their structure and function and providing flexibility to plants for photosynthetic acclimation to changing environmental conditions [180,331]. Recent reports highlight that while the two main chloroplast Trxs (m and f) are involved in CBC reduction *in vivo* [183,278], Trx m seems to be more specifically engaged in the control of processes balancing photosynthetic reactions [182, 254, 256, 259,285].

Photosynthetic performance is highly regulated by environmental factors such as temperature, nutrients and especially light. Changes in light quality cause unequal distribution of excitation energy between the two photosystems. It is known that preferential excitation of PSII promotes the activation of a redox-sensitive kinase that allows the phosphorylation of LHCII. The phosphorylated LHCII (pLHCII) migrates from PSII towards PSI and shifts the excitation energy in favor of PSI (the so-called state 2). Conversely, under light conditions favoring PSI excitation, the kinase is deactivated and the pLHCII becomes dephosphorylated and relocated to PSII, thus increasing its cross-section and balancing the energy towards PSII (reversion to state 1). This rebalancing process, called state transitions, has been described as a fast post-translational acclimation mechanism operating in photosynthetic organisms under limiting light intensities [20–22,332]. In vascular plants, LHCII comprises different homo- and heterotrimers of Lhcb1, Lhcb2 and Lhcb3 apoproteins [5]. According to their affinity binding to the PSII core, LHCII trimers can be classified into at least three different types: S (strong), M (moderate) and L (loose) [6]. Both S and M trimers play a minor role in state transitions, whereas the peripherically associated L trimer comprises the mobile fraction of the LHCII pool [5,333,334]. Recent studies in Arabidopsis have demonstrated that S and M trimers still remain associated with PSII upon phosphorylation [333,334], and that phosphorylated L trimers may also serve as an antenna for PSI in most natural light conditions [335], suggesting that association of

pLHCII to PSI in higher plants may also represent a long-term response against changes in light intensity under most natural light conditions.

LHCII phosphorylation is triggered by the redox state of the plastoquinone (PQ) pool through the activation of a thylakoid-associated LHCII kinase [24,336]. Two orthologous LHCII kinases called Stt7 and STN7 have been identified in *Chlamydomonas* and Arabidopsis, respectively [24,337]. These are transmembrane proteins with catalytic domains exposed to the stroma that contain two conserved cysteine (Cys) residues, essential for their activity, located at the N-terminus on the lumenal side [338,339]. The LHCII kinase requires an intact Cytb_6f complex to be active [340–342] and is mainly regulated by the redox state of the PQ pool, with an interaction between plastoquinol and the quinol-oxidation site of the Cytb_6f complex being critical for its activation [25,26]. The interaction of Stt7/STN7 with the Cytb_6f complex occurs by means ofthe Rieske protein (PetC) [338]. Previous studies have shown that maximal Stt7/STN7 activity *in vivo* occurs at low light (LL) intensities, whereas it is drastically inhibited at higher irradiances [28,343]. This inhibition has been reported to be mediated by the redox state of the chloroplast, most likely via the Fd-Trx system [29]. The two well-conserved lumenal Cys residues have been reported to be the obvious target for stromal Trxs [337], although they are located on opposite sides of the thylakoid membrane. If this were the case, a trans-thylakoid redox pathway would be required to make the kinase inactive [20,344]. Recent findings, however, have demonstrated that the disulfide bridge formed by the two conserved lumenal Cys residues is maintained during both activation and deactivation of the kinase [27], indicating that mechanisms others than thiol reduction of these Cys residues should be involved in the regulation of the STN7 deactivation under high light (HL) conditions. Rather, other authors propose the two conserved Cys residues located in the stroma as alternative substrates for Trxs [29,30]. In this case, [29] postulated that the Trx target site of STN7 is hidden in the active kinase, whereas in HL it becomes exposed and thus is made available for Trx inhibition. However, these stromal Cys residues are conserved in land plants but not in unicellular green algae [27,30] and, moreover, seem to not be required for STN7 activity and state transitions [27]. Therefore, the mechanistic basis for explaining the STN7 shut off through the Fd/Trx system is still the subject of debate.

The specificity of chloroplast Trxs in controlling the inactivation of STN7 under HL likewise remains largely unsolved. The first report on this, conducted with an *in vitro* phosphorylation assay of thylakoid membranes, involved both Trx f and m in the inhibition of LHCII phosphorylation, with Trx f being more efficient at low concentrations [29]. Later, a direct physical interaction between STN7 and Trx f was demonstrated *in vitro* [345]. Recently, a plausible STN7 activation has been proposed in Arabidopsis *trxm1m2* mutants as a compensatory mechanism that allows increased photosynthesis during the low-light periods of fluctuating light [285]. Here we have analyzed the specificity of chloroplast Trxs f or m in the redox regulation of STN7 and its impact on

photosynthesis. This analysis was performed in wild-type (Wt) tobacco plants, as well as in lines overexpressing Trx f or m (o/exTrxf and o/exTrxm, respectively) from the plastid genome. Our findings demonstrate that overexpression of Trx m, but not Trx f, was associated with a complete loss of LHCII phosphorylation under LL conditions. In addition, the photosynthetic machinery was severely impaired in o/exTrxm plants. A putative role of Trx m in altering LHCII phosphorylation and its consequences in modifying thylakoid architecture and photosynthetic performance in tobacco plants is discussed.

1.2 Materials and methods

Plant material and experimental conditions

Wt tobacco plants (*Nicotiana tabacum* cv. Petite Havana SR1) and plants overexpressing the mature *Trxf* or *Trxm* sequence from the chloroplast genome under the control of the P*rrnG10*L regulatory sequence [305] were used in this study. Transformed and Wt plants were grown in a phytotron under the following conditions: 16 h light photoperiod, 80 $\mu mol.m^{-2}.s^{-1}$ photosynthetic photon flux density (PPFD) and 28ºC. Samples were taken from young fully-expanded leaves of 7-week-old plants after 16 h light or 8 h dark, if not indicated otherwise. When necessary, plants were adapted to different light regimes: dark (D); low light (LL) at 80 $\mu mol.m^{-2}.s^{-1}$; high light (HL) at 800 $\mu mol.m^{-2}.s^{-1}$ generated by a high-pressure sodium lamp (SON-T Agro 400; Philips, Amsterdam, Netherlands); or far-red light (FR; which preferentially excites PSI) obtained by covering the sodium lamp with a Rosco-27 filter (Rosco Labs, Port Chester, NY).

Tobacco plants overexpressing a redox mutant variant of Trx m (o/exTrxm-mut) were generated. The mutation was produced by site-directed mutagenesis using the following oligonucleotides: forward-5′-CTCCGTGGAGTGGTCCAAGCCGAATG-3′ and reverse-5′-CATTCGGCTTGGACCACTCCACGGAG-3′, which included a double change to replace Cys37 and Cys40 with serine. The Trxm-mut fragment was then generated by PCR as previously described [346] and the resulting cDNA was sequenced to check for the correct introduction of the mutation. The PCR product was finally cloned into the pL3 chloroplast transformation vector under the control of the *rrnG10L* promoter. Plastid transformation, homoplasmy and protein expression verification was performed as previously described [305].

Chlorophyll *a* fluorescence: Fast transient and steady-state measurements

Fast transient chlorophyll (Chl) *a* fluorescence was measured using the portable FluorPen FP 100 (Photon Systems Instruments, Drasov, Czech Republic) in dark

adapted leaves (8 h) to allow the complete oxidation of reaction centers. Chl *a* fluorescence transients were induced by the exposure of plants to high irradiance (3000 $\mu mol.m^{-2}.s^{-1}$), and fluorescence was recorded for 2 seconds. The data are shown as the relative fluorescence at time t (Vt), defined as (Ft−Fo)/(Fm−Fo).

Steady-state Chl *a* fluorescence measurements were carried out with the fluorometer of a Li-Cor 6400XT gas exchange portable photosynthesis system (Li-Cor, Lincoln, Nebraska, USA) at a PPFD of 1200 $\mu mol.m^{-2}.s^{-1}$. The quantum yield of PSII (Φ_{PSII}) was calculated as (Fm′–Fs)/(Fm′ [347]. Photochemical energy quenching (qP or qL) was calculated using either qP = (Fm′–Fs)/(Fm′–Fo′) or qL = (Fm′–Fs)/(Fm′–Fo′) × Fo′/Fs [348]. The fraction of closed (reduced) PSII reaction centers, also known as the excitation pressure, was calculated as either 1–qP or 1–qL.

Gas exchange and photosynthetic electron transport rate determinations

Fully expanded apical leaves were used to measure gas exchange with a Li-Cor 6400XT. The gas exchange response to [CO_2] was measured by changing the [CO_2] entering the leaf chamber with the following steps: 400, 300, 250, 200, 150, 100, 50, 400, 500, 600, 700, 800, 1000, 1200 and 1500 $\mu mol.mol^{-1}$, with 2-3 minutes between each step. The net rate of CO_2 assimilation (A_N), stomatal conductance (g_s), transpiration rate (*E*) and sub-stomatal CO_2 concentration (C_i) were estimated at a PPFD of 1200 $\mu mol.m^{-2}.s^{-1}$ and 400 $\mu mol.mol^{-1}$ [CO_2] using equations [349]. Estimations of the maximum carboxylation velocity of Rubisco (Vc_{max}), the maximum electron transport rate contributing to ribulose 1,5-bisphosphate (RuBP) regeneration (J_{max}) and the triose phosphate utilization rate (TPU) were determined [350].

Simultaneous measurements of Chl *a* fluorescence and CO_2 exchange under non-photorespiratory conditions (2% O_2 in vol.) were performed with the Li-Cor 6400XT by varying light intensity in a stepwise manner (from 2000 to 0 $\mu mol.m^{-2}.s^{-1}$). This procedure allows estimation of the rate of photosynthetic electron transport (ETR) as follows [347]: ETR= 4[(Φ_{PSII}– b)/a]PPFD, with a, b and PPFD being, respectively, the slope, the ordinate axis intercept of the relationship between Φ_{PSII} and Φ_{CO2}, and the incident PPFD [351].

Finally, we calculated the distribution of energy between the two photosystems (f) from ETR= Φ_{PSII} x PPFD x leaf absorptance x f [352], assuming a maximum leaf absorptance of 0.875, based on the constancy of light absorption for the leaf Chl concentrations found in our experiments [353].

Chlorophyll content

Photosynthetic pigments were extracted from leaf disks collected from fully expanded leaves and crushed in 5 ml 80% acetone. After centrifugation, the amount of

Chl *a* and *b* was measured spectrophotometrically and calculated according to Lichtenthaler equations [354].

Detection of thylakoid phosphoproteins and the STN7 amount

Leaf samples (100 mg) were ground in liquid nitrogen and thylakoid membranes were isolated [355]. All of the extraction buffers contained 10 mM NaF (phosphatase inhibitor) to maintain the *in vivo* phosphorylation state. Protein concentration was measured using the RC protein assay (Bio-Rad, Hercules, CA), according to the manufacturer's instructions. Thylakoid extracts (15 µg of protein) were electrophoresed in a 15% polyacrylamide gel containing 6 M urea, and separated proteins were transferred to a PVDF membrane for immunoblotting. Phosphoproteins were immunodetected using a rabbit polyclonal phospho-threonine antibody (Cell Signaling Technology, Danvers, MA), at a dilution of 1:1000, and a peroxidase-conjugated goat anti-rabbit antibody (Sigma-Aldrich, St Louis, MO) at a 1:10,000 dilution. Detection was performed using the ECL Prime western blotting detection reagent (GE Healthcare, Buckinghamshire, UK), according to the manufacturer's instructions. To determine the amount of STN7 in these samples, blots were immunoprobed with a specific STN7 antibody (Agrisera AB, Vännäs, Sweden) at a dilution of 1:2000. Protein bands were detected using the ECL Select western blotting detection reagent (GE Healthcare).

Structure and protein composition of thylakoid membranes

Thylakoid membranes, isolated as described before, were solubilized with 1.5% digitonin, a milder detergent that preserves weak interactions between protein complexes and gives information on protein complexes in the stroma lamellae as well as in grana margins and end membranes [356]. Thylakoid proteins (80 µg) were analyzed by blue-native polyacrylamide gel electrophoresis (BN-PAGE) using 4-16% NativePAGE Novex Bis-Tris gels (Invitrogen, ThermoFisher Scientific) according to the manufacturer's instructions, which enables the resolving of protein complexes of high molecular weight (up to ≥1000 kDa). Thylakoid proteins were then transferred to a PVDF membrane, immunoprobed against Lhcb1 and Lhcb2 antibodies (1:1000 dilution; Agrisera AB) and detected by ECL Prime.

For transmission electron microscopy (TEM) analysis, leaf samples from Wt and o/exTrxm plants were fixed and processed as previously described [346].

Pull-down of His-tagged proteins

Chloroplasts from tobacco plants were isolated [357] and protein-protein interactions were *in situ* stabilized using the cell-permeable DSP crosslinker (ThermoFisher Scientific). Crosslinked chloroplasts were lysed (50mM BisTris, 6N HCl, 50mM NaCl, 10% (w/v) glycerol, 1% digitonin and protease inhibitor cocktail) and His-tagged Trx target complexes were pulled down using Ni-NTA agarose (Qiagen, Hilden,

Germany) as follows: chloroplast lysates were incubated with 200 µl of Ni-NTA resin for 3-4 h at 4ºC. After centrifugation at 600 *g* for 1 min, the supernatant was discarded and the pellet was washed five times with washing buffer (lysis buffer without digitonin). The pulled-down proteins were eluted with 4x Laemmli buffer (0.5 M Tris–HCl pH 6.5, 4% SDS, 20% glycerol and 10% β-mercaptoethanol). Input extracts and pulled-down proteins were analyzed by SDS-PAGE and immunoblotted with specific antibodies: anti-STN7 (Agrisera AB), anti-Trx m and anti-Trx f [346], anti-2-Cys Prx [358] or anti-Lhcb1.

1.3 Results

Overexpression of Trx m, but not f, impedes LHCII phosphorylation by down-regulating STN7 activity

The phosphorylation status of isolated thylakoids from Wt, o/exTrxf and o/exTrxm plants grown under LL conditions (80 $\mu mol.m^{-2}.s^{-1}$) was monitored by western blot (Figure 1.1A). LHCII phosphorylation, which is predominantly mediated by STN7, was detected in Wt and o/exTrxf plants, whereas it was completely missed in o/exTrxm plants. By contrast, levels of phosphorylated PSII core proteins (regulated by the protein kinase STN8; [359] barely differed among o/exTrxf, o/exTrxm and Wt plants. These results indicate that the overexpression of Trx m in tobacco plants specifically inhibits the phosphorylation status of STN7-specific substrates. Curiously, STN7 was found at even higher levels in o/exTrxm plants than in Wt and o/exTrxf plants (Figure 1.1B), which indicates that the lack of phosphorylation in o/exTrxm plants did not correlate with a decrease in the amount of STN7, but instead may be indicative of a down-regulation of its kinase activity.

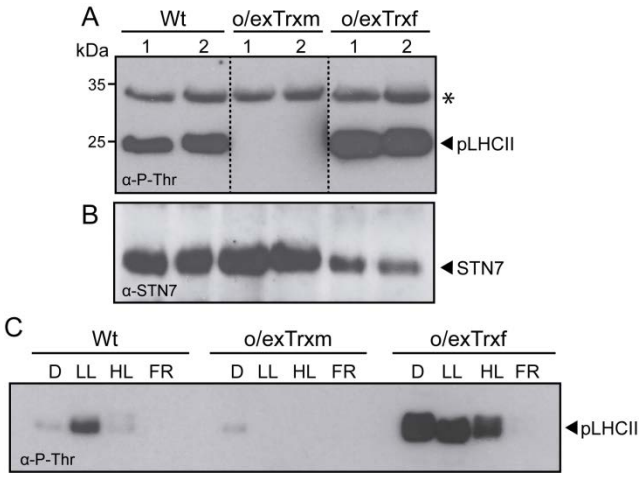

Figure 1.1. **Effect of Trx m or f overexpression in tobacco chloroplasts on thylakoid protein phosphorylation and STN7 accumulation.** A) Thylakoid protein phosphorylation in Wt, o/exTrxm and o/exTrxf plants sampled during the light (16 h at 80 μmol.m^{-2}.s^{-1}) period. Thylakoid proteins (15 μg) were separated by SDS-PAGE (15% + 6M urea), transferred to PVDF membrane and immunoblotted with a phospho-threonine antibody. Phosphorylated LHCII (pLHCII) proteins are indicated. Asterisk represents phosphorylated PSII core proteins (D1 or D2). Molecular weights (kDa) are indicated on the left. B) STN7 protein accumulation in samples described in A. The PVDF membrane was probed with an antibody raised against STN7. C) LHCII phosphorylation pattern under different light regimes. Wt, o/exTrxm and o/exTrxf plants were placed in darkness (D) for 8 h and then transferred for 2 h to low light (LL; 80 μmol.m^{-2}.s^{-1}), followed by exposure to high light (HL; 800 μmol.m^{-2}.s^{-1}) or far red (FR) for 1 h. At the end of light treatments, the LHCII phosphorylation of isolated thylakoids was analyzed by western blot.

To compare the LHCII phosphorylation pattern under different light regimes, Wt, o/exTrxf and o/exTrxm plants were left in darkness for 8 h, and then placed for 2 h in LL, which normally induces state 2. Plants were then exposed to 1 h of either HL or FR conditions to induce state 1. As expected, LHCII phosphorylation in Wt plants was inhibited in darkness and became activated under LL conditions, whereas treatments with HL or FR once more triggered complete dephosphorylation of LHCII (Figure 1.1C). Interestingly, o/exTrxm plants seemed to be arrested in state 1, with LHCII constitutively dephosphorylated. In contrast, o/exTrxf plants retained the LHCII phosphorylation under dark and HL conditions as if they were trapped in state 2 (Figure 1.1C). Subsequently, only a prolonged FR exposure (1 h) allowed the transition from state 2 to 1.

The redox status of the PQ pool is altered in Trx-overexpressing tobacco plants

It is well known that STN7 activation is controlled by reductions in the PQ pool. The fast transient of Chl *a* fluorescence (OJIP; Strasserf *et al.* 1995) has been used to estimate the redox state of the intermediate electron carriers in the transgenic lines. As shown in Figure 1.2A, the shape of the OJIP transient rise was altered in dark-adapted leaves of o/exTrxf and o/exTrxm plants, which exhibited an increase in the J value of about 15 and 60% over Wt plants, respectively. Hence, in both transgenic lines, the area above the J-I curve was smaller than in the Wt (Figure 1.2A). This area is assumed to be a measure for the number of oxidized PQ molecules available at the beginning of the fluorescence measurement [361], suggesting that the fraction of reduced PQ in the dark is increased in both transgenic plants relative to Wt. To corroborate this fact, Wt, o/exTrxf and o/exTrxm leaves were subjected to FR light as a way of removing the electron accumulation in the PSII acceptor side [362]. Leaves were therefore subjected to a 1 min FR pulse followed by 30 sec of dark adaptation to avoid any possible actinic effect induced by the FR pulse. After this treatment, the OJIP transient of dark-adapted Trx-overexpressing leaves almost recovered the Wt shape (Figure 1.2B), which confirms the over-reduction of the PQ pool in both transgenic lines. To investigate the redox state of the PQ pool in light, the fluorescence parameters 1-qL and 1-qP were used. As shown in Figure 1.2C and D, both parameters were significantly increased in o/exTrxm plants, which indicatesthat a more reduced PQ pool also occurs at saturating light conditions and suggests that the PQ pool would be permanently overreduced in this genotype. Therefore, the decreased STN7 activity in o/exTrxm plants under LL does not appear to correlate with an oxidation of the PQ pool.

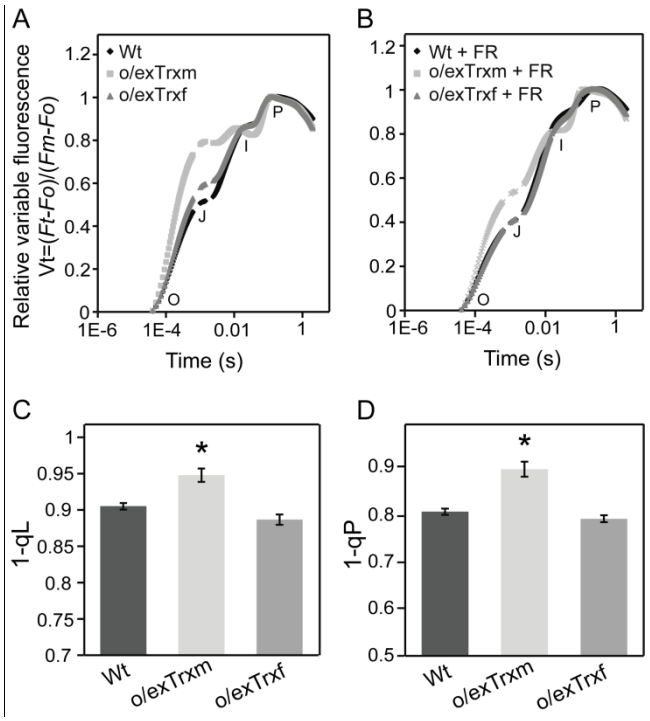

Figure 1.2. Effect of Trx overexpression on Chl *a* fluorescence transients in o/exTrxm, o/exTrxf and Wt tobacco leaves. O, J, I, and P points represent increasing Chl fluorescence values during exposition to short saturating light pulse. A) Normalized Chl *a* fluorescence transients of overnight dark-adapted leaves. B) Normalized Chl *a* fluorescence transients of overnight dark-adapted leaves subjected to 1 min far-red (FR) pulse followed by 30 sec of dark adaptation. C) Redox status of the PQ pool expressed as 1-qL. D) Redox status of the PQ pool expressed as 1-qP. Data shown are mean ± SE (n=6 plants for each line). Statistical significance compared to Wt plants is indicated by asterisks ($P< 0.05$, Student's *t*-test).

Overexpression of Trx m alters the structure and protein composition of thylakoid membranes

To assess the effect of inhibited LHCII phosphorylation on formation of the PSI-LHCII supercomplex during state transitions, BN-PAGE analyses were performed on digitonin-solubilized thylakoid membranes from LL- and dark-adapted Wt, o/exTrxm and o/exTrxf plants (Figure 1.3). The state transition-specific PSI-LHCII supercomplex appeared in Wt thylakoids that were exposed to LL (state 2), whereas it was markedly reduced in Wt thylakoids kept in darkness (state 1) (Figure 1.3A). The BN-PAGE analysis revealed no significant differences between Wt and o/exTrxf under LL conditions, while the PSI-LHCII supercomplex failed to form in o/exTrxm thylakoids (Figure 1.3A). This indicates that the absence of phosphorylation in the o/exTrxm line (Figure 1.1C) impedes migration of LHCII from PSII to PSI, with the concomitant loss of PSI-LHCII supercomplex formation. Conversely, a large portion of the PSI-LHCII

supercomplex persisted in thylakoid membranes from dark-adapted o/exTrxf leaves (Figure 1.3A), which is consistent with the high LHCII phosphorylation level shown by this line in darkness (Figure 1.1C).

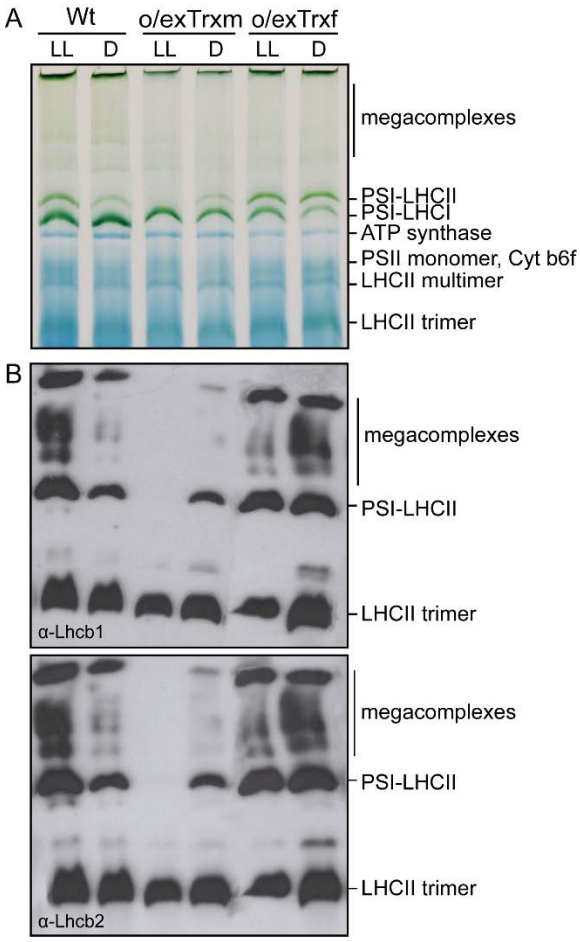

Figure 1.3. Thylakoid protein complex organization and composition. A) Thylakoid protein complexes (80 µg) from Wt, o/exTrxm and o/exTrxf plants were solubilized with 1.5% digitonin and separated by BN-PAGE. Identification of protein complexes was performed in accordance with [339,356]. B) Lhcb1 and 2 protein content in thylakoid complexes. Thylakoid complexes reported above were transferred to PVDF membrane and immunoblotted against Lhcb1 and Lhcb2 antibodies.

The mobile LHCII trimers performing state transitions are mainly composed of Lhcb1 and Lhcb2 proteins [5]. We therefore analyzed the level of these two apoproteins in thylakoid extracts. BN-PAGE combined with immunoblotting showed that in the Wt, Lhcb1 and 2 mainly migrated as LHCII trimers but also as PSI-LHCII complexes and larger megacomplexes under LL, whereas the abundance of these complexes decreased in the dark (Figure 1.3B). The larger digitonin-solubilized megacomplexes mainly represented PSI-LHCII megacomplexes and PSI-PSII complexes migrating together [356]. Trx f-overexpressing plants exposed to LL displayed a similar Lhcb1

and 2 distribution compared to Wt, while the number of state transition-specific complexes considerably increased in thylakoids of o/exTrxf plants kept in the dark. By contrast, Lhcb1 and 2 proteins were not detected at the gel position corresponding to the PSI-LHCII complex nor at the location of the larger megacomplexes in o/exTrxm plants grown under LL (Figure 1.3B). Taken together, our results support the idea that phosphorylation of LHCII proteins strongly influences the formation of such megacomplexes.

The overexpression of Trx m in tobacco plants altered not only the phosphorylation pattern of Lhcb 1 and 2 apoproteins, but also their abundance in chloroplasts. An Lhcb1/2 reduction of about 50% was observed in o/exTrxm compared to Wt and o/exTrxf plants (Figure 1.4). To examine whether changes in the LHCII abundance could influence thylakoid ultrastructure, chloroplasts of Wt and o/exTrxm plants were analyzed by TEM. As shown in Figure 1.5, thylakoids from Wt plants formed a continuous network of stromal lamellae with stacked grana (left panel), whereas thylakoids from o/exTrxm plants were partially unstacked, with stacks exhibiting fewer membrane layers (reduction in grana height) than in the Wt (right panel).

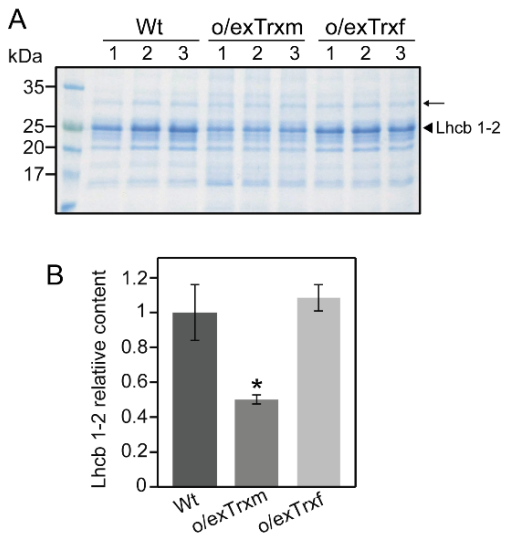

Figure 1.4. Analysis of Lhcb1-2 abundance. A) Thylakoid proteins (30 µg) were separated by SDS-PAGE (13%) and visualized by Coomassie Blue R-250 staining. Identification of protein Lhcb1-2 was performed in accordance with [363]). B) Semiquantitative analysis of the Lhcb1-2 protein amount. Coomassie gel in A was analyzed with GeneTools software. Protein levels in Wt, o/exTrxm and o/exTrxf plants are shown relative to the levels of a constitutively expressed protein (indicated with an arrow). Data are given as means ± SE of three biological replicates. Statistical significance relative to Wt plants are indicated by asterisk (*P*< 0.05, Student's t test).

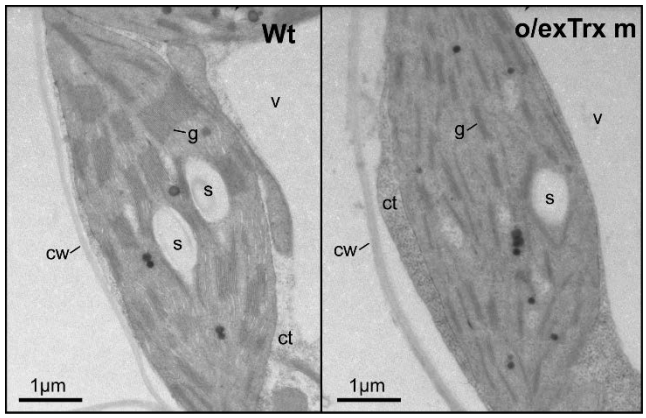

Figure 1.5. **Thylakoid ultrastructure of o/exTrxm plants.** Transmission electron microscopy was performed to examine leaf mesophyll cells from tobacco Wt and Trx m-overexpressing plants. Representative cross-sections of chloroplasts are shown. v, vacuole; ct, cytoplasm; cw, cell wall; g, grana; s, starch.

Overexpression of Trx m negatively affects photosynthesis

Gas exchange analyses conducted in leaves of Wt, o/exTrxm and o/exTrxf plants showed no differences between Wt and o/exTrxf (Table 1.1). On the other hand, while no significant differences were detected on g_s and *E* between the three genotypes, the A_N strongly decreased in o/exTrxm plants. The higher Ci of o/exTrxm may be linked with their lower CO_2 fixation rates. A-Ci curve analyses revealed that depleted photosynthetic rates detected in o/exTrm were associated with the lower values detected on the Vc_{max}, J_{max} and TPU.

Table 1.1. **Photosynthetic parameters of Wt, o/exTrxm and o/exTrxf tobacco plants.** Net photosynthesis (A_N, µmol CO_2 $m^{-2}s^{-1}$), sub-stomatal CO_2 concentration (C_i, µmol CO_2 mol^{-1} air), stomatal conductance (g_s, mol H_2O $m^{-2}s^{-1}$), transpiration (*E*, mmol H_2O $m^{-2}s^{-1}$), maximum carboxylation velocity of Rubisco (Vc_{max}, µmol $m^{-2}s^{-1}$), maximum electron transport rate contributing to RuBP regeneration (J_{max}, µmol $m^{-2}s^{-1}$) and triose phosphate utilization rates (TPU, µmol $m^{-2}s^{-1}$) in 7-week-old wild-type, Trx m-and f-overexpressing plants (Wt, o/exTrxm and o/exTrxf respectively). Values are means ± SE (*n*= 6-9). Different letters denote significantly different values (*P*< 0.05, ANOVA).

	A_N	C_i	g_S	*E*	Vc_{max}	J_{max}	TPU
Wt	11.7±0.5^a	292.0±5.7^b	0.21±0.02^a	2.8±0.5^a	56.6±3.9^a	66.6±1.9^a	3.7±0.1^a
o/exTrxm	7.0±0.3^b	326.9±7.55^a	0.21±0.02^a	3.3±0.3^a	32.3±1.2^b	38.4±1.4^b	2.1± 0.1^b
o/exTrxf	11.0±0.4^a	294.6±9.1^b	0.20±0.02^a	2.9±0.4^a	49.5±2.8^a	61.0±1.7^a	3.3± 0.1^a

Effects of Trx m overexpression on photochemistry were further confirmed by simultaneous measurements of the light response curves of photosynthesis and fluorescence at low O_2, which allows quantification of photosynthetic ETR in the absence of photorespiration. The data revealed lower photosynthetic ETR in o/exTrxm than in the Wt plants (Table 1.2), in line with the above-mentioned decreased J_{max} values. In addition, this approach allows estimation of the light distribution between PSII and PSI (f). These results indicated a lower distribution of light to PSII in o/exTrxm than in the Wt plants (Table 1.2), suggesting changes in the stoichiometry of PSII with respect to PSI in o/exTrxm plants. The Chl *a* and *b* concentrations were also reduced in o/exTrxm compared to Wt and o/exTrxf plants (Table 1.2). Moreover, significant differences in the Chl *a*/*b* ratio were found between lines, the ratio being higher in o/exTrxm plants as a consequence of a more prominent decrease in Chl *b* than in the Chl *a* concentration (Table 1.2). This result can be explained by decreases in antenna size and/or alterations in the stoichiometry of thylakoid pigment-protein complexes of the photosystems. The latter would be in agreement with the described alteration of light distribution between photosystems.

Table 1.2. **Chlorophyll content, energy transport and distribution.** Chl *a* and *b* concentration (µg cm^{-2}), Chl *a/b* ratio, photosynthetic electron transport rate (ETR, µmol $e^- m^{-2}s^{-1}$) and energy distribution between photosystem II to photosystem I (f) in 7-week-old wild-type, Trx m- and f-overexpressing plants (Wt, o/exTrxm and o/exTrxf respectively). Values are means ± SE (n= 6). Different letters denote significantly different values ($P< 0.05$, ANOVA). n.d, not determined.

	Chl *a*	Chl *b*	Chl *a/b*	ETR	f
Wt	27.77±1.38^a	8.73± 0.30^a	3.18± 0.08^b	62.50±1.45^a	0.54± 0.00^a
o/exTrxm	13.67±0.48^b	3.8 ±0.08^b	3.60± 0.12^a	30.67±2.05^b	0.46±0.00^b
o/exTrxf	26.97±1.37^a	8.51±0.67^a	3.17 ± 0.12^b	n.d	n.d

Tobacco plants overexpressing the Trx m redox mutant variant recovered the Wt phenotype

To ascertain whether the STN7 inactivation observed in o/exTrxm plants was triggered by the reductase activity of the overexpressed Trx m, the two Cys residues within its catalytic domain were replaced by serine (C37/40S) to generate the redox mutant. Transplastomic tobacco plants overexpressing this mutant (o/exTrxm-mut) were generated by chloroplast transformation as previously described [305] and integration of the transgene into plastid DNA and homoplasmy was confirmed (Figure 1.6A and B). O/exTrxm-mut plants almost recovered the Wt phenotype, with the expression level of the mutated variant being similar to that of Trx m in o/exTrxm plants

(Figure 1.6C and D). Regarding the LHCII phosphorylation status, pLHCII was detected in LL-adapted o/exTrxm-mut plants at similar levels as in the Wt (Figure 1.7A), which indicates that STN7 conserves its phosphorylation capacity in this line. Accordingly, BN-PAGE analyses of thylakoid protein complexes clearly revealed that o/exTrxm-mut plants also recovered the state transition-specific PSI-LHCII complex under LL conditions (Figure 1.7B). When the fast Chl *a* fluorescence transient was analyzed in leaves of o/exTrxm-mut plants, the OJIP shape shifted towards that of the Wt plants (Figure 1.7C). In agreement with these findings, the A_N and ETR in o/exTrxm-mut plants reached values similar to those of Wt plants (Figure 1.7D). Taken together, our results provide evidence for the recovery of the Wt phenotype when the Trx m redox mutant was overexpressed in tobacco chloroplasts, suggesting that, in o/exTrxm plants, the overexpressed Trx m inhibits STN7 activity and impairs the photosynthetic performance of tobacco plants in a redox-dependent way.

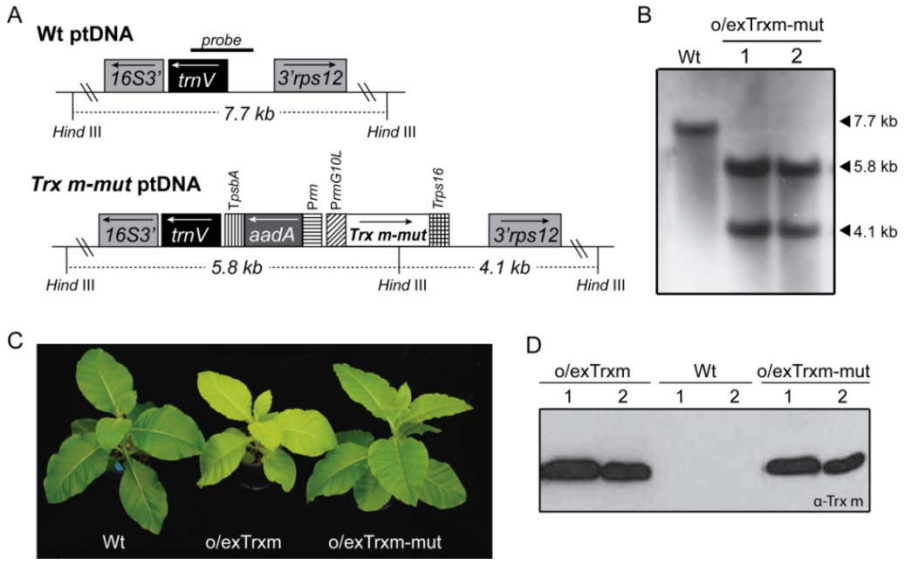

Figure 1.6. **Generation of o/exTrxm-mut transplastomic tobacco plants and analysis of the transgene expression.** A) Map of the Wt and transformed Trxm-mut plastid genomes. The probe for the Southern blot is shown over the corresponding sequence. The sizes of the predicted bands after DNA digestion with *HindIII* are indicated. The arrows in the boxes show the direction of transcription. *16S3', trnV and 3'rps12*: original sequences of the chloroplast genome; *aadA*: aminoglycoside 3'-adenylytransferase gene; P*rrn*: *16S* rRNA promoter and 5'-untranslated region; P*rrnG10L*: *16S* rRNA promoter fused to the leader region of the bacteriophage T7 gene *10*; T*psbA*: terminator region of the *psbA* gene; T*rps16*: terminator region from the chloroplast *rps16 gene.* B) Southern blot analysis. Total DNA (10 μg) of two Trxm-mut plants and a Wt control were digested with HindIII and probed. C) Visual appearance of Wt, o/exTrxm and o/exTrxm-mut plants. Representative photographs are shown. D) Immunoblot analysis of protein extracts from mature leaves of Wt, o/exTrxm and o/exTrxm-mut plants. Ten μg of total protein are loaded per line. Specific anti-Trx m antibody was used.

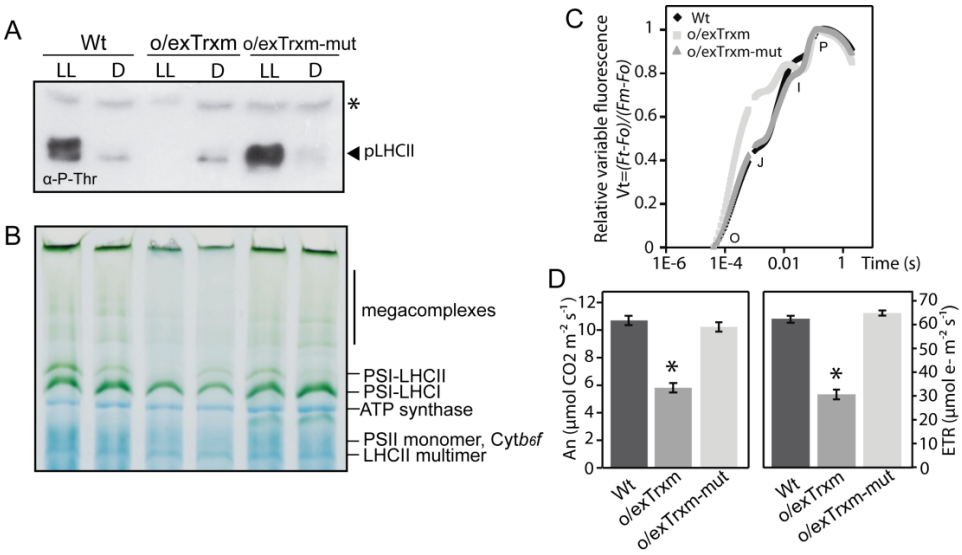

Figure 1.7. Recovery phenotype in tobacco plants overexpressing the redox mutant variant of Trx m. A) LHCII protein phosphorylation in Wt, o/exTrxm and o/exTrxm-mut plants sampled under low light (LL, 80 µmol.m−2.s−1) or dark (D) conditions. Thylakoid proteins (15 µg of protein) were separated by SDS-PAGE (15% + 6M urea), transferred to PVDF membrane and immunoblotted with a phosphothreonine-specific antibody. Asterisk represents phosphorylated photosystem II (PSII) core proteins (D1 or D2). B) Pigment-protein complexes from thylakoids (80 µg) were separated by BN-PAGE. The identity of protein complexes is shown. C) Normalized OJIP transients of overnight dark-adapted leaves. D) Net rate of CO_2 assimilation (A_N) and photosynthetic electron transport rate (ETR).

Putative protein-protein interaction between Trx m and STN7/PetC proteins

To investigate a putative protein-protein interaction between Trx m and STN7 or proteins involved in the kinase activation such as PetC, an *in vivo* pull-down assay using chloroplasts from His-tagged Trx m-overexpressing tobacco plants was performed. Chloroplasts from Wt, o/exTrxf and o/exTrxm-mut were used as controls. The pull-down assay allowed recovery of substantial amounts of overexpressed Trxs, which correlated with the amount present in the respective input extracts (Figure 1.8). Input extracts and pulled-down proteins were analyzed by SDS-PAGE and then immunoblotted with anti-STN7 and anti-PetC (Figure 1.8). The results indicated that STN7 and PetC were barely detected in the pulled-down fraction from Wt, o/exTrxf and o/exTrxm-mut plant extracts, whereas they were enriched in the fraction from o/exTrxm extracts (Figure 1.8). The input and pulled-down fractions from each line were also immunoblotted with anti-2-Cys peroxiredoxin (Prx), a well-known Trx target protein [364], and anti-Lhcb1 (non-target protein) as positive and negative controls, respectively. While no presence of Lhcb1 was found in any pulled-down fraction, 2-Cys

Prx co-precipitated with both the Trx m and f proteins (Figure 1.8). Altogether, these results demonstrate a putative protein-protein interaction, either directly or through associated partners, between Trx m and the STN7/PetC proteins.

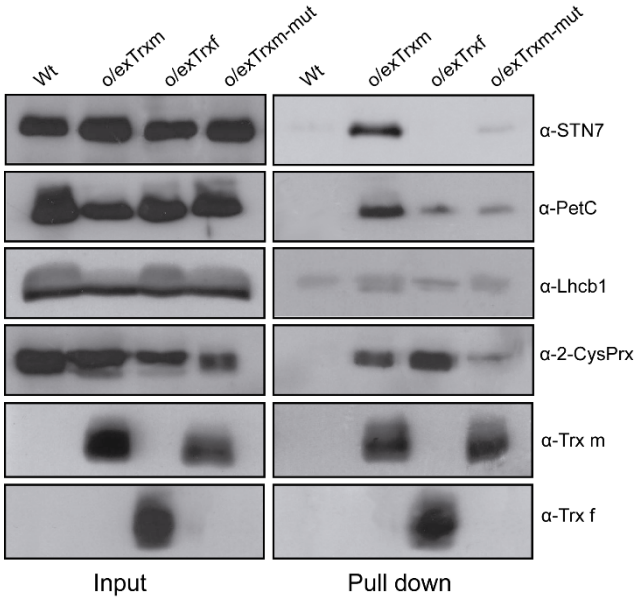

Figure 1.8. ***In vivo*** **pull down assay showing interaction between Trx m and STN7/PetC.** Protein complexes from Wt and His-tagged o/exTrxm, o/exTrxf and o/exTrxm-mut crosslinked-chloroplasts were pulled-down with Ni-NTA resin. After washing the beads, bound proteins were eluted by boiling and analyzed, together with input fractions, by western blot using anti-STN7, anti-PetC, anti-2-Cys Prx, anti-Lhcb1, anti-Trxm and anti Trx f antibodies.

1.4 Discussion

Phosphorylation pattern of LHCII proteins in Trx-overexpressing tobacco plants

Our study highlighted that, under typical inhibitory light conditions (such as HL and darkness [28], the overexpression of Trx f in tobacco chloroplasts is associated with an induction of LHCII phosphorylation (Figure 1.1). In fact, pLHCII levels in the o/exTrxf line were comparable (under HL) or even higher (in the dark) to those induced by LL. Similar results were reported in transgenic Arabidopsis lines overexpressing STN7 [339]. However, in our case, differences in the LHCII phosphorylation pattern between o/exTrxf and Wt plants could not be explained by an increase in the STN7 amount since it was even lower than in Wt (Figure 1.1B). Indeed, regulation of LHCII phosphorylation might be due not only to light conditions but also to the metabolic

status of the chloroplast [365]. In particular, increased LHCII phosphorylation in darkness has been observed in Arabidopsis by feeding leaves with glucose [366]. Previous studies have shown that Trx f overexpression in tobacco chloroplasts increases the soluble sugar content in leaves, and particularly glucose [305]. Therefore, we presume that the STN7 activation observed in o/exTrxf tobacco plants could be due to the metabolic status of the chloroplast. More specifically, the sugar accumulation would favor production of NADPH from the oxidative pentose phosphate pathway leading to a non-photochemical reduction of the PQ pool (Figure 1.2A and B) via NDH [367] and the subsequent STN7 activation. In agreement, an increase in the NADPH/NADP ratio was recorded in this transgenic line (Supplementary material, Figure S1.1). The overreduced PQ pool in o/exTrxf plants is only apparent in OJIP measurement but not in 1-qL and 1-qP (Figure 1.2C and D) probably because the pressure of electron flow at the saturating light conditions employed for these measurements may overcome the PQ pool overreduction in this genotype.

In o/exTrxm plants, however, STN7 seems to be insensitive to the reduction state of the PQ pool (Figure 1.1 and 1.2), and the pattern of LHCII phosphorylation resembles that of *stn7* mutants [339]. Nevertheless, the lack of LHCII phosphorylation in o/exTrxm leaves could not be explained by a downregulation of the STN7 amount, rather, STN7 tends to accumulate at even higher levels than in Wt (Figure 1.1B). It is known that STN7 abundance is regulated at both the transcriptional and post-translational level in a light- and redox-dependent manner [339]. Accordingly, the STN7 accumulation in o/exTrxm plants clearly correlated with a more reduced PQ pool (Figure 1.1 and 1.2). The PQ pool overreduction in o/exTrxm plants may be linked to a decrease in the PSI activity, mainly caused by the lack of state 2 transition (i.e., smaller PSI antenna size) and decreased Fd amount at the PSI acceptor side (Supplementary material, Figure S1.2). An overreduction of transthylakoid redox carriers such as CcdA and HCF164, caused by the Trx m overexpression (discussed below), could likewise cause an unbalanced PQ pool. The STN7 accumulation in o/exTrxm plants was however not accompanied by an increase in the STN7 kinase activity, as reported from several photosynthetic mutant lines with constitutively overreduced PQ pools [339], but instead resulted in a complete STN7 deactivation (Figure 1.1). The increase in STN7 levels in o/exTrxm plants could therefore be a compensatory response to the absence of state transitions. Similar results were reported in Arabidopsis mutants lacking Lhcb1, where STN7 also tends to accumulate in the absence of state transitions [368].

In summary, we demonstrated *in vivo* that the overexpression of Trx m, but not its counterpart f, downregulates the STN7 activity, while earlier reports, based on *in vitro* experiments, involved both f and m in the STN7 inhibition [29,345]. This discrepancy may be explained by the lack of specificity for different target enzymes that Trxs f and m usually revealed when *in vitro* studies were used [180].

How Trx m overexpression induces STN7 inactivation

The current knowledge of Trx-mediated STN7 inactivation under HL supports two working hypotheses: (i) reduced Trx directly breaks the stromal disulfide bridge of STN7 thus interfering with ATP-binding and leading to its inactivation [29,30]; (ii) reduction of the lumenal bridge involves a trans-thylakoid redox pathway for the delivery of reducing equivalents from the stroma to the lumen, with the CcdA and HCF164 proteins [289,290] being the most suitable candidates [20,344]. Recent studies, however, speculate that the reactive oxygen species (ROS) generated in HL conditions might affect kinase folding in the thylakoid membrane, blocking its activity [27]. However, comparable ROS contents were shown in all genotypes (Supplementary material, Figure S1.3), so ROS accumulation cannot account for the deactivation of STN7 in o/exTrxm plants. Within this context, our results would provide support *in vivo* that Trx m serves as the stromal source of reducing power for thiol-dependent regulation of STN7 activity.

It is well known that Stt7/STN7 interacts with the Cytb_6f complex by means of PetC [338], interaction that critically affects the kinase activity [25,26]. Reverse genetic approaches have also unveiled a relevant role for PetC in state transitions and LHCII phosphorylation [339,369]. However, our study showed that the amount of PetC protein in o/exTrxm plants was similar to (or even higher than) the quantity found in Wt plants (Supplementary material, Figure S1.4), indicating that the STN7 deactivation in this line should neither be attributed to PetC downregulation. The movement of the lumenal PetC domain (which typically occurs during electron transfer within the Cytb_6f complex [370]) could be coupled to a transitory dimer formation of the kinase, leading to its activation [27]. The direct interaction between STN7 and PetC raises the possibility that the same redox system operates during regulation of their redox states. In this sense, it is known that the CcdA/HCF164 trans-thylakoid redox pathway is required for Cytb_6f assembly, Trx m likely being the stromal electron donor for this system [211,212,289,290]. Therefore, Trx m overexpression could be causing the overreduction of the STN7 lumenal Cys residues (by means of the CcdA/HCF164 pathway) with the consequent impact on transitory dimer formation, as has been shown after prolonged anaerobic treatment [27]. However, the fact that the overexpressed Trx m specifically associates with STN7 inside the chloroplast (Figure 1.8), along with previous results showing that the mutation of the lumenal STN7 Cys does not affect its interaction with Trx [345], rather support the idea that Trx m exerts changes in the redox state of Cys residues placed in the kinase domain, hampering its activity [30]. Consistent with this, three m-type Trxs (m1, m2 and m4) have been identified in the peripheral fraction of the thylakoid membrane proteome from Arabidopsis chloroplasts, indicating that these isoforms are associated with the stromal side of the thylakoid membrane [371]. Some of the discrepancies with this model [27] could be explained by a dynamically buried/exposed Trx target site in STN7 as originally proposed [29]. With

regard to the pulled-down PetC found in o/exTrxm plants (Figure 1.8), it would better result from isolation of in-chloroplast crosslinked endogenous protein complexes, most probably by means of the CcdA/HCF164 redox pathway, than from a direct interaction with Trx m.

Overexpression of Trx m shows altered protein complex composition and thylakoid architecture, as well as impaired photosynthetic performance in tobacco plants

The overexpression of Trx m in tobacco chloroplasts affected both the protein composition of photosynthetic complexes and the thylakoid structure, and consequently impacted photosynthesis (Figure 1.3, 1.4, 1.5 and Table 1.1). The PSI-LHCII supercomplex (characteristic of state transitions) is formed when a subpopulation of pLHCII migrates from PSII to PSI so as to increase their optical absorption cross-section [356,372–374]. In this study, BN-PAGE fractionation of digitonin-solubilized thylakoid proteins revealed a clear correlation between LHCII phosphorylation and the amount of PSI-LHCII supercomplex and the related larger megacomplexes (Figure 1.1 and 1.3). Thus, state transition-specific complexes were absent in o/exTrxm plants grown under LL conditions, reaffirming that in the absence of phosphorylation no migration of LHCII from PSII to PSI occurs, whereas they were abundant in o/exTrxf plants kept in the dark, for which a strong kinase activity is presumed (discussed above). Curiously, a small amount of PSI-LHCII supercomplex was perceived in both Wt and o/exTrxm plants in the dark (Figure 1.3), in agreement with the residual LHCII phosphorylation level (Figure 1.1C). Low STN7 activity in the dark has previously been reported in Arabidopsis, and was attributed to a stromal electron source triggering PQ pool reduction [339]. Therefore, our results indicate that the overexpressed Trx m must be reduced (using photosynthetic electrons provided by Fd during the day) to efficiently abolish LHCII phosphorylation and this reinforces the importance of Trx m reductase activity in this process.

The overexpression of Trx m in tobacco chloroplasts likewise resulted in partial unstacking of grana (Figure 1.5). Unstacking of thylakoid membranes may be induced by LHCII phosphorylation in the transition from state 1 to 2 [375] or by PSII core phosphorylation under HL stress [376,377]. However, in o/exTrxm plants, partial unstacking occurs in the absence of LHCII phosphorylation (plants blocked in state 1) and with a phosphorylation pattern of PSII core proteins similar to that of Wt (Figure 1.1A). Therefore, other factors such as the amount of LHCII or curvature thylakoid 1 (CURT1) proteins [378] may account for the observed phenotype. Along these lines, our results show a downregulation of Lhcb1-2 in o/exTrxm plants (Figure 1.4), which could explain the observed rearrangement in the thylakoids. Accordingly, a similar thylakoid architecture phenotype has been reported from an Arabidopsis line deficient in Lhcb1 [368]. Likewise, the light distribution difference in favor of PSI seen in

o/exTrxm plants could easily be explained by the smaller PSII antenna size (Lhcb1-2 reduction), which agrees with the higher Chl a/b ratio of these plants (Table 1.2).

The observed diminishment in LHCII proteins in o/exTrxm plants suggests a marked LHCII degradation process in this genotype. According to previous studies [379,380], dephosphorylated LHCII seems to be the preferred substrate for protease enzymes. Thus, the lack of LHCII phosphorylation in o/exTrxm plants suggests that protease enzymes may have degraded these proteins. There are several lines of evidence that FtsH, a metalloprotease essential for the repair of photodamaged D1, is also responsible for degradation of several LHCII apoproteins [381,382]. Interestingly, redox control of the FtsH proteolytic activity has recently been demonstrated in *Chlamydomonas* [383], suggesting that the overexpressed Trx m in tobacco chloroplasts might induce a reactivation of FtsH protease. Similarly, the PQ pool overreduction in o/exTrxm plants could also downregulate the transcription of *cab* genes [384,385], which may also contribute to decreased LHC II level.

Energy required to sustain functioning of the photosynthetic apparatus requires an adjusted and coordinated light energy capture, which then needs to be transported through the photosynthetic electron chain and used in carboxylation. The absence of significant differences in stomatal opening or increases in sub-stomatal CO_2 concentration revealed that the impaired photosynthetic rates in o/exTrxm plants could not have been due to the availability of CO_2 at the Rubisco carboxylation site. Instead, the reduced photosynthesis was due to a lower energetic status that negatively affected the photosynthetic machinery and CO_2 fixation. In fact, our data showed that the depleted ETR of o/exTrxm plants was the main factor explaining the lower V_{Cmax} and J_{max}, which are both energy-demanding processes. O/exTrxm plants showed an impairement not only in the linear photosynthetic ETR, as described in this work, but also the cyclic ETR has been reported as being markedly affected [254]. In green algae, the absence of state transitions could also affect the photosynthetic cyclic electron flow (CEF) [386]. However, it seems that the failure to undergo state transitions does not affect the CEF in the *stn7* mutant [373], implying that state transitions and CEF act independently in land plants. Rather, the absence of CEF in o/exTrxm plants could be related to the reduced thylakoid stacking observed in this line, as has recently been proposed [387,388]. Overall, our results highlight the fact that the inhibited photosynthetic performance of o/exTrxm plants could be a consequence of depleted phosphorylated LHCII protein, which negatively affects the energetic status, photosynthetic machinery and CO_2 fixation in those plants. However, previous studies conducted with SNT7 mutants demonstrated that state transitions do not become critical for plant performance [24,389], suggesting that factors other than STN7 deactivation should account for the observed o/exTrxm phenotype. In this sense, the overexpressed Trx m could be affecting the redox regulation of relevant chloroplast

metabolic pathways such as the carbon and nitrogen metabolism, influencing thereby the photosynthetic performance of this genotype.

1.5 Supplementary material

1.5.1 Supplementary methods

Pyridine nucleotide determination. NADP and NADPH were measured as described in [390], using phenazine methosulfate that catalyzed the reduction of dichlorophenolindophenol in the presence of glucose 6-phosphate and glucose 6-phosphate dehydrogenase.

***In situ* detection of ROS.** Detection was carried out according to [391] with some modifications. For hydrogen peroxide detection 3,3′-diaminobenzidine (DAB) was used: detached leaves were vacuum-infiltrated with 1mg/ml DAB water solution, pH 3.8, for 2 min and incubated in the same solution under growth light for 90 min. *In situ* histochemical staining for superoxide detection was performed using nitroblue tetrazolium chloride (NBT): detached leaves were vacuum-infiltrated with 10mM potassium phosphate buffer pH 7.8 containing 10mM NaN_3 for 2 min and incubated in 0.1% NBT for 90 min under growth light. In both cases, pigments were removed by boiling 5 min in acetic acid-glycerol-ethanol (1/1/3) and leaves were immediately photographed. The quantification of the histochemical staining intensity was performed with Adobe Photoshop CS software.

Immunoblot analysis. Leaves of Wt, o/exTrxm and o/exTrxf plants were ground in liquid nitrogen and used to extract total protein in Laemmli buffer. Protein quantification was performed using the RC-DC protein assay (Bio-Rad, Hercules, CA) with bovine serum albumin as a standard, according to the manufacturer's instructions. Proteins were separated using SDS-PAGE, electro-transferred onto PVDF membranes (Hybond C, GE Healthcare, Fairfield, CT) and probed with anti-Fd and anti-PetC antibodies (Agrisera AB, Vännäs, Sweden). A peroxidase-conjugated goat anti-rabbit antibody (1:10,000; Sigma-Aldrich, St Louis, MO) was used as secondary antibody. Detection was performed using the ECL Prime detection system (GE Healthcare, Buckinghamshire, UK).

1.5.2 Supplementary figures

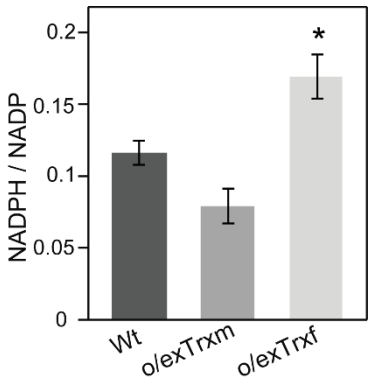

Figure S1.1. Pyridine nucleotide NADPH/NADP ratio in leaves. Leaves from Wt, o/exTrxm and o/exTrxf plants were harvested after 4 hours illumination and pyridine nucleotides measured. Values are mean ± SE of measurements of 5 biological replicates. Statistical significance compared to Wt plants is indicated by asterisks (*P*< 0.05, Student's t-test).

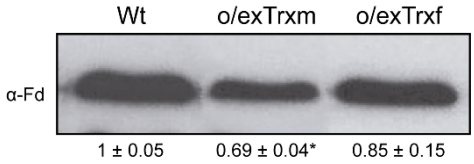

Figure S1.2. Abundance of Fd, the main electron acceptor from PSI. The Fd protein content in Wt, o/exTrxm and o/exTrxf plants was determined by western blot. 50 µg of total protein were separated by SDS-PAGE (18%). Immunoblotting was performed using specific Fd antibody at a dilution of 1:1000. Numbers below the blot show signal strength in the Trx lines relative to Wt ± standard error obtained from analysis of protein extracts of three plants in three biological replicates. Statistical significance compared to Wt plants is indicated by asterisks (*P*< 0.05, Student's t-test).

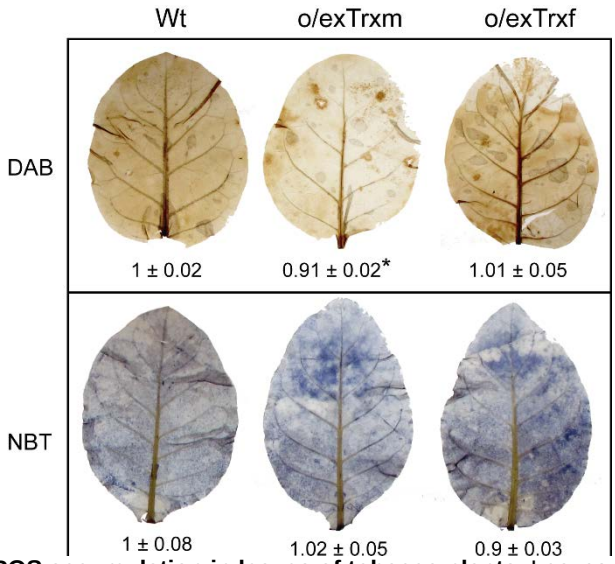

Figure S1.3. **ROS accumulation in leaves of tobacco plants.** Leaves from 4-week-old Wt, o/exTrxm and o/exTrxf plants grown under 16 h light/8 h dark photoperiod were harvested after 7 h of illumination. The upper panel shows 3,3′-diaminobenzidine (DAB) *in situ* histochemical staining for hydrogen peroxide production. The lower panel illustrates nitroblue tetrazolium chloride (NBT) *in situ* histochemical staining for superoxide detection. The experiment was conducted three times with similar results. For each treatment, a representative infiltrated leaf is shown. Numbers under pictures indicate quantitative measurements as mean ± SE of 6 biological replicates. Statistical significance compared to Wt plants is indicated by asterisks (P< 0.05, Student's t-test).

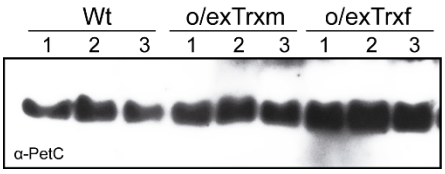

Figure S1.4. Abundance of PetC protein. Western blot analysis was performed to determine the amount of PetC protein in Wt, o/exTrxm and o/exTrxf plants. Similar amounts of protein were loaded for each line, separated on 15% SDS-PAGE containing 6 M urea, transferred to a PVDF membrane and immunoblotted against a PetC antibody at a dilution of 1:5000.

.

CAPÍTULO II

NTRC and thioredoxin f overexpression differentially induces starch accumulation in tobacco leaves.

2.1 Introduction

Post-translational redox modifications play a major role in different cell processes. Thioredoxins (Trxs) are among the protagonists in this regulatory mechanism [135]. Trxs modulate target protein activities via a thiol-disulfide exchange mechanism involving the two redox-active cysteines (Cys) of the canonical WC(G/P)PC active site [392]. In plants, the Trx system is particularly complex, with a great number of Trx isoforms [393] and more than 400 potential Trx targets [226]. The first experimental evidence of redox regulation and signalling was reported years ago in plant chloroplasts [13]. In illuminated chloroplasts, ferredoxin (Fd) and Fd-Trx reductase (FTR) are responsible for feeding the electrons generated in the photosynthetic electron transport chain into the regulatory Trx system. In the dark, or in non-photosynthetic plastids, the NADPH generated from the oxidative pentose phosphate pathway (OPPP) is the source of reducing power for Fd reduction via Fd–NADPH reductase (FNR) [311]. Plastid Trxs act as transmitters of the redox signal by transferring electrons from Fd to downstream target enzymes. Five types of classical Trxs (MW about 10–12 kDa) have been reported for plastids (Trx f, m, x, y, z) [169,185], as well as four “Trx-like” proteins with non-canonical active sites, and two “atypical Trxs”, in which the Trx motifs are associated with other domains [142].

C-type NADPH-dependent Trx reductase (NTRC), which was first identified in rice [191], has been classified as an atypical Trx [142] but also as a Trx reductase [124]. Its Trx domain is an extension (at the C-terminus) of the NADPH-Trx reductase (NTR) domain. NTRC is found only in photosynthetic organisms such as plants, algae and certain cyanobacteria [191,394], both in chloroplasts and non-green plastids [192]. It has been described as a bifunctional enzyme that reduces target proteins using NADPH as an electron donor [193,194,200]. The homodimer of NTRC is reported to be catalytically active [220]. Electrons donated by NADPH are transferred from the NTR domain of one subunit to the Trx domain of the other [220]. The discovery of NTRC thus unveiled the existence of a redox regulatory system in chloroplasts, other than that provided by Fd/Trx, which operates during both light and dark periods using the NADPH generated from photosynthesis and OPPP, respectively. Some authors suggest that NTRC becomes a key reducing system during the night, when the level of reduced Fd is low [358,394].

Starch is the most abundant storage carbohydrate in plants, which is composed of amylose and amylopectin. Transitory starch is considered as a carbohydrate reservoir, which buffers the diurnal changes in the supply of photoassimilates. ADP-glucose pyrophosphorylase (AGPase), which catalyzes the first committed step of starch synthesis in higher plants, is considered a key enzyme in this process, controlling the flux from carbon to starch [395]. Additionally, an alternative model considering the transport of ADP-glucose (generated in the cytosol through the sucrose synthase

activity) into the chloroplast has also been proposed [32,41,42]. Three major enzymes act simultaneously in starch synthesis: starch synthases (SSs), branching enzymes (BEs) and debranching enzymes (DBEs). Soluble SSs are believed to be primarily responsible for amylopectin synthesis, catalyzing the formation of a polymer of α-1,4-glycosidic bonds using ADP-glucose. BEs create branches from existing chains via glucanotransferase reactions, and DBEs (ISA1 and ISA2) hydrolyze some of the branches again during the synthesis of amylopectin [396]. About starch degradation, starch granule surface solubilization is required in order to provide hydrolases access to the glucan chains. This process is dependent on the reversible phosphorylation and dephosphorylation of glucans, which are completed by glucan, water dikinases (GWDs), phosphoglucan phosphatases (PWDs) and a glucan-binding phosphatase (DSP4) [38]. Complete degradation of starch is achieved by endo-acting α-amylases (AMYs) and exo-acting β-amylases (BAMs) enzymes, but also DBEs (ISA3 and LDA) are required to hydrolyze the branch points [38].

Starch metabolism is extraordinarily well-tuned by the presence of very sophisticated regulatory mechanisms. Post-translational modifications, including redox regulation, are considered the main way by which the activity of enzymes involved in transient starch metabolism are regulated [48,397]. In higher plants, AGPase was described as a heterotetramer consisting of two large (AGPS) and two small (AGPB) subunits. *In vitro* experiments demonstrated that Trxs mediate its activation by the reduction of a disulfide bridge between the two small subunits [302,398]. The *in vivo* relevance of these findings was verified in Arabidopsis *trxf* and/or *ntrc* mutants, which showed a decreased starch accumulation and redox activation of AGPase [197, 202, 223, 278,304]. From these works, it is proposed that Trx f is a key enzyme involved in light-dependent activation of AGPase, while NTRC has been identified as AGPase regulator in the dark or in response to sugars. However, the impact of the redox regulation of AGPase *in vivo* and its role in starch synthesis have fallen under discussion [32,399–401]. Other starch biosynthetic enzymes has been reported to be susceptible to reducing agents, such as ISA1/ISA2, SS1 and SS3 [307]. However, only SS1 has been well confirmed as a redox-regulated enzyme being mainly *in vitro* activated by Trxf, but also by Trx m and NTRC [308].

In addition to starch synthesis, enzymes involved in starch degradation have been shown to be under redox control [48,307]. Among them, chloroplastic localized Arabidopsis AMY3 could be activated by reduced Trxs, being Trx f the most effective [318]. The same applies to BAM1, which could be also partially activated by NTRC [34,317]. The enzyme GWD that catalyzes the phosphorylation of starch and the DSP4 required for glucan desphosphorylation can also be reduced and activated by Trxs *in vitro*, with Trx f being the more efficient activator in both cases [313,315,316]. Nevertheless, Arabidopsis *gwd* mutant plants expressing a redox-insensitive GWD displayed normal starch turnover [314]. According to the widely accepted model for the

night-active starch degradation pathway [38,78], the reductive activation of starch degradative enzymes by Trxs (during the day) may seem contradictory. However, there are several evidences that starch degradation also takes place in such conditions, mainly associated with certain stress conditions or guard cell opening [34,37], indicating the existence of a starch futile cycle in leaves as previously proposed [32,402] Despite this, NTRC could also provide the reducing power to redox-activate starch turnover during the night.

Combination of *in vitro* and *in vivo* evidence indicates that both Trx f and NTRC clearly modulate the transitory starch metabolism in leaves, although a distinguishable role for each Trx type *in vivo* is unclear. So as to examine whether NTRC and Trx f perform discernible and specific functions on starch metabolism, in the present work we examine the effect of overexpressing and silencing *NTRC* and *Trxf* genes in *Nicotiana* plants on starch metabolism. Our results help to gain insights into Trx specificity *in vivo*.

2.2 Material and methods

Plant material and growth conditions

Tobacco plants overexpressing*Trxf*, from the chloroplast genome, under the control of the *psbA* promoter [305] (hereafter referred to as o/exTrxf) or *NTRC* (generated in this study and named o/exNTRC) were used. To generate o/exNTRC plants, *Arabidopsis thaliana NTRC* coding sequence (GenBanK: NM_129731), excluding the putative transit peptide, was amplified by PCR using the primers described in Supplementary Table S2.1. The amplified *NTRC* sequence, which includeda 6xHis tag to facilitate protein purification, was cloned into a pKS intermediate vector (Stratagene, La Jolla, CA, USA) for fusion to the promoter and 5'UTR of the tobacco *psbA* gene. Finally, the NTRC expression cassette was introduced into the chloroplast transformation vector pAF [403] to generate pAF-NTRC. Gold microprojectiles coated with pAF-NTRC vector were bombarded into *Nicotiana tabacum* (Petite Havana SR1) *in vitro*-grown leaves as described previously [346]. Regenerated plants were transplanted and grown in a phytotron (16 h light/8 h dark, 150 µmol.m^{-2}.$s^{-1}$and 28ºC) for homoplasmy confirmation and seed production.

Silenced plants, in which the expression of *NTRC* or *Trxf* genes was strongly reduced, were also used in this study (hereafter referred to as VIGS-NTRC and VIGS-Trxf). To obtain these plants, tobacco rattle virus-based virus-induced gene silencing (VIGS) was applied in *Nicotiana benthamiana* [404]. A database search (*Nicotiana benthamiana* Genome and Transcriptome Sequencing Consortium: http://benthgenome.com) identified the tobacco orthologous *NTRC* and *Trxf* genes in *N. benthamiana* by BLAST homology. In both cases, all found sequences had high similarity and a conserved region was used to specifically silence each gene. *NTRC*

and *Trxf* conserved fragments were amplified from RT-PCR-generated *N. benthamiana* cDNA using the primers described in Supplementary Table S2.1 and cloned into the pTRV2 vector. pTRV1, which contains replication and movement viral genes, and pTRV2-NTRC or -Trxf derivatives were introduced into Agrobacterium GV3101 and co-agroinfiltrated into 2-3-week-old *N. benthamiana* plants according to a standard protocol [405,406]. The non-silencing TRV control, containing a 396-bp fragment of the β-glucuronidase gene (GUS), was used as described previously [407]. Silencing of the endogenous phytoene desaturase gene (PDS), which causes photobleaching, was used as a positive control for VIGS efficiency (VIGS-PDS). Silenced plants were grown in a phytotron in 16h light/8h dark light regime at 80 $\mu mol.m^{-2}.s^{-1}$ and 24°C. Plants were grown for 3 weeks prior to analysis, allowing for the post-infiltration development of at least 2-3 full leaves.

DNA, RNA and protein analysis

To confirm homoplasmy in plants overexpressing NTRC, a Southern blot analysis was performed. Leaf discs from o/exNTRC and wild-type (Wt) tobacco plants were finely powdered in liquid nitrogen. Total plant DNA was extracted by using the cetyltrimethylammonium bromide (CTAB) procedure; 10 µg were digested with *Bgl*II, separated on a 0.8% (w/v) agarose gel, transferred to a nylon membrane and hybridized with a 0.8 kb probe homologous to the flanking sequences. Probe labelling and hybridization were performed using the DIG High Prime DNA Labelling and Detection Starter Kit II (Roche, Mannheim, Germany).

Analysis of *NTRC* and *Trxf* mRNA levels was carried out in VIGS-NTRC and VIGS-Trxf plants. Total RNA from silenced leaf tissues was extracted using Trizol® Reagent (Thermo Fisher Scientific, CA, USA) following the manufacturer's protocol. Generation of cDNA and RT-qPCR analysis were performed [408]. The efficiency of the primers used in RT-qPCR was no lower than 98%. To normalize the mRNA levels of target genes between samples, relative actin mRNA levels were determined using actin-specific primers (Supplementary material, Table S2.1) and a relative quantification method [409].

Protein expression was analysed in o/exNTRC and VIGS plants. Total protein was extracted in Laemmli buffer (0.5 M Tris–HCl pH 6.5, 4% SDS, 20% glycerol and 10% β-mercaptoethanol) and quantified using the DC Protein Assay (Bio-Rad, Hercules, CA, USA) with bovine serum albumin as a standard. Proteins were electrophoresed on a 10% or 15% SDS-polyacrylamide gels for NTRC and Trx f, respectively, transferred to a PVDF membrane and immunoblotted with specific antibodies: 1:750 dilution for NTRC [191] and 1:5000 for Trx f [346]. A peroxidase-conjugated goat anti-rabbit antibody (1:10,000; Sigma-Aldrich, St Louis, MO) was used as secondary antibody. Detection was performed using the ECL Prime detection system (GE Healthcare, Buckinghamshire, UK).

Protein purification and activity assays

Fully expanded leaves of o/exNTRC plants were ground in liquid nitrogen and homogenized 1:5 (w/v) in protein extraction buffer [20 mM sodium phosphate pH 7.4, 500 mM NaCl, 0.1% (v/v) Triton X-100 including a cocktail of protease inhibitors from Roche (Mannheim, Germany)]. The homogenate was incubated on ice for 45 min and cell debris was pelleted by centrifugation (20,000 *g,* 20 min, 4ºC). Overexpressed NTRC was purified from plant protein extracts by affinity chromatography on a Ni-NTA column (Qiagen, Hilden, Germany). The protein content of eluates was measured with the DC Protein Assay (Bio-Rad) and the purity of NTRC was checked by SDS-PAGE and Coomassie Blue staining (Supplementary Figure S2.1). The Trx activity of the purified NTRC protein (2, 4 or 8 µM) was determined according to the DTT-dependent insulin reduction assay [392] as described previously [132]. The NTR activity was determined by the reduction of 5,5'-dithiobis(2-nitrobenzoic acid) (DTNB) [191].

Starch determination

The starch determination was performed using an amyloglucosidase-based test kit (R-Biopharm AG, Darmstadt, Germany) according to the manufacturer's instructions. Starch content was analysed in young well-expanded leaves of o/exNTRC and o/exTrxf plants harvested just before the inflorescence emission (7-week-old plants) at the end of the light (16 h) and dark (8 h) periods. Starch was also analyzed in silenced plants (VIGS-NTRC and VIGS-Trxf) using fully expanded leaves collected 3 weeks after infection.

For starch synthesis and degradation rate determination, starch content at the end of the dark (8 h) and the light (16 h) periods were measured and slopes between both of those times were calculated. For each rate determination, paired samples were collected at the same position of the leaf blade at both sides of the central vein.

Enzyme activities associated with starch synthesis and degradation

Leaves from tobacco Wt, o/exNTRC, o/exTrxf plants and *N. benthamiana* VIGS-GUS, VIGS-NTRC and VIGS-Trxf plants were harvested after 8 h illumination or 4 h darkness and immediately frozen and ground in liquid nitrogen.

Enzymatic analysis of soluble starch synthase activity was carried out in protein extracts from leaves sampled in the light [410]. One unit of activity was defined as the amount of enzyme causing an increase of one unit per min in absorbance at 340 nm.

Activities of AMY and BAM were measured in leaves harvested in the dark using the Ceralpha® and Betamyl-3® assay kits (Megazyme, Ireland). Both assays are highly specific and selective for each enzyme and avoid interferences from DBEs. For LDA assay, the PullG6 Method (Megazyme) was used according to the manufacturer's instructions in leaves harvested in dark conditions.

AGPB redox status

The AGPase redox status was determined by immunoblotting, analysing the degree of AGPB monomerization in leaf samples collected at the end of the light (16 h) and dark (8 h) periods. Protein extraction was performed as previously described [398]. Proteins from 1 mg of fresh weight were subjected to 10% non-reducing SDS-PAGE, transferred to nitrocellulose membrane and probed with a specific AGPase antibody (Agrisera AB, Vännäs, Sweeden) at a dilution of 1:1000. A peroxidase-conjugated goat anti-rabbit antibody (Sigma-Aldrich) at a 1:10,000 dilution was used as secondary antibody.

Zymograms of starch hydrolytic activities

Leaf samples (300 mg) harvested after 8 h light or 4 h dark were ground in liquid nitrogen, homogenised in 1 ml of soluble protein extraction buffer (50mM Hepes pH 7.5, 2mM EDTA and 10% glycerol) and incubated for 5 min on ice. The supernatant was obtained after 10 min of centrifugation at 14,000*g* at 4ºC and soluble protein concentration was measured by Bradford assay (Bio-Rad) using bovine serum albumin as a standard. Protein extracts (35 µg) were incubated in presence or absence of 40 mM DTT or 200 µM $CuCl_2$ for 2 h on ice in the dark and loaded on native PAGE (7.5% acrylamide) containing 0.2% (w/v) potato amylopectin (Sigma-Aldrich) as substrate in the separating gel. After migration (under native condition for 4 h at 4ºC at 15 $V.cm^{-1}$), gels were incubated overnight at room temperature in 100 mM Tris-HCl pH 7, 1 mM $MgCl_2$ and 1 mM $CaCl_2$ containing buffer. Activities were revealed by iodine staining (Lugol solution; Sigma-Aldrich).

2.3 Results

Generation of transplastomic tobacco plants overexpressing fully functional NTRC

The mature Arabidopsis *NTRC* coding sequence was expressed into tobacco chloroplasts under the control of the plastid *psbA* promoter and terminator, and inserted together with the selectable spectinomycin resistance gene (aadA) into the plastid genome between the *trnI* and *trnA* genes (Figure 2.1A). Southern blotting was performed to verify site-specific integration and to confirm the homoplasmy of the regenerated spectinomycin-resistant plants. The flanking region probe (Figure 2.1A) identified a 4.5 kb hybridizing fragment in Wt plants, and recognized two fragments (5.2 and 2.3-kb) in the NTRC-overexpressing lines (Figure 2.1A and B), hereafter referred to as o/exNTRC. The absence of 4.5 kb bands in o/exNTRC plants indicated homoplasmy. Since insertion of transgenes into the plastid DNA occurs via homologous

recombination at the specific *trnI-trnA* insertion site, all transplastomic lines are identical [411] and the o/exNTRC line 1 was therefore used in further experiments.

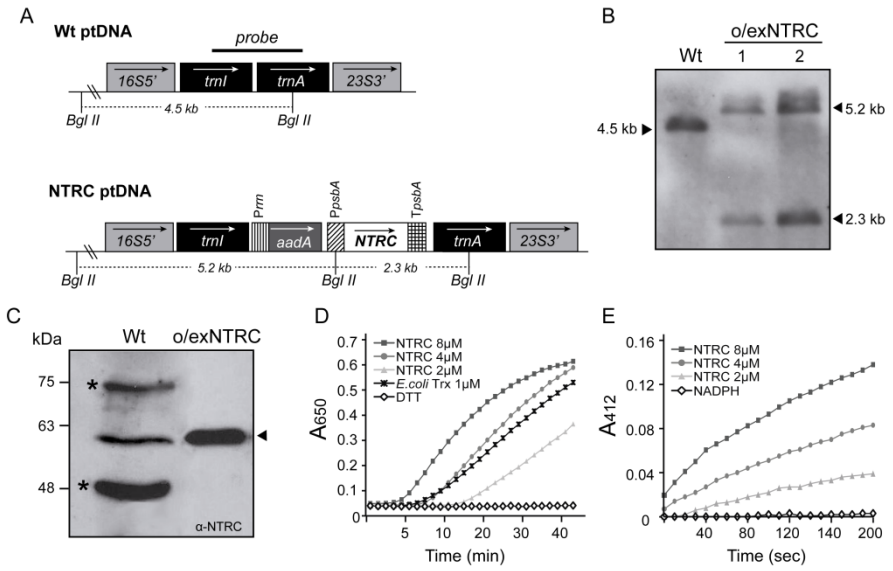

Figure 2.1. Integration, overexpression and functionality of the NTRC protein in transplastomic tobacco plants. A) Map of the Wt and transformed NTRC plastid genomes. The *NTRC* gene, driven by the *psbA* promoter and terminator, was cloned into the intergenic region between *trnI* and *trnA*. The arrows in the boxes show the direction of transcription. The probe for the Southern blot is shown over the corresponding sequence. The sizes of the predicted bands after DNA digestion with *BglII* are indicated. *16S5', trnI, trnA, 23S3'*: original sequences of the chloroplast genome; *aadA*: aminoglycoside 3'-adenylytransferase gene; P*rrn*: *16S*rRNA promoter and 5'-untranslated region; P*psbA*: *psbA* promoter and 5'-untranslated region; T*psbA*: terminator region of the *psbA* gene. B) Southern blot analysis of Wt and o/exNTRC plants. The sizes of the bands after DNA digestion with *BglII* are indicated. C) Immunoblot analysis of total protein extracts from fully-expanded leaves of 7 week-old plants. Protein loading for o/exNTRC (1 μg) and Wt (50 μg) extracts was adjusted to make it visible in the blot. An specific primary anti-NTRC antibody [191] at 1:750 dilution was used. The arrowhead indicates the NTRC band. Asterisks indicate non-specific bands. D) DTT-dependent insulin reduction assay of NTRC was performed in a reaction mixture containing 2, 4 and 8 μM of purified NTRC, supplemented with 0.5 mM DTT. Negative control runs were performed in the absence of NTRC (line DTT in graph). Trx from *E. coli* (1 μM) was used as a positive control. E) NADPH-dependent reduction of DTNB was assayed at room temperature in a buffer containing 2, 4 and 8 μM of NTRC supplemented with 150 μM NADPH. Negative controls runs were performed in the absence of NTRC (line NADPH in graph).

NTRC overexpression was confirmed by immunodetection, showing both the overexpressed and the endogenous proteins similar mobility (Figure 2.1C). In the Wt plants, the NTRC band was visible in the blot when 50 μg of total protein were loaded,

whereas 1 µg of total protein was sufficient for the o/exNTRC plants. Densitometric analysis of several immunoblots showed the NTRC in the transplastomic plants to be some 200 times more abundant than endogenous NTRC in the Wt plants. Moreover, the affinity-purified NTRC from tobacco chloroplasts catalysed both the reduction of insulin in the presence of DTT (Figure 2.1D) and the reduction of DNTB in the presence of NADPH (Figure 2.1E) in a concentration-dependent manner. Thus, the NTRC overexpressed in tobacco chloroplasts was fully functional, and showed both Trx and NTR activities.

Phenotypically, o/exNTRC plants were slightly (but significantly) smaller than Wt plants (Supplementary Figures S2.2A and B). Moreover, its leaf chlorophyll content was about 30% below that recorded for Wt (Figure S2.2C), consistent with the pale-green color noticed in o/exNTRC plants (Figure S2.2A). However, these differences disappeared by the adult stage (Supplementary Table S2.2).

Production of *Nicotiana benthamiana* plants with reduced expression of NTRC or Trx f

The tobacco rattle virus-based VIGS approach was applied to efficiently silence *NTRC* or *Trxf* genes in *N. benthamiana*. To construct the gene-silencing vectors, *NTRC* and *Trxf* cDNA conserved regions were individually cloned into the pTRV2 vector [412]. Co-infiltration with pTRV1 and pTRV2-Trxf or –NTRC derivatives into *N. benthamiana* seedlings showed no apparent phenotype after three weeks of infection in VIGS-NTRC and VIGS-Trxf plants compared to non-silencing control plants (VIGS-GUS) under the assayed growing conditions (Figure 2.2A). By contrast, VIGS-PDS plants, used as positive gene silencing controls, efficiently induced photobleaching in *N. benthamiana* leaves (Figure 2.2A). The RT-qPCR analysis revealed that *NTRC* and *Trxf* gene expression was efficiently and specifically reduced in each VIGS-silenced line (Figure 2.2B). Hence, VIGS-NTRC plants exhibited a reduction of 92% in the *NTRC* expression without any effect on *Trxf* gene expression. Similarly VIGS-Trxf plants specifically reduced *Trxf* gene expression by approximately 96% compared to VIGS-GUS, while NTRC expression remains unchanged (Figure2.2B). The high silencing efficiency achieved in these plants was also confirmed at protein level by western blot (Figure 2.2C). The bands corresponding to those of NTRC and Trx f proteins were significantly reduced in total protein extracts of VIGS-NTRC and VIGS-Trxf plants, respectively (Figure 2.2C).

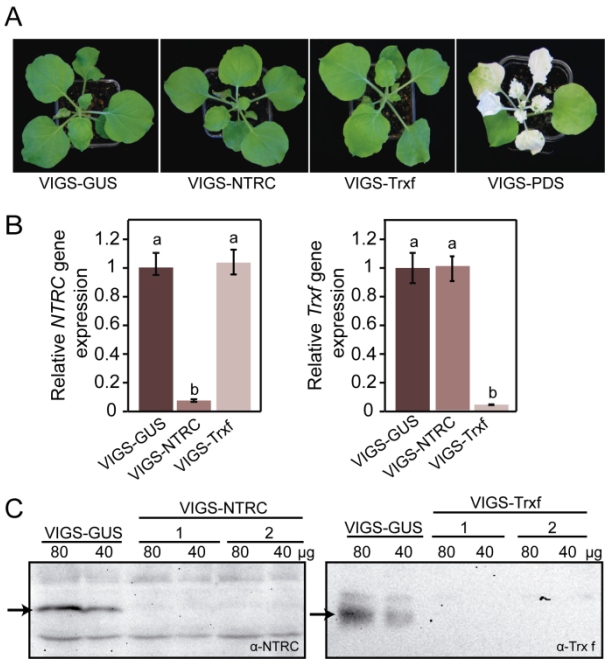

Figure 2.2. NTRC and Trx f silencing confirmation in *N. benthamiana* plants. A) Representative photographs of VIGS-NTRC and VIGS-Trxf taken 3 weeks after infiltration. The negative control VIGS-GUS and the positive control VIGS-PDS were also shown. At least ten biological replicates were performed, and similar results were obtained. B) Suppression rate of *NTRC* and *Trxf* genes in VIGS plants analyzed by qRT-PCR 3 weeks after infiltration. The relative transcript levels of *NTRC and Trxf* in VIGS-NTRC and VIGS-Trxf plants were expressed relative to that of the negative control (VIGS-GUS), previously normalized to 1. The data represent means ± SE of six biological replicates. Statistical significance compared to control plants is indicated by different letters ($P < 0.05$, ANOVA). C) Immunoblot analysis of NTRC and Trx f protein level in silenced plants compared to VIGS-GUS plants. 40 and 80 µg of total protein extracts from each line were separated by electrophoresis on 10% and 15 % SDS-PAGE for NTRC and Trx f, respectively. Protein detection was performed with a primary antibody, anti-NTRC [191] or anti-Trx f [346], at 1:750 or 1:5000 dilution respectively, and a secondary antibody (anti-rabbit peroxidase conjugated, Sigma-Aldrich) at 1:10,000 dilution. Each protein is indicated by an arrow.

Starch accumulation pattern in leaves of tobacco plants with altered NTRC or Trx f levels

To gather additional evidence about the role of plastid Trxs on starch metabolism, we further investigated the leaf starch accumulation pattern in plants with increased (o/exNTRC and o/exTrxf) or reduced (VIGS-NTRC and VIGS-Trxf) levels of NTRC and Trx f, respectively. Our results showed an increased leaf starch content in both o/exNTRC and o/exTrxf plants compared to Wt at the end of the day (16 h light) by about 35% and 60%, respectively (Figure 2.3A). The same, but even more pronounced,

trend was shown in these plants at the end of the night period (8 h dark), with a similar increase in both lines that almost tripled the starch content over the Wt plants (Figure 2.3A). Curiously, when the starch content was analyzed in leaves of silenced plants, only VIGS-Trxf plants showed a significant decrease on starch accumulation whereas VIGS-NTRC plants achieved similar starch quantities compared to VIGS-GUS control plants (Figure 2.3B).

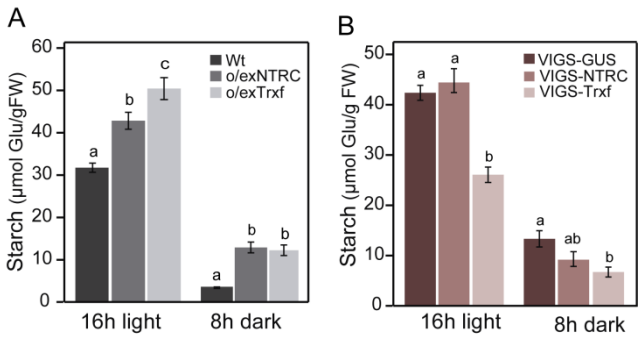

Figure 2.3. Starch accumulation in plants with altered NTRC or Trx f levels. A) Starch content in fully-expanded leaves from 7-week-old o/exNTRC and o/exTrxf plants grown in phytotron under 150 µmol.m^{-2}.s^{-1} after 16 h-light or 8 h-dark periods. B) Starch accumulation levels from mature leaves of phytotron-growing silenced plants harvested 21 days after infiltration at the end of the light (16 h; 80 µmol.m^{-2}.s^{-1}) and dark (8 h) periods. Results are the mean ± SE of six individual plants. Different letters above the bars indicate significant differences among lines for each specific harvesting period (P< 0.05, ANOVA).

Comparative analysis of enzymes related to starch synthesis

In order to check if o/exNTRC and o/exTrxf plants show a higher starch synthesis capacity, the activity of two well confirmed redox regulated enzymes such as SS and AGPase [48] was analyzed. Interestingly, o/exTrxf plants displayed a clear increase on SS activity while o/exNTRC plants showed no differences compared to Wt plants (Figure 2.4A). Accordingly, when the silenced plants were analyzed, VIGS-Trxf plants showed significantly lower SS activity compared to VIGS-GUS control plants (Figure 2.4B), while no differences were found in VIGS-NTRC plants.

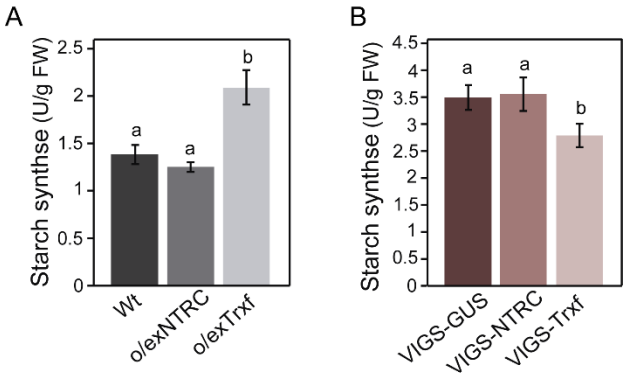

Figure 2.4. Starch synthase activity in leaves of plants overexpressing or silencing Trx f or NTRC. Protein extracts from leaves of tobacco overexpressing plants (A) and *N. benthamiana* silenced plants (B) harvested after 8 h illumination were used to analyze the soluble SS activity as described in "Materials and Methods". Each value is the mean ± SE of six individual plants. Different letters above bars indicate significant differences ($P< 0.05$, ANOVA).

Regarding AGPase,we previously demonstrated that its redox state, as a proxy of its *in vivo* activity, was not affected in o/exTrxf plants [305]. To assess the AGPase redox activation in o/exNTRC plants, in this study the degree of AGPB monomerization was analysed by western blotting under non-reducing conditions. Densitometric quantification of the oxidized (~100 kDa, dimer) and reduced (~50 kDa, monomer) forms of AGPB revealed no differences in AGPB reduction between o/exNTRC and Wt plants at the end of the light phase (Figure 2.5A). By contrast, o/exNTRC plants showed a in the AGPB monomerization compared to Wt at the end of the dark period (Figure 2.5A). A surprising increase of 2-Cys peroxiredoxin (Prx) monomerization, another well-known NTRC target [280], during the dark period also occurred in o/exNTRC plants (Supplementary Figure S2.3), suggesting that the overexpressed NTRC is mainly operating as a reducer in tobacco plants during the night. When VIGS-NTRC plants were analyzed, a reduction in the AGPB monomerization was shown at the end of the light period compared with control plants (Figure 2.5B), while no differences were detected under dark conditions.

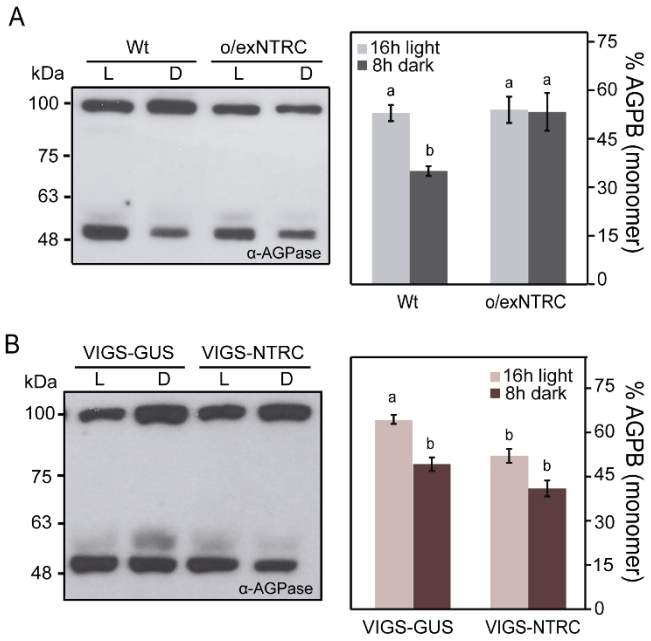

Figure 2.5. Redox activation of AGPase in plants with altered levels of NTRC. A) Leaves of Wt and o/exNTRC plants were sampled at the end of the light (L; 150 µmol.m^{-2}.s^{-1}) and dark (D) periods. B) Leaves of VIGS-GUS and VIGS-NTRC plants were harvested at the end of the light (L; 80 µmol.m^{-2}.s^{-1}) and dark (D) periods. A representative non-reducing western blot of AGPB is shown in each case. AGPB monomerization is presented as the percentage of the 50 kDa monomer relative to the total amount of AGPB. Each value is the mean ± SE of four individual plants. Different letters above bars represent significant differences (P< 0.05, ANOVA).

Overall, once analyzed the activities of two major enzymes involved in starch biosynthesis, our results point to a putative specific regulation of SS by Trx f, and suggest that the starch related phenotype observed in o/exNTRC plants may probably be a consequence of altered night-time starch metabolism having regard to the higher reduction of AGPase during this period.

Comparative analysis of enzymes related to starch degradation

We also analyzed whether the starch accumulation observed in NTRC- or Trx f-overexpressing tobacco leaves could be related to a downregulation of enzymes involved in starch degradation. To this end, the capacity of AMY, BAM and LDA were measured in leaves harvested after 4 hours of darkness from plants overexpressing NTRC or Trx f. Our results showed no differences in any of these enzyme activities among Wt, o/exNTRC and o/exTrxf plants (Figure 2.6A-C). When plants with reduced levels of NTRC or Trx f were analyzed, no differences between lines were also found in AMY, BAM and LDA activities (Figure 2.6D-F), suggesting that neither NTRC nor Trx f

seem to alter the overall activity of these amylolytic enzymes in tobacco leaves, at least in the assayed growing conditions. In addition, these results indicate that the increased starch accumulation in o/exNTRC or o/exTrx f leaves does not occur at the expense of a deactivation of these starch-degrading enzymes.

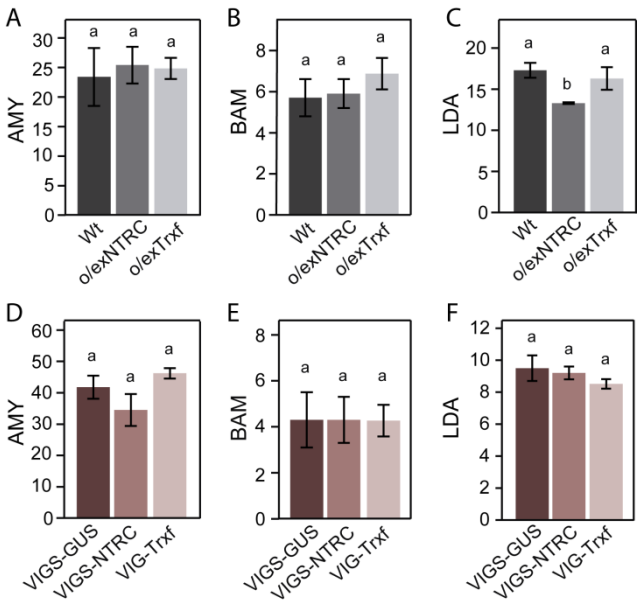

Figure 2.6. **Starch-degrading enzyme activities in leaves of Wt and transgenic plants overexpressing or silencing NTRC or Trx f.** Measurements were performed in leaves harvested after 4 h of darkness. Data are shown as units.mg^{-1} FW calculated according to Ceralpha®, Betamyl-3® and PullG6 methods (Megazyme). Data are given as means ± SE of six extracts, each made from an individual plant. Statistical significance is indicated by different letters above bars (P< 0.05, ANOVA).

Qualitative study of redox sensitive amylolytic enzymes in tobacco plants

To know the amylolytic enzyme profiles of tobacco extracts, zymographic analysis were additionally performed. We first analyzed the redox sensitivity of starch-degrading enzymes in Wt tobacco plants by incubating protein samples in presence of the reducing reagent DTT or the oxidizing reagent $CuCl_2$ followed by zymogram analysis. Under these conditions, several starch-modifying activities were observed in tobacco leaf extracts, including AMYs, BAMs and DBEs (Figure 2.7A) that were identified according as in previous works [413]. We found that the activity of a band corresponding to a putative DBE was less noticeable when incubate with DTT (Figure 2.7A, indicated by an arrowhead). On the contrary, a putative AMY was shown to be active only under reducing conditions (Figure 2.7A, indicated by an asterisk). Oxidant

conditions, however, did not appear to modify the activity of the amylolytic enzyme profile (Figure 2.7A). Based on these qualitative assay, we zymographically analyzed the activity of starch degradative enzymes in o/exNTRC and o/exTrxf extracts compared to Wt. Our results revealed a similar amylolytic enzyme pattern between o/exNTRC and Wt plants in light conditions, while a slight decrease in the activity of a putative DBE was shown in o/exNTRC extracts in the dark (Figure 2.7B). Conversely, there was no difference in the activity of starch-degrading enzymes between Wt and o/exTrxf plants under light or dark conditions (Figure 2.7C). These findings suggest that the overexpression of NTRC in tobacco plants leads to a downregulation of a putative DBE during the night, which could explain, at least to some extent, the starch increase seen in these plants. Although any enzyme involved in starch degradation was described to be redox deactivated, these results suggest this possibility, at least in tobacco leaves.

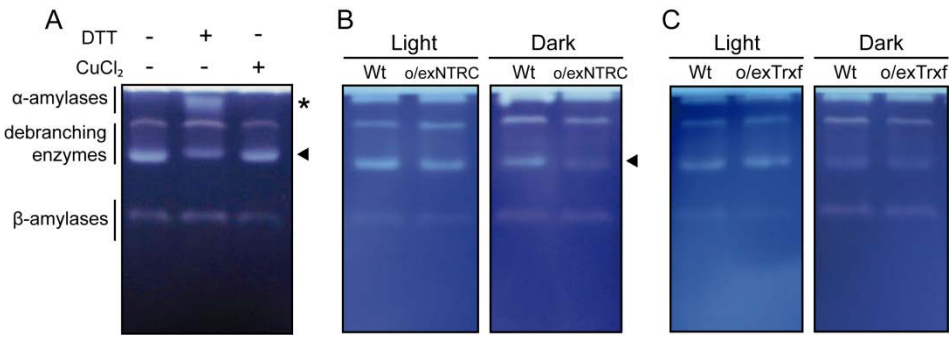

Figure 2.7. Analysis of amylolytic enzymes using native PAGE in Wt and NTRC- or Trx f-overexpressing tobacco leaves. Soluble proteins were extracted from leaves harvested after 8 h light or 4 h dark periods and separated (35µg) in native polyacrylamide gels containing 0.2% potato amylopectin. After electrophoresis, gels were incubated overnight and then stained with iodine solution to reveal pale bands where the amylopectin had been hydrolyzed. Putative activities of α-amylases, β-amylases and debranching enzymes were identified according to [413]. Asterisks indicate enzymes activated by reduction; arrowheads indicate enzymes deactivated by reduction. A) Redox mediated changes in starch amylolytic activities. Extracted proteins were treated with 40 mM DTT or 200 µM $CuCl_2$ for 2 h prior to gel loading. B) Differences between Wt and o/exNTRC plants in light and dark conditions. C) Differences between Wt and o/exTrxf plants in light and dark conditions.

NTRC and Trx f overexpression differentially alters the starch synthesis and degradation rates

To further investigate the differential role of NTRC and Trx f overexpression in promoting starch accumulation, starch synthesis and degradation rates were determined. Our results showed that, during the light period, NTRC overexpression in the chloroplasts did not alter the starch synthesis rate compared to Wt (≈ 1.8 µmol

glucose.g $FW^{-1}.h^{-1}$ in both lines), whereas this rate was greatly increased by about 30% in o/exTrxf leaves (Figure 2.8A). However, opposed results were found when nocturnal starch degradation rates were analyzed (Figure 2.8B). After 8 h of darkness, only o/exNTRC plants exhibited a significant reduction of about 40% in the starch degradation rate compared to o/exTrxf and Wt plants. Overall, these results indicate that the overexpression of NTRC or Trxf into the chloroplast leads to an increased leaf starch content, albeit different mechanisms seem to be governing starch metabolism in each transplastomic line.

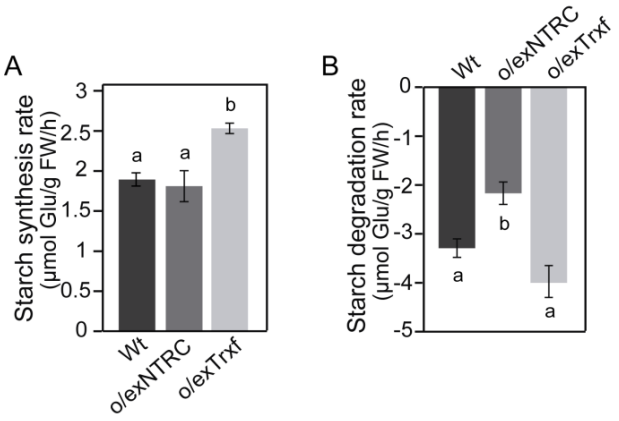

Figure 2.8. Rate of starch synthesis and degradation in plants overexpressing NTRC or Trx f. Pairs of samples were harvested from equivalent leaves of Wt, o/exNTRC and o/exTrxf plants in the same phenological growth stage (before inflorescence emission) at the end of the dark and light periods. The synthesis and degradation rates were calculated as explained in "Material and methods". Results are the mean ± SE for seven individual plants. Different letters above each bar indicate significant differences (P< 0.05, ANOVA).

2.4 Discussion

Chloroplasts contain a rich diversity of Trxs, the reduction of which is dependent on Fd reduced by the photosynthetic electron transport chain, and ultimately on light. In addition, there is a chloroplast NADPH-dependent Trx reductase, NTRC, which contains a complete Trx system in a single polypeptide that relies on NADPH and, thus, may be operative also during the night. Both Trxs and NTRC are reported to control different plant processes including the biosynthesis of starch [48,180]. Previous studies led to the view that these two different systems may have non-overlapping functions in plants [222]. In this work, we have explored the specificity of NTRC and Trx f in the regulation of starch metabolism by using overexpression and reverse genetics approaches.

Phenotype of *Nicotiana* plants with altered NTRC protein levels

We show that the overexpression of a fully functional NTRC protein in chloroplasts induces a significant increase in transitory starch accumulation in the tobacco leaves (Figure2.3A) and partially alters its phenotype (slight growth delay and lower chlorophyll content than Wt) during the younger growth stages (Figure S2.2). However, o/exNTRC tobacco plants recover the Wt phenotype in their adult stage (Table S2.2). NTRC has been unveiled as a redox regulatory system in chloroplasts that operates reducing target proteins at the expense of NADPH [191]. Thus, the recovery of Wt phenotype may indicate that the overexpressed NTRC in tobacco plants competes for NADPH with the accelerated chloroplast metabolism of growing tissues, but not in adult stages. In agreement with our results, overexpression of NTRC in Arabidopsis was previously shown to increase the accumulation of starch in illuminated leaves, which also displayed a chlorophyll reduction [196]. The importance of redox regulatory mechanisms in the maintenance of well-adjusted tetrapyrrole biosynthesis during plant development has broadly been demonstrated, with NTRC a key player in this regulation [198]. Hence, NTRC overexpression may alter the redox status of the chloroplast in young plants, thereby affecting chlorophyll synthesis.

In contrast, we found that *N. benthamiana* silenced VIGS-NTRC plants showed no apparent phenotypic changes compared with non-silencing control VIGS-GUS plants, and both lines accumulated similar amounts of transitory starch (Figures 2.2A and 2.3B). Likewise, it was determined that Arabidopsis *ntrc* mutant plants grown at low irradiance did not show differences compared to Wt in either plant growth or the patterns and rates of starch accumulation [400]. On the contrary, an attenuation of starch accumulation has widely been reported in *ntrc* Arabidopsis single mutants [196,197, 202, 223,306], which generally exhibited an impaired growth phenotype. It should be noted, however, that all these works were carried out at light intensities exceeding 125 $\mu mol.m^{-2}.s^{-1}$, where plants grown under photo-oxidative stress conditions and NTRC would play an important role in protecting plants against such stress [400]. Recently, the impaired growth of Arabidopsis *ntrc* mutant has been associated with an increased electron flow, from the Trx pool to 2-Cys Prx (involved in reducing H_2O_2) that indirectly may downregulate the Calvin-Benson cycle [201]. Thus, the lack of phenotype in VIGS-NTRC silenced plants may be explained by the low-irradiance growing conditions, where a limited H_2O_2 production is presumed. Under such conditions, the influence of NTRC silencing on starch metabolism can therefore be better analyzed.

Enhanced starch accumulation in o/exNTRC leaves as a consequence of impaired starch metabolism at night

The increased transitory starch accumulation seen in o/exNTRC leaves was not accompanied by either upregulation of SS activity (Figure 2.4A) or redox-activation of AGPase during the day (Figure 2.5A). Accordingly, no differences were found in the starch synthesis rate calculated for o/exNTRC plants compared to the Wt (Figure 2.8A). There is a general agreement about the role of NTRC in regulating starch synthesis via AGPase reduction [197, 223,306]. In this work, o/exNTRC plants showed a significant increase of AGPB monomerization but only during the night (Figure 2.5A). It may be that, in illuminated chloroplasts, overexpressed NTRC competes with the active chloroplast metabolism for photosynthetically-generated NADPH, while the availability of NADPH generated via the OPPP in the dark would supply more electrons to the NTRC system. To confirm this hypothesis, we analysed the reduction pattern of a well-known NTRC target (2-Cys Prx) in o/exNTRC plants, and demonstrated that it is also more efficiently reduced at night, with up to a 4-fold increase in 2-Cys-Prx reduction compared to light conditions (Supplementary Figure S2.3). In agreement with these results, it was previously shown that 2-Cys Prx, besides other Calvin-Benson cycle enzymes, was more reduced in Arabidopsis plants overexpressing NTRC under dark conditions than in Wt plants [221]. All in all, the present findings point to higher reductive activation of both AGPase and 2-Cys Prx by overexpressed NTRC at night, when NADPH availability is apparently better. Interestingly, during the night, increased AGPB monomerization in o/exNTRC plants converged with a reduction in starch turnover (Figure 2.8B). Thus, AGPase redox activation in darkness could account for the modified starch turnover rate in the o/exNTRC leaves by supporting starch synthesis. Similarly, it was previously suggested that Arabidopsis lines expressing a mutagenized and permanently active AGPase accumulated more leaf starch probably due to a slow starch turnover during the night [399]. When VIGS-NTRC silenced plants (grown under non-stressed conditions) were analyzed for AGPase reduction, the proportion of fully reduced AGPB in the light was significantly decreased compared to Wt (Figure 2.5B), which is in agreement with previously reported result [197,223]. However, contrary to these other works, no changes in the transitory starch accumulation occurred in VIGS-NTRC silenced plants (Figure 2.3B). Our findings suggest that NTRC is involved in AGPase redox regulation, although this fact does not appear to have a direct impact on starch biosynthesis during the day, at least under the assayed conditions. The role of AGPase redox-activation in starch biosynthesis has also been questioned by other authors [400,401], and starch synthesis stimulation *in vivo* has been demonstrated independent of such reductive activation [305,414].

In recent years, further candidates have been added to the list of reductively activated starch metabolizing enzymes, some of which are related to starch degradation [48,307]. Besides the Fd/Trx system, which is presumed to upregulate

starch degradation during stress conditions or in guard cells under light conditions [34,37], NTRC could also provide a reductive regulation of these enzymes in the night. Indeed, BAM1 from Arabidopsis has been described to be partially reduced by NTRC *in vitro* [34]. Therefore, a role for the overexpressed NTRC in the redox control of starch degradative enzymes in tobacco leaves during the night cannot be ruled out. However, in the present work we show that the activity of AMY, BAM and LDA enzymes in o/exNTRC or VIGS-NTRC plants did not differ from that of control plants (Figures 2.6), suggesting that the level of NTRC accumulated in chloroplasts does not affect the overall amylase and LDA activities *in vivo* under the assayed conditions. Interestingly, zymographic analysis performed with o/exNTRC extracts revealed a decrease in the activity of a hydrolytic enzyme in dark conditions compared to Wt (Figure 2.7B). Therefore, our results rather argue for an amylolytic enzyme deactivation in o/exNTRC plants, which is in agreement with the reduction of its starch degradation rate (Figure 2.8B). Although Trx-mediated deactivation of other chloroplastic enzymes such as glucose-6-phosphate dehydrogenase has previously been described [415,416], this may be the first evidence for an starch-degrading enzyme. The mobility of this downregulated degradative enzyme in the zymogram, which also seems to be deactivated in Wt tobacco extracts incubated with DTT (Figure 2.7A), indicates that it may correspond with a putative DBE [413]. Two DBEs involved in starch breakdown has been reported: ISA3 and LDA proteins. LDA was previously described as a redox-sensitive enzyme, although it seems to be more active under reducing conditions [307,319,320]. However, as stated before, no differences in LDA activity were seen between NTRC transgenic plants and their respective controls (Figure 2.6C and F). On the other hand, a small but significant activation of the Arabidopsis recombinante ISA3 activity was observed under reducing conditions [307]. *In vivo* analysis of DBE mutants show that Arabidopsis *isa3* mutants accumulate more leaf starch and have a slower rate of starch breakdown than Wt plants [56,417], a similar phenotype as o/exNTRC plants. All in all, these findings could suggest a downregulation of ISA3 in o/exNTRC tobacco plants exerted by the overexpressed NTRC that could explain, at least in part, the increased starch accumulation and reduced starch turnover found in these plants. Further investigations are, however, required to shed light on this matter.

Finally, it should be noted that qualitative zymogram analysis also showed a putative AMY isoform [413] that appears to be activated in Wt extracts treated with DTT as reducing agent (Figure 2.7A). This enzyme could be an ortholog of the Arabidopsis plastid localised AMY3, being the unique redox-regulated AMY reported in chloroplasts [307,318]. However, our results showed that neither NTRC nor Trx f overexpression appear to alter the redox status of this AMY isoform in tobacco leaf extracts.

Starch synthase as the main determinant of starch accumulation in Trx f transgenic *Nicotiana* plants

We previously demonstrated that overexpression of Trx f into tobacco chloroplasts has a positive effect on transitory starch accumulation and leaf biomass production [305,418,419]. Accordingly, here we show a decrease of starch content in the corresponding Trx f silenced plants, which did not display any visible phenotype (Figures 2.2A and 2.3B). Previous works also showed that Arabidopsis *trxf1* mutants lead to a decrease in starch content without altering plant phenotype [223,304]. However, double *trxf1-f2* mutants also accumulated less starch but showed some phenotypic defects [202,278]. All these studies made with Arabidopsis mutants attributed the decrease in transitory starch to the AGPase deactivacion [223,304]. However, we have previously demonstrated that the redox state of AGPase was not altered in Trx f-overexpressing tobacco plants [305].

Here, we further analyse the activity of other starch metabolic enzymes. Our results demonstrated that neither increasing nor decreasing Trx f content inside the chloroplast alters the activity of AMY, BAM and LDA enzymes (Figure 2.6). Therefore, Trx f does not appear to be involved in the *in vivo* redox modulation of those enzymes, despite being one of the most efficient Trx in the *in vitro* reductive activation [317,318]. Similarly, the overexpression of Trx f did not alter the amylolytic enzyme profile of tobacco leaf extracts (Figure 2.7C). By contrast, SS activity in o/exTrxf plants was higher than in Wt plants (Figure 2.4A), while VIGS-Trxf plants showed a decreased SS capacity (Figure 2.4B). It must be specified that there are five classes of SS in higher plants (SSI, SSII, SSIII, SSIV and GBSS) involved in starch biosynthesis. Based on mutant phenotypes, each SS class appears to have a distinct role during amylopectin synthesis, although their relative contribution varies in different tissues and among species [396]. It was reported that SSI constitutes the major soluble SS and is a major determinant for the synthesis of amylopectin in Arabidopsis leaves [420]. Moreover, according to the crystal structure of barley SSI, it was proposed that a disulfide bridge between two Cys can be formed [421]. Interestingly, the ability of Arabidopsis SS1 to be redox activated was confirmed, being Trx f the most effective activator *in vitro* [308]. Supporting this idea, Arabidopsis plants overexpressing Trx f from different species displayed an increased SS expression and activity [310,422]. Taken together, our results support the view of a specific role of Trx f in the redox regulation of starch synthases also in tobacco plants. Moreover, the rate of starch synthesis was increased in o/exTrxf plants while the degradation rate remained unaltered (Figure 2.8), supporting the idea that Trx f seems to be mainly involved in starch biosynthesis modulation.

2.5 Supplementary material

2.5.1 Supplementary methods

Redox status of 2-Cys Prx. The redox status of 2-Cys Prx was determined by immunoblotting, analysing the degree of monomerization in leaf samples collected at the end of the light (16 h; 150 µmol photons m^{-2} s^{-1}) and dark (8 h) periods. Protein extraction was performed as previously described [423]. Proteins from 1 mg of fresh weight were subjected to 10% non-reducing SDS-PAGE, transferred to nitrocellulose membrane and probed with a specific 2-Cys Prx antibody at a dilution of 1:1500. A peroxidase-conjugated goat anti-rabbit antibody (Sigma-Aldrich) at a 1:10,000 dilution was used as secondary antibody.

Plant growth and characterization. Wt and o/exNTRC plants were grown in a phytotron (16-h light/8-h dark; 150µmol photons m^{-2} s^{-1}) at 28ºC. The relative leaf chlorophyll concentration was measured using a Minolta SPAD 502 chlorophyll metre (Konica Minolta Optics Inc, Tokyo, Japan), examining four fully expanded leaves per plant in different developmental stages.

2.5.2 Supplementary figures

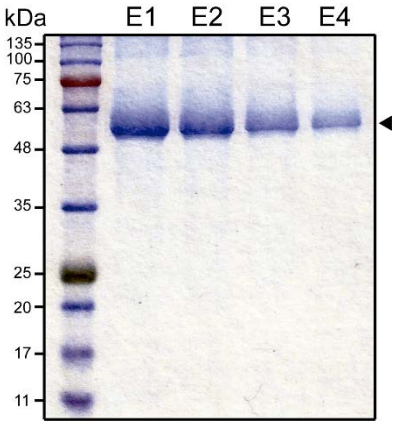

Figure S2.1. SDS-PAGE analysis of purified NTRC from transplastomic o/exNTRC tobacco plants. His-tagged NTRC was purified by Ni-NTA affinity chromatography. The four eluates (E1-E4) were loaded onto a 12%SDS-PAGE gel and stained with Coomassie Blue.

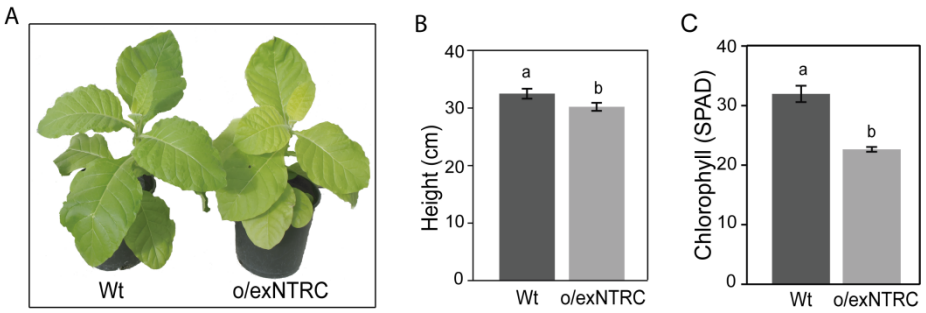

Figure S2.2. Phenotypic characterization of the NTRC-overexpressing line. A) Wt and o/exNTRC plants were grown in phytotron for 7 weeks under standard conditions (150 µmol photons m^{-2} s^{-1}, 16-h photoperiod and 28ºC). Mean stem height (B) and chlorophyll content (C) (SPAD value) was measured. Values ± SE (bars) were obtained from 15 plants per line. Different letters represent significant differences between lines (P< 0.05, ANOVA).

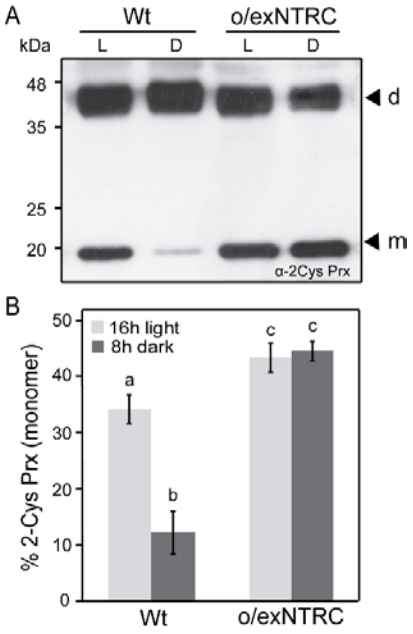

Figure S2.3. Redox status of 2-Cys Prx in o/exNTRC plants. Redox activation of 2-Cys Prx in leaves from 7-week-old o/exNTRC tobacco plants grown in phytotron and sampled at the end of the light (L) and dark (D) periods. A) A representative non-reducing western blot of 2-Cys Prx in leaves of Wt and o/exNTRC plants is shown. B) Quantification of 2-Cys Prx monomerization shown as the percentage of the 20 kDa monomer relative to the total amount of 2-Cys Prx. Results are the mean ± SE for five plants. m: monomer; d: dimer. Different letters above each bar indicate significant differences (P< 0.05, ANOVA).

2.5.3 Supplementary tables

Table S2.1. List of primers used in these work.

Primers used for *NTRC* amplification (5'-3')[a,b]	
NTRC_for	ccatgggt**catcaccatcaccatcac**GGATCCTCTTCTTCAGAGGCGAG
NTRC_rev	gcggccgcTTATTTATTGGCCTCAA
Primers used for VIGS vector construction	
pTRV2-NTRC_for	AGTgaattcCTGATACTCAGGAAGAATC
pTRV2-NTRC_rev	CTAggatccACTGTACACATGGAGTAC
pTRV2-trxf_for	AGTgaattcGTTGCAGGAGATTATGGC
pTRV2-trxf_rev	CTAggatccCTTTGGAGCAATCAC
Primers used for RT-qPCR analysis	
Actin_for	CAGCAACTGGGATGATATGG
Actin_rev	GGCGCTTCAGTTAAGAGGAC
NTRC_for	TGACTTAATGGATAGGATGAG
NTRC_rev	GTTCACTACTTTGGATAGTAA
trx f_for	CAAGTAAACGGCGTATCATT
trx f_rev	CAGACCACCGATTGCTTGCT

[a] Restriction sites are indicated in lowercase

[b] 6xHis tag is indicated in bold

Table S2.2. Phenotypic characterization of o/exNTRC plants grown in phytotron under standard conditions at different developmental stages. Values are the mean ± SE for 6 individual plants. *****Significantly different to the Wt (P< 0.05, Student's t-test).

	Wt	**o/exNTRC**
Flowering stage		
Height (cm)	82.5 ± 4.2	70.0 ± 2.7*
Chlorophyll content (SPAD)	32.8 ± 1.5	30.5 ± 0.9
Maturity		
Height(cm)	87.0 ± 4.5	86.7 ± 4.5
Chlorophyll content (SPAD)	26.5 ± 1.9	26.8 ± 0.9

CAPÍTULO III

Thioredoxin m overexpression in chloroplasts alters carbon and nitrogen partitioning in tobacco plants

3.1 Introduction

The carbon (C) and nitrogen (N) metabolisms of higher plants are tightly and multiply coordinated in order to maintain optimal growth and development. This strong connection ensures that amino acids and C skeletons are available for plant metabolic requirements, which entails that photosynthetic products must be partitioned between carbohydrate and amino acid biosynthesis. The control of this partitioning is mediated by an extremely complex network involving signals that emanate from different metabolites, proteins and hormones. Moreover, the redox status of the cell has been proposed as an important factor that might impact the integration of plant C and N assimilation [112].

Within chloroplasts, the thiol-based redox regulatory system includes plastid thioredoxins (Trxs), which are ubiquitous small disulfide reductases containing a redox-active disulfide group that is involved in light-dependent regulation of target proteins through thiol-disulfide exchanges. Hence, Trxs transfer reducing power from photosynthetically reduced ferredoxin (Fd) to target enzymes through the action of Fd-Trx reductase, thus modulating their activity related to various metabolic pathways. Five Trx types, termed f, m, x, y and z, have been found within the chloroplast. Originally, f- and m-type Trxs were identified as regulators of thiol enzymes involved in photosynthetic C assimilation in the chloroplast [13,140], whereas Trx x, y and z have been more closely linked to the regulation of antioxidant enzymes [142]. However, proteomic approaches revealed a great number of chloroplast-localized Trx targets that basically cover all the main chloroplast functions [226]. *In vitro* experiments using recombinant proteins provided new insights into Trx selectivity for redox regulation in the stroma [177] and, more recently, genetic studies have been used to dissect specific roles for plastid Trxs *in vivo* [179,180,424]. According to previous studies, Trx f is mainly associated with the redox regulation of C reactions, including enzymes of both the Calvin-Benson cycle (CBC) and starch metabolism [177, 228, 277,278,304,305]. By contrast, Trx m is proposed to control a wider range of processes such as biogenesis of cytochrome (Cyt) b_6f and PSII [212,259], cyclic electron flow around PSI [254], tetrapyrrole synthesis [258], export of reducing power via the malate valve [285], non photochemical quenching-dependent photoprotection [256], and the activation of antioxidant [177,182] as well as CBC enzymes [183]. However, the involvement of plastid Trxs in the regulation of N metabolism and, more precisely, N assimilation and partitioning has been poorly studied.

Previous studies suggest a role of Trxs in the regulation of N assimilation via redox regulation of chloroplast glutamine synthetase (GS2) and Fd-dependent glutamate synthase (Fd-GOGAT) in algae [322, 324,425] and cyanobacteria [325,426]. Fd-GOGAT catalyzes the conversion of glutamine (Gln) and 2-oxoglutarate to two molecules of glutamate (Glu), whereas GS2 catalyzes the ATP-dependent formation of

Gln from Glu and ammonia, thus participating in the re-assimilation of ammonia released from a variety of metabolic pathways such as photorespiration, catabolism of amino acids and metabolism of phenylpropanoids [102]. Both enzymes constitute the GS-GOGAT cycle, which is essential for N assimilation and photorespiration in chloroplasts. *In vitro* experiments also provide evidence that these two enzymes may be subjected to redox regulation in higher plants: (i) spinach and soybean Fd-GOGAT enzymes were reported to be preferentially activated by Trx m [181]; and (ii) the GS2 activity has been suggested as being directly redox modulated in chloroplasts [326]. Moreover, both enzymes were identified as Trx targets in different proteomic studies [226], and a redox regulation of the GS-GOGAT cycle *in vivo* was suggested to take place in Arabidopsis leaves treated with the reductant DTT [328].

The present study aims to shed light on the Trx-mediated redox regulation of N metabolism in plant leaves. Previous work has indicated that the increased redox state of tobacco chloroplasts achieved by Trx m overexpression might impair the C status of the cell [305], involving processes like photosynthesis [254] and chloroplast redox homeostasis [182]. However, the effect of Trx m overexpression on chloroplast C and N metabolism still remains to be analyzed. Here we conducted a wide metabolomic characterization of Trx m-overexpressing tobacco plants, concluding that Trx m alters C and N partitioning by promoting N instead of C metabolism. Moreover, a putative role of Trx m in GS2 redox modulation is discussed, linked to its effect on the photorespiratory N cycle. Taken together, our results suggest an important role for Trx m in controlling the N metabolism in plant chloroplasts.

3.2 Materials and methods

Plant material and growth conditions

The study was carried out with tobacco (*Nicotiana tabacum* cv. Petit Havana SR1) wild-type (Wt) plants and transplastomic plants overexpressing the mature *Trxm* coding sequence (o/exTrxm plants) from the chloroplast genome under the control of the *rrnG10*L promoter [305]. Because insertion of transgenes into plastid DNA occurs via homologous recombination at a specific insertion site, all transplastomic lines are identical [411] and therefore a single transplastomic line was used. Two-week-old seedlings, germinated *in vitro*, were transferred to 3 L pots filled with soil and grown in a phytotron under the following conditions: 16 h light/8 h dark, 150 $\mu mol.m^{-2}.s^{-1}$ and 28°C. Plants were watered twice a week with 0.5x Hoagland nutrient solution. In order to test the behavior of o/exTrxm plants under N-limiting conditions, a second experiment was conducted. In this case, plants were grown under hydroponic conditions in 3 L pots filled with an inert substrate such as perlite. Plants were irrigated daily with nutrient solution (3 mM KH_2PO_4, 1 mM $MgSO_4$, 1 mM $CaCl_2$ and 2 g/L Nutrel

C commercial micronutrient mixture [Yara Iberian, Madrid, Spain], pH 5.8-6.2) containing 1 mM or 2 mM KNO_3 [427]. For the 1 mM KNO_3 treatment, 1 mM KCl was added to supplement potassium levels in line with the 2 mM KNO_3 treatment. Pots were washed every week with distilled water to prevent salt accumulation. All analyses were carried out on the youngest fully expanded leaves of 6-week-old plants.

Determination of starch, soluble sugars, protein and amino acids

Soluble sugars and starch contents were determined at the end of the light and dark periods in tobacco leaf ethanol extracts and pellets by using, respectively, HPLC and an amyloglucosidase-based test kit (R-Biopharm AG, Darmstadt, Germany) as previously described [305]. For protein determination, leaf samples (100 mg) harvested after 4 h illumination were ground in liquid nitrogen, resuspended in 200 µL of soluble protein extraction buffer (100 mM Tricine-NaOH pH 8, 8 mM $MgCl_2$ and 2 mM EDTA) and incubated for 15 min on ice. The supernatant was obtained after 5 min of centrifugation at 10,000 *g* and the soluble protein concentration was measured with an RC-DC protein assay (Bio-Rad, Hercules, CA, USA) using bovine serum albumin as a standard. For amino acid quantification, 4 h light-harvested leaf samples (50 mg) were ethanol extracted, derivatized and analyzed on a reverse-phase HPLC column using the fluorescing reagent, AQC [428].

Metabolomics

Frozen leaf samples harvested after 4 h illumination were ground in 2 ml microcentrifuge tubes using stainless steel beads and a Retsch Mixer Mill MM 400 (Retsch, Haan, Germany) under cryogenic conditions. From these samples, metabolites were extracted, derivatized and analyzed via gas chromatography-time of flight mass spectrometry (GC–TOF–MS) analyses as described before [429]. The GC–TOF–MS system consisted of a CTC CombiPAL autosampler (CTC Analytics, Zwingen, Switzerland), an Agilent 6890N gas chromatograph (Agilent Technologies, Santa Clara, CA, USA) and a LECO Pegasus III time-of-flight mass spectrometer running in EI+ mode (Leco Instruments, St. Joseph, MI, USA). Metabolites were identified by comparison with database entries of authentic standards [430,431] using TagFinder software [432]. Peak intensity of a representative fragment was normalized with that of the internal standard ribitol and fresh sample weight and referred to as relative abundance.

Enzyme assays

Leaves harvested after 4 h illumination were immediately frozen and ground under liquid nitrogen. Aliquots of ~20 mg FW were extracted with 500 µL of extraction buffer according to [433]. Phosphoglycerokinase (PGK), NADP-dependent glyceraldehyde-3-phosphate dehydrogenase (NADP-GAPDH), fructose-bisphosphatase (FBPase),

glutamine synthetase (GS), Fd-dependent glutamate synthase (Fd-GOGAT), NAD-dependent glutamate dehydrogenase (NAD-GDH) and phospho*enol*pyruvate carboxylase (PEPC) were assayed as previously reported [433] and triose-phosphate isomerase (TPI) according to [434]. All assays were performed on microplates using 96-head pipetting robots (Hamilton, Villebon-sur-Yvette, France) and UV-visible readers (SAFAS, Monaco). Assay optimization and calculations were conducted as in [435].

Gene Expression Analysis

Total RNA was extracted from tobacco plants with with Trizol® reagent (Invitrogen). One µg of DNAse treated total RNA was used for cDNA synthesis by reverse transcription with PrimeScript™ RT-PCR Kit (Takara Bio) according to the manufacturer's instructions. Quantitative PCR analysis was carried out using gene-specific primers (Figure 3.3) to amplify *gln2*, *pgk* and *gapB* genes. The analysis was performed with SYBR® Premix Ex Taq™ (Takara Bio), and the comparative Ct (threshold cycles) method (ΔΔCt) was applied for relative quantification of gene expression using an AriaMx real-time PCR System (Agilent Technologies). Relative expression levels were normalized to *16s rRNA* expression.

Determination of the redox state of Trx m *in vivo*

Leaves of plants overexpressing Trx m in light and dark conditions were ground in liquid nitrogen and protein was extracted and incubated with or without 50 mM DTT reducing agent or 50mM diamide or H_2O_2 oxidant agents. Extracts were precipitated with 10% (w/v) TCA and washed twice with 100% ice-cold acetone before the protein pellet was resuspended in 2% SDS and 150 mM Tris-HCl, pH 7.5 buffer. One part of the samples was incubated with 10 mM AMS (4-acetamido-4′-maleimidylstilbene-2,2′-disulfonate) (Invitrogen) to alkylate Cys residues, for 1 h at room temperature in the dark. Both AMS-treated and untreated samples were separated by 15% non-reducing SDS-PAGE and immunoblotted with anti-Trx m specific antibody (1:5000). The *in vivo* reduced form becomes labelled with AMS and migrates slower in SDS-PAGE.

Chlorophyll, nitrate and ammonium quantification

Photosynthetic pigments were extracted from leaf disks collected from fully expanded leaves and crushed in 5 ml 80% acetone. After centrifugation, the amount of chlorophyll (Chl) *a* and *b* was measured spectrophotometrically and calculated according to Lichtenthaler equations [354].

Aliquots of ~30 mg of frozen leaf material were homogenized with 600 µL of ultrapure water. Samples were then incubated at 80ºC for 5 min and centrifuged at 20,000 g and 4ºC for 20 min. The supernatant was recovered and used for nitrate [436] and ammonium [437] determination.

Gas exchange and chlorophyll fluorescence determinations

Gas exchange measurements were carried out with the LI 6400XT gas exchange portable photosynthesis system (LI-COR, Lincoln, Nebraska, USA) in fully expanded leaves. Determinations were conducted between 4 and 7 h after the onset of illumination. The light-saturated rate of CO_2 assimilation was measured at 1000 $\mu mol.m^{-2}.s^{-1}$ photosynthetic photon flux density, with 400 $\mu mol.s^{-1}$ air flow rate, 25ºC and 60% RH. Photosynthetic parameters were obtained using the equations of von Caemmerer and Faraquhar [349]. Dark respiration (R_d) measurement was determined in the early onset of the dark period. Photorespiration was expressed as the reduction % in the net photosynthetic rate by photorespiration. Briefly, after performing the net photosynthesis determinations at ambient CO_2 and O_2 conditions, leaves were kept in the chamber and N_2 from a tank (Air Liquide) was plugged into the Li-6400XT inlet to remove O_2 from the air entering the leaf chamber to allow photorespiration determinations.

The rate of oxygenation by Rubisco (V_o) was estimated as previously described [349], as $V_o=(V_c x\ pO_2)/(SrXC_i)$ where V_c refers to the rate of carboxylation of RuBP, pO_2 refers to the ambient partial pressure of O_2, Sr refers to the relative specificity of Rubisco, and C_i refers to the sub-stomatal CO_2 concentration. The rate of carboxylation by Rubisco (V_c) was estimated as $Vc=(A+R)/[1-pO_2/(2xSrxC_i)]$, where R refers to the rate of day respiration [438]. The electron transport through photosynthetic C reduction (ETRc) and the electron transport through photorespiratory C oxidation (ETRo) were determined as ETRc=4xVc and ETRo=4xVo, respectively [439].

Redox dependent structure and activity of glutamine synthetase

Frozen tobacco leaf material (~100 mg) from Wt and o/exTrxm plants was homogenized in 3 volumes of extraction buffer (100 mM HEPES, pH 7.5, and 2 mM EDTA) and incubated for 30 min in the dark on ice. After centrifugation at 20,000 g for 10 min, Wt samples were incubated in the presence or absence of 10 mM DTT or 1 mM $CuCl_2$ for 1 h on ice in the dark. Samples were then subjected to 10% non-reducing SDS-PAGE and blotted onto PVDF membrane (Hybond C, GE Healthcare, Fairfield, CT). The chloroplast GS2 isoform was detected with a primary antibody (anti-GS2, Agrisera AB) at 1:5000 dilution and a secondary antibody (anti-rabbit peroxidase conjugated, Merck KGaA, Darmstadt, Germany) at 1:10,000 dilution. Immunoblot detection was performed by chemiluminescence (ECL Prime Western blotting, GE Healthcare).

Protein complexes were analyzed from intact chloroplasts solubilized with 1.5% digitonin by blue native (BN)-PAGE using a 4–16% NativePAGE Novex Bis-Tris gel (Invitrogen, ThermoFisher Scientific) according to the manufacturer's instructions. After electrophoresis, protein complexes were transferred to a PVDF membrane and probed

with anti-GS2 antibody. Protein samples were incubated for 30 min on ice in the presence or absence of 10 mM DTT or 1 mM $CuCl_2$ before loading.

GS redox dependent activity was performed, as previously described [100], on protein extracts from Wt plants incubated with or without 5 mM DTT or 100 µM $CuCl_2$ for 30 min on ice. Recovery of GS activity by reduction was performed by incubating oxidized samples (after treatment with 100 µM $CuCl_2$) with 5 mM DTT for 30 min on ice.

For GS2 quantification, ground leaf samples were homogenized in 2 volumes of total protein extraction buffer (125 mM Tris-HCl pH 6.8, 4% SDS and 20% glycerol). Samples were incubated on ice for 15 min and supernatant was recovered after centrifugation. Protein extracts were quantified by a RC-DC protein assay (Bio-Rad), separated (2.5 µg) by SDS–PAGE on 10% polyacrylamide gels and transferred to a PVDF membrane for immunoblotting with anti-GS2 antibody. Immunoblots were quantified using the GeneTools analyzer software (SynGene, Cambridge, UK).

Bimolecular fluorescence complementation tests

To generate the bimolecular fluorescence complementation (BiFC) constructs, *Trxm* (GenBank HQ338525) and *gln2* (GenBank XM_016584731.1), full-length coding sequences were PCR-amplified and cloned into both pSPYCE-35S and pSPYNE-35S binary BiFC vectors [440], carrying the C and N-terminal fragments, respectively, of yellow fluorescent protein (YFP). Constructs were checked by sequencing and electroporated into *Agrobacterium tumefaciens* (GV3101) cells. Transformed cells were grown in liquid LB and co-infiltrated, together with an *Agrobacterium* strain carrying the p19 gene-silencing suppressor plasmid, into *Nicotiana benthamiana* leaves [441]. Epidermal cell layers of co-infiltrated leaves were assayed for fluorescence 3 days after infiltration using a D-Eclipse C1 confocal microscope (NIKON, Japan).

3.3 Results

Trx m overexpression alters the balance of C and N in tobacco plants

We firstly investigate the accumulation of C and N-derived metabolites in tobacco plants overexpressing the endogenous *Trxm* gene from the plastid genome, hereafter named o/exTrxm, grown in a phytotron under controlled conditions. Starch levels were significantly decreased in o/exTrxm leaves, by approximately 40% and 80% in light and dark conditions, respectively (Figure 3.1A). Likewise, the sucrose level was significantly lower in the transplastomic line, showing a similar pattern to starch (Figure 3.1B). On the other hand, o/exTrxm leaves showed a dramatic decrease in the glucose and fructose content compared to Wt, with levels being very similar in the light and dark (Figure 3.1C and D). These results indicate that, as suspected from previous works

[305], the leaf carbohydrate metabolism is somewhat impaired by the overexpression of Trx m in tobacco chloroplasts.

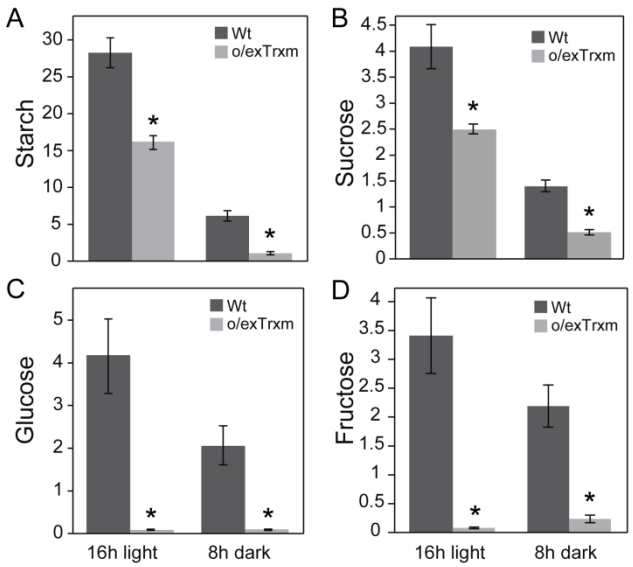

Figure 3.1. Starch and sugar levels in Wt and o/exTrxm tobacco leaves. A) Starch (µmol Glu.g^{-1} FW); B) sucrose (nmol.g^{-1} FW); C) glucose (nmol.g^{-1} FW) and D) fructose (nmol.g^{-1} FW) accumulation in young fully expanded leaves of phytotron-grown plants harvested after 16-h light and 8-h dark periods. Results are the mean ± SE of six individual plants. Statistical significance compared to Wt plants is indicated by asterisks (P< 0.05, Student's t-test).

By contrast, the amounts of both soluble protein and total amino acids were higher in o/exTrxm leaves (~40%) compared to Wt (Table 3.1). To further analyze the impact of Trx m overexpression on N metabolism, the leaf free amino acid profile was analyzed. Ten amino acids were significantly higher in the o/exTrxm genotype: alanine, asparagine, aspartic acid, GABA, Glu, Gln, isoleucine, leucine, serine (Ser) and valine. In contrast, only phenylalanine (Phe) levels decreased by around 14% in the transplastomic plants compared to Wt (Table 3.1). Therefore, both the observed decrease in starch and sugars and the increase in protein and amino acids suggest that the overexpression of Trx m in tobacco chloroplasts induces an imbalance between C and N.

Table 3.1. Soluble protein and amino acid contents in Wt and o/exTrxm plants. Leaf samples were taken after 4 h illumination. Results are given in µg.mg^{-1} FW for soluble protein and nmol.g^{-1} FW for amino acids. Values are means ± SE (n=4-5). Values that are significantly different from Wt are indicated in bold (P < 0.05, Student's t-test).

	Wt	o/exTrxm	P value
Soluble Protein	6.37 ± 0.15	9.01 ± 0.43	**0.000**
Amino acids	5064.21 ± 167.18	6974.90 ± 296.03	**0.001**
Alanine	1265.3 ± 72.2	2166 ± 107.5	**0.000**
Arginine	98.9 ± 1.9	103.8 ± 1.7	0.111
Asparagine	110 ± 17.2	310.1 ± 41.7	**0.005**
Aspartic acid	399.7 ± 50	591.7 ± 19.9	**0.005**
GABA	234.4 ± 10.2	276.7 ± 11.9	**0.033**
Glutamic acid	845.5 ± 38.5	984 ± 38.1	**0.039**
Glutamine	196.7 ± 20.8	292.5 ± 17	**0.008**
Glycine	187 ± 8.4	204.4 ± 12.6	0.330
Isoleucine	96.3 ± 1.4	105 ± 2	**0.009**
Leucine	199.5 ± 6.7	231.7 ± 6.6	**0.010**
Lysine	55.8 ± 4.5	48.1 ± 2.5	0.187
Methionine	84.4 ± 1.1	87.9 ± 1.6	0.134
Phenylalanine	168.2 ± 3.4	144.2 ± 3.7	**0.002**
Proline	176.4 ± 13.7	162.6 ± 7.7	0.416
Serine	294.5 ± 26	513 ± 23.1	**0.000**
Threonine	571.7 ± 49.8	476.9 ± 88.8	0.43
Tyrosine	204.3 ± 6	204.3 ± 5	0.998
Valine	66.2 ± 1.6	72.1 ± 3	**0.022**

Metabolomic analysis supports C and N imbalance in the o/exTrxm genotype

GC-TOF MS-based metabolite profiling was performed to investigate the global effect of Trx m overexpression on plant metabolism. A total of 42 metabolites were annotated including amino acids, sugars, organic acids and other metabolites (Supplementary material, Table S3.1). All amino acids and some sugars were previously quantified by HPLC and presented similar trends in both analyses; sugar levels were decreased in o/exTrxm compared to Wt plants, while most amino acids were increased except for Phe (Figure 3.1, Table 3.1). Metabolites not overlapping with those detected by HPLC are shown in Table 3.2 as proportions relative to Wt. Among sugars, a general downward trend was observed in the o/exTrxm metabolome, with fucose being significantly decreased and maltose and trehalose being below the level of detection. Some organic acids, most of them related to the phenylpropanoid pathway, were also significantly lower in the o/exTrxm genotype including threonic acid, cis-3-caffeoylquinic acid, trans-3-caffeoylquinic acid and quinic acid. Altogether, the metabolomic results corroborate that the overexpression of Trx m in chloroplasts alters

C and N partitioning in tobacco plants promoting N (rather than C) metabolism and also affecting phenylpropanoid precursors.

Table 3.2. Changes in leaf metabolite levels after 4 h illumination in o/exTrxm plants relative to Wt. Metabolite profiling was performed using GC-TOF-MS analysis. Results are means ± SD (n=4). Values that are significantly different from Wt according are indicated in bold (*P*< 0.05, Student's *t*-test). n.d, not detected.

	Wt	o/exTrx m
Sugars		
1,6-anhydro-beta-D-glucose	1 ± 0.15	0.96 ± 0.07
DL-rhamnose	1 ± 0.13	0.90 ± 0.06
DL-fucose	**1 ± 0.18**	**0.53 ± 0.04**
Gentiobiose	1 ± 0.24	0.48 ± 0.08
D-xylose	1 ± 0.30	0.32 ± 0.05
D-maltose	**1 ± 0.03**	**n.d**
alpha-alpha'-D-trehalose	**1 ± 0.31**	**n.d**
Organic acids		
trans-caffeic acid	1 ± 0.25	1.30 ± 0.09
Nicotinic acid	1 ± 0.09	1.18 ± 0.20
Citric acid	1 ± 0.21	1.13 ± 0.40
Fumaric acid	1 ± 0.18	1.12 ± 0.18
n-nonanoic acid	1 ± 0.22	0.93 ± 0.14
4-amino-butyric acid	1 ± 0.11	0.87 ± 0.16
Pyruvic acid	1 ± 0.15	0.86 ± 0.25
Succinic acid	1 ± 0.16	0.86 ± 0.07
DL-malic acid	1 ± 0.18	0.85 ± 0.17
Phosphoric acid	1 ± 0.32	0.60 ± 0.19
2-oxo-glutaric acid	1 ± 0.21	0.41 ± 0.13
Threonic acid	**1 ± 0.15**	**0.39 ± 0.09**
cis-3-caffeoylquinic acid	**1 ± 0.18**	**0.35 ± 0.06**
trans-3-caffeoylquinic acid	**1 ± 0.19**	**0.25 ± 0.06**
DL-glyceric acid	1 ± 0.41	0.15 ± 0.03
D(-)-quinic acid	**1 ± 0.37**	**0.08 ± 0.02**
Others		
Putrescine	1 ± 0.13	1.60 ± 0.24
myo-inositol	1 ± 0.23	0.55 ± 0.11
Tyramine	1 ± 0.31	0.42 ± 0.06

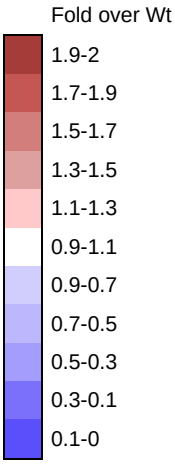

Activity of C and N metabolism enzymes

We further analyzed the activity of several enzymes involved in primary C and N metabolism in Wt and o/exTrxm leaves harvested after a 4-h light period. Consistent with the proposal that Trx m plays an important role in the activation of CBC enzymes *in vivo* [183], a significant increase in PGK, NADP-GAPDH and FBPase activities was observed in the o/exTrxm genotype compared to Wt, whereas TPI activity was invariant between genotypes (Figure 3.2). When the activity of N cycle-related enzymes was analyzed, the o/exTrxm genotype also showed a general increase in the capacity of the GS/GOGAT cycle enzymes. GS and Fd-GOGAT activities were higher in o/exTrxm leaves, although this was only significant for GS (Figure 3.2). NAD-GDH and PEPC capacities were also measured because of their central position at the interface between C and N metabolism. In both cases the o/exTrxm genotype displayed higher extractable activities for these enzymes (Figure 3.2). It is also worth mentioning that all these enzyme activities were still increased when expressed on a protein basis. With the exception of FBPase activity, the observed increase in enzyme capacities seemed to be specific to Trx m because tobacco plants overexpressing its counterpart, Trx f [305], did not show the same effect (Supplementary material, Table S3.2).

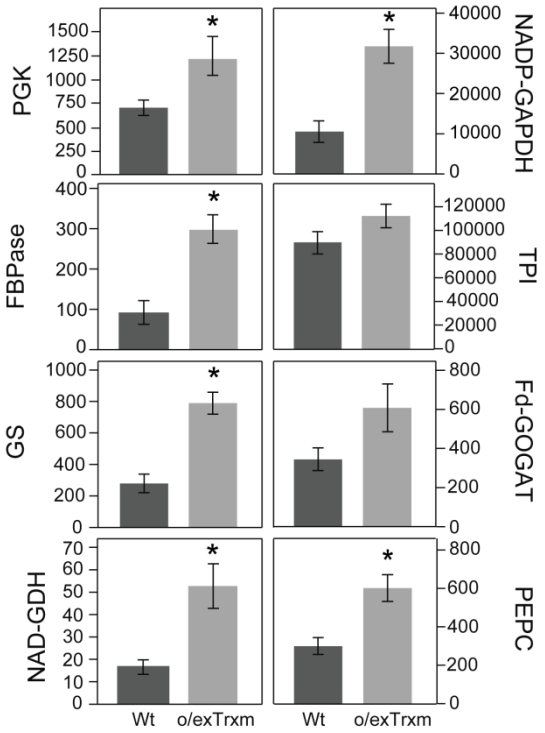

Figure 3.2. C and N metabolism enzyme activities in o/exTrxm tobacco plants. Samples were harvested after 4 h illumination from the youngest fully expanded leaves of plants grown in a phytotron under a 16-h light photoperiod and assayed for phosphoglycerokinase (PGK), NADP-dependent glyceraldehyde-3-phosphate dehydrogenase (NADP-GAPDH), fructose-1,6-bisphosphatase (FBPase), triose-phosphate isomerase (TPI), glutamine synthetase (GS), ferredoxin-dependent glutamate synthase (Fd-GOGAT), NAD-dependent glutamate dehydrogenase (NAD-GDH) and phospho*enol*pyruvate carboxylase (PEPC). Results, expressed as nmol.g^{-1} FW min^{-1}, are the mean ± SE of five individual plants. Statistical significance compared to Wt plants is indicated by asterisks ($P < 0.05$, Student's *t*-test).

To assess whether the significant and specific increase observed in the chloroplastic enzyme activities of Trx m-overexpressing plants resulted from a transcriptional or posttranscriptional regulation, the levels of mRNA transcripts of PGK, NADP-GAPDH and GS2 protein-coding genes were analyzed using RT-qPCR. The transcript levels of all these genes remained unchanged in the o/exTrxm genotype (Figure 3.3), revealing that their increased capacity likely resulted from a posttranscriptional regulation specifically promoted by the Trx m overexpression in chloroplasts.

A

Primers[a]	Forward (5'-3')	Reverse (5'-3')
gln2 (XM_016584731.1)	GCTTCAAACATGGACCCCTA	TTTGAGCAGCAAGAGCTTCA
pgk (Z48977.1)	CAAGGCGAAAGGAGTCAGTC	GATAGCAGATGCAGGCACAA
gapB (M14418.1)	TGTGTGACATTTTCCAACAAAG	AACAGGGGTTGATCTTGTGG
16S rRNA (Z00044.2)	CTTTTTAAGTCCGCCGTCAAA	TCTTTCCGATCTCTACGCATTTC

[a]GenBank accession numbers (NCBI) are indicated in parenthesis

B

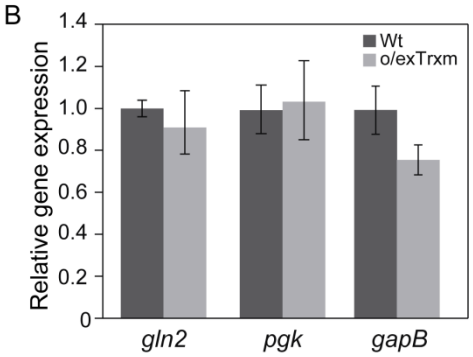

Figure 3.3. RT-qPCR analysis of *gln2*, *pgk* and *gapB* expression in tobacco Wt and o/exTrxm plants. A) Gene-specific primers used for quantitative PCR analysis. B) Graphical representation of relative expression levels normalized to *16s rRNA* expression that shows the fold change as the mean of the different biological repeats (n=3). Error bars represent SE.

Impact of Trx m overexpression on GS2 redox state, activity and stability

Taking that the overexpressed Trx m was mostly reduced in the light (Figure 3.4) and presumably was able to transfer the reducing equivalents from photosynthesis to their target enzymes, we investigated whether Trx m is involved in the redox regulation of GS2 by analyzing the redox state, activity and stability of this enzyme in o/exTrxm and Wt plants (Figure 3.5). When samples were analyzed under non-reducing conditions, our results indicated that overexpression of Trx m in tobacco chloroplasts resulted in increased amounts of GS2 monomers compared to Wt plants (Figure 3.5A,

right panel). In fact, the GS2 protein pattern of o/exTrxm resembles that of Wt samples treated with the reducing reagent DTT (Figure 3.5A). However, even when incubating with high levels of DTT (100 mM), the monomerization of GS2 was not complete, indicating that protein interactions other than disulfide bonds should account for GS2 oligomerization. Since GS2 polypeptides must be assembled into decameric complexes to be active [442], we further analyzed whether changes in the redox state of GS2 might affect the formation of decamers (~420 kDa). BN-PAGE analyses, followed by immunoblotting, were performed on protein extracts from o/exTrxm and Wt chloroplasts. Our results showed that the oligomeric GS2 enzyme migrated with a size compatible with a decameric structure in both Wt and o/exTrxm plants (Figure 3.5B). Similarly, GS2 decamers were not affected by DTT treatment, while significant structural changes (aggregation) were observed when chloroplast proteins were oxidized with $CuCl_2$ (Figure 3.5B). In addition, we noticed that GS activity was increased by DTT treatment and decreased when incubated with the oxidant $CuCl_2$ (Figure 3.5C). However, GS activity was restored when protein extracts were incubated with 5 mM DTT after an oxidation treatment (100 µM $CuCl_2$ for 30 min) (Figure 3.5C). Finally, it was observed that the amount of GS2 protein was clearly increased in o/exTrxm plants compared to Wt (by 40%, Figure 3.5D). As shown before (Figure 3.3) GS2 transcripts were unaltered in the o/exTrxm genotype, suggesting that Trx m might have an influence on maintaining GS2 stability. In combination, our results suggest that Trx m may alter the redox state of GS2, increasing its stability.

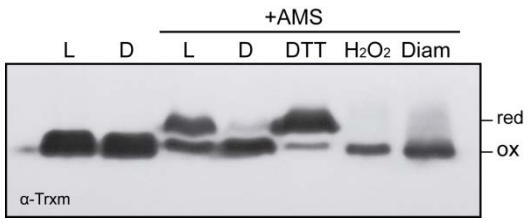

Figure 3.4. Redox status of overexpressed Trx m in tobacco chloroplasts. AMS alkylation and western blot analysis after non-reducing SDS–PAGE of Trx m. Protein leaf extracts incubated with DTT, H_2O_2 or diamide (Diam) prior to the treatment with AMS were undertaken as reduced and oxidized controls respectively. Protein extracts not incubated with AMS were used as non-alkylated controls. Specific Trx m antibody was used.The mobility of the alkylated (reduced, red) and non-alkylated (oxidized, ox) form is indicated.

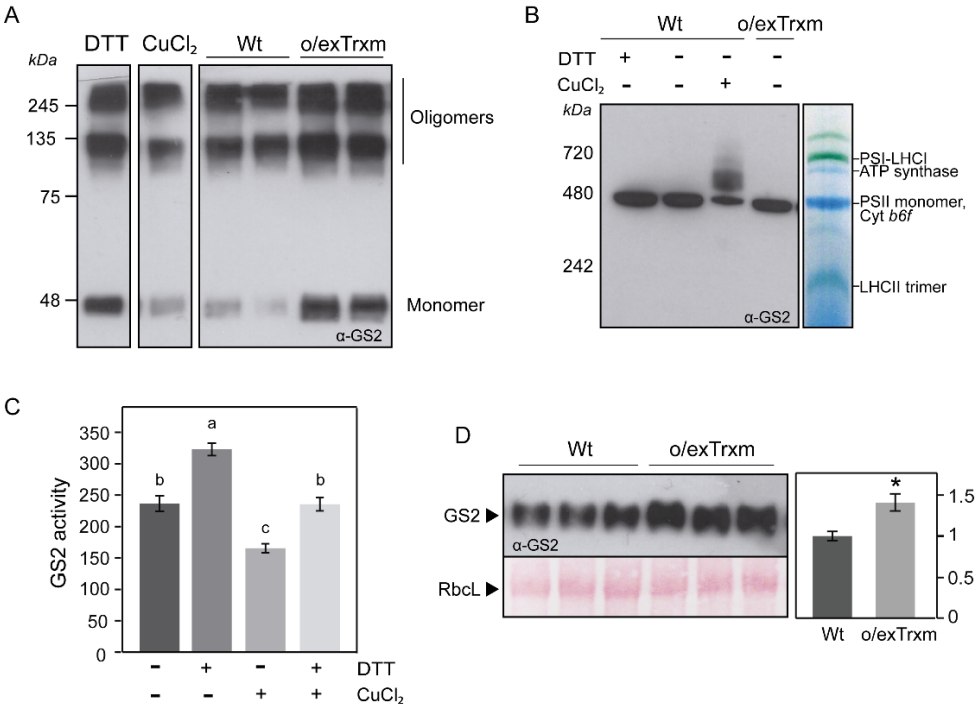

Figure 3.5. Determination of GS2 redox state, activation and stability. A) Redox structural changes of chloroplastic glutamine synthetase (GS2) in Wt and o/exTrxm plants. Proteins were extracted under non-reducing conditions and analyzed (25 µg) on 10% non-reducing SDS-PAGE gels, electrotransferred onto PVDF sheets, and probed with the anti-GS2 antibody (right panel). Wt protein samples were incubated for 1 h on ice in the presence of 10 mM DTT or 1 mM $CuCl_2$ and analyzed as before (left and middle panels, respectively). Positions of molecular weight markers are indicated on the left. B) GS2 protein complexes. Proteins from Wt and o/exTrxm chloroplasts were extracted under non-reducing conditions, separated (50 µg) by BN-PAGE and analyzed by western blot with anti-GS2 antibody. Photosynthetic thylakoid complexes are shown on the right and the molecular weight marker on the left. C) Redox-sensitive GS activity. Protein extracts from Wt plants were incubated with or without 5 mM DTT or 100 µM $CuCl_2$ for 30 min on ice, and the activity was then measured. Recovery of GS activity by reduction was performed by incubating with 5 mM DTT on ice after sample oxidation treatment (100 µM $CuCl_2$). Results are expressed as $nmol.g^{-1}$ $FW.min^{-1}$ ± SE (n=3). Different letters above each bar indicate significant differences ($P< 0.05$, ANOVA) D) GS2 quantification in the o/exTrxm genotype. Total protein extracts (2.5 µg) were loaded on SDS-PAGE and analyzed by western blot. Three different plants per line are shown in the blot. Immunoblots were analyzed with Gene Tools Analyzer software (SynGene). Data are given as means ± SE with Wt relativized to 1. Statistical significance relative to Wt plants is indicated by asterisks ($P< 0.05$, Student's *t*-test).

Trx m interacts with GS2 *in vivo*

Our findings suggest that Trx m could play a regulatory role in the GS/GOGAT cycle through a putative interaction with GS2. To test this hypothesis, we performed a BiFC analysis by *A. tumefaciens*–mediated infiltration in the chloroplasts of *N. benthamiana* leaves. GS2 fused with the sequence encoding the N-terminal fragment of YFP (GS2-YN) was co-expressed with Trx m fused with the C-terminal fragment of YFP (Trx m-YC). YFP fluorescence was detected in the chloroplasts, thereby confirming the interaction of GS2 and Trx m in this plant organelle (Figure 3.6). Similarly, we observed YFP fluorescence when combinations of GS2-YN and GS2-YC were co-expressed, indicating a self-interaction of this protein as was previously reported [442]. In this BiFC assay, agro-infiltration with bZIP63-YN and bZIP63-YC was used as a positive control [440]. While co-expression of Trx m-YC and empty YN vector, as well as GS2-YN and empty YC vector, which did not result in the production of yellow fluorescent signals, served as negative controls (Figure 3.6).

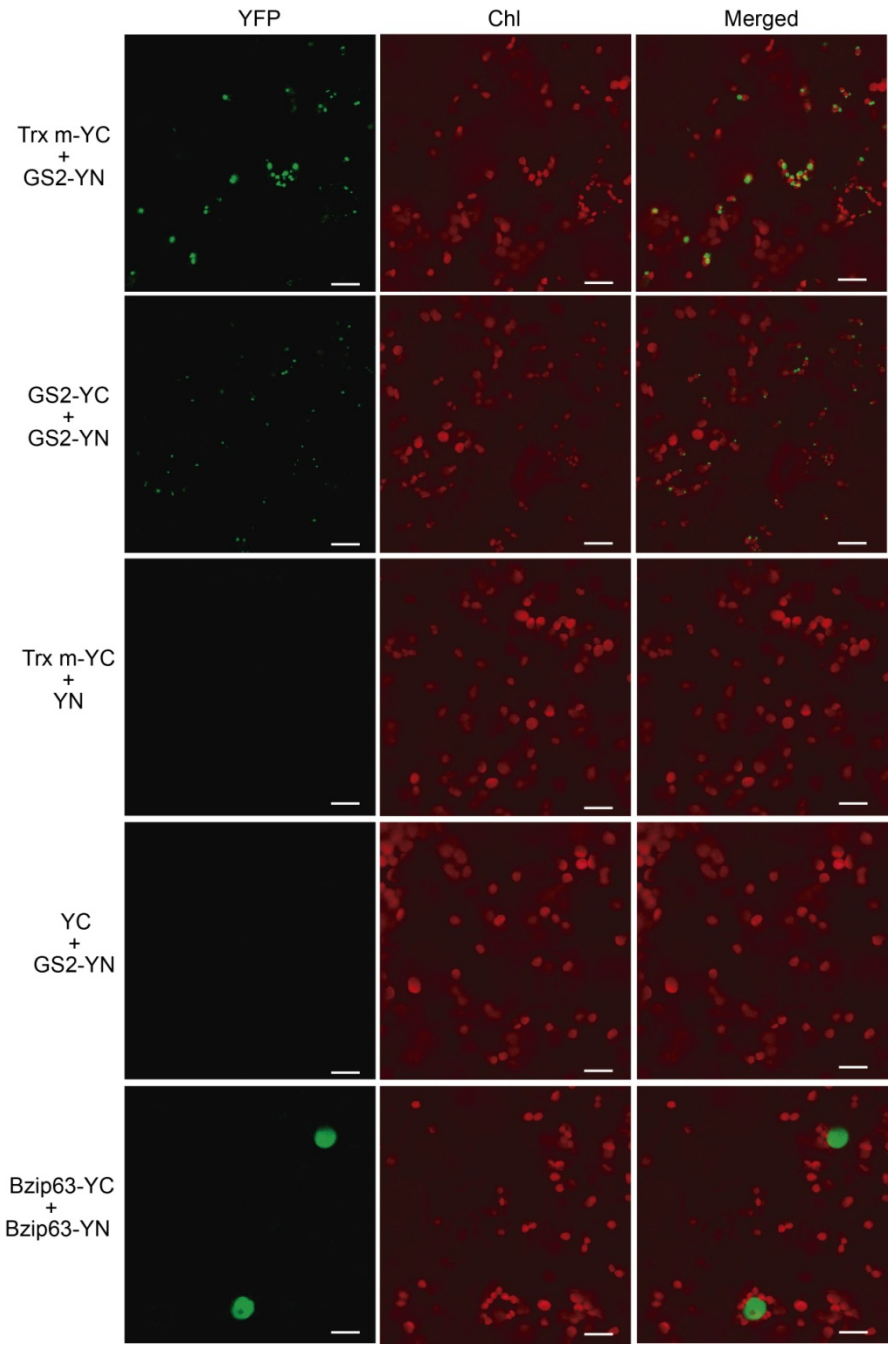

Figure 3.6. BiFC assay to identify *in vivo* interactions of Trx m and GS2. Confocal microscopy micrographs of agro-infiltrated *N. benthamiana* leaves analyzed 3 days after infiltration. The co-expressed constructs are indicated on the top of each panel. The images shown are representative of three independent BiFC tests. Scale bar: 15 μm. YFP, yellow fluorescence; Chl, chlorophyll autofluorescence.

Integrating C and N metabolisms with photorespiration and respiration

We further analyzed the photorespiration in the o/exTrxm genotype given its influence over the interaction between C and N metabolisms. Gas exchange analyses showed that net photosynthesis (A_N, determined at 21% O_2) decreased significantly in o/exTrxm plants relative to Wt, whereas no significant differences in CO_2 fixation rates were observed between lines when analyzed at 2% O_2 ($A_{N2\%}$, Table 3.3).

Table 3.3. Photorespiration in o/exTrxm plants. Net photosynthesis (A_n, µmol CO_2 $m^{-2}.s^{-1}$), net photosynthesis determined at 2% O_2 ($A_{N2\%}$, µmol CO_2 $m^{-2}.s^{-1}$) and photorespiration (R_p, µmol CO_2 $m^{-2}.s^{-1}$) in Wt and o/exTrxm tobacco plants grown in a 16h-light/8h-dark photoperiod. Results are the mean ± SE of six individual plants. Asterisks indicate statistical differences (P< 0.05, Student's *t*-test).

	A_N	$A_{N2\%}$	Rp
Wt	9.39 ± 0.64	11.57 ± 0.57	2.18 ± 0.24
o/exTrxm	6.32 ± 0.36*	9.92 ± 0.63	3.60 ± 0.45*

In Wt plants, photorespiration reduced the net photosynthetic rate by about 25%, whereas this reduction in o/exTrxm plants was twice as high as that observed in Wt (Figure 3.7A). This result indicates that photorespiration strongly contributes to the diminution of the net photosynthesis observed in the o/exTrxm genotype. In agreement with this finding, electron transport flux analyses revealed an increase in the electron flux to oxygenation relative to carboxylation (ETRo/ETRc) in o/exTrxm compared to Wt plants (Figure 3.7B). However, no significant differences in dark respiration (R_d) were detected between the genotypes (Figure 3.7C). Because photorespiration is intimately associated with N assimilation, nitrate and ammonium content was also analyzed in these plants. The levels of ammonium and, most importantly, nitrate were significantly increased in the o/exTrxm genotype relative to Wt (Figure 3.7D). These results collectively indicate that Trx m overexpression in chloroplasts also alters the so-called photorespiratory N cycle.

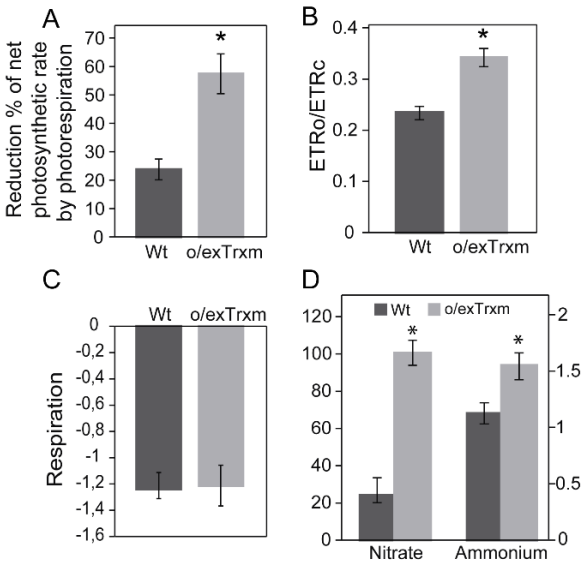

Figure 3.7. Photorespiration, ETRo/ETRc, dark respiration and N status in o/exTrxm tobacco plants. A) Percentage reduction in the net photosynthetic rate by photorespiration. B) The electron flux of oxygenation relative to carboxylation, ETRo/ETRc. C) Respiration (µmol CO_2 $m^{-2}.s^{-1}$) of Wt and o/exTrxm tobacco plants grown in a 16-h light photoperiod. D) Nitrate and ammonium content (nmol.mg^{-1} FW) in Wt and o/exTrxm plants harvested after 4 h illumination. Results are the mean ± SE of six individual plants. Asterisks indicate statistical differences (P< 0.05, Student's t-test).

Influence of Trx m overexpression in plant development under N-limiting conditions

Given that Trx m overexpression in chloroplasts affected the N status of the tobacco plants, we next analyzed the influence of nitrate supply on plant growth. Wt and o/exTrxm plants were grown in perlite and irrigated with nutrient solution containing low N amounts (1 or 2 mM KNO_3). In all assayed conditions, the o/exTrxm genotype exhibited slower growth and reduced Chl content compared to Wt (Figure 3.8A and B), as previously reported [182,305]. However, we observed a significant decrease in the biomass of Wt plants when grown at 1 mM nitrate compared to 2 mM that did not occur in o/exTrxm plants (Figure 3.8A). The same behavior was observed when Chl content was measured (Figure 3.8B), indicating that the low N supply exerts a greater impact on plant performance in Wt than in o/exTrxm plants. It should be noted that, under N-limiting conditions, o/exTrxm leaves also accumulated more nitrate and ammonium than Wt (Figure 3.8C and D). In fact, nitrate accumulated in Wt leaves at very low levels compared to those detected in Wt plants irrigated with full nutrient solution (Figure 3.7D and 3.8C), while nitrate levels were still high in the o/exTrxm genotype grown under these conditions. Conversely, ammonium accumulation in leaves seems to be less

sensitive to N deficiency because only Wt plants grown at 1 mM nitrate showed a significant decrease (Figure 3.7D and 3.8D). Together, these results indicate that the o/exTrxm behavior is relatively unaffected by the N-limiting conditions.

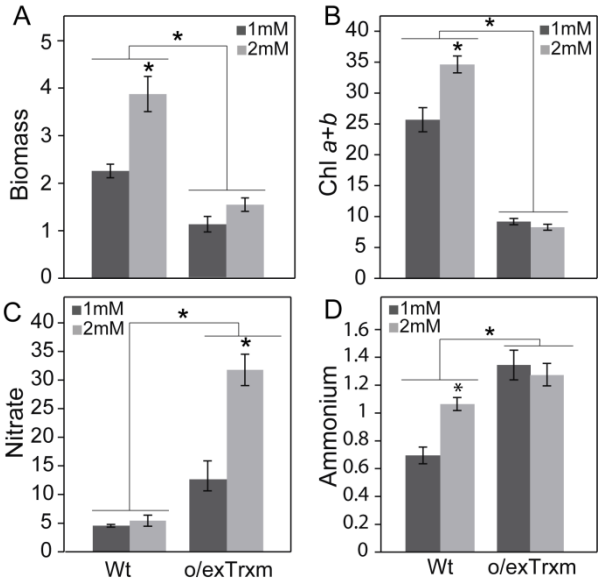

Figure 3.8. Response to nitrate supply. Plants were grown in a 16-h light photoperiod and watered daily with 1 or 2 mM KNO_3. After 30 days, plants were harvested after 4 h illumination and analyzed for A) plant biomass (g DW); B) total chlorophyll (µg.cm^{-2}); C) nitrate; and D) ammonium content (nmol.g^{-1} FW). Results are the mean ± SE of four individual plants. Statistical significance between treatments is indicated by asterisks (P< 0.05, Student's t-test).

3.4 Discussion

C and N assimilation in leaves requires the partitioning of reductant and photosynthates to sustain the demands of amino acid and carbohydrate biosynthesis. These processes are regulated at different levels according to prevailing environmental conditions. The ability of plants to coordinate C and N metabolism consists both of a complex sensory system and an intricate associated signaling network [112]. The redox status of the cell may have a key role in this coordination, with chloroplast Trxs serving as crucial components of the redox network [15]. In the current study, we have characterized the C and N metabolism of tobacco plants overexpressing Trx m from the chloroplast genome, and we found that Trx m is a central regulator of N metabolism.

C and N imbalance associated with Trx m overexpression in tobacco chloroplasts

Tobacco plants overexpressing Trx m exhibited an altered C and N partitioning, promoting the accumulation of N-related metabolites at the cost of C-related ones (Figure 3.1, Table 3.1 and 3.2). This effect seems to be specific to the m-type Trx because it does not occur when Trx f is overexpressed at the same levels [305,419]. Several enzymes of the starch degradation pathway have been reported as being redox-activated by Trxs [48]. However, this is an unlikely explanation for the low starch content reported in this genotype because the major starch breakdown products (maltose and glucose, [38]) did not accumulate in the o/exTrxm genotype (Figure 3.1 and Table 3.2). The lower photosynthetic rates of o/exTrxm (Table 3.3) could, furthermore, have contributed to the observed reduction in carbohydrate levels. To identify candidates that might explain the photosynthetic down-regulation, the activities of some CBC enzymes were determined (Figure 3.2). Curiously, such determinations revealed that PGK and NADP-GAPDH activities were higher in o/exTrxm than in Wt and o/exTrxf plants (Figure 3.2 and Supplementary material Table S3.2). Considering that their expression levels were unaltered (Figure 3.3), a specific post-translational regulation of both enzymes by Trx m can be suggested. However, the increased activities of PGK and NADP-GAPDH were not in line with the lower photosynthetic rates. These results suggest that while Trx m seems to redox activate CBC enzymes, as previously reported [183], the limitation in net photosynthesis could rather be associated with an impairment of the photosynthetic machinery in the o/exTrxm plants [443] that produces the reducing power and energy necessary for CO_2 fixation.

While C metabolism was severely impaired, our study showed that Trx m overexpression favored N metabolism. The content of amino acids and, consequently, soluble protein was increased in the o/exTrxm genotype relative to Wt (Table 3.1). Amino acid levels basically depend on their relative rates of production and consumption and/or transport [112]. Several enzymes involved in amino acid biosynthesis have been postulated as potential Trx targets, either in the spinach chloroplast [245] or in *Chlamydomonas reinhardtii* [251], and some of these are involved in the synthesis of the amino acids that were found to be upregulated in the o/exTrxm genotype (Table 3.1). Therefore, a direct Trx m-dependent regulation of some of these chloroplastic enzymes cannot be ruled out. Moreover, the general increase in amino acids and, in particular, the higher Glu and Gln pools shown in the o/exTrxm genotype (Table 3.1) may be indicative of an upregulation of the GS/GOGAT cycle via posttranslational reductive activation, as was previously shown in Arabidopsis leaves treated with DTT [328]. In fact, our results revealed a significant GS activity increase in the o/exTrxm genotype (Figure 3.2). Hence, the increased amino acid content observed in the present study could be caused by a reductive activation of the GS/GOGAT cycle *in vivo*, exerted by Trx m. The mitochondrial GDH, which operates at

the interface of C and N metabolism and participates in the balancing of the cellular levels of three major components (ammonium, 2-oxoglurarate and Glu), also exhibited higher GDH activity in the o/exTrxm genotype (Figure 3.2). Assuming that in leaves, GDH, which is coupled to respiration, mostly operates in the deaminating direction [444], one hypothesis is that the flux through the futile cycle involving GS, Fd-GOGAT and GDH could be increased in the o/exTrxm genotype. Such a cycle would be in line with sugar depletion (energy is mostly used by GS and Fd-GOGAT reactions) and with increased nitrate and ammonia, as well as increased photorespiration. Indeed, more N would be cycled and less N would be used for growth, even if the amino acid and protein contents increase, which may also account for the slower growth exhibited by the o/exTrxm genotype. Altogether, our results indicated that Trx m could have a role in controlling the cellular C/N balance associated with the chloroplast redox status.

Trx m overexpression redox-modulates GS2 in tobacco chloroplasts

Our findings showed that the overexpression of Trx m in tobacco chloroplasts leads to an increase in both GS2 activity and content (Figure 3.2 and 3.5D), while transcript levels were unaltered (Figure 3.3). These results point to a post-translational regulation of GS2 by Trx m, thus improving its stability or activity (or both). Supporting this hypothesis, it was shown that the addition of reducing agents, especially DTT, increases the activity of recombinant GS2 from *Canavalia lineata* [326]. These authors demonstrated that the redox sensitivity of GS2 is due to two conserved Cys residues found exclusively in the chloroplast isoform, albeit mutations in one of these Cys residues still retained GS2's redox activation. In agreement, the activity and stability of GS2 from *Lotus japonicus*, which preserves only one of the two conserved Cys residues, were considerably improved in the presence of thiol compounds [445]. It should be noted that GS2 from tobacco also conserves only one of these Cys residues (Supplementary material, Figure S3.1), indicating that this unique conserved Cys should be sufficient for the Trx m-mediated redox regulation of GS2, as occurs in *L. japonicus* plants. This fact suggests that Trx m could operate by reducing intermolecular disulfide bonds, thus affecting GS2 oligomerization. Along these lines, when the tobacco enzyme was analyzed under non reducing conditions, an increase in GS2 monomers was observed in o/exTrxm protein extracts, which electrophoresed like Wt samples treated with DTT (Figure 3.5A). The analysis of the quaternary structure revealed that the o/exTrxm genotype maintain the ability to form GS2 decamers (Figure 3.5B), the protein complex shown to be catalytically active in chloroplasts [84,442]. However, the GS2 redox state, as well as its complex formation and activity, seem to be affected by oxidant agents (Figure 3.5A and C). In agreement with this, it was previously demonstrated that GS2 displays an extreme sensitivity to oxidants in plants, resulting in its aggregation and cleavage [446,447]. It is known that the metal-catalyzed oxidation (MCO) system inflicts damage on GS2, which precedes its selective

degradation [446,448]. Curiously, peroxiredoxins (Prx) have been proposed as principal actors in the mechanism protecting GS against MCO-induced inactivation [449–451], which in the case of 2-Cys Prx from Chinese cabbage is tightly linked to the thiol-specific reducing group of the enzyme [452]. Our results point to an increase in GS2 stability in the o/exTrxm genotype (Figure 3.3 and 3.5D) and suggest that Trx m could be involved in regulating GS2 protection and stabilization, either directly or through Prxs, thus preventing GS2 oxidation and its subsequent degradation. In this work, BiFC assays showed that Trx m interacts with GS2 *in vivo* (Figure 3.6), suggesting that this mechanism may involve a direct interaction between both proteins. However, given that multiple Prxs have been reported as Trx targets in chloroplasts [177, 201,226], we cannot rule out that Trx m may also be activating this protection system through Prxs. The findings presented above provide evidence for an *in vivo* post-translational regulation of GS2 activity and/or stability accomplished by Trx m.

Overexpression of Trx m in chloroplasts favors the photorespiratory N cycle rather than nitrate assimilation

In the o/exTrxm genotype, we observed a higher photorespiratory rate than in Wt plants (Figure 3.7). Photorespiration is known to interact with several primary metabolic pathways [453], including the GS/GOGAT cycle [108,454]. The conversion from glycine (Gly) to Ser in the photorespiratory cycle results in the production of ammonia at a rate far exceeding that of primary N assimilation, by up to 10-fold [82]. Meanwhile, GS2 controls the re-assimilation of the released ammonia in chloroplasts [112], a process known as the photorespiratory N cycle. Interestingly, the pool of Ser was higher in the o/exTrxm genotype than in Wt, while the pool of Gly remained unaltered (Table 3.1), indicating a higher rate of Gly to Ser conversion that correlates with a significant increase in ammonium in o/exTrxm leaves (Figure 3.7D). Therefore, the enhanced photorespiratory capacity in this transplastomic line may be linked to the activation of the GS/GOGAT cycle. The re-assimilation of ammonia into chloroplasts is accurately regulated by the transport of dicarboxylates across the chloroplast envelope via the 2-oxoglutarate/malate transporter (OMT or DiT1) and the general dicarboxylate transporter (DCT or DiT2) [95,455]. Both DiT1 and DiT2 constitute a double translocator system that functions to coordinate the photorespiration and GS/GOGAT pathways [94,456]. We demonstrated by qPCR that the o/exTrxm genotype showed an increase in the expression of DiT2 relative to Wt (Supplementary material, Figure S3.2), thus reinforcing the proposal for an upregulated photorespiratory N cycle in these plants.

It was reported that the occurrence of photorespiratory N recycling may result in a lower net rate of inorganic N assimilation in the leaf [112]. In agreement with this affirmation, the o/exTrxm genotype accumulated extremely large amounts of nitrate in leaves (Figure 3.7D), a phenotype that resembles nitrate reductase (NR) mutant plants

[100]. In addition, we showed that the o/exTrxm genotype was less sensitive than Wt to nitrate deprivation (Figure 3.8). This behavior could be due to an inhibition of the NR enzyme causing a deficiency in nitrate reduction. Because NR is located in the cytosol, Trx m overexpression might exert an indirect control over its activity. It is well known that a decrease in reductant availability in the cytosol may limit NR activity [457–459]. Interestingly, a decrease in the NADPH/$NADP^+$ ratio and NADP pool size was observed in the o/exTrxm genotype (Supplementary material, Figure S3.3), indicating a reduced flux of reducing power to the cytosol, which may explain the large nitrate accumulation occurring in o/exTrxm leaves. However, other aspects occurring in the o/exTrxm genotype may also account for nitrate accumulation via a downregulation of the NR activity. Among them, sugar depletion [460] and decreases in net photosynthesis [461] have been reported to result in a massive reduction in NR protein levels. Our results collectively demonstrate that the overexpression of Trx m in chloroplasts favors the re-assimilation of photorespired ammonium rather than primary nitrate assimilation.

Putative role of Trx m in phenylpropanoid metabolism

Central metabolism is an important source of precursors for the synthesis of secondary metabolites. There are several lines of evidence that the range and levels of secondary metabolites are regulated in response to the C and N status in tobacco [101,462]. Phenylpropanoids represent a diverse group of secondary metabolites, with roles in plant structure, defense and signaling [463]. They are synthesized via the shikimate pathway in the plastid, with aromatic amino acids as precursors. In the o/exTrxm genotype there was a dramatic decrease in two shikimate pathway-related compounds such as quinic and caffeoylquinic acids (Table 3.2), the latter being one of the predominant soluble phenylpropanoids in the *Solanaceae* [464]. This result is in accordance with a previous work where a stimulation of phenylpropanoid metabolism in response to low nitrate was demonstrated [462]. Hence, the higher accumulation of nitrate (Figure 3.7D) in the o/exTrxm genotype could account for the decrease in quinic and caffeoylquinic acids. Moreover, phenylpropanoids are synthesized from Phe, and we also show a specific decrease in this amino acid in the o/exTrxm genotype (Table 3.1). Alternatively, the decreased phenylpropanoid content in the o/exTrxm genotype could be related to a decrease in the phospho*enol*pyruvate (PEP) translocator activity [119]. Interestingly, an increase in PEPC activity, which catalyzes the conversion of PEP and HCO^-_3 to oxaloacetate and inorganic phosphate, occurred in these plants (Figure 3.2). Oxaloacetate is the precursor of most of the amino acids that are increased in the o/exTrxm genotype. Hence, our results suggest that in the o/exTrxm genotype PEP preferentially serves as PEPC substrate instead of being exported through the PEP translocator to the chloroplast, thus negatively affecting the phenylpropanoid content. In agreement with this, Arabidopsis PEPC mutants largely reduced the flux from PEP to oxaloacetate and, thereby, suppressed the GS/GOGAT

cycle and subsequent ammonium assimilation [465], a phenotype completely opposite to that of the o/exTrxm genotype.

3.5 Supplementary material

3.5.1 Supplementary figures

```
A.thaliana      MAQILAASPTCQMRVPKHSSV-IASSSKLWSSVVLKQKKQSN-NKVRGFRVLALQSDNST
C.lineata       MAQILAPSTQWQMRITKTSPNASPVTSNMWSSLLMKQNKKAT--SSAKFRVLAIKSENGT
N.tabacum       MAQILAPSAQWQMRMTKSSTDANPLTSKMWSSVVLKQNKRLAVKSSAKFRVFALQSDSGT
L.japonicus     MAQILAPSTQWQTRITKTSPNASPITSNMWSSLLWKQNKKVA--RASKFRVLAIKSDGST

A.thaliana      VNRVETLLNLDTKPYSDRIIAEYIWIGGSGIDLRSKSRTIEKPVEDPSELPKWNYDGSST
C.lineata       INRLENLLDLDITPYTDKIIAEYIWVGGTGIDVRSKSRTIARPVEHPSELPKWNYDGSST
N.tabacum       VNRVEQLLNLDVTPYTDKIIAEYIWIGGSGIDMRSKSRTISKPVKHASELPKWNYDGSST
L.japonicus     INRLEGLLNLDVTPYTDKFIAEYIWIGGTGVDVRSKSRTISKPVSHPSELPKWNYDGSST

A.thaliana      GQAPGEDSEVILYPQAIFRDPFRGGNNILVICDTWTPAGEPIPTNKRAKAAEIFSNKKVS
C.lineata       GQAPGDDSEVILYPQAIFKDPFRGGNNILVICDAYTPAGEPIPTNKRHRAAEIFSNPKVQ
N.tabacum       GQAPGEDSEVILYPQAIFKDPFRGGNNILVICDAYTPAGEPIPTNKRHKAAQIFSDSKVV
L.japonicus     GQAPGDDSEVILYPQAIFRDPFRGGNNILVICDAYTPQGEPIPTNKRHRAAEIFSNPKVQ

A.thaliana      GEVPWFGIEQEYTLLQQNVKWPLGWPVGAFPGPQGPYYCGVGADKIWGRDISDAHYKACL
C.lineata       AEVPWYGIEQEYTLLQTNVNWPLGWPVGGYPGPQGPYYCSAGADKSFGRDISDAHYKACL
N.tabacum       SEVPWFGIEQEYTLLQQNVKWPLGWPVGGYPGPQGPYYCGAGADKSFGRDISDAHYKACL
L.japonicus     AEIPWYGIEQEYTLLQTDVKWPLGWPVGGYPGPQGPYYCAAGADKSFGRDISDAHYKACL

A.thaliana      YAGINISGTNGEVMPGQWEFQVGPSVGIDAGDHVWCARYLLERITEQAGVVLTLDPKPIE
C.lineata       YAGINISGTNGEVMPGQWEFQVGPSVGIEAGDHIWAARYILERITEQAGVVLSLDPKPIQ
N.tabacum       YAGINISGTNGEVMPGQWEFQVGPSVGIEAGDHIWCARYILERITEQAGVVLSLDPKPIE
L.japonicus     YAGINISGTNGEVMPGQWEYQVGPSVGIEAGDHIWASRYLLERITEQAGVVLTLDPKPIE
*
A.thaliana      GDWNGAGCHTNYSTKSMREEGGFEVIKKAILNLSLRHKEHISAYGEGNERRLTGKHETAS
C.lineata       GDWNGAGCHTNYSTKSMREEGGFEVIKKAILNLSLRHSDHIRAYGEGNERRLTGKHETAD
N.tabacum       GDWNGAGCHTNYSTLSMREEGGFEVIKKAILNLSLRHKEHISAYGEGNERRLTGKHETAS
L.japonicus     GDWNGAGAHTNYSTKSMREEGGFEVIKKAILNLSLRHQDHIRAYGEGNERRLTGKHETAD
*
A.thaliana      IDQFSWGVANRGCSIRVGRDTEAKGKGYLEDRRPASNMDPYIVTSLLAETTLLWEPTLEA
C.lineata       INTFSWGVANRGCSIRVGRDTEKNGKGYLEDRRPASNMDPYVVTSLLAETTLLWEPTLEA
N.tabacum       IDKFSWGVANRGASIRVGRDTEKQGKGYLEDRRPASNMDPYVVTGLLAETTILWEPTLEA
L.japonicus     INTFSWGVANRGCSIRVGRDTEKEGKGYLEDRRPASNMDPYVVTALLAETTLLWEPTLEA

A.thaliana      EALAAQKLSLNV
C.lineata       EALAAQKIALKV
N.tabacum       EALAAQKLALNV
L.japonicus     EALAAQKIQLKV
```

Figure S3.1. Alignment of the amino acid sequence of GS2 using the CLUSTALW software. *Arabidopsis thaliana* (Q43127), *Canavalia lineata* (AAF17703), *Nicotiana tabacum* (XP_016440217) and *Lotus japonicus* (AAN84563). The chloroplast-specific conserved cysteine residues (asterisks) are highlighted in a yellow box [326,445].

A

Primers[a]	Forward (5'-3')	Reverse (5'-3')
DiT1 (XM_016606358.1)	GGGACTTGGTGCTTGTGTTT	GCAATTAACCATGGGATTGG
DiT2 (NM_001325346)	GATCTCCCGGATGTCTTCAA	GACCCAAGAACTTCCACCAA

[a]GenBank accession numbers (NCBI) are indicated in parenthesis

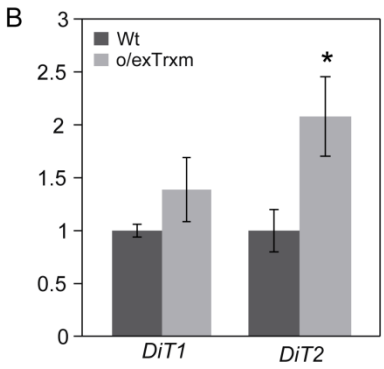

Figure S3.2. RT-qPCR analysis of *DiT1* and *DiT2* expression in tobacco Wt and o/exTrxm plants. Accumulation of mRNA was analysed by quantitative RT-PCR using the specific primers shown in (A). Relative expression levels were normalized to 16s rRNA expression. Graphical representation (B) shows the fold change as the mean of the different biological repeats (n=3). Error bars represent SE. Statistical significance compared with Wt plants is indicated by asterisks (*P*< 0.05, Student's t-test).

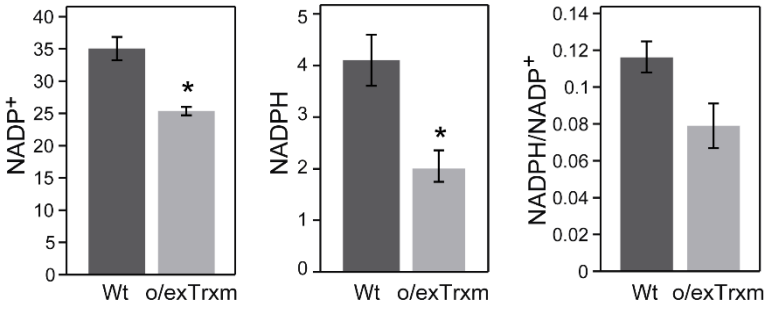

Figure S3.3. Effect of Trx m overexpression on the pyridine nucleotide content. Concentration of $NADP^+$ and NADPH ($nmol.g^{-1}$ FW) in Wt and o/exTrxm tobacco leaves after 4 h illumination were measured as described in Chapter I, section 1.5.1. Results are the mean ± SE of 4 individual plants. Statistical significance compared with Wt plants is indicated by asterisks (*P*< 0.05, Student's *t*-test).

3.5.2 Supplementary tables

Table S3.1. **Changes in the levels of the 42 annotated metabolites after 4 h illumination in o/exTrxm plants relative to Wt.** Metabolite profiling was performed using GC-TOF-MS analysis. Results are means ± SD (n=4). Values that are significantly different from the Wt according to the Student's *t*-test are indicated in bold (*P* value < 0.05). n.d, not detected.

	Wt	o/exTrxm
Amino acids		
DL-serine	**1 ± 0.19**	**2.06 ± 0.27**
DL-alanine	**1 ± 0.09**	**1.76 ± 0.28**
DL-pyroglutamic acid	1 ± 0.25	1.45 ± 0.27
L-aspartic acid	1 ± 0.34	1.42 ± 0.30
DL-glutamine	1 ± 0.42	1.41 ± 0.19
DL-asparagine	1 ± 0.13	1.25 ± 0.16
DL-glutamic acid	1 ± 0.08	0.89 ± 0.11
DL-methionine	1 ± 0.11	0.69 ± 0.11
DL-threonine	1 ± 0.21	0.53 ± 0.28
DL-phenylalanine	**1 ± 0.07**	**0.49 ± 0.07**
Glycine	1 ± 0.32	0.49 ± 0.12
L-proline	1 ± 0.41	0.39 ± 0.14
Sugars		
1.6-anhydro-beta-D-glucose	1 ± 0.15	0.96 ± 0.07
DL-rhamnose	1 ± 0.13	0.90 ± 0.06
D-sucrose	1 ± 0.08	0.77 ± 0.12
DL-fucose	**1 ± 0.18**	**0.53 ± 0.04**
D-fructose	1 ± 0.31	0.48 ± 0.21
Gentiobiose	1 ± 0.24	0.48 ± 0.08
D-xylose	1 ± 0.30	0.32 ± 0.05
D-glucose	1 ± 0.53	0.17 ± 0.06
D-maltose	**1 ± 0.03**	**n.d**
alpha-alpha'-D-trehalose	**1 ± 0.31**	**n.d**
Organic acids		
trans-caffeic acid	1 ± 0.25	1.30 ± 0.09
Nicotinic acid	1 ± 0.09	1.18 ± 0.20
Citric acid	1 ± 0.21	1.13 ± 0.40
Fumaric acid	1 ± 0.18	1.12 ± 0.18
DL-malic acid	1 ± 0.06	1.01 ± 0.09
n-nonanoic acid	1 ± 0.22	0.93 ± 0.14
4-amino-butyric acid	1 ± 0.11	0.87 ± 0.16
Pyruvic acid	1 ± 0.15	0.86 ± 0.25
Succinic acid	1 ± 0.16	0.86 ± 0.07
DL-malic acid	1 ± 0.18	0.85 ± 0.17
Phosphoric acid	1 ± 0.32	0.60 ± 0.19
2-oxo-glutaric acid	1 ± 0.21	0.41 ± 0.13
cis-3-caffeoylquinic acid	**1 ± 0.18**	**0.35 ± 0.06**
Threonic acid	**1 ± 0.15**	**0.39 ± 0.09**
trans-3-caffeoylquinic acid	**1± 0.19**	**0.25 ± 0.06**
DL-glyceric acid	1 ± 0.41	0.15 ± 0.03
D(-)-quinic acid	**1 ± 0.37**	**0.08 ± 0.02**
Others		
Putrescine	1 ± 0.13	1.60 ± 0.24
myo-inositol	1 ± 0.23	0.55 ± 0.11
Tyramine	1 ± 0.31	0.42 ± 0.06

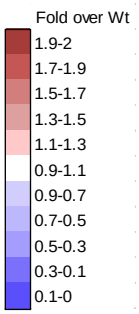

Table S3.2. **Enzyme activities in plants overexpressing Trx f from the chloroplasts genome**. Samples were taken after 4 h illumination from leaves of plants grown in phytotron under 16h-light/8h-dark photoperiod and assayed for phosphoglycerokinase (PGK), NADP-dependent glyceraldehyde-3-phosphate dehydrogenase (NADP-GAPDH), fructose-1,6-bisphosphatase (FBPase), triose-phosphate isomerase (TPI), glutamine synthetase (GS), ferredoxin-dependent glutamate synthase (Fd-GOGAT), NAD-dependent glutamate dehydrogenase (NAD-GDH) and phospho*enol*pyruvate carboxylase (PEPC) activities. Results, expressed as nmol.g^{-1} FW.min^{-1}, are the mean ± SE of five individual plants. Statistical significance compared with Wt plants is indicated by asterisks (P< 0.05, Student's *t*-test).

	Wt	**o/exTrxf**
PGK	706.9 ± 81.0	545.9 ± 55.2*
NADP-GAPDH	10472.7 ± 2679.2	9837.0 ± 2284.1
FBPase	92.0 ± 29.4	240.7 ± 62.0*
TPI	90539.5 ± 9493.0	112228.6 ± 9964.7
GS	279.2 ± 58.7	256.7 ± 35.5
Fd-GOGAT	342.2 ± 58.2	342.2 ± 18.5
NAD-GDH	16.9 ± 3.2	20.6 ± 1.0
PEPC	300.8 ± 43.9	218.9 ± 16.2*

CAPÍTULO IV

In vivo **trapping of plastid thioredoxin targets in** ***Nicotiana benthamiana*** **plants**

4.1 Introduction

Plant thioredoxins (Trxs), initially identified as light-dependent regulators of key photosynthetic metabolism enzymes in chloroplasts [13], constitute a complex redox system supported by multiple Trx isoforms [393]. In chloroplasts, several types of typical and atypical Trxs have been reported [142, 169,185]. Among them, Trx f, m and NTRC (C-type NADPH dependent Trx reductase) are the most studied plastid Trxs. The typical Trxs f and m play a key role in the ferredoxin (Fd)/Trx system of oxygenic photosynthetic organisms [225]. In this system, electrons flow from light-reduced Fd to Trxs via Fd-Trx reductase (FTR) so as to regulate the activity of target proteins through the reduction of specific disulfide groups. Both Trxs f and m have been involved in multiple functions such as stress response [182], starch metabolism [308,316], lipid biosynthesis [466], chlorophyll synthesis and breakdown [258], biogenesis of photosystem II (PSII) [259], Calvin-Benson cycle [183,228], protein folding and import [467], translation and chaperone activity [132] have been reported for these Trxs in recent years. Conversely, the atypical Trx NTRC constitutes *per se* a redox regulatory system in chloroplasts that reduces target proteins using NADPH as electron donor [191,200]. NTRC was suggested to be responsible of regulatory functions sometimes similar but, in other cases, distinct from those of the classically known Fd/Trx system [222], being an efficient reductant of proteins involved in antioxidant defence [200,221], chlorophyll synthesis [199,253] or gene expression [468].

Given this outlook, with plants exhibiting the most versatile Trx system, the specificity of each Trx type for their targets become fundamental for understanding Trx controlled redox-regulated physiological processes. Before the advent of proteomics, target proteins were identified by biochemical approaches [225]. But it was not until 2001 when the repertoire of Trx-target proteins considerably expanded, reaching to more than 400 potential Trx targets identification in plants [226] thanks to the development of proteomics. Two main approaches were employed for this purpose. The first method, named reductome approach, uses thiol specific probes to label Trx targets in a crude extract *in vitro*. In this procedure, the enzymatic Trx system (NADPH, NTR and Trx) is reconstituted and used to reduce disulfide bonds allowing detection of Trx-targeted proteins and their identification by mass spectrometry (MS). Free sulfhydryl groups (−SH) are labelled with different probes such as monobromobimane fluorescent probe [216, 233, 235,236,469,470], cyanine 5 maleimide fluorescent dye [237], biotinylated probes [230], radioactive iodoacetamide [238], cleavable isotope-coded affinity tag reagents [239,471] or cysteine-reactive tandem mass tags [240]. The advantage of the last two probes over other methods relies on the accurate quantification of the cysteine (Cys) redox status and localization of the Trx target Cys residues.

The second approach is based on the covalent binding between a mutant monocysteinic Trx mutant and its target proteins. It takes advantage of the two-step disulfide bridge reduction reaction [472] where the more N-terminal catalytic Cys of the Trx attacks the disulfide bridge of the target protein, reducing one Cys of the target and establishing a heterodisulfide bridge that is then attacked by the more C-terminal Cys, allowing the release of both the reduced target and the oxidized Trx. Therefore, mutation of the second Cys residue (buried Cys), into serine or alanine, allows to stabilize the heterodimer trapping potential Trx targets from different cell lysates. This strategy was performed for the first time in yeast [243], but a modification of the technique consisting of mutant Trx immobilization on a resin (batch method), Trx-bound targets elution by adding a chemical reductant such as DTT and identification by MS, was then broadly used in plants [157, 244–248,467]. Moreover, some authors have compared different proteomic procedures in parallel [229–231,287]. An interesting point emerging from these studies is the apparent lack of specificity shown by proteomic procedures applied to screen for Trx targets. Thus, the column-bound mutant Trx interacts with potential targets irrespective of the type used (Trx m, Trx f, Trx h or *Escherichia coli* Trx) [245]. Even using a cytosolic Trx, it was possible to identify chloroplastic or mitochondrial target enzymes [246,247].

Considering the loss of specificity for different Trx types showed by these *in vitro* approaches, and with the aim of gaining insight into such specificity, here we developed an *in vivo* strategy based on *Agrobacterium tumafaciens*-mediated monocysteinic Trx f, Trx m or NTRC mutant overexpression in *Nicotiana benthamiana* plants, combined with MS-based proteomics. Our method led to the identification of numerous proteins that potentially associated with plastid Trxs. To our knowledge, this study is the first to distinguish among three types of Trxs *in vivo*.

4.2 Material and methods

Plant material and growth conditions

N. benthamiana plants were grown in pots (organic soil/vermiculite, 70/30 v/v) in a phytotron under 16-h light/8-h dark photoperiod at 28°C under a photosynthetic photon flux density of 80 $\mu mol.m^{-2}.s^{-1}$ and a relative humidity of 65%. Plants were watered once a week with 50% diluted Hoagland's solution. After 5 weeks, fully developed leaves were used for agroinfiltration.

Construction of monocysteinic Trx mutants and plant transformation

Site-directed mutagenesis was performed by PCR using *NtTrxf, NtTrxm* [346] or *AtNTRC* (GenBanK: NM_129731) cDNAs as templates. The *Trxf-C47S* mutant was produced with C47S-fand C47S-r primers (Supplementary material, Table S4.1) in

order to introduce a single change to replace Cys47 with Ser, and Trxf-f and Trxf-r primers (Supplementary material, Table S4.1) to amplify full gene length. The transit peptide of the tobacco Rubisco small subunit was amplified using Rbcs-f and Rbcsf-r primers, and translationally fused to Trxf-C47S by overlapping PCR with Rbcs-f and Trxf-r primers (Supplementary material, Table S4.1). Trxm-C40S and NTRC-C457S were obtained following the same strategy using the corresponding primers (Supplementary material, Table S4.1). In case of NTRC, the Cys457 correspond to the nucleophilic Cys in the Trx domain of the protein. The chimeric genes were introduced into a pBin20 binary vector [473] under the control of the Cauliflower Mosaic Virus 35S promoter and transformed into GV3101 *A. tumefaciens* strain.

N. benthamiana plants were co-infiltrated into the abaxial air spaces of 5-week-old leaves with two *A. tumefaciens* clones harboring the single mutant constructions (Trxf-C47S, Trxm-C40S or NTRC-C457S) and the P19 gene silencing suppressor, as previously described by [441] using a 1-ml syringe without needle.

Protein preparation and purification of target proteins

Leaf tissue within the infiltrated area was collected 5 days post-agroinfiltration and ground immediately in liquid nitrogen. Leaves were resuspended in extraction buffer [20 mM sodium phosphate pH 7.4, 150 mM NaCl, 25 mM imidazole, 0.1% Triton X-100 and complete protease inhibitor cocktail (Roche Diagnostics, Mannheim, Germany)] and incubated 45 min on ice. The homogenate was filtered through two layers of Miracloth (Calbiochem, Nottingham, UK), and centrifuged at 15,800 *g* for 20 min at 4°C. Supernatant was then recovered, passed through 0.45 µm filter and purified by chromatography on affinity columns packed with Ni-NTA agarose (Qiagen, Hilden, Germany) according to manufacturer's instructions. The resin was washed with 20 column volumes of wash buffer (20 mM sodium phosphate pH 7.4, 150 mM NaCl, 45 mM imidazole and protease inhibitor cocktail) to fully remove non-specifically bound proteins. Target proteins were then eluted in wash buffer containing 20 mM DTT. Finally, monocysteinic Trxs were removed from the column using wash buffer with 500 mM imidazole.

Proteomic analysis

Sample preparation. Eluates were homogenized in lysis buffer (7 M urea, 2 M thiourea, 50 mM DTT) and protein concentration was quantified with the Bradford assay kit (Bio-Rad, Hercules, CA, USA) and then precipitated with the ReadyPrep 2-D cleanup kit (BioRad, USA). The protein extract for each sample was diluted in Laemmli buffer and loaded into a 1.5 mm thick polyacrylamide gel with a 4% stacking gel casted over a 15% resolving gel. The run was stopped as soon as the front entered 3 mm into the resolving gel to concentrate the whole proteome in the stacking/resolving gel interface. Bands were stained with Coomassie Brilliant Blue and excised from the gel.

Purification and concentration of peptides was performed using C18 Zip Tip Solid Phase Extraction (Millipore, USA).

Mass Spectrometry analysis. Peptide mixtures were separated by reverse phase chromatography using an Eksigent nanoLC ultra 2D pump fitted with a 75 μm ID column (Eksigent 0.075 × 250). Samples were first loaded for desalting and concentration into a 0.5 cm length 100 μm ID precolumn packed with the same chemistry as the separating column. Mobile phases were 100% water 0.1% formic acid (FA) (buffer A) and 100% Acetonitrile 0.1% FA (buffer B). Column gradient was developed in a 200 min two step gradient from 5% B to 25% B in 160 min and 25%B to 40% B in 21 min. Column was equilibrated in 95% B for 8 min and 5% B for 11 min. During all process, precolumn was in line with column and flow maintained all along the gradient at 300 nl/min. Eluting peptides from the column were analyzed using a Sciex 5600 Triple-TOF system. Information data was acquired upon a survey scan performed in a mass range from 350 m/z up to 1250 m/z in a scan time of 250 ms. Top 35 peaks were selected for fragmentation. Minimum accumulation time for MS/MS was set to 100 ms giving a total cycle time of 3.8 s. Product ions were scanned in a mass range from 230 m/z up to 1500 m/z and excluded for further fragmentation during 15 s.

Data Analysis. The MS/MS data acquisition was performed using Analyst 1.7.1 (Sciex) and spectra files were processed through Protein Pilot Software (v 5.0.1-Sciex) using Paragon™ algorithm (v 5.0.1) for database search [474]and Progroup™ for data grouping, and searched against the concatenated target-decoy UniProt proteome database (*Nicotiana tabacum)*. False discovery rate was performed using a non-lineal fitting method [475] and displayed results were those reporting a 1% Global false discovery rate or better.

The peptide quantification was performed using the Progenesis LC−MS software (ver. 2.0.5556.29015, Nonlinear Dynamics). Using the accurate mass measurements from full survey scans in the TOF detector and the observed retention times, runs were aligned to compensate for between-run variations in our nanoLC separation system. To this end, all runs were aligned to a reference run automatically chosen by the software, and a master list of features considering m/z values and retention times was generated. The quality of these alignments was manually supervised with the help of quality scores provided by the software. The peptide identifications were exported from Protein Pilot software and imported in Progenesis LC−MS software where they were matched to the respective features. Output data files were managed for subsequent statistical analyses and representation. Proteins identified by site (identification based only on a modification), reverse proteins (identified by decoy database) and potential contaminants were filtered out. Proteins quantified with at least two unique peptides, *p*-value lower than 0.05, and a Log2 fold change >1.8 were considered as potential interacting partners of Trx f, Trx m or NTRC proteins.

Bioinformatics and annotations. For this purpose, homology search was first performed for all the identified sequences with NCBI blastp program against NCBI nr database. In this way, Arabidopsis (*Arabidopsis thaliana*) orthologs were identified in order to facilitate the following information gathering process. Then, to determine the functional properties of the identified proteins, the protein sequences were mapped with Gene Ontology Terms (http://geneontology.org/)

4.3 Results

Identification of proteins captured as Trx targets

To increase the number and specificity of proteins targeted by Trx f, Trx m and NTRC, we developed an *in vivo* approach based on the ability of monocysteinic Trxs to form a covalent disulfide-bonded heterodimer with its targets [476,477]. To this end, we generated three monocysteinic His-tagged Trx mutants (Trxf-C47S, Trxm-C40S or NTRC-C457S) that were overexpressed in *N. benthamiana* plants by agroinfiltration. The Trx-target heterodimers covalently bounded inside the chloroplast were purified by Ni affinity chromatography from leaf protein extracts 5 days after infiltration, when the expression of the mutant variants in leaf tissues was higher. Plants agroinfiltrated with a strain containing the empty pBin20 vector were used as negative control, considering that their eluates enclose proteins that interact unspecifically with the isolation system used. After elution with DTT to recover the trapped targets, columns were eluted with imidazole in order to release and visualize resin bound Trxs (Figure 4.1), confirming the overexpression level achieved in the agroinfiltrated plants.

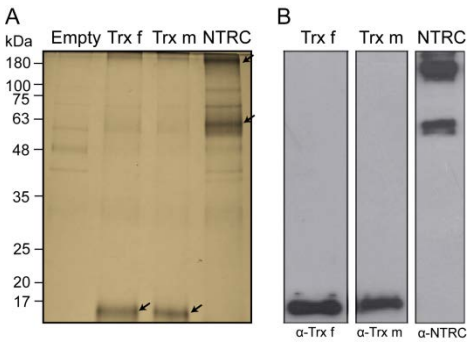

Figure 4.1. **Silver staining and western blot analysis of fractions collected with imidazole from *N. benthamiana* plants agroinfiltrated with the monocysteinic mutant variants of Trx f, Trx m and NTRC or the empty vector as control.** Similar volumes were separated in 13.5% acrylamide gels and then proteins were visualized by silver staining (A) or immunoblotted (B) with specific anti-Trxf, anti-Trx m (1: 5000; [132]) or anti-NTRC (1:1000; [191]) antibodies. Arrows indicate the corresponding overexpressed Trx for each fraction.

This analysis allowed identifying hundreds of proteins in the *N. tabacum* database (Figure 4.2). Amog them, candidate targets were selected on the basis of a Log2 fold change > 1.8 relative to those identified in extracts from *N. benthamiana* plants agroinfiltrated with empty vector. This selection led to the identification of 39, 41 and 120 proteins for Trx f, Trx m and NTRC, respectively, in the *N. tabacum* database (Supplementary material, Tables S4.2, S4.3 and S4.4).

Although genome assembly for *N. tabacum* has recently improved [478], Arabidopsis remains the best annotated plant [479,480]. Therefore, the predicted proteins were also matched to their closest Arabidopsis orthologs by a BLASTp search [481] to assess their likely subcellular location. This analysis showed the dominance of plastid proteins over other suborganellar locations, considering that 48, 58 and 61% of the candidate proteins for Trx f, Trx m and NTRC, respectively, were plastid localized. The rest of proteins were discarded as plastid Trx target candidates. Probably, the identification of extraplastidial proteins was a consequence of the use of crude leaf extracts for the purification assay, which allows interaction of non-plastidic proteins with monocysteinic Trx mutants during the extraction process.

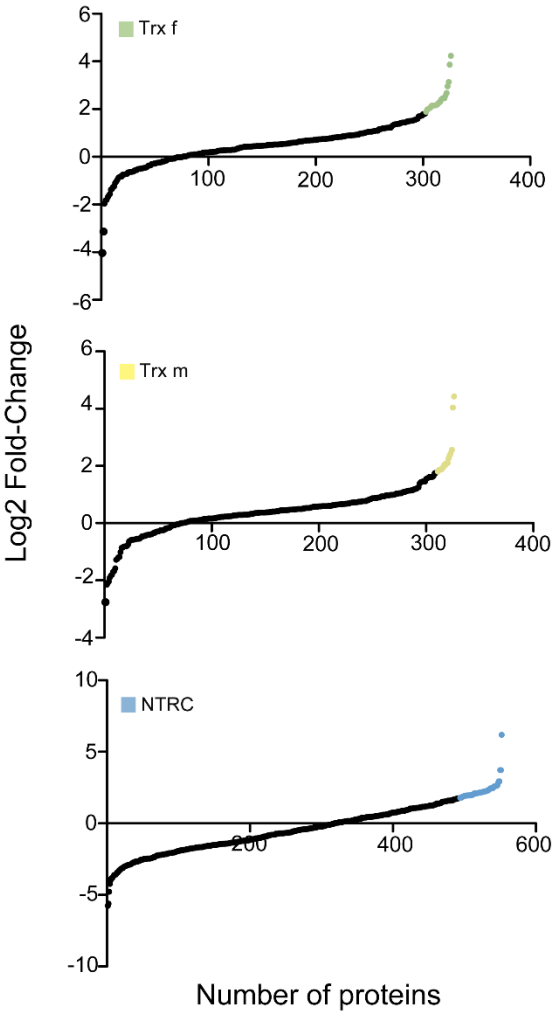

Figure 4.2. Proteomic analysis of the Trx interacting proteins. Using quantitative mass spectrometry, eluting Trxs proteomes were compared with eluting empty vector proteome. The candidate interacting Trx proteins are shown in green for Trx f, yellow for Trx m and blue for NTRC.

Analysis of candidate Trx partners

Tables 4.1 and 4.2 summarize the plastid-localized proteins identified as potential targets for Trx f (15 proteins), Trx m (18 proteins) and NTRC (68 proteins). These tables also provide information about the location of target proteins inside the chloroplast, distinguishing between stroma, membrane thylakoid and lumen. It should be note that some of the identified proteins are well-known Trx targets, such as NADP-glyceraldehyde-3-phosphate dehydrogenase (NADP-GAPDH), sedoheptulose-bisphosphatase (SBPase) or Rubisco activase [15], confirming the applicability of the approach. Because Trx target proteins often form an inter- or intramolecular Trx-reducible disulfide, we further analyzed the number of conserved Cys residues in the new potential Trx partners by CLUSTALW amino acid sequence alignment and the result was also indicated in Tables 4.1 and 4.2. We found 6 previously undescribed targets for Trx f and 9 for Trx m (with grey background in Table 4.1). Concerning NTRC, 5 proteins were previously described as NTRC partners: 2-Cys Prx B, Trx m, FTR, FBPase and AGPase small subunit. From de remaining proteins, 28 have already been described as targets of other Trx types (with green colour background in Table 4.2), 15 are totally new (with grey background in Table 4.2), 6 have a lumenal localization and the remaining 14 proteins had no conserved Cys and therefore cannot be considered as redox-interacting proteins.

Table 4.1. List of plastid proteins identified as potential Trx f and Trx m targets. The table shows identified proteins in *N. tabacum* database, as well as its homologous in Arabidopsis with the corresponding identity %. Localization inside the chloroplast is indicated. The potential new targets are indicated with a grey background for which the number of conserved Cys is shown.

Nicotiana tabacum		*Arabidopsis thaliana*			Trx f	Trx m	Cys	Subcellular localization
UniProtKB	**Protein name**	**UniProtKB**	**Protein name**	**Identity %**				
Cell redox homeostasis								
A0A1S4A3V7	2-Cys peroxiredoxin BAS1	Q9C5R8	2-Cys peroxiredoxin BAS1-like (2-Cys Prx B)	77	x	x		stroma
A0A1S4A969	Glutathioneperoxidase	P52032	Phospholipid hydroperoxide glutathione peroxidase 1 (PHGPx)	72.4		x		stroma
A0A1S4C620	Peptide methionine sulfoxide reductase-like	P54150	Peptide methionine sulfoxide reductase A4 (MSRA4)	62		x		stroma
A0A1S4B900	Peroxiredoxin Q	Q9LU86	Peroxiredoxin Q (Prx Q)	76.3	x	x		lumen
A0A1S4D678	Peroxiredoxin-2E-2	Q949U7	Peroxiredoxin-2E (Prx IIE)	57.7	x			stroma
A0A1S4ASD9	Thioredoxin-like 2	Q8LCT3-2	Thioredoxin-like 2-2 (Lilium 2)	65.5		x	2	stroma
A0A1S4D2Y9	Thioredoxin-like 4	Q9C5C5	Thioredoxin-like 4 (Lilium 5)	66.3	x	x	2	stroma
Photosynthesis								
A0A1S4CIH3	PGR5-like protein 1A	Q8H112	PGR5-like protein 1A (PGRL1)	72.8	x	x		Thylakoid membrane
Carbon metabolism								
A0A1S4ATB8	Glyceraldehyde-3-phosphate dehydrogenase	P25857	Glyceraldehyde-3-phosphate dehydrogenase GAPB (NADP-GAPDH)	85.8	x			stroma
A0A1S3YQS9	Malate dehydrogenase (NADP)	Q8H1E2	Malate dehydrogenase (NADP-MDH)	79.4		x		stroma
A0A1S4CZ71	Phosphogluca nwaterdikinase	Q6ZY51	Phosphogluca nwaterdikinase (PWD)	61.2	x	x	7	stroma
A0A1S4A3L9	Ribulose bisphosphate carboxylase/oxygenase activase 1	P10896	Ribulose bisphosphate carboxylase/oxygenase activase (Rubisco activase)	78.6	x	x		stroma
A0A1S3YEX0	Sedoheptulose-1,7-bisphosphatase	P46283	Sedoheptulose-1,7-bisphosphatase (SBPase)	81.5		x		stroma
A0A1S4DEY3	Starch synthase	Q9MAQ0	Granule-bound starch synthase 1 (GBSS1)	74.1		x	6	stroma

Table 4.1. List of plastid proteins identified as potential Trx f and Trx m targets (continuación).

Protein folding									
A0A1S4DGW7	Peptidylprolylisomerase	Q9LYR5	Peptidyl-prolyl cis-transisomerase FKBP19 (PPIase FKBP19)	87.7	x				lumen
Transcription and translation regulation									
A0A1S4DL03	50S ribosomal protein L18	Q9SX68	50S ribosomal protein L18	83.8		x	1		stroma
Q6T7F3	Amidophosphoribosyltransferase	Q9STG9	Amidophosphoribosyltransferase 2 (ATase2)	77.6	x	x	9		stroma
A0A140G1V5	Ribosomalprotein S3	P56798	30S ribosomalprotein S3	87.6	x	x	3		stroma
A0A1S4CR05	Uridinekinase	Q9FKS0	Uridine kinase-like protein 1 (UK)	87.4	x	x	#		stroma
Secondary metabolism									
A0A1S4B8Q6	Cis-abienolsynthase	G3CCC1	Cis-abienolsynthase (ABS) *		x	x	#		stroma
Amino acid biosynthesis									
A0A1S4DHJ8	5'-adenylylsulfate reductase 2	P92981	5'-adenylylsulfate reductase 2 (APR2)	75.4	x	x			stroma
Unknown function									
A0A1S4CQQ3	Thylakoid lumenal 29 kDaprotein	P82281	Thylakoid lumenal 29 kDa protein (TL29)	69.4	x				lumen

*No orthologs are present in the A rabidopsis genome
Database is not sufficiently developed to permit the assignment of conserved amino acids

Table 4.2. List of plastid proteins identified as potential NTRC targets. The table shows identified proteins in *N. tabacum* database, as well as its homologous in Arabidopsis with the corresponding identity %. Localization inside the chloroplast is indicated. The new potential targets, located in the stroma or the thylakoid membrane, are indicated with a grey background and their number of conserved Cys is shown. The proteins previously identified as targets of other Trx types are indicated with a green background.

Nicotiana tabacum		*Arabidopsis thaliana*			Cys	Subcellular localization
UniProtKB	**Protein name**	**UniProtKB**	**Protein name**	**Identity %**		
Cell redox homeostasis						
A0A1S4A3V7	2-Cys peroxiredoxin BAS1	Q9C5R8	2-Cys peroxiredoxin BAS1-like (2-Cys Prx B)	77		stroma
A0A1S4B1Q8	CBS domain-containing protein CBSX1	O23193	CBS domain-containing protein CBSX1 (CDCP2)	63.6		stroma
A0A1S3Y8V8	Glutathione S-transferase DHAR3	Q8LE52	GSH-dependent dehydroascorbate reductase 3 (DHAR3)	72.5		stroma
A0A1S3ZZS2	Probable L-ascorbateperoxidase 6	Q42593	L-ascorbateperoxidase T (tAPX)	73.7		thylakoid membrane
A0A1S4A969	Glutathioneperoxidase	P52032	Phospholipid hydroperoxide glutathione peroxidase 1 (PHGPx)	72.4		stroma
W0KRH1	Superoxidedismutase	Q9LU64	Superoxide dismutase [Fe] 2 (FSD2)	59.1	0	thylakoid membrane
A0A1S4CCB3	Thioredoxin-like	Q9SEU6	Thioredoxin M4 (Trx m4)	53.3		stroma
Photosynthesis						
A0A140G1P8	ATP synthase CF0 B subunit	P56759	ATP synthase subunit b	88.6	1	thylakoid membrane
A0A1S4CSA5	ATP synthase delta chain	Q9SSS9	ATP synthase subunit delta	60.5		thylakoid membrane
P00823	ATP synthase subunit alpha	P56757	ATP synthase subunit alpha	94		thylakoid membrane
A0A140G1S2	ATP synthase subunit beta	P19366	ATP synthase subunit beta	93		thylakoid membrane
A0A1S4CBW5	Chlorophyll a-b binding protein	Q9SY97	Photosystem I chlorophyll a-b binding protein 3-1 (Lhca3.1)	89.4	0	thylakoid membrane
Q0PWS6	Chlorophyll a-b binding protein	Q9C639	Photosystem I chlorophyll a-b binding protein 5 (Lhca5)	38	0	thylakoid membrane
Q40512	Chlorophyll a-b binding protein	Q01667	Photosystem I chlorophyll a-b binding protein 6 (Lhca1)	87.4		thylakoid membrane
A0A1S4BMB0	Chlorophyll a-b binding protein	Q9SHR7	Photosystem II chlorophyll a-b binding protein 2.1 (Lhcb2.1)	89		thylakoid membrane
A0A1S4DIE1	Chlorophyll a-b binding protein	Q9S7M0	Photosystem II chlorophyll a-b binding protein 3 (Lhcb3)	87.5		thylakoid membrane

Table 4.2. List of plastid proteins identified as potential NTRC targets (continuación)**.**

Q0PWS7	Chlorophyll a-b binding protein	Q07473	Photosystem II chlorophyll a-b binding protein CP29.1 (Lhcb4.1)	86.6		thylakoid membrane
A0A140G1T3	Cytochrome b559 subunit alpha	P56779	Cytochrome b559 subunitalpha	99	0	thylakoid membrane
A0A1S3XVT6	Cytochrome b6	P56773	Cytochrome b6	98	2	thylakoid membrane
A0A1S4B832	Cytochrome b6-f complex iron-sulfur subunit	Q9ZR03	Cytochrome b6-f complexiron-sulfur subunit (RISP)	77.8	4	thylakoid membrane
A0A140G1S8	Cytochrome f	P56771	Cytochrome f	90	2	thylakoid membrane
A0A1S3YVN4	Ferredoxin	P16972	Ferredoxin-2 (Fd2)	65.7	4	stroma
A0A1S4B5N2	Ferredoxin-thioredoxin reductase	A0A1P8BDN6	Ferredoxin-thioredoxin reductase subunit A (Variable subunit) 2	46.5		stroma
Q84QE8	Oxygen evolving complex 33 kDa photosystem II protein	Q9S841	Oxygen-evolving enhancer protein 1-2 (OEE-1)	81.3		thylakoid lumenal side
A0A1S4BMY9	Oxygen-evolving enhancer protein 2-2	Q42029	Oxygen-evolving enhancer protein 2-1 (OEE-2)	72.9		thylakoid lumenal side
A0A1S3XRM3	Oxygen-evolving enhancer protein 3-2	Q41932	Oxygen-evolving enhancer protein 3-2 (OEE-3)	68.8	0	thylakoid lumenal side
A0A140G1X0	Photosystem I iron-sulfur center	P62090	Photosystem I iron-sulfur center (PSI-C)	100	9	thylakoid membrane
A0A140G1R3	Photosystem I P700 chlorophyll a apoprotein A1	P56766	Photosystem I P700 chlorophyll a apoprotein A1 (PSI-A)	98	4	thylakoid membrane
A0A140G1R2	Photosystem I P700 chlorophyll a apoprotein A2	P56767	Photosystem I P700 chlorophyll a apoprotein A2 (PSI-B)	98	2	thylakoid membrane
A0A1S3ZIE1	Photosystem I reaction center subunit II	Q9SA56	Photosystem I reaction center subunit II-2 (PSI-D2)	76.6	1	thylakoid membrane
A0A1S4CFV4	Photosystem I reaction center subunit IV A	Q9S831	Photosystem I reaction center subunit IV A (PSI-E1)	71	0	thylakoid membrane
A0A1S4CYN6	Photosystem I reaction center subunit IV B	Q9S714	Photosystem I reaction center subunit IV B (PSI-E2)	58.4	0	thylakoid membrane
D2K7Z2	Photosystem I reaction center subunit	P49107	Photosystem I reaction center subunit N (PSI-N)	69.1		thylakoid membrane
A0A1S4CR54	Photosystem I reaction center subunit VI-1	Q9SUI7	Photosystem I reaction center subunit VI-1 (PSI-H1)	77.2	0	thylakoid membrane
A0A1S4BQS3	Photosystem I reaction center subunit XI	Q9SUI4	Photosystem I reaction center subunit XI (PSI-L)	80.7	1	thylakoid membrane
A0A1S3YQ87	Photosystem II 22 kDaprotein	Q9XF91	Photosystem II 22 kDa protein (CP22)	73.2	0	thylakoid membrane
A0A140G1Q8	Photosystem II CP43 reaction center protein	P56778	Photosystem II CP43 reaction center protein	98		thylakoid membrane

Table 4.2. List of plastid proteins identified as potential NTRC targets (continuación).

Nicotiana tabacum		*Arabidopsis thaliana*			Cys	Subcellular localization
UniProtKB	**Protein name**	**UniProtKB**	**Protein name**	**Identity %**		
A0A140G1U3	Photosystem II CP47 reaction center protein	P56777	Photosystem II CP47 reaction center protein	98.6		thylakoid membrane
A0A140G1Q7	Photosystem II D2 protein	P56761	Photosystem II D2 protein	99		thylakoid membrane
A0A140G1P2	Photosystem II D1 protein	P83755	Photosystem II D1 protein	99.7		thylakoid membrane
A0A1S4A1K3	Plastocyanin	P42699	Plastocyaninmajorisoform	67.7	0	thylakoid lumenal side
Carbon metabolism						
A0A1S4AA023	Fructose-1,6-bisphosphatase	P25851	Fructose-1,6-bisphosphatase 1 (FBPase 1)	86.5		stroma
A7XAQ5	Glucose-1-phosphate adenylyltransferase	P55228	Glucose-1-phosphate adenylyltransferase small subunit (AGPase B)	87.5		stroma
A0A1S3Z1X1	Probable ribose-5-phosphate isomerase 3	Q9S726	Probable ribose-5-phosphate isomerase 3	68.3		stroma
A0A140G1S3	Ribulose bisphosphate carboxylase large chain	O03042	Ribulose bisphosphate carboxylase large chain (Rubisco LSU)	94		stroma
A0A1S3X2Z0	Triosephosphate isomerase	Q9SKP6	Triosephosphate isomerase (TPI)	79.4		stroma
Protein folding						
A0A1S4AH01	10 kDa chaperonin-like	Q9M1C2	10 kDa chaperonin 1	71	2	stroma
A0A077DBL2	20 kDa chaperonin	O65282	20 kDa chaperonin	74	0	stroma
A0A1S4AWT3	Peptidyl-prolyl cis-trans isomerase	Q9ASS6	Peptidyl-prolyl cis-trans isomerase CYP20-2	69.3		thylakoid luminal side
A0A1S3ZH83	Peptidyl-prolyl cis-trans isomerase CYP38	Q9SSA5	Peptidyl-prolyl cis-trans isomerase CYP38	76.8		lumen
A0A1S3XJV2	Peptidyl-prolyl isomerase	O22870	Peptidyl-prolyl cis-trans isomerase FKBP16-3	65.5		lumen
A0A1S4DIY1	Rubisco large subunit-binding protein subunit beta	P21240	Chaperonin 60 subunit beta 1	81.8		stroma
Trancription and translation regulation						
A0A1S4CYJ5	29 kDa ribonucleoprotein A	Q9ZUU4	RNA-binding protein CP29B	59.9		stroma
A0A1S3XX03	31 kDa ribonucleoprotein	Q04836	31 kDa ribonucleoprotein	53	0	stroma

Table 4.2. List of plastid proteins identified as potential NTRC targets (continuación).

A0A1S3Z334	Chloroplast stem-loop binding protein of 41 kDa b	Q9SA52	Chloroplast stem-loop binding protein of 41 kDa b (CSP41-b)	85.8		stroma
A0A1S3ZRR1	Nucleoid-associated protein At4g30620	Q9M098	Nucleoid-associated protein At4g30620	76.4	1	stroma
A0A1S4CGA5	Pentatricopeptide repeat-containing protein At4g30825	O65567	Pentatricopeptide repeat-containing protein At4g30825	63.8	9	stroma
A0A1S3YRF9	Ribosome-recycling factor	Q9M1X0	Ribosome-recycling factor (RRF)	64.4	0	stroma
Amino acid biosynthesis						
A0A1S4CUE0	Ferredoxin-dependent glutamate synthase	Q9ZNZ7	Ferredoxin-dependent glutamate synthase 1 (Fd-GOGAT 1)	83.9		stroma
A0A1S3YTZ2	Ketol-acid reductoisomerase	Q05758	Ketol-acid reductoisomerase	84.8		stroma
A0A1S4APF3	Ornithine carbamoyl transferase	O50039	Ornithine carbamoyl transferase	75.3		stroma
Response to stress						
A0A1S4A194	Soluble inorganic pyrophosphatase 6	Q9LXC9	Soluble inorganic pyrophosphatase 6 (Ppase 6)	74.6	0	stroma
Chlorophyll synthesis						
A0A1S4C5X4	Oxygen-dependent coproporphyrinogen-III oxidase	Q9LR75	Coproporphyrinogen-III oxidase 1 (CPOX)	80.4	2	stroma
Photorespiration						
A0A1S3X073	Phosphoglycolate phosphatase 1B	P0DKC4	Phosphoglycolate phosphatase 1B	66.8	4	stroma
PSII assembly						
A0A1S4DN09	Photosystem II repair protein PSB27-H1	Q9LR64	Photosystem II repair protein PSB27-H1	64.5		thylakoid luminal side
A0A1S4DKC9	Photosystem II stability/assembly factor HCF136	O82660	Photosystem II stability/assembly factor HCF136	78.3		thylakoid lumenal side
Sulfur metabolism						
A0A1S4CCJ9	Cysteine synthase	P47999	Cysteine synthase	83.5		stroma
Unknown function						
A0A1S4BU42	Thylakoid luminal protein TL20.3	Q8H1Q1	Thylakoid luminal protein TL20.3	75.8		lumen

When the identified targets were grouped into different chloroplast processes, we found that they are involved in diverse biological functions (Figure 4.3). Trx f and Trx m targets placed mostly in to cell redox homeostasis (up to 30%) and carbon metabolism (~19 and 28% respectively). However, the main represented group for NTRC was photosynthesis (~50%), followed by cell redox homeostasis, protein folding and transcription and translation regulation (~9% each one).

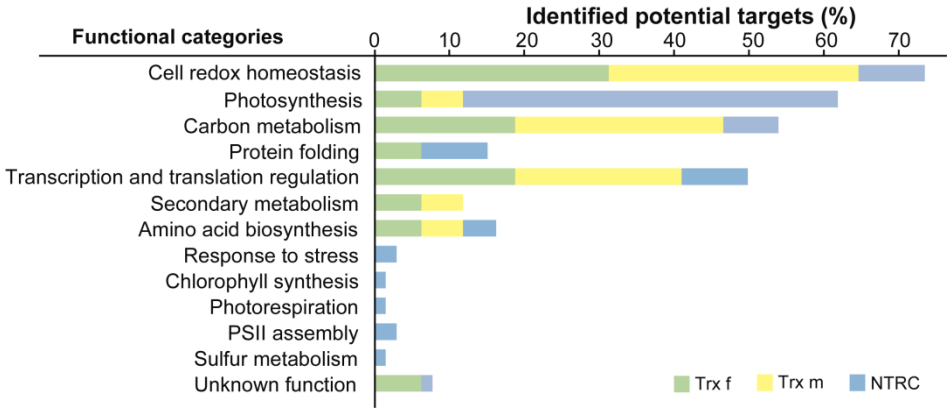

Figure 4.3. Functional classification of proteins identified as putative Trx f, Trx m or NTRC partners in chloroplasts. The plot represents the % of total targets for each Trx in each functional category.

Analyzing the specificity among different Trxs in our system, we observed that targets associated with Trx f and Trx m were mainly coincident (Table 4.1). Among the selected candidate targets, 11 proteins are shared between Trx f and m (Figure 4.4 and Table 4.1), which implies that the specificity between these Trxs and their targets is also poorly conserved in this *in vivo* approach. By contrast, NTRC seems to better conserve the specificity for their targets considering that only two proteins were also identified as Trx f and/or m targets in this assay (Figure 4.4). Such proteins were 2-Cys peroxiredoxin (Prx), which was captured as partner of the three Trxs, and glutathione peroxidase that is listed as Trx m and NTRC target protein (Tables 4.1 an 4.2).

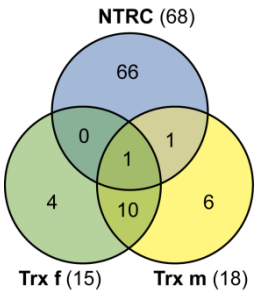

Figure 4.4. Comparison of Trx specificity represented with a Venn diagram showing the overlap between candidate target proteins for Trx f, Trx m and NTRC.

4.4 Discusion

For decades, numerous approaches have been contribute to increase the knowledge of plant Trx interacting proteins, not only in chloroplasts but also in other compartments [226,240]. However, all of them has been performed *in vitro* and consequently, the specificity for each Trx type has not been greatly improved. In case of NTRC, there is only one previous work where some putative targets of its Trx domain were identified [222]. Taking this background, in this study we have developed a new *in vivo* strategy to identify Trx f, Trx m and NTRC targets with the aim of gaining insights into type specificity.

Novelty and specificity of the approach

Unlike the *in vitro* mutant Trx affinity trapping based methods, here we perform an alternative approach where Trxs-target protein interactions were *in vivo* stabilized inside the plant chloroplasts. Usually, infiltration of *A. tumefaciens* into leaves of *N. benthamiana* is used to facilitate the mass production of valuable proteins, a procedure known as molecular farming [482]. In this work, using this technique, we overexpressed a monocysteinic His-tagged Trx mutant that was targeted to the chloroplast by means of the Rubisco small subunit transit peptide. Inside the chloroplast, these mutant variant formed a stable heterodimer with their targets, which were finally trapped via affinity purification. This approach allowed the *in vivo* identification of 15, 18 and 68 potential targets for Trx f, m and NTRC, respectively (Tables 4.1 and 4.2). A similar approach has been broadly used to identify protein-protein interactions in mammalian cells. In this case, cells are transfected with a plasmid coding for a tagged-bait protein that is then isolated, together with bound proteins, using a specific chemical or biological ligand linked to a solid suppor [483]. However, this technique has not been used to trap redox interactors. Only two *in vivo* approaches were used to identify Trx targets: (i) yeast overexpressing an His-tagged-Trx h mutant variant [243], and (ii) potato plants overexpressing the atypical CDSP32 [249] in chloroplasts. Therefore, our approach represents the first attempt to identify Trx f, m and NTRC targets *in vivo*.

With regard to the specificity against Trx partners of this *in vivo* approach, our results show little specificity between the classical Trxs f and m and their targets, while specificity seems to be more preserved in the case of NTRC (Figure 4.4). The lack of Trx type specificity is common to both the affinity column and reductome approaches, as was appreciated in a previous work by comparing targets trapped on mutant Trx f and m columns [245]. This was partially explained by assuming that the replacement of one Cys of the active site by serine causes a slight change in the microenvironment of the protein that abolished specificity. This view could also be applied in our study, where such interaction occurs *in vivo*. Similarly, it was found [244] that the mutant Trx m protein trapped several chloroplast targets known to prefer Trx f, which itself, when

mutated, was ineffective in binding such target enzymes. Moreover, some well known Trx targets were even trapped by mutant forms of Trx-like proteins such as CDSP32 or HCF164 [211,249], or by glutaredoxins (Grx) [484]. However, our results showed a gain of specificity of NTRC for its targets (Figure 4.4) that could be explained by the important differences between classical Trxs and NTRC with regard to protein structure.

The lack of specificity is also reflected in the processes accomplished by these targets. So that Trx f and m identified targets share the same main processes (cell redox homeostasis, carbon metabolism or transcription and translation regulation), while NTRC targets are mainly involved in photosynthesis. Moreover, there are processes that are exclusively represented by Trx f or m targets (secondary metabolism) or NTRC (response to stress, chlorophyll synthesis, photorespiration, PSII assembly or sulfur metabolism) (Figure 4.3). This is in agreement with a regulatory role of NTRC in the chloroplast redox network distinct from those of the FTR/Trx system [221,222], although their activities seem to be interconnected [201,485]. Actually, there is only one work to date where NTRC targets have been identified by affinity chromatography and compared with those obtained for Trx f mutant [222]. Despite using an *in vitro* approach, they found that several targets had distinct interaction efficiencies with NTRC and Trx f, demonstrating that type specificity could be achieved.

New potential Trx f, m and NTRC target proteins

This study led to the identification of 102 proteins linked to Trx f, m and NTRC (Tables 4.1 and 4.2). Most of them were previously identified as potential Trx targets by distinct methodologies. However, some of them were newly identified partners, which must fulfil two requirements to be considered as really feasible Trx targets: (i) to harbor conserved Cys residues; and (ii) because Trxs are located in the stroma, a similar location is expectable for its targets, at least for its conserved Cys residues. Trapped proteins with no conserved Cys residues were considered as part of complexes that could be eluted linked to Trx targets. This kind of proteins, such as superoxide dismutase [Fe]2, PSI reaction center subunit IV A or B, PSII 22 kDa protein, cytochrome (Cyt) b559 subunit alpha or peptidyl-prolyl cis-trans isomerase FKBP19 (Tables 4.1 and 4.2), will not be recognized as putative redox interactors. On the other hand, we have also identified some lumenal located proteins, like immunophilins FKBP19, FKBP16-3, CYP20-2, CYP38 or 29kDa thylakoid lumenal protein TL29 or TL20.3 (Table 4.1 and 4.2) that will neither be considered as potential targets in this study. Below, we briefly discuss feasible targets (with conserved Cys and stromal or thylakoid membrane location) identified in this approach.

Trx f and Trx m

Cell antioxidant and redox homeostasis. Among 7 proteins identified as Trx f and m targets in this group, we found two Prxs localized in the stroma (Table 4.1), the typical 2-Cys Prx B and the atypical Prx IIE, which are important elements of the antioxidant defense system and redox signaling of the plant cell [486]. Both of them were shown to be *in vitro* reduced by typical and atypical Trxs or Grxs [170, 177, 185,487–489] and were previously identified as putative Trx targets by proteomic approaches [216, 230,231, 244, 249,490].

Two atypical Trxs belonging to the Lilium or ACHT family (Lilium 2 and 5) were also identified for Trx f and only Lilium 2 for Trx m (Table 4.1). It was shown that Llilium 2 was not efficiently reduced by neither NTRC nor FTR, but it was efficiently regenerated by glutathione [489]. However, our results indicate that Trx f and/or m could be direct reductants of this family through FTR. In agreement with these findings, two conserved Cys residues were found for these two proteins (Table 4.1).

Peptide methionine sulfoxide reductase (MSRA4), which acts as an antioxidant against oxidative damage [491], was also identified as a putative Trx m target (Table 4.1). Accordingly, we previously demonstrated that tobacco plants overexpressing Trx m specifically displayed increased capacity for MSRs [182]. However, other authors proposed Trx z as the reducer of MSR4 *in vitro* [224], or the y-type Trxs as the physiological electron donor to plastidial MSRs [187]. MSR was also identified as a putative Trx target by proteomic approaches in Arabidopsis [230,238].

Other enzyme with a role in protecting cells against oxidative damage, PHGPx [492], was detected as Trx m partner (Table 4.1). Both y- and z-type Trxs were able to efficiently reduce PHGPx *in vitro* [186,224]. About proteomic approaches, only mitochondrial PHGPx were identified as a putative Trx interactor [157,247].

Photosynthesis. A single protein involved in photosynthetic light reactions was identified as a Trx target in this assay, PGR5-like protein (PGRL1) (Table 4.1), which participates in the cyclic electron flow around PSI in chloroplasts [493]. An *in vitro* interaction between PGRL1 and Trx m, and less efficiently with Trx f, was demonstrated [270]. Moreover, *in vitro* experiments revealed an inhibitory effect of Arabidopsis Trx m4 on PGR-dependent pathway, as well as an inhibition of this pathway in tobacco plants overexpressing Trx m *in vivo* [254], pointing to Trx m as the principal regulator of PGR-dependent electron flow, although in this work it was also identified as Trx f partner.

Carbon metabolism. Two Calvin-Benson cycle enzymes, NADP-GAPDH subunit B and SBPase were identified as Trx targets in this assay (Table 4.1). Both are known as classical Trx target proteins and have been reported to be *in vitro* regulated by Trx f [15, 222, 228,277]. However, there are *in vivo* evidences for the contribution of Trx m in

their activation [183]. Both enzymes were also proposed as Trx targets based on different proteomic approaches [230, 238,244].

Rubisco activase, an enzyme that regulates the activity of the entire Calvin-Benson cycle via regulation of the Rubisco, was identified as Trx f and m target (Table 4.1). It was previously reported to be specifically activated by Trx f [282], and it was subsequently identified as Trx target by different proteomic approaches [230, 238, 244,469]. There were also *in vivo* evidences of its modulation by Trx f, showing retarded and incomplete reduction upon illumination in Arabidopsis Trx f1f2 mutant plants [278].

We also found two enzymes that participate in starch metabolism: (i) a starch synthetasa (SS) that could be identified as a granule-bound starch synthase (GBSS1) according to its homology with Arabidopsis sequences, and (ii) phosphoglucan water dikinase (PWD), which catalyzes the phosphorylation of starch requires for its degradation. There were evidences of a redox regulation of Arabidopsis soluble SS1 and SS3 [307] and more recently, it was demonstrated that SS1 isoform were *in vitro* activated by Trx f1, Trx m4 and NTRC [308]. However, there is no evidence to date relating GBSSs with Trx modulation, but sequence alignment among different species led to identify 6 conserved Cys residues (Table 4.1). It cannot be discarded that, as in AtSS1, some of these residues could affect both activity and redox sensitivity of the enzyme, but further work is required to assess this assumption. Other starch dikinase (GWD) was previously found to be activated through Trx f reduction [313], however our work constitute the first evidence of a putative regulation of PWD by both Trx f and m. In fact, it contains 7 conserved Cys residues (Table 4.1).

Chloroplastic malate dehydrogenase (NADP-MDH), which functions in the malate valve exporting excess reductive power from the chloroplasts [494], was also identified as a Trx m partner (Table 4.1). It is another classical Trx target [15] that could be activated by different Trxs *in vitro*, although the highest efficiency was displayed by Trx f1 [177, 222,228]. However, *in vivo* evidence indicate that it is preferentially activated by Trx m [183,285]. This enzyme was also identified as a putative Trx target in different proteomic approaches [230, 238,467], although Trx f/m specificity has not been completely addressed.

Transcription and translation regulation. In the present work, we have identified two translation-related proteins as potential Trx targets: 50s ribosomal protein L18 and 30s ribosomal protein S3 (Table 4.1). These proteins are generally not considered to undergo Cys oxidoreduction, however, in a previous work a large number of ribosomal proteins were identified as potential Trx targets [239]. There are further evidences about the role of Trxs in protein translation, as the known capability of light to activate translation [261] and to stabilize mRNA [495]. We found that ribosomal protein L18 and S3 showed 1 and 3 conserved Cys, respectively (Table 4.1), suggesting that Trx could

redox-modulate the formation of ribosomal complexes as occurs with GAPDH/PRK/CP12 complex [496].

Two enzymes involved in nucleotide metabolism were found as putative Trx f and m targets: uridine kinase-like protein 1 and amidophosphoribosyltransferase 2 (Table 4.1) [497,498]. In both cases no evidences about a possible redox regulation has been shown to date. For the second one, the sequence alignment showed the presence of 9 conserved Cys (Table 4.1). For uridine kinase-like protein 1 the database was not sufficiently developed to permit the assignment of conserved amino acids, although both *N. tabacum* and Arabidopsis sequences present 10 Cys along its sequence.

Secondary metabolism. An enzyme involved in Z-abeniol biosynthesis was also identified as Trx putative target (Table 4.1). Cis-abienol synthase participates in the biosynthesis of this diterpene, which is a precursor of important flavours and aromas in tobacco glandular trichomes [499]. Due to its specificity is not possible to perform an alignment to permit the assignment of conserved Cys, but the tobacco sequence contains 20 Cys residues.

Amino acid biosynthesis. We also found a protein involved in the metabolism of amino acids that belongs to the 5'-adenylylsulfate reductase family, APR 2. This is a key enzyme in the plant sulfate assimilation pathway that reduces sulfate to sulfite [500]. It contains a Trx-like domain at its C-terminus [501,502] and pre-incubations with high concentrations of DTT or Trx m leads to inactivation of the enzyme [503]. This indicated, together with our results, a putative interaction with Trxs.

NTRC

***Cell redox homeostasis*.** It was shown that the enzyme 2-Cys Prx B, also identified as a putative Trx f and m target (Tables 4.1 and 4.2), can directly interact [504] or be efficiently reduced by NTRC [193,194,358]. Although NTRC has been identified as the primary electron donor for 2-Cys Prx *in vivo* [195, 221,222,280], it was also shown that redox balance of 2-Cys Prx is linked to both NTRC and Fd/Trx system [201,485], confirming our results.

PHGPx was detected as potential NTRC target, as well as for Trx m in this study (Tables 4.1 and 4.2). PHGPx have 2 conserved Cys involveed in the catalytic mechanism and it uses preferentially the Trx system as reductant [186]. Nevertheless, any direct relationship with NTRC was shown to date.

Two proteins involved in the chloroplastic ascorbate-glutathione cycle have been identified as NTRC putative targets (Table 4.2): GSH-dependent dehydroascorbate reductase 3 and L-ascorbate peroxidase. These proteins were proposed to remove large amounts of H_2O_2 produced during photosynthetic operations in the light [505]. Dehydroascorbate reductase 3 is considered a monomeric GST-like protein, with a Cys in place of serine at the active site, which has the capacity for reversible disulfide bond

formation with glutathione [506]. Both proteins were previously identified as putative Trx [229,230, 235,238] and 2-Cys Prx [507] targets by proteomic approaches, but any direct relation with NTRC has been demonstrated so far.

Inside this group, we found a single cystathionine β-synthase domain containing protein (CBSX1) that controls cellular H_2O_2 levels and modulates plant development by sensing changes in adenosine nucleotides [508]. It was reported that the plastid located CBSX1 was able to interact and activate Trx f, m, x, and y [509]. With these findings, it cannot be discarded the possibility of being an NTRC interactor.

Trx m4 protein was also found to probably interact with NTRC in this assay (Table 4.2). It was recently described an *in vivo* interaction between NTRC and Trx m1 and m3 by bimolecular fluorescence complementation (BIFC) test [221], although *in vitro* experiments showed that NTRC could not reduce Trx m [222].

Photosynthesis. Our approach allowed identifying 34 putative partners involved in photosynthesis light reactions (Table 4.2). Among the nine identified PSI core subunits, only N subunit was previously reported as a disulfide-containing protein in Arabidopsis [510] and as a Trx partner in thylakoid membranes [469]. Some of the remaining subunits, presented one or more conserved Cys residues but not others (Table 4.2). Among them, the PSI iron-sulfur center (PSI-C) that harbored 9 conserved Cys (Table 4.2) is located in the stromal side of the thylakoid membrane making possible a putative interaction with NTRC. The identification of so many subunits, some of them with no conserved Cys, could be as a result of the PSI complex capture, as previously resported for NTRC and some NDH complex subunits [271].

PSII core proteins (D1, D2, CP43 and CP47) were also identified as potential NTRC partners (Table 4.2). It was previously reported a direct interaction between Trx m and D1, D2, and CP47 subunits assisting the biogenesis of PSII [259], but any relation with NTRC was described to date. We also identified six chlorophyll *a*/*b* binding proteins (Table 4.2), which are apoproteins of the light harvesting complex of PSI (Lhca) and PSII (Lhcb). Lhcb were previously identified as Trx target in thylakoid membranes [469], but not Lhca. Among the three identified proteins associated to PSI, only Lhca1 has 3 conserved Cys (Table 4.2).

Oxygen evolving enhancer protein were also identified (Table 4.2) as NTRC targets. Prior to our experiments, only isoforms 1 and 2 were described as putative Trx partners in proteomic approaches [238,469]. Taking that these proteins are located in the thylakoid lumen associated with the PSII complex, they could have been also trapped as part of this complex.

Three components of Cytb_6f complex (Cyt b6, Cyt b6-f complex iron sulfur subunit and Cyt f) were identified as potential NTRC partners since they have 2, 4 and 2 conserved Cys respectively (Table 4.2), although an interaction with the atypical Trx HCF164 was shown previously [211].

Fd and FTR were also identified as putative NTRC targets in this study (Table 4.2). It was previously shown an *in vivo* interaction between the catalytic subunit of FTR and NTRC by BIFC analysis [221]. As it is known, Fd interacts with FTR, so its identification in this case could be as part of a protein complex formation with FTR.

Finally, four subunits of the ATP synthase were found (Table 4.2). Among them α, β and δ subunits of CF1 were previously identified as putative Trx partners by proteomic approaches [211,469]. However only the (γ) subunit was described to be subjected to redox regulation by Trxs [183,262] and NTRC [221,222,267,268]. The remaining fourth subunit (ATP synthase subunit b) has never been identified as a target Trx target although it conserved 1 Cys (Table 4.2).

Overall, although a direct interaction between NTRC and some of the above identified membrane thylakoid proteins cannot be excluded, our results suggest that others could be eluted as part of protein complexes linked to the monocysteinic NTRC mutant.

Carbon metabolism. Among proteins involved in carbon metabolism, four Calvin-Benson cycle enzymes were identified (Table 4.2). Rubisco large subunit was reported to have 2 Cys residues able to form a disulfide bond in the non-activated form of the tobacco enzyme [511]. Moreover it was also identified Rubisco subunits as Trx targets in spinach chloroplasts [244,245,469] or Arabidopsis leaves [230]. However, the impact of Trx on Rubisco reduction remains unresolved. About fructose-1,6-bisphosphatase (FBPase), *in vitro* experiments showed that it was specifically activated by f-type Trxs, while NTRC failed [177,228], although it was previously captured as an NTRC partner in affinity column [222]. Moreover, recent results indicate a role of NTRC in FBPase regulation *in vivo*, as well as a direct NTRC-FBPase interaction [221], confirming our results. The next enzyme, triosephosphate isomerase, was previously identified by different proteomic approaches as a Trx target [230, 238,245]. Primary sequence alignments showed 3 conserved Cys in chloroplast isoforms, however it was shown that it is not susceptible to redox agents [512]. Finally, ribose-5-phosphate isomerase, which catalyzes the reversible isomerization of ribose-5P to ribulose-5P, was previously found as a Trx partner by proteomic approaches [230,238], however it has not been possible to demonstrate redox regulation on the basis of activity [513] and no evidence for NTRC interaction was shown to date.

The other enzyme identified in this group was the small subunit of glucose-1-phosphate adenylyltransferase (AGPase B), which is considered a key enzyme in starch synthesis [78]. A redox activation of the enzyme exerted by NTRC was demonstrated both *in vitro* and *in vivo* [197]. A direct interaction between both proteins was also confirmed by yeast two-hybrid analysis [306]. Such evidence, together with our results, strongly indicate a role of NTRC in AGPase redox modulation.

Protein folding. Our approach allowed identifying three chaperonins involved in protein folding as NTRC targets (Table 4.2). The β subunit of the chaperonine 60 kDa (CPN60) was previously identified as a potential Trx target candidate [193, 229,246]. CPN20 and CAPN10 are co-chaperonins of CPN60 [514,515], suggesting, therefore that these proteins could be purified as part of a protein complex. Only CPN10 has 2 conserved Cys residues, although any direct relation with NTRC was shown to date.

Transcription and translation regulation. We have identified transcription and translation-related proteins as potential NTRC targets (Table 4.2). RNA-binding protein CP29B and chloroplast stem-loop binding protein of 41 kDa b were previously identified as potential Trx targets by proteomic approaches [230]. Pentatricopeptide repeat-containing protein At4g30825 and nucleoid-associated protein At4g30620 have never been related to a putative redox modulation, but their sequences present 9 and 1 conserved Cys (Table 4.2).

Amino acid biosynthesis/Nitrogen assimilation. Three plastidial proteins involved in nitrogen assimilation were identified as NTRC interactors (Table 4.2). Among them we found Fd-dependent glutamate synthase 1, which participates in glutamate synthesis and photorespiration, a protein reported to be activated by DTT and reduced Trxs, more efficiently by Trx m [181]. Moreover, it was found as a potential Trx target in amyloplasts [216]. Ketol-acid reductoisomerase, involved in valine and isoleucine biosynthesis, andornithine carbamoyltransferase, implicated in the synthesis of arginine, were previously reported as a potential Trx targets in cereal and medicago seeds [229,231], as well as in amyloplasts [216]. For all of them this is the first time where an interaction with NTRC is reported.

Sulfur metabolism. Cystein synthase was identified as NTRC target in this approach (Table 4.2). It was shown that this enzyme requires DTT for activity [516] and it was also found as a Trx target [245] but any evidence about a putative interaction with NTRC was previously shown.

Other processes. Two enzymes involved in tetrapyrrole pathway (CPOX) and photorespiration (phosphoglycolate phosphatase 1B) were identified as new putative NTRC targets (Table 4.2). There is no previous evidence of a redox regulation of these enzymes, however they contain 2 and 4 conserved Cys (Table 4.2).

In summary, our new strategy based on *in vivo* trapping of Trx interactors using monocysteinic mutant forms of Trx f, Trx m and NTRC, led to the identification of 30 potential new target proteins in *N. benthamiana* chloroplasts. Although the apparent lack of specificity shown between Trx f and m, a significant specificity for NTRC was observed. The newly identified proteins contain conserved Cys residues, are located in the stroma or in the thylakoid membrane (although the putative stromal location of the conserved Cys residues remains to be analyzed), and function in a spectrum of processes.

4.5 Supplementary material

4.5.1 Supplementary tables

Table S4.1. List of primers used for monocysteinic Trxs expression

Trxf-C47S	Site-directed mutagenesis (5'-3')[a] C47S-f: CTCAGTGGTGTGGTCCTAGCAAAGTG C47S-r: CACTTTGCTAGGACCACACCACTGAG Full gene length (5'-3')[b,c] Trxf-f: ATGCAGGTGTGGAGCTCCGATGCTACTGCTAC Trxf-r: tctaga*TTAATGGTGATGGTGATGGTG*ACTTGACCGCACATCCTC Rubisco small subunit transit peptide (5'-3') Rbcs-f: ccatggCTTCCTCAGTTCTTTCC Rbcsf-r: ATCGGAGCTCCACACCTGCATGCATTGCAC
Trxm-C40S	Site-directed mutagenesis (5'-3') C40S-f: CTCCGTGGTGTGGTCCAAGCCGAATG C40S-r: CATTCGGCTTGGACCACACCACGGAG Full gene length (5'-3') Trxm-f: ATGCAGGTGTGGGAAGCGCAAAATACTGCC Trxm-r: tctaga*TTAATGGTGATGGTGATGGTG*CAAGAATTTCTCTATGCAGG Rubisco small subunit transit peptide (5'-3') Rbcs-f: ccatggCTTCCTCAGTTCTTTCC Rbcsm-r: TTGCGCTTCCCACACCTGCATGCATTGCAC
NTRC-C457S	Site-directed mutagenesis (5'-3') C457S-f: CACCAACATGTGGCCCCAGTAGGACTC C457S-r: AGTCCTACTGGGGCCACATGTTGGTG Full gene length (5'-3') NTRC-f: ATGCAGGTGTGGTCTTCTTCAGGAGGCGAG NTRC-r: tctaga*TTAATGGTGATGGTGATGGTG*TTTATTGGCCTCAATGAATTC Rubisco small subunit transit peptide (5'-3') Rbcs-f: ccatggCTTCCTCAGTTCTTTCC RbcsNTRC-r: TGAAGAAGACCACACCTGCATGCATTGCAC

[a] Restriction sites are indicated in lowercase
[b] Single nucleotide changes to replace Cys with Ser are underlined
[c] Italics indicate 6xHis tag sequences

Table S4.2. Proteomic analysis of Trx f candidate targets. Specified criteria: al least two unique peptides, p-Value < 0.05 and a Log2 fold change > 1.8.

Accession	Description	Subcellular localization	Unique peptides	Peptide count	Confidence score	p-Value	Fold Change
A0A1S3Z4R9	12-oxophytodienoate reductase 3-like	Peroxisome	2	2	12	0.00	2.42
L7UU40	26S protease regulatory subunit 8 homolog A-like	Nucleus, cytoplasm	2	2	13	0.00	3.33
A0A1S4BDA7	2-Cys peroxiredoxin BAS1	Chloroplast	9	18	419	0.00	7.79
A0A1S4DBQ8	40S ribosomalprotein S15a-1	Cytoplasm	3	3	37	0.05	2.49
A0A1S4DHJ8	5'-adenylylsulfate reductase 2	Chloroplast	4	4	67	0.00	5.80
Q6T7F3	Amidophosphoribosyl transferase	Chloroplast	9	9	150	0.01	2.13
A0A1S3ZQZ9	Annexin	Unknown	2	5	46	0.00	2.74
A0A1S4APY2	Aspartate--tRNA ligase 2	Cytoplasm	3	3	35	0.00	2.10
A0A1S4A4L1	Aspartyl protease family protein 1-like	Plasma membrane	2	2	27	0.00	1.83
A0A1S4D2D2	BTB/POZ domain-containing protein At1g03010-like isoform X2	Unknown	2	2	16	0.00	1.96
A0A1S4B8Q6	Cis-abienol synthase	Chloroplast	2	2	13	0.01	2.26
A0A1S3YJX2	Dihydropyrimidinase isoform X1	Endoplasmic reticulum	2	2	15	0.00	14.95
A0A1S3XYZ9	GDSL esterase/lipase 2-like	Secreted	2	7	82	0.00	4.99
A0A1S4ATB8	Glyceraldehyde-3-phosphate dehydrogenase	Chloroplast	8	20	294	0.00	3.19
A0A1S4AKJ1	Golgin candidate 1-like	Golgi apparatus	2	2	17	0.01	1.98
A0A1S3Y7P2	Patatin-like protein 3	Plasma membrane	3	3	23	0.00	1.90
A0A1S4C620	Peptide methionine sulfoxide reductase-like	Cytosol	3	3	44	0.00	4.84
A0A1S4DGW7	Peptidyl prolyl isomerase	Chloroplast	3	3	28	0.01	1.86

Table S4.2. Proteomic analysis of Trx f candidate targets (continuación).

A0A1S4A0A5	Protein FLX-like 3 isoform X1	Unknown	2	2	10	0.00	2.64
A0A1S4C9Y8	Putative late blight resistance protein homolog R1A-3	Unknown	2	2	16	0.00	2.46
A0A1S4BBZ3	Putative uridine kinase C227.14 isoform X2	Cytosol	2	2	24	0.00	3.48
A0A140G1V5	Ribosomal protein S3	Chloroplast	2	2	13	0.01	2.53
A0A1S32VC8	Obg-like ATPase 1	Cytosol	7	7	104	0.00	2.77
A0A1S4A3L9	Ribulose bisphosphate carboxylase/oxygenase activase 1	Chloroplast	2	15	248	0.01	2.13
A0A1S4BTX2	Stress response protein NST1-like	Unknown	2	2	19	0.01	1.94
A0A1S4D2Y9	Thioredoxin-like 4	Chloroplast	7	7	94	0.00	5.02
A0A1S4CQQ3	Thylakoid lumenal 29 kDa protein	Chloroplast	2	4	55	0.00	1.90
A0A1S4AFW1	Tryptophan--tRNA ligase, cytoplasmic-like isoform X2	Cytoplasm	2	2	28	0.00	2.58
A0A1S4DKS1	UBP1-associated protein 2B-like	Nucleus	5	6	68	0.02	2.97
A0A1S4B454	Uncharacterized protein LOC107804229	Unknown	2	2	25	0.00	5.14
A0A1S4CK21	Uncharacterized protein LOC107819880	Unknown	2	2	14	0.00	8.33
A0A1S4CR05	Uridine kinase	Chloroplast	2	2	18	0.00	2.50

Table S4.3. Proteomic analysis of Trx m candidate targets. Specified criteria: al least two unique peptides, p-Value < 0.05 and a Log2 fold change > 1.8.

Accession	Description	Subcellular localization	Unique peptides	Peptide count	Confidence score	p-Value	Fold Change
A0A1S3Z4R9	12-oxophytodienoate reductase 3-like	Peroxisome	2	2	12	0.00	2.01
L7UU40	26S protease regulatory subunit 8 homolog A-like	Nucleus	2	2	13	0.00	2.80
A0A1S4A3V7	2-Cys peroxiredoxin BAS1	Chloroplast	7	17	350	0.05	3.75
A0A1S4DBQ8	40S ribosomalprotein S15a-1	Cytoplasm	3	3	37	0.00	1.95
A0A1S3ZK73	40S ribosomal protein S25-like	Cytosol	2	3	21	0.00	1.93
A0A1S4DL03	50S ribosomal protein L18	Chloroplast	2	2	27	0.01	3.23
A0A1S4DHJ8	5'-adenylylsulfate reductase 2	Chloroplast	4	4	67	0.00	19.89
A0A1S3XPC1	Altered inheritance of mitochondria protein 32-like	Unknown	2	2	17	0.01	1.85
Q6T7F3	Amidophosphoribosyl transferase	Chloroplast	9	9	150	0.00	2.94
A0A1S3ZQZ9	Annexin	Unknown	2	5	46	0.04	1.88
A0A1S4B8Q6	Cis-abienol synthase	Chloroplast	2	2	13	0.00	2.14
A0A1S3YJX2	Dihydropyrimidinase isoform X1	Endoplasmic reticulum	2	2	15	0.00	4.52
A0A1S3XYZ9	GDSL esterase/lipase 2-like	Secreted	2	7	82	0.01	4.66
A0A1S4A969	Glutathione peroxidase	Chloroplast	6	6	69	0.02	2.66
A0A1S4AKJ1	Golgin candidate 1-like	Golgi apparatus	2	2	17	0.01	1.99
A0A1S4DEY3	Granule-bound starch synthase 1	Chloroplast	2	3	22	0.00	2.71
A0A1S4B4B2	Histone-lysine N-methyl transferase setd3-like	Unknown	3	3	46	0.00	3.68
A0A1S3YQS9	Malate dehydrogenase (NADP)	Chloroplast	12	12	171	0.00	1.83
A0A1S4BQQ0	Nudix hydrolase 8-like	Unknown	2	2	24	0.00	9.46

Table S4.3. Proteomic analysis of Trx m candidate targets (continuación).

A0A1S4A0A5	Protein FLX-like 3 isoform X1	Unknown	2	2	10	0.01	2.10
A0A1S4C9Y8	Putative late blight resistance protein homolog R1A-3	Unknown	2	2	16	0.01	2.23
A0A1S4BBZ3	Putative uridine kinase C227.14 isoform X2	Cytosol	2	2	24	0.01	3.53
A0A140G1V5	Ribosomal protein S3	Chloroplast	2	2	13	0.00	2.44
A0A1S4A3L9	Ribulose bisphosphate carboxylase/oxygenase activase 1	Chloroplast	2	15	248	0.02	2.16
A0A1S3YEX0	Sedoheptulose-1,7-bisphosphatase	Chloroplast	6	16	246	0.01	2.11
A0A1S4ASD9	Thioredoxin-like 2	Chloroplast	2	3	49	0.01	2.65
A0A1S4D2Y9	Thioredoxin-like 4	Chloroplast	7	7	94	0.00	8.60
A0A1S4AFW1	Tryptophan--tRNA ligase, cytoplasmic-like isoform X2	Cytoplasm	2	2	28	0.00	1.95
A0A1S4DKS1	UBP1-associated protein 2B-like	Nucleus	5	6	68	0.00	2.22
A0A1S3Y1A3	Uncharacterized protein LOC107771070	Unknown	2	2	15	0.00	5.43
A0A1S3ZX69	Uncharacterized protein LOC107791394	Unknown	4	4	68	0.01	3.63
A0A1S4CK21	Uncharacterized protein LOC107819880	Unknown	2	2	14	0.02	2.93
A0A1S3Y9V3	UPF0061 protein azo1574-like	Unknown	2	3	29	0.00	3.20
A0A1S4CR05	Uridine kinase-like protein 1	Chloroplast	2	2	18	0.01	1.96

Table S4.4. Proteomic analysis of NTRC candidate targets. Specified criteria: al least two unique peptides, p-Value < 0.05 and a Log2 fold change > 1.8.

Accession	Description	Subcellular localization	Unique peptides	Peptide count	Confidence score	p-Value	Fold Change
A0A1S4AH01	10 kDa chaperonin-like	Chloroplast	4	4	68	0.00	3.24
Q43590	1-amniocyclopropane-1-carboxylate oxidase	Unknown	8	8	145	0.00	2.19
A0A1S3XWD3	2,3-bisphosphoglycerate-independent phosphoglycerate mutase	Cytoplasm	6	6	102	0.00	2.38
A0A077DBL2	20 kDa chaperonin	Chloroplast	4	4	75	0.00	4.59
A0A1S4CYJ5	29 kDa ribonucleoprotein A	Chloroplast	6	6	144	0.00	2.24
A0A1S4A3V7	2-Cys peroxiredoxin BAS1	Chloroplast	3	15	256	0.00	13.15
A0A1S3XXX03	31 kDa ribonucleoprotein	Chloroplast	3	3	47	0.01	4.42
A0A1S3ZYM9	5-methyltetrahydropteroyl triglutamate homocysteine methyltransferase-like	Cytosol	4	12	168	0.01	2.51
A0A1S4DLA0	60S ribosomal protein L35-like	Cytosol	2	2	34	0.00	2.79
P17514	Acidic endochitinase Q	Vacuole	7	7	150	0.00	5.53
Q9AT16	Ankyrin-repeat protein HBP1	Nucleus	5	5	82	0.00	5.53
A0A140G1P8	ATP synthase CF0 B subunit	Chloroplast	9	10	113	0.00	2.47
A0A1S4CSA5	ATP synthase delta chain	Chloroplast	3	3	41	0.00	3.71
P00823	ATP synthase subunit alpha	Chloroplast	2	35	642	0.01	2.23
A0A140G1S2	ATP synthase subunit beta	Chloroplast	27	31	689	0.00	3.42
A0A1S4C3F4	Calreticulin isoform X2	Endoplasmicreticulum	5	5	89	0.01	2.87
A0A1S4B1Q8	CBS domain-containing protein CBSX1	Chloroplast	2	2	20	0.00	3.05
A0A1S4DIE1	Chlorophyll a-b binding protein 13	Chloroplast	5	5	100	0.00	7.68

Table S4.4. Proteomic analysis of NTRC candidate targets (continuación).

A0A1S4CCJ9	Cysteine synthase	Mitochondrion	7	10	213	0.01	2.62
A0A140G1T3	Cytochrome b559 subunit alpha	Chloroplast	2	2	22	0.00	3.87
A0A1S4ACF7	Cytochrome b561 and DOMON domain-containing protein At3g25290-like	Unknown	2	2	18	0.00	3.03
A0A1S3XVT6	Cytochrome b_6	Chloroplast	2	2	38	0.01	2.86
A0A1S4B832	Cytochrome b_6f complex iron-sulfur subunit	Chloroplast	5	5	84	0.00	2.14
A0A1S4CNA9	Cytochrome c-like	Mitochondrion	2	2	21	0.00	3.10
A0A140G1S8	Cytochrome f	Chloroplast	12	12	241	0.01	3.03
A0A1S4BMJ4	Earlynodulin-like protein 2	Plasma membrane	2	4	53	0.00	3.95
A0A1S4D7J1	Endochitinase B	Vacuola	2	2	49	0.01	5.57
A0A1S4CDZ9	Fasciclin-like arabinogalactan protein 1	Plasma membrane	2	2	61	0.00	2.30
A0A1S4AMD8	Fasciclin-like arabinogalactan protein 8	Plasma membrane	2	2	33	0.00	4.52
A0A1S3YVN4	Ferredoxin	Chloroplast	5	5	148	0.01	4.73
A0A1S4CUE0	Ferredoxin-dependent glutamate synthase	Chloroplast	2	4	75	0.01	2.34
A0A1S4B5N2	Ferredoxin-thioredoxin reductase	Chloroplast	4	4	40	0.00	2.39
A0A1S4A023	Fructose-1,6-bisphosphatase	Chloroplast	6	6	102	0.00	1.90
A0A1S3YQI2	Fructose-bisphosphate aldolase	Cytosol	7	8	156	0.00	2.21
P23547	Glucan endo-1,3-beta-glucosidase, acidic isoform GI9	Secreted	3	3	41	0.00	2.31
A7XAQ5	Glucose-1-phosphate adenylyltransferase	Chloroplast	4	4	72	0.00	1.84
A0A1S4CUX2	Glutaredoxin	Cytoplasm	3	4	55	0.00	2.38
A0A1S4A969	Glutathione peroxidase	Chloroplast	4	4	43	0.00	4.06

Table S4.4. Proteomic analysis of NTRC candidate targets (continuación).

Accession	Description	Subcellular localization	Unique peptides	Peptide count	Confidence score	p-Value	Fold Change
A0A1S3ZX72	Haloacid dehalogenase-like hydrolase domain-containing protein At3g48420	Chlotoplast	5	5	49	0.01	1.94
A0A1S3YTZ2	Ketol-acid reductoisomerase	Chloroplast	2	2	20	0.01	2.47
A0A1S3YXG6	Malate dehydrogenase	Mitochondrion	9	17	376	0.00	5.91
A0A1S3Y6M1	Malate dehydrogenase	Cytoplasm	2	7	149	0.00	3.09
A0A1S3ZW53	Malate dehydrogenase	Mitochondrion	4	12	251	0.00	7.67
A0A1S3YUT4	Monodehydroascorbate reductase	Peroxisome	6	6	94	0.01	2.62
A0A1S4BWK5	NADP-dependent glyceraldehyde-3-phosphate dehydrogenase-like	Cytoplasm	4	4	82	0.00	2.19
A0A1S4CLH1	Nascent polypeptide-associated complex subunit alpha-like protein 1	Cytosol	2	4	53	0.00	4.69
A0A1S3ZRR1	Nucleoid-associated protein At4g30620	Chloroplast	2	2	30	0.00	5.47
A0A1S4APF3	Ornithine carbamoyl transferase	Chloroplast	2	2	40	0.00	3.37
Q84QE8	Oxygen evolving complex 33 kDa photosystem II protein	Chloroplast	10	18	316	0.00	3.87
A0A1S4C5X4	Oxygen-dependent coproporphyrinogen-III oxidase	Chloroplast	3	3	34	0.01	1.96
A0A1S3ZHB8	Oxygen-evolving enhancer protein 1	Chloroplast	6	21	431	0.00	4.60
A0A1S4BMY9	Oxygen-evolving enhancer protein 2-2	Chloroplast	8	9	215	0.00	3.86
A0A1S3XRM3	Oxygen-evolving enhancer protein 3-2	Chloroplast	16	17	266	0.00	3.89
A0A1S4CGA5	Pentatricopeptide repeat-containing protein At4g30825	Chloroplast	2	2	8	0.00	73.37

Table S4.4. Proteomic analysis of NTRC candidate targets (continuación).

A0A1S4AWT3	Peptidyl-prolyl cis-trans isomerase	Chloroplast	7	8	124	0.00	4.14
A0A1S3X073	Phosphoglycolate phosphatase 1B	Chloroplast	2	3	27	0.01	3.86
Q1W375	Phosphomannomutase	Cytoplasm	2	2	18	0.01	2.09
A0A140G1X0	Photosystem I iron-sulfur center	Chloroplast	10	10	209	0.00	4.33
A0A140G1R3	Photosystem I P700 chlorophyll a apoprotein A1	Chloroplast	7	7	70	0.00	6.14
A0A140G1R2	Photosystem I P700 chlorophyll a apoprotein A2	Chloroplast	4	4	52	0.01	5.42
A0A1S3ZIE1	Photosystem I reaction center subunit II	Chloroplast	20	20	400	0.00	3.67
A0A1S4CFV4	Photosystem I reaction center subunit IV A	Chloroplast	4	4	75	0.00	4.29
A0A1S4CYN6	Photosystem I reaction center subunit IV B	Chloroplast	6	6	113	0.00	4.46
D2K7Z2	Photosystem I reaction center subunit	Chloroplast	5	6	118	0.00	2.26
A0A1S4CR54	Photosystem I reaction center subunit VI-1	Chloroplast	3	3	40	003	2.10
A0A1S4BQS3	Photosystem I reaction center subunit XI	Chloroplast	2	2	59	001	4.77
A0A1S3YQ87	Photosystem II 22 kDaprotein	Chloroplast	2	2	44	0.04	2.39
A0A140G1Q8	Photosystem II CP43 reaction center protein	Chloroplast	14	16	294	0.00	4.94
A0A140G1U3	Photosystem II CP47 reaction center protein	Chloroplast	26	26	502	0.00	4.96
A0A140G1Q7	Photosystem II D2 protein	Chloroplast	7	7	186	0.00	6.16
A0A140G1P2	Photosystem II protein D1	Chloroplast	2	2	36	0.01	4.37
A0A1S4DN09	Photosystem II repair protein PSB27-H1	Chloroplast	6	6	129	0.00	4.49
A0A1S4DKC9	Photosystem II stability/assembly factor HCF136	Chloroplast	7	7	114	0.01	3.49
A0A1S4A1K3	Plastocyanin	Chloroplast	5	5	78	0.00	4.39
A0A1S3ZZS2	Probable L-ascorbate peroxidase 6, chloroplastic isoform X2	Chloroplast	3	3	70	0.00	2.34

Table S4.4. Proteomic analysis of NTRC candidate targets (continuación).

A0A1S4A194	Soluble inorganic pyrophosphatase 6	Chloroplast	3	3	36	0.00	3.97
A0A1S3ZTX1	Superoxide dismutase [Cu-Zn]	Nucleus, cytosol	3	3	53	0.00	3.47
W0KRH1	Superoxide dismutase	Chloroplast	3	3	44	0.00	2.39
A0A1S4CCB3	Thioredoxin-like	Chloroplast	2	6	82	0.00	2.28
A0A1S4BU42	Thylakoid luminal protein TL20.3	Chloroplast	3	3	72	0.00	3.78
A0A1S3X2Z0	Triosephosphate isomerase	Chloroplast	3	4	44	0.02	3.25
A0A1S3XK44	Uncharacterized protein At4g15545-like	Unknown	2	2	17	0.01	2.06
A0A1S3Z0H0	Uncharacterized protein LOC107781661	Nucleus	2	2	24	0.00	3.24
A0A1S4BZK6	Uncharacterized protein LOC107813570	Mitochondrion	4	4	58	0.00	3.03
A0A1S4D357	Uncharacterized protein LOC107825453	Nucleus	2	7	107	0.01	2.12
A0A1S4D8Y5	Uncharacterized protein LOC107827263	Unknown	4	5	59	0.00	5.22
A0A1S4DQW8	Uncharacterized protein LOC107832223	Chloroplast	2	2	31	0.02	2.13
A9CM22	Voltage-dependent anion channel	Mitochondrion	4	5	54	0.00	3.08
A0A097BTV9	V-type proton ATPase catalytic subunit A	Vacuole	2	52	1059	0.00	2.06
A0A1S4AP74	V-type proton ATPase subunit a	Vacuole	8	8	119	0.02	2.88
A0A1S3ZYF9	V-type proton ATPase subunit	Vacuole	3	3	34	0.00	2.91
A0A1S4DC16	V-type proton ATPase subunit H	Vacuole	2	2	19	0.00	2.12
A0A1S4AQ72	Xyloglucanendotransglucosylase/hydrolase	Secreted	4	4	59	0.00	2.00

PERSPECTIVAS FUTURAS

PERSPECTIVAS FUTURAS

Las Trxs son enzimas ubícuas que contienen un grupo ditiol en su sitio redox activo que les permite catalizar la formación reversible de puentes disulfuro en una gran cantidad de proteínas diana, regulando así su estructura y función. En plantas, el sistema Trx es muy versátil, y está formado por dos tipos TR, una dependiente de Fd (FTR) y otra de NADPH (NTR) como fuente de poder redactor, y distintos tipos de Trxs (f, m, x, y, z, h, o y otras enzimas tipo Trx). En los cloroplastos se utilizan los electrones provenientes de la Fd reducida para reducir las Trxs a través de FTR, aunque también se ha encontrado un tipo inusual de NTR, denominada NTRC. NTRC contiene además del dominio reductasa un dominio Trx, conformando por sí sola un sistema Trx independiente del sistema Fd/Trx. De esta manera, en los cloroplastos las Trxs constituyen un complejo sistema de regulación redox que permite modular la actividad de muchas proteínas involucradas en diversos procesos.

En los últimos años se ha avanzado mucho en el estudio del papel de las Trxs, utilizando principalmente métodos bioquímicos y técnicas de genética reversa para su análisis *in vivo*. Estos estudios han revelado un papel específico para las Trxs clásicas en la regulación del transporte electrónico y en la adaptación de la fotosíntesis y el metabolismo del estroma a condiciones de intensidad de luz fluctuante (revisado en [180,424]). Por este motivo, en el capítulo I de este trabajo de tesis se analizó el papel de las Trxs plastidiales m y f en los estados de transición, mecanismo que permite equilibrar de forma rápida la energía absorbida por ambos fotosistemas para mantener una capacidad fotosintética óptima en plantas. Mediante la sobreexpresión de las Trxs m y f en cloroplastos de tabaco, se observó que sólo Trx m parece tener un papel relevante *in vivo* en la regulación de este mecanismo, produciendo una completa inhibición de la actividad de la enzima STN7 kinasa responsable de la fosforilación de los LHCII, que son capaces de migrar entre los dos fotosistemas conformando los estados de transición. Teniendo en cuenta que la inhibición de la fosforilación de los LHCII no era debida a una disminución en la cantidad de STN7, y que la sobreexpresión al mismo nivel de una Trx m con su centro activo mutado revertía la capacidad de fosforilación de STN7, se deduce que Trx m regula de manera redox dependiente esta enzima. Además, la ausencia de fosforilación en las plantas que sobreexpresan Trx m conllevó una disminución en la cantidad de LHCII. Existen evidencias de que la enzima FtsH, una metaloproteasa esencial en la reparación de los daños inducidos por la luz de la proteína D1, también es responsable de la degradación de algunas apoproteinas de los LHCII [381,382]. Recientemente se ha descrito una regulación redox de la actividad proteolítica de FtsH en *Chlamydomonas* [383], que aumenta en presencia de DTT gracias a la reducción de sus puentes disulfuro intermolecuales. También se han identificado algunas isoformas de FtsH como potenciales dianas de Trxs [211] y aunque no todas sus Cys conservadas se

encuentran en el lado estromático [383], no se puede descartar que la sobre expresión de Trx m pueda inducir una reactivación de FtsH, con la consiguiente degradación de los LHCII (sobre todo de las formas no fosforiladas), que finalmente produzcan una alteración de la estequiometria y ultraestrucutra de las proteínas de los tilacoides en estas plantas. Junto a FtsH, por otro lado, sería interesante analizar también el papel de otros factores que puedan influir en el fenotipo observado en estas plantas. Se ha observado que la proteína CURT1 (del inglés *curvaturethylakoid 1)*, tiene una influencia importante en la estructura de los grana [378]. CURT1 forma oligómeros y se encuentra de manera más abundante en los márgenes de los grana donde controla el nivel de apilamiento induciendo la curvatura en las membranas [517,518]. Esta proteína también se fosoforila de manera reversible, proceso que regula su nivel de oligomerización y por tanto, su actividad [517]. Dada la estructura tilacoidal observada en las plantas o/exTrxm, una posible implicación de la Trx m en la desoligomerizacion de CURT1 no se puede descartar. Aunque la secuencia madura de CURT1 no presenta Cys conservadas (analizado a partir de las secuencias disponibles en UniProt), el papel regulador de la Trx m podría ser vía activación/desactivación de alguna kinasa/fosfatasa. En este sentido, realizar un análisis fosfoproteómico en plantas con sobreexpresión de Trxs podría resultar de interés, ya que las Trxs podrían tener un papel en la regulación redox de kinasas o fosfatasas [519], que a su vez regulen otras proteínas involucradas en diferentes procesos.

Dada la relevancia de las Trxs plastidiales en la regulación de los procesos relacionados con la fijación y el metabolismo del carbono fotosintético [424], en el capítulo II se aborda el estudio del papel del las Trxs plastidiales f y NTRC en el metabolismo del almidón, molécula aceptora final del carbono fijado en la fotosíntesis. Si bien, ya se conocía la implicación de ambas proteínas en el metabolismo del almidón [197,304–306], todavía no se han esclarecido los mecanismos específicos por los que actúan. Según nuestros resultados, Trx f estaría implicada en la regulación del proceso de síntesis favoreciendo la actividad de las SSs. Sin embargo, la acumulación de almidón transitorio en plantas que sobreexpresan NTRC se relaciona más con la regulación de la AGPasa y/o alguna enzima involucrada en la degradación del almidón en los periodos de oscuridad. Teniendo en cuenta también que el metabolismo del almidón puede estar influenciado por otros factores como la fosforilación reversible de proteínas o la formación de complejos enzimáticos [40,397], sería interesante realizar un estudio *in planta* de estos procesos con las plantas generadas en este trabajo.Así, junto con el estudio fosfoproteómico propuesto anteriormente, se podría analizar también la presencia de Trx f y NTRC en los gránulos de almidón. En cereales, diversas enzimas relacionadas con la síntesis de almidón se localizan unidas a los gránulos, y dicha unión parece estar regulada por modificaciones postraduccionales y/o interacciones proteina-proteina [520]. Tanto Trx f como NTRC presentan propiedades tipo chaperona [132,133], pudiendo jugar un papel importante en este tipo

de interacciones en plantas de tabaco con sobreexpresión de las mismas. Por tanto, un análisis proteómico de los gránulos de almidón en estas plantas podría resultar igualmente interesante.

Además del metabolism del C, las Trxs plastidiales, y más concretamente Trx m, también parecen ejercer un papel relevante en el metabolism del N tal y como se pone de manifiesto en el capítulo III de esta tesis. Los resultados obtenidos muestran que la sobreexpresión de Trx m produjo un aumento en el contenido de aminoácidos y proteína soluble a expensas del almidón y azúcares soluble en hojas de tabaco. Además, se observó un aumento en la fotorrespiración y una gran acumulación de nitrato en hoja, indicando una activación del flujo fotorrespiratorio del nitrógeno en estas plantas. Un motivo que puede explicar este efecto, al menos en parte, es la activación del ciclo GS/GOGAT en cloroplastos. Los análisis metabolómicos y enzimáticos realizados en estas plantas también lo sugieren. Dicha activación podría ser debida a una regulación positive y/o estabilización de GS2 ejercida por la Trx m, con la que se ha comprobado que interactúa físicamente. Teniendo en cuenta que ya existen numerosos precedentes que demuestran la capacidad de las Trxs para modular la actividad, plegamiento o estabilidad de varias proteínas [198, 221,521–523], GS2 constituiría un nuevo ejemplo en plantas. Por otro lado, no se pueden descartar la influencia de otros factores en el fenotipo observado. Teniendo en cuenta que uno de los precursores para la asimilación del amonio es el 2OG, que es producido fuera del cloroplasto, sería interesante analizar un posible papel de la Trx m en la regulación de los transportadores DiT1/DiT2 necesarios para la entrada de 2OG en el cloroplasto [92]. Ya existen evidencias de algunos transportadores que son susceptibles a regulación redox en plantas [216,312]. En este sentido, los resultados obtenidos hasta la fecha apuntan a un aumento en la expression de DiT2 en las plantas que sobreexpresan Trx m.

Finalmente, y viendo la cantidad de proteínas que podrían ser susceptibles a una regulación redox por parte de las Trxs, se planteó el interés de identificar nuevas proteínas diana. Si bien existe un gran número de trabajos encaminados a determinar nuevas dianas de Trxs, las condiciones *in vitro* utilizadas en ellos no han servido para dilucidar la especificidad entre los diferentes tipos de Trxs. Por este motivo, en el capítulo IV se aborda una nueva estrategia para la identificación de proteínas diana de Trx f, m y NTRC *in vivo*, con el objetivo de ganar en especificidad respecto a los trabajos previos realizados. Esta estrategia, en la que se sobreexpresó *in planta* mutantes monocisteínicos de Trxs f, m o NTRC, permitió identificar hasta 30 nuevas proteínas diana. Sin embargo, no se consiguió aumentar la especificidad entre Trx f y m, aunque sí se mejoró entre las Trxs clásicas y NTRC. Así por ejemplo, de este trabajo se deduce que es más probable una intercacción de la SSs con las Trxs clásicas (aunque se identificó con Trx m, indicar que con Trx f también fue dentificada con un valor de significación de 0.07), mientras que la enzima AGPasa sería una

candidata a interaccionar más específicamente con NTRC. Esta distinción respalda los resultados obtenidos en el capítulo II sobre el papel de estas Trxs en el metabolismo del almidón. Sin embargo, STN7 o GS2, enzimas que parecen asociarse específicamente con Trx m según los resultados de los capítulos I y II, no fueron identificadas como proteínas diana en este trabajo. Por ultimo, la validación tanto a nivel bioquímico como molecular de las nuevas dianas identificadas abre un interesante abanico de posibilidades para futuros trabajos.

CONCLUSIONES

CONCLUSIONES

1. La sobreexpresión de Trx m, pero no de Trx f, desde el genoma plastidial de tabaco produjo la inhibición de la fosoforilación de los LHCII como consecuencia de una inactivación de la kinasa STN7, impidiendo la formación de los supercomplejos PSI-LHCII y por tanto, los estados de transición.

2. Las plantas de tabaco con elevados niveles de Trx m presentaron una menor cantidad de proteínas asociadas a los complejos antena del PSII (Lhcb1 y 2), un aumento en el ratio de clorofila *a*/*b*, así como una alteración en la estructura de los tilacoides, que mostraron un menor grado de apilamiento. Esta modificación en la estequiometría de los fotosistemas se tradujo en una menor tasa de transporte electrónico, produciendo una disminución en la tasa fotosintética en estas plantas.

3. Plantas de tabaco con sobreexpresión de una Trx m mutante sin actividad redox, en la que los residues de Cys de su centro activo fueron sustituidos por serinas, presentaron un fenotipo similar a las plantas control en lo relativo a los niveles de fosforilación de los LHCII, a la formación de supercomplejos PSI-LHCII y, por tanto, a la actividad de la kinasa STN7. Tanto la tasa de transporte electrónico como la fotosíntesis neta también recuperaron los valores de las plantas control. Todo ello indica que Trx m inhibe la actividad de STN7 de manera redox-dependiente.

4. .El estudio realizado sobre las plantas de tabaco que sobreexpresan Trx m permitió arrojar luz sobre el mecanismo por el que la enzima STN7 kinasa es inactivada por las Trxs. Se demostró que Trx m interactúa específicamente con STN7 *in vivo* mediante un ensayo de pull-down, sugiriendo que sería capaz de reducir las Cys se esta enzima presentes en la cara estromática.

5. La sobreexpresión desde el plastoma de tabaco de la secuencia correspondiente a la proteína madura de NTRC, bajo la dirección de la secuencia promotora *psbA*, provocó un elevado nivel de acumulación de esta proteína de forma funcional en hojas. Estas plantas presentaron una ligera disminución en el crecimiento y contenido de clorofila respecto a las plantas control, fenotipo que revirtió cuando estas plantas alcanzaron la fase adulta.

6. La técnica de silenciamiento génico inducido por virus permitió la obtención de plantas de *Nicotiana benthamiana* con una reducción de la expresión, mayor del 90%, de los genes *Trxf* y *ntrc*. El silenciamiento de estos genes no produjo cambios significativos en el fenotipo de las plantas en las condiciones ensayadas.

7. Las plantas con elevados niveles de NTRC acumularon gran cantidad de almidón en hoja debido principalmente a una bajada en la tasa neta de degradación del almidón durante los periodos de oscuridad. Bien mediante una activación por reducción de la enzima AGPase y/o por disminución de la actividad de una posible enzima desrramificadora involucrada en la degradación del almidón.

8. Tanto la sobreexpresión como el silenciamiento de Trx f en plantas confirmó su relevancia en el metabolismo del almidón, estando principalmente involucrada en la activación de la capacidad de las enzimas almidón sintasas.

9. La sobreexpresión de Trx m en cloroplastos de tabaco produjo un desequilibrio entre el metabolismo del carbono y el nitrógeno, con una disminución en la tasa fotosintética y la síntesis de carbohidratos que no se vio acompañada de una inhibición del metabolismo del nitrógeno. Al contrario, se produjo un aumento en la cantidad de proteína y aminoácidos.

10. Las plantas con elevados niveles de Trx m presentaron un aumento en la capacidad de la enzima GS. Además se demuestró *in vivo* que Trx m puede interaccionar físicamente con GS2, regulando la actividad y/o estabilidad de esta proteína de manera redox-dependiente. De esto se deduce que Trx m podría tener un papel en la regulación del ciclo GS/GOGAT, que constituye la principal ruta de asimilación de amonio en plantas.

11. La sobreexpresión de Trx m produjo un aumento de la fotorrespiración, de los niveles de serina y de la acumulación de nitrato en hojas de tabaco, lo que apunta a una activación del ciclo fotorrespiratorio del nitrógeno mediada por la sobreexpresión de Trx m.

12. La bajada en el contenido de fenilpropanoides en las plantas con sobreexpresión de Trx m se relacionó con un aumento en la capacidad de la enzima PEPC, que podría resultar en una reducción del flujo de PEP al cloroplasto, a partir del cual empiezan a sintetizarse estos compuestos.

13. La técnica basada en la sobreexpresión de mutantes redox de Trxs en *N. benthamiana*, en las que la cisteína resolutiva del centro activo fue sustituída por serina, resultó ser una metodología válida para la caza de proteínas dianas de Trxs f, m y NTRC, constituyendo la primera estrategia *in vivo* diseñada para este fin con este tipo de Trxs.

14. Esta metodología permitió identificar 15 posibles nuevas dianas de las Trxs f y m, así como otras 15 para NTRC, si bien estos resultados requieren de una validación posterior tanto a nivel bioquímico como molecular.

15. El método desarrollado en este trabajo de tesis para la caza de dianas *in vivo* permitió mejorar la especificidad entre las Trxs clásicas y NTRC respecto a sus posibles dianas, si bien no resultó válido de cara a esclarecer la distinción entre Trx f y m.

BIBLIOGRAFÍA

BIBLIOGRAFÍA

1. **Horton, P. *et al.*** Regulation of light harvesting in green plants. *Annu. Rev. Plant Physiol. Plant Mol. Biol.* 1996, *47*, 655–684.
2. **Shi, L.X. & Schröder, W.P.** The low molecular mass subunits of the photosynthetic supracomplex, photosystem II. *Biochim. Biophys. Acta - Bioenerg.* 2004, *1608*, 75–96.
3. **Shi, L.X. *et al.*** Photosystem II, a growing complex: Updates on newly discovered components and low molecular mass proteins. *Biochim. Biophys. Acta - Bioenerg.* 2012, *1817*, 13–25.
4. **Bricker, T.M. *et al.*** The extrinsic proteins of Photosystem II. *Biochim. Biophys. Acta - Bioenerg.* 2012, *1817*, 121–142.
5. **Galka, P. *et al.*** Functional analyses of the plant photosystem I-light-harvesting complex II supercomplex reveal that light-harvesting complex II loosely bound to photosystem II is a very efficient antenna for photosystem I in state II. *Plant Cell* 2012, *24*, 2963–2978.
6. **Dekker, J.P. & Boekema, E.J.** Supramolecular organization of thylakoid membrane proteins in green plants. *Biochim. Biophys. Acta - Bioenerg.* 2005, *1706*, 12–39.
7. **Minagawa, J.** Dynamic reorganization of photosynthetic supercomplexes during environmental acclimation of photosynthesis. *Front. Plant Sci.* 2013, *4*, 513.
8. **Croce, R. & Van Amerongen, H.** Light-harvesting in photosystem i. *Photosynth. Res.* 2013, *116*, 153–166.
9. **Quick, W.P. & Neuhaus, H.** The regulation and control of photosynthetic carbon assimilation. In *A molecular approach to primary metabolism in higher plants*; 1997; pp. 39–61.
10. **Raines, C.A.** The Calvin cycle revisited. *Photosynth. Res.* 2003, *75*, 1–10.
11. **Flügge, U.-I.** Phosphate Translocators in Plastids. *Annu. Rev. Plant Physiol. Plant Mol. Biol.* 1999, *50*, 27–45.
12. **Buchanan, B.B.** The Path to Thioredoxin and Redox Regulation in Chloroplasts. *Annu. Rev. Plant Biol.* 2016, *67*, 1–24.
13. **Buchanan, B.B.** Role of Light in the Regulation of Chloroplast Enzymes. *Annu. Rev. Plant Physiol.* 1980, *31*, 341–374.
14. **Jacquot, J.P. *et al.*** Thioredoxins: structure and function in plant cells. *New Phytol.* 1997, *136*, 543–570.
15. **Schürmann, P. & Buchanan, B.B.** The ferredoxin/thioredoxin system of oxygenic photosynthesis. *Antioxid. Redox Signal.* 2008, *10*, 1235–1274.
16. **Pesaresi, P. *et al.*** Dynamics of reversible protein phosphorylation in thylakoids of flowering plants: The roles of STN7, STN8 and TAP38. *Biochim. Biophys. Acta - Bioenerg.* 2011, *1807*, 887–896.
17. **Anderson, J.M.** Photoregulation of the composition, function, and strucutre of thylakoid membranes. *Annu. Rev. Plant Physiol.* 1986, *37*, 93–136.
18. **Ruban, A. V. *et al.*** The photoprotective molecular switch in the photosystem II antenna. *Biochim. Biophys. Acta - Bioenerg.* 2012, *1817*, 167–181.
19. **Minagawa, J.** State transitions-The molecular remodeling of photosynthetic supercomplexes that controls energy flow in the chloroplast. *Biochim. Biophys. Acta - Bioenerg.* 2011, *1807*, 897–905.
20. **Lemeille, S. & Rochaix, J.-D.** State transitions at the crossroad of thylakoid signalling pathways. *Photosynth. Res.* 2010, *106*, 33–46.
21. **Tikkanen, M. *et al.*** Novel insights into plant light-harvesting complex II phosphorylation and “state transitions.” *Trends Plant Sci.* 2011, *16*, 126–131.
22. **Allen, J.F.** Protein phosphorylation in regulation of photosynthesis. *Biochim. Biophys. Acta - Bioenerg.* 1992, *1098*, 275–335.
23. **Allen, K.D. & Staehelin, L.A.** Biochemical characterization of photosystem-II antenna polypeptides in grana and stroma membranes of spinach. *Plant Physiol.* 1992, *100*, 1517–1526.
24. **Bellafiore, S. *et al.*** State transitions and light adaptation require chloroplast thylakoid protein kinase STN7. *Nature* 2005, *433*, 892–895.
25. **Zito, F. *et al.*** The Qo site of cytochrome b_6f complexes controls the activation of the LHCII kinase. *EMBO J.* 1999, *18*, 2961–2969.
26. **Vener, A. V *et al.*** Plastoquinol at the quinol oxidation site of reduced cytochrome *bf* mediates signal transduction between light and protein phosphorylation: Thylakoid protein kinase deactivation by a single-turnover flash. *Proc. Natl. Acad. Sci.* 1997, *94*, 1585–1590.
27. **Shapiguzov, A. *et al.*** Activation of the Stt7/STN7 kinase through dynamic interactions with the cytochrome b_6f complex. *Plant Physiol.* 2016, *171*, 82–92.

28. **Rintamäki, E. *et al.*** Phosphorylation of light-harvesting complex II and photosystem II core proteins shows different irradiance-dependent regulation in vivo. *J. Biol. Chem.* 1997, *272*, 30476–30482.
29. **Rintamäki, E. *et al.*** Cooperative regulation of light-harvesting complex II phosphorylation via the plastoquinol and ferredoxin-thioredoxin system in chloroplasts. *Proc. Natl. Acad. Sci.* 2000, *97*, 11644–11649.
30. **Puthiyaveetil, S.** A mechanism for regulation of chloroplast LHC II kinase by plastoquinol and thioredoxin. *FEBS Lett.* 2011, *585*, 1717–1721.
31. **Martinsuo, P. *et al.*** Dithiol oxidant and disulfide reductant dynamically regulate the phosphorylation of light-harvesting complex II proteins in thylakoid membranes. *Plant Physiol.* 2003, *133*, 37–46.
32. **Baslam, M. *et al.*** Genetic and isotope ratio mass spectrometric evidence for the occurrence of starch degradation and cycling in illuminated Arabidopsis leaves. *PLoS One* 2017, *12*, e0171245.
33. **Fernandez, O. *et al.*** Leaf Starch Turnover Occurs in Long Days and in Falling Light at the End of the Day. *Plant Physiol.* 2017, *174*, 2199–2212.
34. **Valerio, C. *et al.*** Thioredoxin-regulated β-amylase (BAM1) triggers diurnal starch degradation in guard cells, and in mesophyll cells under osmotic stress. *J. Exp. Bot.* 2011, *62*, 545–555.
35. **Thalmann, M. *et al.*** Regulation of Leaf Starch Degradation by Abscisic Acid Is Important for Osmotic Stress Tolerance in Plants. *Plant Cell* 2016, *28*, 1860–1878.
36. **Zanella, M. *et al.*** β-amylase 1 (BAM1) degrades transitory starch to sustain proline biosynthesis during drought stress. *J. Exp. Bot.* 2016, *67*, 1819–1826.
37. **Santelia, D. *et al.*** New insights into redox control of starch degradation. *Curr. Opin. Plant Biol.* 2015, *25*, 1–9.
38. **Zeeman, S.C. *et al.*** Starch: its metabolism, evolution, and biotechnological modification in plants. *Annu. Rev. Plant Biol.* 2010, *61*, 209–234.
39. **Zeeman, S.C. *et al.*** The breakdown of starch in leaves. *New Phytol.* 2004, *163*, 247–261.
40. **Geigenberger, P.** Regulation of starch biosynthesis in response to a fluctuating environment. *Plant Physiol.* 2011, *155*, 1566–1577.
41. **Baroja-Fernandez, E. *et al.*** Most of ADP-glucose linked to starch biosynthesis occurs outside the chloroplast in source leaves. *Proc. Natl. Acad. Sci.* 2004, *101*, 13080–13085.
42. **Pozueta-Romero, J. *et al.*** ADP-Glucose Transport by the Chloroplast Adenylate Translocator Is Linked to Starch Biosynthesis. *Plant Physiol.* 1991, *97*, 1565–72.
43. **Nielsen, T.H. *et al.*** Intermediary glucan structures formed during starch granule biosynthesis are enriched in short side chains, a dynamic pulse labeling approach. *J. Biol. Chem.* 2002, *277*, 20249–20255.
44. **Recondo, E. & Leloir, L.F.** Adenosine diphosphate glucose and starch synthesis. *Biochem. Biophys. Res. Commun.* 1961, *6*, 85–88.
45. **Seung, D. *et al.*** Protein targeting to starch is required for localising granule-bound starch synthase to starch granules and for normal amylose synthesis in Arabidopsis. *PLoS Biol.* 2015, *13*, e1002080.
46. **Nakamura, T. *et al.*** Production of waxy (amylose-free) wheats. *Mol. Gen. Genet. MGG* 1995, *248*, 253–259.
47. **Jacobsen, E. *et al.*** Phenotypic and genotypic characterization of an amylose-free starch mutant of the potato. *Euphytica* 1989, *44*, 43–48.
48. **Skryhan, K. *et al.*** Redox Regulation of Starch Metabolism. *Front. Plant Sci.* 2018, *9*, 1–8.
49. **Nakamura, Y. *et al.*** Characterization of the reactions of starch branching enzymes from rice endosperm. *Plant Cell Physiol.* 2010, *51*, 776–794.
50. **Dumez, S. *et al.*** Mutants of Arabidopsis lacking starch branching enzyme II substitute plastidial starch synthesis by cytoplasmic maltose accumulation. *Plant Cell* 2006, *18*, 2694–2709.
51. **Yan, H.B. *et al.*** Comparison of the starch synthesis genes between maize and rice: copies, chromosome location and expression divergence. *Theor. Appl. Genet.* 2009, *119*, 815–825.
52. **Han, Y. *et al.*** Three orthologs in rice, *Arabidopsis*, and *Populus* encoding starch branching enzymes (SBEs) are different from other *SBE* gene families in plants. *Gene* 2007, *401*, 123–130.
53. **Streb, S. *et al.*** Starch granule biosynthesis in *Arabidopsis* is abolished by removal of all debranching enzymes but restored by the subsequent removal of an endoamylase. *Plant Cell* 2008, *20*, 3448–3466.
54. **Hussain, H. *et al.*** Three isoforms of isoamylase contribute different catalytic properties for the debranching of potato glucans. *Plant Cell* 2003, *15*, 133–149.
55. **Delatte, T. *et al.*** Arabidopsis mutants *Atisa1* and *Atisa2* have identical phenotypes and lack

the same multimeric isoamylase, which influences the branch point distribution of amylopectin during starch synthesis. *Plant J.* 2005, *41*, 815–830.
56. **Delatte, T. *et al.*** Evidence for distinct mechanisms of starch granule breakdown in plants. *J. Biol. Chem.* 2006, *281*, 12050–12059.
57. **Yun, M.S. *et al.*** Rice debranching enzyme isoamylase3 facilitates starch metabolism and affects plastid morphogenesis. *Plant Cell Physiol.* 2011, *52*, 1068–1082.
58. **Zhang, X. *et al.*** Overlapping functions of the starch synthases SSII and SSIII in amylopectin biosynthesis in *Arabidopsis*. *BMC Plant Biol.* 2008, *8*, 96.
59. **Pfister, B. *et al.*** Genetic evidence that chain length and branch point distributions are linked determinants of starch granule formation in Arabidopsis. *Plant Physiol.* 2014, *165*, 1457–1474.
60. **Hennen-Bierwagen, T.A. *et al.*** Starch biosynthetic enzymes from developing maize endosperm associate in multisubunit complexes. *Plant Physiol.* 2008, *146*, 1892–1908.
61. **Hennen-Bierwagen, T.A. *et al.*** Proteins from multiple metabolic pathways associate with starch biosynthetic enzymes in high molecular weight complexes: A model for regulation of carbon allocation in maize amyloplasts. *Plant Physiol.* 2009, *149*, 1541–1559.
62. **Tetlow, I.J. *et al.*** Analysis of protein complexes in wheat amyloplasts reveals functional interactions among starch biosynthetic enzymes. *Plant Physiol.* 2008, *146*, 1878–1891.
63. **Ahmed, Z. *et al.*** Protein-protein interactions among enzymes of starch biosynthesis in high-amylose barley genotypes reveal differential roles of heteromeric enzyme complexes in the synthesis of A and B granules. *Plant Sci.* 2015, *233*, 95–106.
64. **Crofts, N. *et al.*** Amylopectin biosynthetic enzymes from developing rice seed form enzymatically active protein complexes. *J. Exp. Bot.* 2015, *66*, 4469–4482.
65. **Niittylä, T. *et al.*** A previously unknown maltose transporter essential for starch degradation in leaves. *Science (80-.).* 2004, *303*, 87–89.
66. **Cho, M.H. *et al.*** Role of the plastidic glucose translocator in the export of starch degradation products from the chloroplasts in *Arabidopsis thaliana*. *New Phytol.* 2011, *190*, 101–112.
67. **Edner, C. *et al.*** Glucan, water dikinase activity stimulates breakdown of starch granules by plastidial β-amylases. *Plant Physiol.* 2007, *145*, 17–28.
68. **Baunsgaard, L. *et al.*** A novel isoform of glucan, water dikinase phosphorylates pre-phosphorylated α-glucans and is involved in starch degradation in Arabidopsis. *Plant J.* 2005, *41*, 595–605.
69. **Kötting, O. *et al.*** Identification of a novel enzyme required for starch metabolism in Arabidopsis leaves. The Phosphoglucan, water dikinase. *Plant Physiol.* 2004, *137*, 242–252.
70. **Ritte, G. *et al.*** Phosphorylation of C6- and C3-positions of glucosyl residues in starch is catalysed by distinct dikinases. *FEBS Lett.* 2006, *580*, 4872–4876.
71. **Hejazi, M. *et al.*** Glucan, water dikinase phosphorylates crystalline maltodextrins and thereby initiates solubilization. *Plant J.* 2008, *55*, 323–334.
72. **Kotting, O. *et al.*** STARCH-EXCESS4 Is a Laforin-Like Phosphoglucan Phosphatase Required for Starch Degradation in Arabidopsis thaliana. *Plant Cell Online* 2009, *21*, 334–346.
73. **Santelia, D. *et al.*** The phosphoglucan phosphatase like sex four2 dephosphorylates starch at the C3-position in *Arabidopsis*. *Plant Cell* 2011, *23*, 4096–4111.
74. **Meekins, D.A. *et al.*** Phosphoglucan-bound structure of starch phosphatase Starch Excess4 reveals the mechanism for C6 specificity. *Proc. Natl. Acad. Sci.* 2014, *111*, 7272–7277.
75. **Fulton, D.C. *et al.*** β-AMYLASE4, a noncatalytic protein required for starch breakdown, acts upstream of three active β-Amylases in *Arabidopsis* chloroplasts. *Plant Cell* 2008, *20*, 1040–1058.
76. **Stanley, D. *et al.*** Characterisation of putative α-amylases from apple (*Malus domestica*) and Arabidopsis thaliana. *Biologia (Bratisl).* 2002, *57*, 137–148.
77. **Streb, S. & Zeeman, S.C.** *Starch metabolism in Arabidopsis*; 2012;
78. **Stitt, M. & Zeeman, S.C.** Starch turnover: Pathways, regulation and role in growth. *Curr. Opin. Plant Biol.* 2012, *15*, 282–292.
79. **Krapp, A.** Plant nitrogen assimilation and its regulation: A complex puzzle with missing pieces. *Curr. Opin. Plant Biol.* 2015, *25*, 115–122.
80. **Meyer, C. & Stitt, M.** Nitrate reduction and signalling. In *Plant Nitrogen*; Lea, P.J., Morot-Gaudry, J.-F., Eds.; Springer Berlin Heidelberg: Berlin, Heidelberg, 2001; pp. 37–59 ISBN 978-3-662-04064-5.
81. **Lea, P.J. & Miflin, B.J.** Nitrogen Assimilation and its Relevance to Crop Improvement. In *Nitrogen Metabolism in Plants in the Post-genomic Era*; 2010; Vol. 42, pp. 1–40 ISBN 9781444328608.
82. **Keys, A.J. *et al.*** Photorespiratory nitrogen cycle. *Nature* 1978, *2758*, 741–743.
83. **Bittsánszky, A. *et al.*** Overcoming ammonium toxicity. *Plant Sci.* 2015, *231*, 184–190.
84. **Kimata-Ariga, Y. & Hase, T.** Multiple complexes of nitrogen assimilatory enzymes in spinach

chloroplasts: Possible mechanisms for the regulation of enzyme function. *PLoS One* 2014, *9*, e108965.

85. **Seabra, A.R. *et al.*** Novel aspects of glutamine synthetase (GS) regulation revealed by a detailed expression analysis of the entire GS gene family of *Medicago truncatula* under different physiological conditions. *BMC Plant Biol.* 2013, *13*, 137.
86. **Taniguchi, M. & Miyake, H.** Redox-shuttling between chloroplast and cytosol: Integration of intra-chloroplast and extra-chloroplast metabolism. *Curr. Opin. Plant Biol.* 2012, *15*, 252–260.
87. **Diaz, C. *et al.*** Nitrogen recycling and remobilization are differentially controlled by leaf senescence and development stage in Arabidopsis under low nitrogen nutrition. *Plant Physiol.* 2008, *147*, 1437–1449.
88. **Masclaux-Daubresse, C. *et al.*** Leaf nitrogen remobilisation for plant development and grain filling. *Plant Biol.* 2008, *10*, 23–36.
89. **Tercé-Laforgue, T. *et al.*** New insights towards the function of glutamate dehydrogenase revealed during source-sink transition of tobacco (*Nicotiana tabacum*) plants grown under different nitrogen regimes. *Physiol. Plant.* 2004, *120*, 220–228.
90. **Kojima, S. *et al.*** NADH-dependent glutamate synthase participated in ammonium assimilation in Arabidopsis root. *Plant Signal. Behav.* 2014, *9*, e29402.
91. **Weber, A. & Flügge, U.-I.** Interaction of cytosolic and plastidic nitrogen metabolism in plants. *J. Exp. Bot.* 2002, *53*, 865–874.
92. **Woo, K.C. *et al.*** A two-translocator model for the transport of 2-oxoglutarate and glutamate in chloroplasts during ammonia assimilation in the light. *Plant Physiol.* 1987, *84*, 624–632.
93. **Schneidereit, J. *et al.*** Antisense repression reveals a crucial role of the plastidic 2-oxoglutarate/malate translocator DiT1 at the interface between carbon and nitrogen metabolism. *Plant J.* 2006, *45*, 206–224.
94. **Kinoshita, H. *et al.*** The chloroplastic 2-oxoglutarate/malate transporter has dual function as the malate valve and in carbon/nitrogen metabolism. *Plant J.* 2011, *65*, 15–26.
95. **Renné, P. *et al.*** The *Arabidopsis* mutant *dct* is deficient in the plastidic glutamate/malate translocator DiT2. *Plant J.* 2003, *35*, 316–331.
96. **Coruzzi, G. & Bush, D.R.** Nitrogen and carbon nutrient and metabolite signaling in plants. *Plant Physiol.* 2001, *125*, 61–64.
97. **Gutiérrez, R.A. *et al.*** Qualitative network models and genome-wide expression data define carbon/nitrogen-responsive molecular machines in *Arabidopsis*. *Genome Biol.* 2007, *8*, 1–13.
98. **Vincentz, M. *et al.*** Regulation of nitrate and nitrite reductase expression in *Nicotiana plumbaginifolia* leaves by nitrogen and carbon metabolites. *Plant J.* 1993, *3*, 315–324.
99. **Kaiser, W.M. & Huber, S.C.** Posttranslational regulation of nitrate reductase in higher plants. *Plant Physiol.* 1994, *106*, 817–821.
100. **Scheible, W.-R. *et al.*** Nitrate acts as a signal to induce organic acid metabolism and repress starch metabolism in tobacco. *Plant Cell* 1997, *9*, 783–798.
101. **Stitt, M. *et al.*** Steps towards an integrated view of nitrogen metabolism. *J. Exp. Bot.* 2002, *53*, 959–970.
102. **Foyer, C.H. *et al.*** Photosynthetic carbon–nitrogen interactions: Modelling inter-pathway control and signalling. In *Annual Plant Reviews: Control of Primary Metabolism in Plants*; Wiley Online Books; 2006; pp. 325–347 ISBN 9780470988640.
103. **Zhu, X.G. *et al.*** What is the maximum efficiency with which photosynthesis can convert solar energy into biomass? *Curr. Opin. Biotechnol.* 2008, *19*, 153–159.
104. **Oaks, A. & Hirel, B.** Nitrogen metabolism in roots. *Annu. Rev. Plant Physiol.* 1985, *36*, 345–365.
105. **Matt, P. *et al.*** The immediate cause of the diurnal changes of nitrogen metabolism in leaves of nitrate-replete tobacco: a major imbalance between the rate of nitrate reduction and the rates of nitrate uptake and ammonium metabolism during the first part of the light peri. *Plant, Cell Environ.* 2001, *24*, 177–190.
106. **Matt, P. *et al.*** Elevated carbon dioxide increases nitrate uptake and nitrate reductase activity when tobacco is growing on nitrate, but increases ammonium uptake and inhibits nitrate reductase activity when tobacco is growing on ammonium nitrate. *Plant, Cell Environ.* 2001, *24*, 1119–1137.
107. **Lillo, C.** Signalling cascades integrating light-enhanced nitrate metabolism. *Biochem. J.* 2008, *415*, 11–19.
108. **Keys, A.J.** The re-assimilation of ammonia produced by photorespiration and the nitrogen economy of C3 higher plants. *Photosynth. Res.* 2006, *87*, 165–175.
109. **Bauwe, H. & Kolukisaoglu, Ü.** Genetic manipulation of glycine decarboxylation. *J. Exp. Bot.* 2003, *54*, 1523–1535.
110. **Hirel, B. & Lea, P.J.** Ammonia assimilation. In *Plant Nitrogen*; Lea, P.J., Morot-Gaudry, J.-F.,

Eds.; Springer Berlin Heidelberg: Berlin, Heidelberg, 2001; pp. 79–99 ISBN 978-3-662-04064-5.
111. **Wingler, A. *et al.*** Photorespiration: metabolic pathways and their role in stress protection. *Philos. Trans. R. Soc. B* 2000, *355*, 1517–1529.
112. **Nunes-Nesi, A. *et al.*** Metabolic and signaling aspects underpinning the regulation of plant carbon nitrogen interactions. *Mol. Plant* 2010, *3*, 973–996.
113. **Hodges, M. *et al.*** Higher plant $NADP^+$-dependent isocitrate dehydrogenases, ammonium assimilation and NADPH production. *Plant Physiol. Biochem.* 2003, *41*, 577–585.
114. **Lancien, M. *et al.*** Enzyme redundancy and the importance of 2-oxoglutarate in higher plant ammonium assimilation. *Plant Physiol.* 2000, *123*, 817–824.
115. **Lemaitre, T. *et al.*** NAD-dependent isocitrate dehydrogenase mutants of Arabidopsis suggest the enzyme is not limiting for nitrogen assimilation. *Plant Physiol.* 2007, *144*, 1546–1558.
116. **Nunes-Nesi, A. *et al.*** Operation and function of the tricarboxylic acid cycle in the illuminated leaf. *Physiol. Plant.* 2007, *129*, 45–56.
117. **Huppe, H.C. & Turpin, D.H.** Integration of carbon and nitrogen metabolism in plant and algal cells. *Annu. Rev. Plant Physiol. Plant Mol. Biol.* 1994, *45*, 577–607.
118. **Voll, L.M. *et al.*** Antisense inhibition of enolase strongly limits the metabolism of aromatic amino acids, but has only minor effects on respiration in leaves of transgenic tobacco plants. *New Phytol.* 2009, *184*, 607–618.
119. **Henkes, S. *et al.*** A small decrease of plastid transketolase activity in antisense tobacco transformants has dramatic effects on photosynthesis and phenylpropanoid metabolism. *Plant Cell* 2001, *13*, 535–551.
120. **Forde, B.G.** Local and long-range signaling pathways regulating plant responses to nitrate. *Annu. Rev. Plant Biol.* 2002, *53*, 203–224.
121. **Foyer, C.H. *et al.*** Markers and signals associated with nitrogen assimilation in higher plants. *J. Exp. Bot.* 2003, *54*, 585–593.
122. **Stitt, M.** Nitrate regulation of metabolism and growth. *Curr. Opin. Plant Biol.* 1999, *2*, 178–186.
123. **Dutilleul, C. *et al.*** Mitochondria-driven changes in leaf NAD status exert a crucial influence on the control of nitrate assimilation and the integration of carbon and nitrogen metabolism. *Plant Physiol.* 2005, *139*, 64–78.
124. **Zaffagnini, M. *et al.*** Redox Homeostasis in Photosynthetic Organisms: Novel and Established Thiol-Based Molecular Mechanisms. *Antioxid. Redox Signal.* 2018, *17*, ars.2018.7617.
125. **Meyer, Y. *et al.*** Thioredoxins and glutaredoxins: unifying elements in redox biology. *Annu. Rev. Genet.* 2009, *43*, 335–367.
126. **Holmgren, A.** Thioredoxin. *Annu. Rev. Biochem.* 1985, *54*, 237–271.
127. **Katti, S.K. *et al.*** Crystal structure of thioredoxin from *Escherichia coli* at 1.68 Å resolution. *J. Mol. Biol.* 1990, *212*, 167–184.
128. **Eklund, H. *et al.*** Conformational and functional similarities between glutaredoxin and thioredoxins. *EMBO J.* 1984, *3*, 1443–1449.
129. **Balmer, Y. *et al.*** Oxidation-reduction and activation properties of chloroplast fructose 1,6-bisphosphatase with mutated regulatory site. *Biochemistry* 2001, *40*, 15444–15450.
130. **Hara, S. *et al.*** Thioredoxin-*h*1 reduces and reactivates the oxidized cytosolic malate dehydrogenase dimer in higher plants. *J. Biol. Chem.* 2006, *281*, 32065–32071.
131. **Berndt, C. *et al.*** Thioredoxins and glutaredoxins as facilitators of protein folding. *Biochim. Biophys. Acta - Mol. Cell Res.* 2008, *1783*, 641–650.
132. **Sanz-Barrio, R. *et al.*** Chaperone-like properties of tobacco plastid thioredoxins f and m. *J. Exp. Bot.* 2012, *63*, 365–379.
133. **Chae, H.B. *et al.*** Thioredoxin reductase type C (NTRC) orchestrates enhanced thermotolerance to *Arabidopsis* by its redox-dependent holdase chaperone function. *Mol. Plant* 2013, *6*, 323–336.
134. **Hölscher, C. *et al.*** Dual-targeting of *Arabidopsis* 6-phosphogluconolactonase 3 (PGL3) to chloroplasts and peroxisomes involves interaction with Trx *m2* in the cytosol. *Mol. Plant* 2014, *7*, 252–255.
135. **Buchanan, B.B. *et al.*** Fifty years in the thioredoxin field and a bountiful harvest. *Biochim. Biophys. Acta - Gen. Subj.* 2012, *1820*, 1822–1829.
136. **Laurent, C.T. *et al.*** Enzymatic synthesis of deoxyribonucleotides. *J. Biol. Chem.* 1964, *239*, 3436–3444.
137. **Buchanan, B.B. *et al.*** Ferredoxin-activated fructose diphosphatase in isolated chloroplasts. *Biochem. Biophys. Res. Commun.* 1967, *29*, 74–79.
138. **Buchanan, B.B. & Wolosiuk, R.A.** Photosynthetic regulatory protein found in animal and bacterial cells. *Nature* 1976, *264*, 669–670.
139. **Holmgren, A. *et al.*** Photosynthetic regulatory protein from rabbit liver is identical with

thioredoxin. *FEBS Lett.* 1977, *82*, 351–354.
140. **Wolosiuk, R.A. & Buchanan, B.B.** Thioredoxin and glutathione regulate photosynthesis in chloroplasts. *Nature* 1977, *266*, 565–567.
141. **Jacquot, J.P. *et al.*** Evidence for the existence of several enzyme-specific thioredoxins in plants. *FEBS Lett.* 1978, *96*, 243–246.
142. **Meyer, Y. *et al.*** Thioredoxin and glutaredoxin systems in plants: molecular mechanisms, crosstalks, and functional significance. *Antioxid. Redox Signal.* 2012, *17*, 1124–60.
143. **Meyer, Y. *et al.*** Thioredoxins in Arabidopsis and other plants. *Photosynth. Res.* 2005, *86*, 419–433.
144. **Rivera-Madrid, R. *et al.*** Evidence for five divergent thioredoxin *h* sequences in *Arabidopsis thaliana*. *Proc. Natl. Acad. Sci.* 1995, *92*, 5620–5624.
145. **Gelhaye, E. *et al.*** The thioredoxin h system of higher plants. *Plant Physiol. Biochem.* 2004, *42*, 265–271.
146. **Traverso, J.A. *et al.*** Roles of N-terminal fatty acid acylations in membrane compartment partitioning: *Arabidopsis* h-type thioredoxins as a case study. *Plant Cell* 2013, *25*, 1056–1077.
147. **Meng, L. *et al.*** A membrane-associated thioredoxin required for plant growth moves from cell to cell, suggestive of a role in intercellular communication. *Proc. Natl. Acad. Sci.* 2010, *107*, 3900–3905.
148. **Reichheld, J.-P. *et al.*** Inactivation of thioredoxin reductases reveals a complex interplay between thioredoxin and glutathione pathways in *Arabidopsis* development. *Plant Cell* 2007, *19*, 1851–1865.
149. **Kobrehel, K. *et al.*** Specific reduction of wheat storage proteins by thioredoxin *h*. *Plant Physiol.* 1992, *99*, 919–924.
150. **Kneeshaw, S. *et al.*** Selective protein denitrosylation activity of thioredoxin-h5 modulates plant immunity. *Mol. Cell* 2014, *56*, 153–162.
151. **Sweat, T.A. & Wolpert, T.J.** Thioredoxin *h5* is required for victorin sensitivity mediated by a CC-NBS-LRR gene in *Arabidopsis*. *Plant Cell* 2007, *19*, 673–687.
152. **Pulido, P. *et al.*** An antioxidant redox system in the nucleus of wheat seed cells suffering oxidative stress. *Plant J.* 2009, *57*, 132–145.
153. **Park, S.K. *et al.*** Heat-shock and redox-dependent functional switching of an h-type Arabidopsis thioredoxin from a disulfide reductase to a molecular chaperone. *Plant Physiol.* 2009, *150*, 552–561.
154. **Laloi, C. *et al.*** Identification and characterization of a mitochondrial thioredoxin system in plants. *Proc. Natl. Acad. Sci.* 2001, *98*, 14144–14149.
155. **Martí, M.C. *et al.*** Mitochondrial and nuclear localization of a novel pea thioredoxin: Identification of its mitochondrial target proteins. *Plant Physiol.* 2009, *150*, 646–657.
156. **Barranco-Medina, S. *et al.*** Hexameric oligomerization of mitochondrial peroxiredoxin PrxIIF and formation of an ultrahigh affinity complex with its electron donor thioredoxin Trx-o. *J. Exp. Bot.* 2008, *59*, 3259–3269.
157. **Yoshida, K. *et al.*** Systematic exploration of thioredoxin target proteins in plant mitochondria. *Plant Cell Physiol.* 2013, *54*, 875–892.
158. **Daloso, D.M. *et al.*** Thioredoxin, a master regulator of the tricarboxylic acid cycle in plant mitochondria. *Proc. Natl. Acad. Sci.* 2015, *112*, E1392–E1400.
159. **Ortiz-Espín, A. *et al.*** Mitochondrial *AtTrxo1* is transcriptionally regulated by AtbZIP9 and AtAZF2 and affects seed germination under saline conditions. *J. Exp. Bot.* 2017, *68*, 1025–1038.
160. **Fonseca-Pereira, P. da *et al.*** The mitochondrial thioredoxin system contributes to the metabolic responses under drought episodes in Arabidopsis. *Plant Cell Physiol.* 2018.
161. **Laughner, B.J. *et al.*** A novel nuclear member of the thioredoxin superfamily. *Plant Physiol.* 1998, *118*, 987–996.
162. **Marchal, C. *et al.*** NTR/NRX define a new thioredoxin system in the nucleus of Arabidopsis thaliana cells. *Mol. Plant* 2014, *7*, 30–44.
163. **Vignols, F. *et al.*** Redox control of Hsp70-co-chaperone interaction revealed by expression of a thioredoxin-like *Arabidopsis* protein. *J. Biol. Chem.* 2003, *278*, 4516–4523.
164. **Serrato, A.J. *et al.*** AtCXXS: Atypical members of the *Arabidopsis thaliana* thioredoxin h family with a remarkably high disulfide isomerase activity. *Physiol. Plant.* 2008, *133*, 611–622.
165. **Liu, Q. *et al.*** An Atypical Thioredoxin Imparts Early Resistance to *Sugarcane Mosaic Virus* in Maize. *Mol. Plant* 2017, *10*, 483–497.
166. **Alkhalfioui, F. *et al.*** A novel type of thioredoxin dedicated to symbiosis in legumes. *Plant Physiol.* 2008, *148*, 424–435.
167. **Lemaire, S.D. *et al.*** Characterization of thioredoxin y, a new type of thioredoxin identified in the genome of *Chlamydomonas reinhardtii*. *FEBS Lett.* 2003, *543*, 87–92.

168. **Mestres-Ortega, D. & Meyer, Y.** The *Arabidopsis thaliana* genome encodes at least four thioredoxins *m* and a new prokaryotic-like thioredoxin. *Gene* 1999, *240*, 307–316.
169. **Arsova, B. *et al.*** Plastidial thioredoxin z interacts with two fructokinase-like proteins in a thiol-dependent manner: Evidence for an essential role in chloroplast development in Arabidopsis and Nicotiana benthamiana. *Plant Cell Online* 2010, *22*, 1498–1515.
170. **Bohrer, A.-S. *et al.*** New insights into the reduction systems of plastidial thioredoxins point out the unique properties of thioredoxin z from *Arabidopsis*. *J. Exp. Bot.* 2012, *63*, 6315–6323.
171. **Belin, C. *et al.*** A comprehensive study of thiol reduction gene expression under stress conditions in *Arabidopsis thaliana*. *Plant, Cell Environ.* 2015, *38*, 299–314.
172. **Hartman, H. *et al.*** Contrasting evolutionary histories of chloroplast thioredoxins *f* and *m*. *Mol. Biol. Evol.* 1990, *7*, 247–254.
173. **Sahrawy, M. *et al.*** Intron position as an evolutionary marker of thioredoxins and thioredoxin domains. *J. Mol. Evol.* 1996, *42*, 422–431.
174. **Tsugita, A. *et al.*** Spinach chloroplast thioredoxins in evolutionary drift. *Biochem. Biophys. Res. Commun.* 1983, *115*, 1–7.
175. **Capitani, G. *et al.*** Crystal structures of two functionally different thioredoxins in spinach chloroplasts. *J. Mol. Biol.* 2000, *302*, 135–154.
176. **Lemaire, S.D. *et al.*** *Chlamydomonas reinhardtii*: a model organism for the study of the thioredoxin family. *Plant Physiol. Biochem.* 2003, *41*, 513–521.
177. **Collin, V. *et al.*** The Arabidopsis plastidial thioredoxins. *J. Biol. Chem.* 2003, *278*, 23747–23752.
178. **Geck, M.K. *et al.*** Identification of residues of spinach thioredoxin f that influence interactions with target enzymes. *J. Biol. Chem.* 1996, *271*, 24736–24740.
179. **Geigenberger, P. & Fernie, A.R.** Metabolic control of redox and redox control of metabolism in plants. *Antioxid. Redox Signal.* 2014, *21*, 1389–1421.
180. **Geigenberger, P. *et al.*** The unprecedented versatility of the plant thioredoxin system. *Trends Plant Sci.* 2017, *22*, 249–262.
181. **Lichter, A. & Häberlein, I.** A light-dependent redox signal participates in the regulation of ammonia fixation in chloroplasts of higher plants - ferredoxin: glutamate synthase is a thioredoxin-dependent enzyme. *J. Plant Physiol.* 1998, *153*, 83–90.
182. **Rey, P. *et al.*** Overexpression of plastidial thioredoxins f and m differentially alters photosynthetic activity and response to oxidative stress in tobacco plants. *Front. Plant Sci.* 2013, *4*, 390.
183. **Okegawa, Y. & Motohashi, K.** Chloroplastic thioredoxin *m* functions as a major regulator of Calvin cycle enzymes during photosynthesis *in vivo*. *Plant J.* 2015, *84*, 900–913.
184. **Benitez-Alfonso, Y. *et al.*** Control of *Arabidopsis* meristem development by thioredoxin-dependent regulation of intercellular transport. *Proc. Natl. Acad. Sci.* 2009, *106*, 3615–3620.
185. **Collin, V. *et al.*** Characterization of plastidial thioredoxins from Arabidopsis belonging to the new y-type. *Plant Physiol.* 2004, *136*, 4088–4095.
186. **Navrot, N. *et al.*** Plant glutathione peroxidases are functional peroxiredoxins distributed in several subcellular compartments and regulated during biotic and abiotic stresses. *Plant Physiol.* 2006, *142*, 1364–1379.
187. **Laugier, E. *et al.*** Involvement of thioredoxin y2 in the preservation of leaf methionine sulfoxide reductase capacity and growth under high light. *Plant, Cell Environ.* 2013, *36*, 670–682.
188. **Vieira Dos Santos, C. *et al.*** Specificity of thioredoxins and glutaredoxins as electron donors to two distinct classes of Arabidopsis plastidial methionine sulfoxide reductases B. *FEBS Lett.* 2007, *581*, 4371–4376.
189. **Diaz, M.G. *et al.*** Redox regulation of PEP activity during seedling establishment in Arabidopsis thaliana. *Nat. Commun.* 2018, *9*.
190. **Wimmelbacher, M. & Börnke, F.** Redox activity of thioredoxin z and fructokinase-like protein 1 is dispensable for autotrophic growth of *Arabidopsis thaliana*. *J. Exp. Bot.* 2014, *65*, 2405–2413.
191. **Serrato, A.J. *et al.*** A novel NADPH thioredoxin reductase, localised in the chloroplast, which deficiency causes hypersensitivity to abiotic stress in *Arabidopsis thaliana*. *J. Biol. Chem.* 2004, *279*, 43821–43827.
192. **Kirchsteiger, K. *et al.*** NADPH Thioredoxin Reductase C Is Localized in Plastids of Photosynthetic and Nonphotosynthetic Tissues and Is Involved in Lateral Root Formation in *Arabidopsis*. *Plant Cell* 2012, *24*, 1534–1548.
193. **Alkhalfioui, F. *et al.*** Unique properties of NADP-thioredoxin reductase C in legumes. *J. Exp. Bot.* 2007, *58*, 969–978.
194. **Moon, J.C. *et al.*** The C-type Arabidopsis thioredoxin reductase ANTR-C acts as an electron donor to 2-Cys peroxiredoxins in chloroplasts. *Biochem. Biophys. Res. Commun.* 2006, *348*,

478–484.
195. **Puerto-Galán, L. *et al.*** The contribution of NADPH thioredoxin reductase C (NTRC) and sulfiredoxin to 2-Cys peroxiredoxin overoxidation in *Arabidopsis thaliana* chloroplasts. *J. Exp. Bot.* 2015, *66*, 2957–2966.
196. **Toivola, J. *et al.*** Overexpression of chloroplast NADPH-dependent thioredoxin reductase in *Arabidopsis* enhances leaf growth and elucidates *in vivo* function of reductase and thioredoxin domains. *Front. Plant Sci.* 2013, *4*, 389.
197. **Michalska, J. *et al.*** NTRC links built-in thioredoxin to light and sucrose in regulating starch synthesis in chloroplasts and amyloplasts. *Proc. Natl. Acad. Sci.* 2009, *106*, 9908–13.
198. **Richter, A.S. & Grimm, B.** Thiol-based redox control of enzymes involved in the tetrapyrrole biosynthesis pathway in plants. *Front. Plant Sci.* 2013, *4*, 371.
199. **Pérez-Ruiz, J.M. *et al.*** NADPH thioredoxin reductase C is involved in redox regulation of the Mg-chelatase I subunit in *Arabidopsis thaliana* chloroplasts. *Mol. Plant* 2014, *7*, 1252–1255.
200. **Perez-Ruiz, J.M.** Rice NTRC Is a High-Efficiency Redox System for Chloroplast Protection against Oxidative Damage. *Plant Cell Online* 2006, *18*, 2356–2368.
201. **Pérez-Ruiz, J.M. *et al.*** NTRC-dependent redox balance of 2-Cys peroxiredoxins is needed for optimal function of the photosynthetic apparatus. *Proc. Natl. Acad. Sci.* 2017, *114*, 12069–12074.
202. **Ojeda, V. *et al.*** NADPH thioredoxin reductase C and thioredoxins act concertedly in seedling development. *Plant Physiol.* 2017, *174*, 1436–1448.
203. **Rey, P. *et al.*** A novel thioredoxin-like protein located in the chloroplast is induced by water deficit in *Solanum tuberosum* L. plants. *Plant J.* 1998, *13*, 97–107.
204. **Broin, M. *et al.*** Involvement of CDSP 32, a drought-induced thioredoxin, in the response to oxidative stress in potato plants. *FEBS Lett.* 2000, *467*, 245–248.
205. **Broin, M. & Rey, P.** Potato plants lacking the CDSP32 plastidic thioredoxin exhibit overoxidation of the BAS1 2-cysteine peroxiredoxin and increased lipid peroxidation in thylakoids under photooxidative stress. *Plant Physiol.* 2003, *132*, 1335–1343.
206. **Tarrago, L. *et al.*** Plant thioredoxin CDSP32 regenerates 1-Cys methionine sulfoxide reductase B activity through the direct reduction of sulfenic acid. *J. Biol. Chem.* 2010, *285*, 14964–14972.
207. **Martin, M.N. *et al.*** The role of 5′-adenylylsulfate reductase in controlling sulfate reduction in plants. *Photosynth. Res.* 2005, *86*, 309–323.
208. **Bick, J.A. *et al.*** Glutaredoxin function for the carboxyl-terminal domain of the plant-type 5'-adenylylsulfate reductase. *Proc. Natl. Acad. Sci.* 1998, *95*, 8404–8409.
209. **Dangoor, I. *et al.*** A small family of chloroplast atypical thioredoxins. *Plant Physiol.* 2009, *149*, 1240–1250.
210. **Yoshida, K. *et al.*** Thioredoxin-like2/2-Cys peroxiredoxin redox cascade supports oxidative thiol modulation in chloroplasts. *Proc. Natl. Acad. Sci.* 2018, *115*, E8296–E8304.
211. **Motohashi, K. & Hisabori, T.** HCF164 receives reducing equivalents from stromal thioredoxin across the thylakoid membrane and mediates reduction of target proteins in the thylakoid lumen. *J. Biol. Chem.* 2006, *281*, 35039–35047.
212. **Motohashi, K. & Hisabori, T.** CcdA is a thylakoid membrane protein required for the transfer of reducing equivalents from stroma to thylakoid lumen in the higher plant chloroplast. *Antioxid. Redox Signal.* 2010, *13*, 1169–1176.
213. **Brooks, M.D. *et al.*** A thioredoxin-like/β-propeller protein maintains the efficiency of light harvesting in *Arabidopsis*. *Proc. Natl. Acad. Sci.* 2013, *110*, E2733–E2740.
214. **Karamoko, M. *et al.*** Lumen thiol oxidoreductase1, a disulfide bond-forming catalyst, is required for the assembly of photosystem II in *Arabidopsis*. *Plant Cell* 2011, *23*, 4462–4475.
215. **Jacquot, J.P. *et al.*** Arabidopsis thaliana NAPHP thioredoxin reductase: cDNA characterization and expression of the recombinant protein in *Escherichia coli*. *J. Mol. Biol.* 1994, *235*, 1357–1363.
216. **Balmer, Y. *et al.*** A complete ferredoxin/thioredoxin system regulates fundamental processes in amyloplasts. *Proc. Natl. Acad. Sci.* 2006, *103*, 2988–2993.
217. **Barajas-López, J. de D. *et al.*** Localization in roots and flowers of pea chloroplastic thioredoxin *f* and thioredoxin *m* proteins reveals new roles in nonphotosynthetic organs. *Plant Physiol.* 2007, *145*, 946–960.
218. **Hanke, G.T. *et al.*** Fd:FNR electron transfer complexes: evolutionary refinement of structural interactions. *Photosynth. Res.* 2004, *81*, 317–327.
219. **Hanke, G.T. *et al.*** Multiple iso-proteins of FNR in *Arabidopsis*: evidence for different contributions to chloroplast function and nitrogen assimilation. *Plant, Cell Environ.* 2005, *28*, 1146–1157.
220. **Pérez-Ruiz, J.M. & Cejudo, F.J.** A proposed reaction mechanism for rice NADPH thioredoxin

reductase C, an enzyme with protein disulfide reductase activity. *FEBS Lett.* 2009, *583*, 1399–1402.
221. **Nikkanen, L. *et al.*** Crosstalk between chloroplast thioredoxin systems in regulation of photosynthesis. *Plant Cell Environ.* 2016, *39*, 1691–1705.
222. **Yoshida, K. & Hisabori, T.** Two distinct redox cascades cooperatively regulate chloroplast functions and sustain plant viability. *Proc. Natl. Acad. Sci.* 2016, *113*, E3967–E3976.
223. **Thormählen, I. *et al.*** Thioredoxin *f1* and NADPH-dependent thioredoxin reductase C have overlapping functions in regulating photosynthetic metabolism and plant growth in response to varying light conditions. *Plant Physiol.* 2015, *169*, 1766–1786.
224. **Chibani, K. *et al.*** Biochemical properties of poplar thioredoxin z. *FEBS Lett.* 2011, *585*, 1077–1081.
225. **Buchanan, B.B. *et al.*** The ferredoxin/thioredoxin system: from discovery to molecular structures and beyond. *Photosynth. Res.* 2002, *73*, 215–222.
226. **Montrichard, F. *et al.*** Thioredoxin targets in plants: the first 30 years. *J. Proteomics* 2009, *72*, 452–74.
227. **Wolosiuk, R.A. *et al.*** Isolation of three thioredoxins from spinach leaves. *J. Biol. Chem.* 1979, *254*, 1627–1632.
228. **Yoshida, K. *et al.*** Thioredoxin selectivity for thiol-based redox regulation of target proteins in chloroplasts. *J. Biol. Chem.* 2015, *290*, 14278–14288.
229. **Wong, J.H. *et al.*** Thioredoxin targets of developing wheat seeds identified by complementary proteomic approaches. *Phytochemistry* 2004, *65*, 1629–1640.
230. **Marchand, C. *et al.*** Comparative proteomic approaches for the isolation of proteins interacting with thioredoxin. *Proteomics* 2006, *6*, 6528–6537.
231. **Alkhalfioui, F. *et al.*** Thioredoxin-linked proteins are reduced during germination of *Medicago truncatula* seeds. *Plant Physiol.* 2007, *144*, 1559–1579.
232. **Pérez-Pérez, M.E. *et al.*** The deep thioredoxome in *Chlamydomonas reinhardtii*: New insights into redox regulation. *Mol. Plant* 2017, *10*, 1107–1125.
233. **Yano, H. *et al.*** A strategy for the identification of proteins targeted by thioredoxin. *Proc. Natl. Acad. Sci.* 2001, *98*, 4794–4799.
234. **Kobrehel, K. *et al.*** Role of the NADP/thioredoxin system in the reduction of α-amylase and trypsin inhibitor proteins. *J. Biol. Chem.* 1991, *266*, 16135–16140.
235. **Wong, J.H. *et al.*** Unraveling thioredoxin-linked metabolic processes of cereal starchy endosperm using proteomics. *FEBS Lett.* 2003, *547*, 151–156.
236. **Marx, C. *et al.*** Thioredoxin and germinating barley: targets and protein redox changes. *Planta* 2003, *216*, 454–60.
237. **Maeda, K. *et al.*** Cy5 maleimide labelling for sensitive detection of free thiols in native protein extracts: identification of seed proteins targeted by barley thioredoxin h isoforms. *Biochem. J.* 2004, *378*, 497–507.
238. **Marchand, C. *et al.*** New targets of Arabidopsis thioredoxins revealed by proteomic analysis. *Proteomics* 2004, *4*, 2696–2706.
239. **Hägglund, P. *et al.*** Identification of thioredoxin disulfide targets using a quantitative proteomics approach based on isotope-coded affinity tags. *J. Proteome Res.* 2008, *7*, 5270–5276.
240. **Zhang, T. *et al.*** Identification of thioredoxin targets in guard cell enriched epidermal peels using cysTMT proteomics. *J. Proteomics* 2016, *133*, 48–53.
241. **Wynn, R. *et al.*** Mixed disulfide intermediates during the reduction of disulfides by *Escherichia coli* thioredoxin. *Biochemistry* 1995, *34*, 11807–11813.
242. **Qin, J. *et al.*** Solution structure of human thioredoxin in a mixed disulfide intermediate complex with its target peptide from the transcription factor NFκB. *Structure* 1995, *3*, 289–297.
243. **Verdoucq, L. *et al.*** *In vivo* characterization of a thioredoxin h target protein defines a new peroxiredoxin family. *J. Biol. Chem.* 1999, *274*, 19714–19722.
244. **Motohashi, K. *et al.*** Comprehensive survey of proteins targeted by chloroplast thioredoxin. *Proc. Natl. Acad. Sci.* 2001, *98*, 11224–11229.
245. **Balmer, Y. *et al.*** Proteomics gives insight into the regulatory function of chloroplast thioredoxins. *Proc. Natl. Acad. Sci.* 2003, *100*, 370–375.
246. **Yamazaki, D. *et al.*** Target proteins of the cytosolic thioredoxins in *Arabidopsis thaliana*. *Plant Cell Physiol.* 2004, *45*, 18–27.
247. **Balmer, Y. *et al.*** Thioredoxin links redox to the regulation of fundamental processes of plant mitochondria. *Proc. Natl. Acad. Sci.* 2004, *101*, 2642–2647.
248. **Marchand, C.H. *et al.*** Thioredoxin targets in *Arabidopsis* roots. *Proteomics* 2010, *10*, 2418–2428.
249. **Rey, P. *et al.*** Analysis of the proteins targeted by CDSP32, a plastidic thioredoxin participating

in oxidative stress responses. *Plant J.* 2005, *41*, 31–42.
250. **Pérez-Pérez, M.E. *et al.*** Selecting thioredoxins for disulphide proteomics: Target proteomes of three thioredoxins from the cyanobacterium Synechocystis sp. PCC 6803. *Proteomics* 2006, *6*, S186–S195.
251. **Lemaire, S.D. *et al.*** New thioredoxin targets in the unicellular photosynthetic eukaryote Chlamydomonas reinhardtii. *Proc. Natl. Acad. Sci.* 2004, *101*, 7475–7480.
252. **Sturm, N. *et al.*** Identification of proteins targeted by the thioredoxin superfamily in plasmodium falciparum. *PLoS Pathog.* 2009, *5*.
253. **Richter, A.S. *et al.*** Posttranslational influence of NADPH-dependent thioredoxin reductase C on enzymes in tetrapyrrole synthesis. *Plant Physiol.* 2013, *162*, 63–73.
254. **Courteille, A. *et al.*** Thioredoxin m4 controls photosynthetic alternative electron pathways in Arabidopsis. *Plant Physiol.* 2013, *161*, 508–520.
255. **Brzezowski, P. *et al.*** Regulation and function of tetrapyrrole biosynthesis in plants and algae. *Biochim. Biophys. Acta* 2015, *1847*, 968–985.
256. **Da, Q. *et al.*** M-type thioredoxins are involved in the xanthophyll cycle and proton motive force to alter NPQ under low-light conditions in Arabidopsis. *Plant Cell Rep.* 2017, *37*, 279–291.
257. **Ikegami, A. *et al.*** The CHLI1 subunit of *Arabidopsis thaliana* magnesium chelatase is a target protein of the chloroplast thioredoxin. *J. Biol. Chem.* 2007, *282*, 19282–19291.
258. **Luo, T. *et al.*** Thioredoxin redox regulates ATPase activity of magnesium chelatase CHLI subunit and modulates redox-mediated signaling in tetrapyrrole biosynthesis and homeostasis of reactive oxygen species in pea plants. *Plant Physiol.* 2012, *159*, 118–130.
259. **Wang, P. *et al.*** Evidence for a role of chloroplastic m-type thioredoxins in the biogenesis of photosystem II in Arabidopsis. *Plant Physiol.* 2013, *163*, 1710–1728.
260. **Trebitsh, T. *et al.*** Translation of chloroplast psbA mRNA is modulated in the light by counteracting oxidizing and reducing activities. *Mol. Cell. Biol.* 2000, *20*, 1116–23.
261. **Trebitsh, T. & Danon, A.** Translation of chloroplast psbA mRNA is regulated by signals initiated by both photosystems II and I. *Proc. Natl. Acad. Sci.* 2001, *98*, 12289–12294.
262. **Hisabori, T. *et al.*** The chloroplast ATP synthase features the characteristic redox regulation machinery. *Antioxid. Redox Signal.* 2013, *19*, 1846–1854.
263. **Ort, D.R. & Oxborough, K.** In situ regulation of chloroplast coupling factor activity. *Annu. Rev. Plant Physiol. Plant Mol. Biol.* 1992, *43*, 269–291.
264. **Nowak, K.F. & McCarty, R.E.** Regulatory role of the C-terminus of the ε subunit from the chloroplast ATP synthase. *Biochemistry* 2004, *43*, 3273–3279.
265. **Mills, J.D. *et al.*** Modulation of coupling factor ATPase activity in intact chloroplasts. *FEBS Lett.* 1980, *112*, 173–177.
266. **Schwarz, O. *et al.*** Kinetics and thioredoxin specificity of thiol modulation of the chloroplast H^+-ATPase. *J. Biol. Chem.* 1997, *272*, 16924–16927.
267. **Carrillo, L.R. *et al.*** Multi-level regulation of the chloroplast ATP synthase: the chloroplast NADPH thioredoxin reductase C (NTRC) is required for redox modulation specifically under low irradiance. *Plant J.* 2016, *87*, 654–663.
268. **Naranjo, B. *et al.*** The chloroplast NADPH thioredoxin reductase C, NTRC, controls non-photochemical quenching of light energy and photosynthetic electron transport in *Arabidopsis*. *Plant Cell Environ.* 2016, *39*, 804–822.
269. **Tikkanen, M. *et al.*** Light-harvesting mutants show differential gene expression upon shift to high light as a consequence of photosynthetic redox and reactive oxygen species metabolism. *Philos. Trans. R. Soc. B* 2014, *369*, 20130229.
270. **Hertle, A.P. *et al.*** PGRL1 is the elusive ferredoxin-plastoquinone reductase in photosynthetic cyclic electron flow. *Mol. Cell* 2013, *49*, 511–523.
271. **Nikkanen, L. *et al.*** Regulation of cyclic electron flow by chloroplast NADPH-dependent thioredoxin system. *Plant Direct* 2018, 1–24.
272. **Dunford, R.P. *et al.*** Location of the redox-active cysteines in chloroplast sedoheptulose-1,7-bisphosphatase indicates that its allosteric regulation is similar but not identical to that of fructose-1,6-bisphosphatase. *Photosynth. Res.* 1998, *58*, 221–230.
273. **Sparla, F. *et al.*** Regulation of photosynthetic GAPDH dissected by mutants. *Plant Physiol.* 2005, *138*, 2210–2219.
274. **Geck, M.K. & Hartman, F.C.** Kinetic and mutational analyses of the regulation of phosphoribulokinase by thioredoxins. *J. Biol. Chem.* 2000, *275*, 18034–18039.
275. **Porter, M.A. *et al.*** Characterization of the regulatory thioredoxin site of phosphoribulokinase. *J. Biol. Chem.* 1988, *263*, 123–129.
276. **Wedel, N. *et al.*** CP12 provides a new mode of light regulation of Calvin cycle activity in higher plants. *Proc. Natl. Acad. Sci.* 1997, *94*, 10479–10484.
277. **Marri, L. *et al.*** Prompt and easy activation by specific thioredoxins of calvin cycle enzymes of

arabidopsis thaliana associated in the GAPDH/CP12/PRK supramolecular complex. *Mol. Plant* 2009, *2*, 259–269.
278. **Naranjo, B. *et al.*** Type-*f* thioredoxins have a role in the short-term activation of carbon metabolism and their loss affects growth under short-day conditions in *Arabidopsis thaliana*. *J. Exp. Bot.* 2016, *67*, 1951–1964.
279. **Eliyahu, E. *et al.*** ACHT4-driven oxidation of APS1 attenuates starch synthesis under low light intensity in *Arabidopsis* plants. *Proc. Natl. Acad. Sci.* 2015, *112*, 12876–12881.
280. **Pulido, P. *et al.*** Functional analysis of the pathways for 2-Cys peroxiredoxin reduction in *Arabidopsis thaliana* chloroplasts. *J. Exp. Bot.* 2010, *61*, 4043–4054.
281. **Portis, A.R.** Rubisco activase - Rubisco's catalytic chaperone. *Photosynth. Res.* 2003, *75*, 11–27.
282. **Zhang, N. & Portis, A.R.** Mechanism of light regulation of Rubisco: a specific role for the larger Rubisco activase isoform involving reductive activation by thioredoxin-f. *Proc. Natl. Acad. Sci. U. S. A.* 1999, *96*, 9438–43.
283. **Zhang, N. *et al.*** Light modulation of Rubisco in Arabidopsis requires a capacity for redox regulation of the larger Rubisco activase isoform. *Proc. Natl. Acad. Sci.* 2002, *99*, 3330–3334.
284. **Heo, J. & Holbrook, G.P.** Regulation of 2-carboxy-D-arabinitol 1-phosphate phosphatase: activation by glutathione and interaction with thiol reagents. *Biochem. J.* 1999, *338*, 409–416.
285. **Thormählen, I. *et al.*** Thioredoxins play a crucial role in dynamic acclimation of photosynthesis in fluctuating light. *Mol. Plant* 2017, *10*, 168–182.
286. **Ojeda, V. *et al.*** 2-Cys peroxiredoxins participate in the oxidation of chloroplast enzymes in the dark. *Mol. Plant* 2018, 1–12.
287. **Hall, M. *et al.*** Thioredoxin targets of the plant chloroplast lumen and their implications for plastid function. *Proteomics* 2010, *10*, 987–1001.
288. **Karamoko, M. *et al.*** Operation of trans-thylakoid thiol-metabolizing pathways in photosynthesis. *Front. Plant Sci.* 2013, *4*, 476.
289. **Page, M.L.D. *et al.*** A homolog of prokaryotic thiol disulfide transporter CcdA is required for the assembly of the cytochrome b_6f complex in *Arabidopsis* chloroplasts. *J. Biol. Chem.* 2004, *279*, 32474–32482.
290. **Lennartz, K. *et al.*** HCF164 encodes a thioredoxin-like protein involved in the biogenesis of the cytochrome b_6f complex in Arabidopsis. *Plant Cell* 2001, *13*, 2539–2551.
291. **Onoa, B. *et al.*** Atomic force microscopy of photosystem II and its unit cell clustering quantitatively delineate the mesoscale variability in *Arabidopsis* thylakoids. *PLoS One* 2014, *9*, e101470.
292. **Lu, Y. *et al.*** Identification of potential targets for thylakoid oxidoreductase AtVKOR/LTO1 in chloroplasts. *Protein Pept. Lett.* 2015, *22*, 219–225.
293. **Gopalan, G. *et al.*** Structural analysis uncovers a role for redox in regulating FKBP13, an immunophilin of the chloroplast thylakoid lumen. *Proc. Natl. Acad. Sci.* 2004, *101*, 13945–13950.
294. **Buchanan, B.B. & Luan, S.** Redox regulation in the chloroplast thylakoid lumen: a new frontier in photosynthesis research. *J. Exp. Bot.* 2005, *56*, 1439–1447.
295. **Gollan, P.J. & Bhave, M.** A thylakoid-localised FK506-binding protein in wheat may be linked to chloroplast biogenesis. *Plant Physiol. Biochem.* 2010, *48*, 655–662.
296. **Lima, A. *et al.*** A redox-active FKBP-type immunophilin functions in accumulation of the photosystem II supercomplex in Arabidopsis thaliana. *Proc. Natl. Acad. Sci.* 2006, *103*, 12631–12636.
297. **Shapiguzov, A. *et al.*** Profound redox sensitivity of peptidyl-prolyl isomerase activity in Arabidopsis thylakoid lumen. *FEBS Lett.* 2006, *580*, 3671–3676.
298. **Kaiser, W.M. & Bassham, J.A.** Light-dark regulation of starch metabolism in chloroplasts: II. Effect of chloroplastic metabolite levels on the formation of ADP-Glucose by chloroplast extracts. *Plant Physiol.* 1979, *63*, 109–113.
299. **Morell, M.K. *et al.*** Subunit structure of spinach leaf ADPglucose pyrophosphorylase. *Plant Physiol.* 1987, *85*, 182–187.
300. **Okita, T.W. *et al.*** The subunit structure of potato tuber ADPglucose pyrophosphorylase. *Plant Physiol.* 1990, *93*, 785–790.
301. **Fu, Y. *et al.*** Mechanism of reductive activation of potato tuber ADP-glucose pyrophosphorylase. *J. Biol. Chem.* 1998, *273*, 25045–25052.
302. **Ballicora, M.A. *et al.*** Activation of the potato tuber ADP-glucose pyrophosphorylase by thioredoxin. *J. Biol. Chem.* 2000, *275*, 1315–1320.
303. **Geigenberger, P. *et al.*** Redox regulation of carbon storage and partitioning in response to light and sugars. *J. Exp. Bot.* 2005, *56*, 1469–1479.
304. **Thormählen, I. *et al.*** Inactivation of thioredoxin *f1* leads to decreased light activation of ADP-

glucose pyrophosphorylase and altered diurnal starch turnover in leaves of *Arabidopsis* plants. *Plant, Cell Environ.* 2013, *36*, 16–29.

305. **Sanz-Barrio, R. *et al.*** Overexpression of plastidial thioredoxin f leads to enhanced starch accumulation in tobacco leaves. *Plant Biotechnol. J.* 2013, *11*, 618–627.
306. **Lepistö, A. *et al.*** Deletion of chloroplast NADPH-dependent thioredoxin reductase results in inability to regulate starch synthesis and causes stunted growth under short-day photoperiods. *J. Exp. Bot.* 2013, *64*, 3843–3854.
307. **Glaring, M.A. *et al.*** Comprehensive survey of redox sensitive starch metabolising enzymes in *Arabidopsis thaliana*. *Plant Physiol. Biochem.* 2012, *58*, 89–97.
308. **Skryhan, K. *et al.*** The role of cysteine residues in redox regulation and protein stability of Arabidopsis thaliana starch synthase 1. *PLoS One* 2015, *10*, e0136997.
309. **Wang, F. *et al.*** The maize plastidic thioredoxin F-type gene *ZmTrxF* increases starch accumulation in transgenic *Arabidopsis*. *Sci. Hortic. (Amsterdam).* 2016, *210*, 205–212.
310. **Wang, F. *et al.*** Enhancement of starch content by constitutive expression of *GmTrxF* in transgenic *Arabidopsis*. *Plant Growth Regul.* 2018, *84*, 351–358.
311. **Balmer, Y. *et al.*** Proteome of amyloplasts isolated from developing wheat endosperm presents evidence of broad metabolic capability. *J. Exp. Bot.* 2006, *57*, 1591–1602.
312. **Kirchberger, S. *et al.*** Molecular and biochemical analysis of the plastidic ADP-glucose transporter (ZmBT1) from *Zea mays*. *J. Biol. Chem.* 2007, *282*, 22481–22491.
313. **Mikkelsen, R. *et al.*** α-glucan, water dikinase (GWD): a plastidic enzyme with redox-regulated and coordinated catalytic activity and binding affinity. *Proc. Natl. Acad. Sci.* 2005, *102*, 1785–90.
314. **Skeffington, A.W. *et al.*** Glucan, water dikinase exerts little control over starch degradation in Arabidopsis leaves at night. *Plant Physiol.* 2014, *165*, 866–879.
315. **Sokolov, L.N. *et al.*** A redox-regulated chloroplast protein phosphatase binds to starch diurnally and functions in its accumulation. *Proc. Natl. Acad. Sci.* 2006, *103*, 9732–9737.
316. **Silver, D.M. *et al.*** Insight into the redox regulation of the phosphoglucan phosphatase SEX4 involved in starch degradation. *FEBS J.* 2013, *280*, 538–548.
317. **Sparla, F. *et al.*** Redox regulation of a novel plastid-targeted β-Amylase. *Plant Physiol.* 2006, *141*, 840–850.
318. **Seung, D. *et al.*** *Arabidopsis thaliana* AMY3 is a unique redox-regulated chloroplastic α-amylase. *J. Biol. Chem.* 2013, *288*, 33620–33633.
319. **Schindler, I. *et al.*** Activation of spinach pullulanase by reduction results in a decrease in the number of isomeric forms. *Biochim. Biophys. Acta - Protein Struct. Mol. Enzymol.* 2001, *1548*, 175–186.
320. **Repellin, A. *et al.*** *In vitro* pullulanase activity of wheat (*Triticum aestivum* L.) limit-dextrinase type starch debranching enzyme is modulated by redox conditions. *J. Cereal Sci.* 2008, *47*, 302–309.
321. **Hase, T. *et al.*** The Interaction of Ferredoxin with Ferredoxin-Dependent Enzymes Photosystem I: The Light-Driven Plastocyanin:Ferredoxin Oxidoreductase. In *Photosystem I: Advances in Photosynthesis and Respiration*; Golbeck, J.H., Ed.; Springer Netherlands: Dordrecht, 2006; pp. 477–498 ISBN 978-1-4020-4256-0.
322. **Florencio, F.J. *et al.*** Thioredoxin-linked activation of the chloroplast and cytosolic forms of *Chlamydomonas reinhardtii* glutamine synthetase. *Plant Physiol. Biochem.* 1993, *31*, 649–655.
323. **Tischner, R. & Schmidt, A.** A thioredoxin-mediated activation of glutamine synthetase and glutamate synthase in Synchronous *Chlorella sorokiniana*. *Plant Physiol.* 1982, *70*, 113–116.
324. **Schmidt, A.** A Thioredoxin Activated Glutamine Synthetase in Chlorella. *Zeitschrift fur Naturforsch. - Sect. C J. Biosci.* 1981, *36*, 396–399.
325. **Papen, H. & Bothe, H.** The activation of glutamine synthetase from the cyanobacterium *Anabaena cylindrica* by thioredoxin. *FEMS Microbiol. Lett.* 1984, *23*, 41–46.
326. **Choi, Y.A. *et al.*** The plastidic glutamine synthetase activity is directly modulated by means of redox change at two unique cysteine residues. *Plant Sci.* 1999, *149*, 175–182.
327. **Taira, M. *et al.*** *Arabidopsis thaliana GLN2*-Encoded Glutamine Synthetase Is Dual Targeted to Leaf Mitochondria and Chloroplasts. *Plant Cell* 2004, *16*, 2048–2058.
328. **Kolbe, A. *et al.*** Combined transcript and metabolite profiling of Arabidopsis leaves reveals fundamental effects of the thiol-disulfide status on plant metabolism. *Plant Physiol.* 2006, *141*, 412–422.
329. **Entus, R. *et al.*** Redox regulation of Arabidopsis 3-deoxy- D -arabino- heptulosonate 7-phosphate synthase. *Plant Physiol.* 2002, *129*, 1866–1871.
330. **Nishizawa, A.N. *et al.*** Chloroplast phenylalanine ammonia-lyase from spinach leaves. *Planta* 1979, *145*, 7–12.
331. **Nikkanen, L. & Rintamäki, E.** Thioredoxin-dependent regulatory networks in chloroplasts

under fluctuating light conditions. *Philos. Trans. R. Soc. B Biol. Sci.* 2014, *369*, 1–7.
332. **Allen, J.F.** State Transitions - a Question of Balance. *Science (80-.).* 2003, *299*, 1530–1532.
333. **Wientjes, E. *et al.*** During state 1 to state 2 transition in *Arabidopsis thaliana*, the photosystem II supercomplex gets phosphorylated but does not disassemble. *J. Biol. Chem.* 2013, *288*, 32821–32826.
334. **Crepin, A. & Caffarri, S.** The specific localizations of phosphorylated Lhcb1 and Lhcb2 isoforms reveal the role of Lhcb2 in the formation of the PSI-LHCII supercomplex in *Arabidopsis* during state transitions. *Biochim. Biophys. Acta - Bioenerg.* 2015, *1847*, 1539–1548.
335. **Wientjes, E. *et al.*** LHCII is an antenna of both photosystems after long-term acclimation. *Biochim. Biophys. Acta - Bioenerg.* 2013, *1827*, 420–426.
336. **Bonardi, V. *et al.*** Photosystem II core phosphorylation and photosynthetic acclimation require two different protein kinases. *Nature* 2005, *437*, 1179–1182.
337. **Depège, N. *et al.*** Role of chloroplast protein kinase Stt7 in LHCII phosphorylation and state transition in *Chlamydomonas*. *Science (80-.).* 2003, *299*, 1572–1575.
338. **Lemeille, S. *et al.*** Analysis of the chloroplast protein kinase Stt7 during state transitions. *PLoS Biol.* 2009, *7*, e1000045.
339. **Wunder, T. *et al.*** Control of *STN7* transcript abundance and transient STN7 dimerisation are involved in the regulation of STN7 activity. *Planta* 2013, *237*, 541–558.
340. **Bennett, J. *et al.*** Cytochrome b_6f complex is required for phosphorylation of light-harvesting chlorophyll a/b complex II in chloroplast photosynthetic membranes. *Eur. J. Biochem.* 1988, *171*, 95–100.
341. **Gal, A. *et al.*** Role of the Cytochrome b_6f complex in the redox-controlled activity of *Acetabularia* thylakoid protein kinase. *J. Biol. Chem.* 1988, *263*, 7785–7791.
342. **Gal, A. *et al.*** Interaction between light harvesting chlorophyll-*a/b* protein (LHCII) kinase and cytochrome b_6/f complex. *J. Biol. Chem.* 1990, *265*, 19742–19749.
343. **Schuster, G. *et al.*** Transient inactivation of the thylakoid photosystem II light-harvesting protein kinase system and concomitant changes in intramembrane particle size during photoinhibition of *Chlamydomonas reinhardtii*. *J. Cell Biol.* 1986, *103*, 71–80.
344. **Dietzel, L. *et al.*** Photosynthetic acclimation: State transitions and adjustment of photosystem stoichiometry - Functional relationships between short-term and long-term light quality acclimation in plants. *FEBS J.* 2008, *275*, 1080–1088.
345. **Wunder, T. *et al.*** The major thylakoid protein kinases STN7 and STN8 revisited: effects of altered STN8 levels and regulatory specificities of the STN kinases. *Front. Plant Sci.* 2013, *4*, 417.
346. **Sanz-Barrio, R. *et al.*** Tobacco plastidial thioredoxins as modulators of recombinant protein production in transgenic chloroplasts. *Plant Biotechnol. J.* 2011, *9*, 639–50.
347. **Genty, B. *et al.*** The relationship between the quantum yield of photosynthetic electron transport and quenching of chlorophyll fluorescence. *Biochim. Biophys. Acta - Gen. Subj.* 1989, *990*, 87–92.
348. **Kramer, D.M. *et al.*** New fluorescence parameters for the determination of Q_A redox state and excitation energy fluxes. *Photosynth. Res.* 2004, *79*, 209–218.
349. **von Caemmerer, S. & Farquhar, G.D.** Some relationships between the biochemistry of photosynthesis and the gas exchange of leaves. *Planta* 1981, *153*, 376–387.
350. **Sharkey, T.D. *et al.*** Fitting photosynthetic carbon dioxide response curves for C_3 leaves. *Plant, Cell Environ.* 2007, *30*, 1035–1040.
351. **Cornic, G. & Briantais, J.-M.** Partitioning of photosynthetic electron flow between CO_2 and O_2 reduction in a C3 leaf (*Phaseolus vulgaris* L.) at different CO_2 concentrations and during drought stress. *Planta* 1991, *183*, 178–184.
352. **Kral, J.P. & Edwards, G.E.** Relationship between photosystem II activity and CO_2 fixation in leaves. *Physiol. Plant.* 1992, *86*, 180–187.
353. **Morales, F. *et al.*** Chlorophyll fluorescence and photon yield of oxygen evolution in iron-deficient sugar beet (*Beta vulgaris* L.) leaves. *Plant Physiol.* 1991, *97*, 886–893.
354. **Lichtenthaler, H.K.** Chlorophylls and carotenoids: Pigments of photosynthetic biomembranes. *Methods Enzymol.* 1987, *148*, 350–382.
355. **Rintamäki, E. *et al.*** Differential D1 dephosphorylation in functional and photodamaged photosystem II centers. *J. Biol. Chem.* 1996, *271*, 14870–14875.
356. **Järvi, S. *et al.*** Optimized native gel systems for separation of thylakoid protein complexes: novel super- and mega-complexes. *Biochem. J.* 2011, *439*, 207–214.
357. **Fernández-San Millán, A. *et al.*** Physiological performance of transplastomic tobacco plants overexpressing aquaporin AQP1 in chloroplast membranes. *J. Exp. Bot.* 2018, *69*, 3661–3673.
358. **Perez-Ruiz, J.M. *et al.*** Rice NTRC is a high-efficiency redox system for chloroplast protection

against oxidative damage. *Plant Cell* 2006, *18*, 2356–2368.
359. **Vainonen, J.P. *et al.*** STN8 protein kinase in *Arabidopsis thaliana* is specific in phosphorylation of photosystem II core proteins. *J. Biol. Chem.* 2005, *280*, 33679–33686.
360. **Strasserf, R.J. *et al.*** POLYPHASIC CHLOROPHYLL a FLUORESCENCE TRANSIENT IN PLANTS AND CYANOBACTERIA. *Photochem. Photobiol.* 1995, *61*, 32–42.
361. **Tóth, S.Z. *et al.*** In intact leaves, the maximum fluorescence level (F_M) is independent of the redox state of the plastoquinone pool: A DCMU-inhibition study. *Biochim. Biophys. Acta - Bioenerg.* 2005, *1708*, 275–282.
362. **Belkhodja, R. *et al.*** Iron deficiency causes changes in chlorophyll fluorescence due to the reduciton in the dark of the Photosystem II acceptor side. *Photosynth. Res.* 1998, *56*, 265–276.
363. **Rumak, I. *et al.*** Correlation between spatial (3D) structure of pea and bean thylakoid membranes and arrangement of chlorophyll-protein complexes. *BMC Plant Biol.* 2012, *12*, 1–18.
364. **König, J. *et al.*** The plant-specific function of 2-Cys peroxiredoxin-mediated detoxification of peroxides in the redox-hierarchy of photosynthetic electron flux. *Proc. Natl. Acad. Sci.* 2002, *99*, 5738–5743.
365. **Hou, C.X. *et al.*** Environmental and metabolic control of LHCII protein phosphorylation: revealing the mechanisms for dual regulation of the LHCII kinase. *Plant, Cell Environ.* 2002, *25*, 1515–1525.
366. **Tikkanen, M. *et al.*** Thylakoid protein phosphorylation in higher plant chloroplasts optimizes electron transfer under fluctuating light. *Plant Physiol.* 2010, *152*, 723–735.
367. **Corneille, S. *et al.*** Reduction of the plastoquinone pool by exogenous NADH and NADPH in higher plant chloroplasts characterization of a NAD(P)H-plastoquinone oxidoreductase activity. *Biochim. Biophys. Acta - Bioenerg.* 1998, *1363*, 59–69.
368. **Pietrzykowska, M. *et al.*** The light-harvesting chlorophyll a/b binding proteins Lhcb1 and Lhcb2 play complementary roles during state transitions in *Arabidopsis*. *Plant Cell* 2014, *26*, 3646–3660.
369. **Wollman, F.-A. & Lemaire, C.** Studies on kinase-controlled state transitions in Photosystem II and b_6f mutants *Chlamydomonas reinhardtii* from which lack quinone-binding proteins. *Biochim. Biophys. Acta - Bioenerg.* 1988, *933*, 85–94.
370. **Breyton, C.** Conformational changes in the cytochrome b_6f complex induced by inhibitor binding. *J. Biol. Chem.* 2000, *275*, 13195–13201.
371. **Friso, G. *et al.*** In-depth analysis of the thylakoid membrane proteome of *Arabidopsis thaliana* chloroplasts: New proteins, new functions, and a plastid proteome database. *Plant Cell* 2004, *16*, 478–499.
372. **Kouřil, R. *et al.*** Structural characterization of a complex of photosystem I and light-harvesting complex II of *Arabidopsis thaliana*. *Biochemistry* 2005, *44*, 10935–10940.
373. **Pesaresi, P. *et al.*** *Arabidopsis* STN7 kinase provides a link between short- and long-term photosynthetic acclimation. *Plant Cell* 2009, *21*, 2402–2423.
374. **Allen, J.F.** Why we need to know the structure of phosphorylated chloroplast light-harvesting complex II. *Physiol. Plant.* 2017, *161*, 28–44.
375. **Chuartzman, S.G. *et al.*** Thylakoid membrane remodeling during state transitions in Arabidopsis. *Plant Cell* 2008, *20*, 1029–1039.
376. **Herbstová, M. *et al.*** Architectural switch in plant photosynthetic membranes induced by light stress. *Proc. Natl. Acad. Sci.* 2012, *109*, 20130–20135.
377. **Tikkanen, M. *et al.*** Phosphorylation-dependent regulation of excitation energy distribution between the two photosystems in higher plants. *Biochim. Biophys. Acta - Bioenerg.* 2008, *1777*, 425–432.
378. **Pribil, M. *et al.*** Structure and dynamics of thylakoids in land plants. *J. Exp. Bot.* 2014, *65*, 1955–1972.
379. **Lindahl, M. *et al.*** Regulatory proteolysis of the major light-harvesting chlorophyll a/b protein of photosystem II by a light-induced membrane-associated enzymic system. *Eur. J. Biochem.* 1995, *231*, 503–509.
380. **Yang, D.-H. *et al.*** Induction of acclimative proteolysis of the light-harvesting chlorophyll a/b protein of photosystem II in response to elevated light intensities. *Plant Physiol.* 1998, *118*, 827–834.
381. **Zelisko, A. *et al.*** AtFtsH6 is involved in the degradation of the light-harvesting complex II during high-light acclimation and senescence. *Proc. Natl. Acad. Sci.* 2005, *102*, 13699–13704.
382. **Luciński, R. & Jackowski, G.** AtFtsH heterocomplex-mediated degradation of apoproteins of the major light harvesting complex of photosystem II (LHCII) in response to stresses. *J. Plant Physiol.* 2013, *170*, 1082–1089.

383. **Wang, F. *et al.*** The high light response and redox control of thylakoid FtsH orotease in *Chlamydomonas reinhardtii*. *Mol. Plant* 2017, *10*, 99–114.
384. **Escoubas, J.M. *et al.*** Light intensity regulation of *cab* gene transcription is signaled by the redox state of the plastoquinone pool. *Proc. Natl. Acad. Sci.* 1995, *92*, 10237–10241.
385. **Yang, D.H. *et al.*** The redox state of the plastoquinone pool controls the level of the light-harvesting chlorophyll *a/b* binding protein complex II (LHC II) during photoacclimation. *Photosynth. Res.* 2001, *68*, 163–174.
386. **Finazzi, G. *et al.*** Involvement of state transitions in the switch between linear and cyclic electron flow in *Chlamydomonas reinhardtii*. *EMBO Rep.* 2002, *3*, 280–285.
387. **Wood, W.H.J. *et al.*** Dynamic thylakoid stacking regulates the balance between linear and cyclic photosynthetic electron transfer. *Nat. Plants* 2018, *4*, 116–127.
388. **Johnson, M.P.** Metabolic regulation of photosynthetic membrane structure tunes electron transfer function. *Biochem. J.* 2018, *475*, 1225–1233.
389. **Frenkel, M. *et al.*** Hierarchy amongst photosynthetic acclimation responses for plant fitness. *Physiol. Plant.* 2007, *129*, 455–459.
390. **Queval, G. & Noctor, G.** A plate reader method for the measurement of NAD, NADP, glutathione, and ascorbate in tissue extracts: Application to redox profiling during *Arabidopsis* rosette development. *Anal. Biochem.* 2007, *363*, 58–69.
391. **Lu, Y. *et al.*** A Small Zinc Finger Thylakoid Protein Plays a Role in Maintenance of Photosystem II in *Arabidopsis thaliana*. *Plant Cell* 2011, *23*, 1861–1875.
392. **Holmgren, A.** Thioredoxin catalyzes the reduction of insulin disulfides by dithiothreitol and dihydrolipoamide. *J. Biol. Chem.* 1979, *254*, 9627–9632.
393. **Chibani, K. *et al.*** Comparative genomic study of the thioredoxin family in photosynthetic organisms with emphasis on Populus trichocarpa. *Mol. Plant* 2009, *2*, 308–322.
394. **Spínola, M.C. *et al.*** NTRC new ways of using NADPH in the chloroplast. *Physiol. Plant.* 2008, *133*, 516–524.
395. **Stitt, M. *et al.*** Arabidopsis and primary photosynthetic metabolism - More than the icing on the cake. *Plant J.* 2010, *61*, 1067–1091.
396. **Pfister, B. & Zeeman, S.C.** Formation of starch in plant cells. *Cell. Mol. Life Sci.* 2016, *73*, 2781–2807.
397. **Kötting, O. *et al.*** Regulation of starch metabolism: the age of enlightenment? *Curr. Opin. Plant Biol.* 2010, *13*, 321–329.
398. **Hendriks, J.H.M. *et al.*** ADP-glucose pyrophosphorylase is activated by posttranslational redox-modification in response to light and to sugars in leaves of Arabidopsis and other plant species. *Plant Physiol.* 2003, *133*, 838–849.
399. **Hädrich, N. *et al.*** Mutagenesis of cysteine 81 prevents dimerization of the APS1 subunit of ADP-glucose pyrophosphorylase and alters diurnal starch turnover in *Arabidopsis thaliana* leaves. *Plant J.* 2012, *70*, 231–242.
400. **Li, J. *et al.*** Post-translational redox modification of ADP-glucose pyrophosphorylase in response to light is not a major determinant of fine regulation of transitory starch accumulation in Arabidopsis leaves. *Plant Cell Physiol.* 2012, *53*, 433–444.
401. **Lunn, J.E. *et al.*** Trehalose metabolism in plants. *Plant J.* 2014, *79*, 544–567.
402. **Bahaji, A. *et al.*** Starch biosynthesis, its regulation and biotechnological approaches to improve crop yields. *Biotechnol. Adv.* 2014, *32*, 87–106.
403. **Fernández-San Millán, A. *et al.*** Human papillomavirus L1 protein expressed in tobacco chloroplasts self-assembles into virus-like particles that are highly immunogenic. *Plant Biotechnol. J.* 2008, *6*, 427–441.
404. **Burch-Smith, T.M. *et al.*** Applications and advantages of virus-induced gene silencing for gene function studies in plants. *Plant J.* 2004, *39*, 734–746.
405. **Liu, Y.L. *et al.*** Virus-induced gene silencing in tomato. *Plant J.* 2002, *31*, 777–786.
406. **Liu, Y. *et al.*** Virus induced gene silencing of a *DEFICIENS* ortholog in *Nicotiana benthamiana*. *Plant Mol. Biol.* 2004, *54*, 701–711.
407. **Wu, C. *et al.*** The reliability of virus-induced gene silencing experiments using tobacco rattle virus in tomato is influenced by the size of the vector control. *Mol. Plant Pathol.* 2011, *12*, 299–305.
408. **Ganusova, E.E. *et al.*** Altered Expression of a Chloroplast Protein Affects the Outcome of Virus and Nematode Infection. *Mol. Plant-Microbe Interact.* 2017, *30*, 478–488.
409. **Pfaffl, M.W.** A new mathematical model for relative quantification in real-time RT-PCR. *Nucleic Acids Res.* 2001, *29*, 45e–45.
410. **Nakamura, Y. *et al.*** Carbohydrate metabolism in the developing endosperm of rice grains. *Plant Cell Physiol.* 1989, *30*, 833–839.
411. **Bock, R.** Engineering Plastid Genomes: Methods, Tools, and Applications in Basic Research

and Biotechnology. *Annu. Rev. Plant Biol.* 2015, *66*, 211–241.
412. **Liu, Y. *et al.*** Tobacco Rar1, EDS1 and NPR1/NIM1 like genes are required for N-mediated resistance to tobacco mosaic virus. *Plant J.* 2002, *30*, 415–429.
413. **Häusler, R.E. *et al.*** Control of carbon partitioning and photosynthesis by the triose phosphate/phosphate translocator in transgenic tobacco plants (*Nicotiana tabacum* L.). I. Comparative physiological analysis of tobacco plants with antisense repression and overexpressi. *Planta* 2000, *210*, 371–382.
414. **Martins, M.C.M. *et al.*** Feedback inhibition of starch degradation in Arabidopsis leaves mediated by trehalose 6-phosphate. *Plant Physiol.* 2013, *163*, 1142–1163.
415. **Née, G. *et al.*** Redox regulation of chloroplastic glucose-6-phosphate dehydrogenase: A new role for f-type thioredoxin. *FEBS Lett.* 2009, *583*, 2827–2832.
416. **Née, G. *et al.*** Redox regulation of chloroplastic G6PDH activity by thioredoxin occurs through structural changes modifying substrate accessibility and cofactor binding. *Biochem. J.* 2014, *457*, 117–125.
417. **Wattebled, F. *et al.*** Mutants of Arabidopsis lacking a chloroplastic isoamylase accumulate phytoglycogen and an abnormal form of amylopectin. *Plant Physiol.* 2005, *138*, 184–195.
418. **Farran, I. *et al.*** Increased bioethanol production from commercial tobacco cultivars overexpressing thioredoxin f grown under field conditions. *Mol. Breed.* 2014, *34*, 457–469.
419. **Aranjuelo, I. *et al.*** Alteration by thioredoxin f over-expression of primary carbon metabolism and its response to elevated CO_2 in tobacco (*Nicotiana tabacum* L.). *Environ. Exp. Bot.* 2015, *118*, 40–48.
420. **Delvallé, D. *et al.*** Soluble starch synthase I: a major determinant for the synthesis of amylopectin in *Arabidopsis thaliana* leaves. *Plant J.* 2005, *43*, 398–412.
421. **Cuesta-Seijo, J.A. *et al.*** Structure of starch synthase I from barley: insight into regulatory mechanisms of starch synthase activity. *Acta Crystallogr. Sect. D Biol. Crystallogr.* 2013, *69*, 1013–1025.
422. **Wang, F.B. *et al.*** Constitutive expression of *SlTrxF* increases starch content in transgenic *Arabidopsis*. *Biol. Plant.* 2017, *61*, 494–500.
423. **Hendriks, J. *et al.*** ADP-glucose pyrophosphorylase is activated by posttranslational redox-modification in response to light and to sugars in leaves of Arabidopsis and other plant. *Plant …* 2003, *133*, 838–849.
424. **Nikkanen, L. *et al.*** Chloroplast thioredoxin systems: prospects for improving photosynthesis. *Philos. Trans. R. Soc. B* 2017, *372*, 20160474.
425. **Tischner, R. & Schmidt, A.** A Thioredoxin-Mediated Activation of Glutamine. *Plant Physiol.* 1982, *70*, 113–116.
426. **Lindahl, M. & Florencio, F.J.** Thioredoxin-linked processes in cyanobacteria are as numerous as in chloroplasts, but targets are different. *Proc. Natl. Acad. Sci.* 2003, *100*, 16107–16112.
427. **Geiger, M. *et al.*** The nitrate and ammonium nitrate supply have a major influence on the response of photosynthesis, carbon metabolism, nitrogen metabolism and growth to elevated carbon dioxide in tobacco. *Plant, Cell Environ.* 1999, *22*, 1177–1199.
428. **Loiret, F.G. *et al.*** Inoculation of sugarcane with *Pantoea* sp. increases amino acid contents in shoot tissues; serine, alanine, glutamine and asparagine permit concomitantly ammonium excretion and nitrogenase activity of the bacterium. *J. Plant Physiol.* 2009, *166*, 1152–1161.
429. **Lisec, J. *et al.*** Gas chromatography mass spectrometry–based metabolite profiling in plants. *Nat. Protoc.* 2006, *1*, 387–396.
430. **Kopka, J. *et al.*** GMD@CSB.DB: the Golm metabolome database. *Bioinformatics* 2005, *21*, 1635–1638.
431. **Schauer, N. *et al.*** GC-MS libraries for the rapid identification of metabolites in complex biological samples. *FEBS Lett.* 2005, *579*, 1332–1337.
432. **Luedemann, A. *et al.*** TagFinder: preprocessing software for the fingerprinting and the profiling of gas chromatography–mass spectrometry based metabolome analyses. In *Plant Metabolomics. Methods in Molecular Biology (Methods and Protocols), vol 860*; Hardy, N.W., Hall, R.D., Eds.; Humana Press: Totowa, NJ, 2012; pp. 255–286 ISBN 978-1-61779-594-7.
433. **Gibon, Y. *et al.*** A robot-based platform to measure multiple enzyme activities in Arabidopsis using a set of cycling assays: Comparison of changes of enzyme activities and transcript levels during diurnal cycles and in prolonged darkness. *Plant Cell* 2004, *16*, 3304–3325.
434. **Biais, B. *et al.*** Remarkable reproducibility of enzyme activity profiles in tomato fruits grown under contrasting environments provides a roadmap for studies of fruit metabolism. *Plant Physiol.* 2014, *164*, 1204–1221.
435. **Bénard, C. & Gibon, Y.** Measurement of enzyme activities and optimization of continuous and discontinuous assays. *Curr. Protoc. Plant Biol.* 2016, *1*, 247–262.
436. **Cataldo, D.A. *et al.*** Rapid colorimetric determination of nitrate in plant tissue by nitration of

salicylic acid. *Commun. Soil Sci. Plant Anal.* 1975, *6*, 71–80.
437. **Sarasketa, A. *et al.*** Exploring ammonium tolerance in a large panel of *Arabidopsis thaliana* natural accessions. *J. Exp. Bot.* 2014, *65*, 6023–6033.
438. **Miyake, C. & Yokota, A.** Determination of the rate of photoreduction of O_2 in the water-water cycle in watermelon leaves and enhancement of the rate by limitation of photosynthesis. *Plant Cell Physiol.* 2000, *41*, 335–343.
439. **Krall, J.P. & Edwards, G.E.** Relationship between photosystem II activity and CO_2 fixation in leaves. *Physiol. Plant.* 1992, *86*, 180–187.
440. **Walter, M. *et al.*** Visualization of protein interactions in living plant cells using bimolecular fluorescence complementation. *Plant J.* 2004, *40*, 428–438.
441. **Liu, L. *et al.*** An efficient system to detect protein ubiquitination by agroinfiltration in *Nicotiana benthamiana*. *Plant J.* 2010, *61*, 893–903.
442. **Unno, H. *et al.*** Atomic structure of plant glutamine synthetase: A key enzyme for plant productivity. *J. Biol. Chem.* 2006, *281*, 29287–29296.
443. **Ancín, M. *et al.*** Thioredoxin m overexpression in tobacco chloroplasts inhibits the protein kinase STN7 and alters photosynthetic performance. *J. Exp. Bot.* 2018.
444. **Fontaine, J.-X. *et al.*** Characterization of a NADH-Dependent Glutamate Dehydrogenase Mutant of *Arabidopsis* Demonstrates the Key Role of this Enzyme in Root Carbon and Nitrogen Metabolism. *Plant Cell* 2012, *24*, 4044–4065.
445. **Betti, M. *et al.*** Molecular analysis of two mutants from *Lotus japonicus* deficient in plastidic glutamine synthetase: Functional properties of purified GLN2 enzymes. *Planta* 2006, *224*, 1068–1079.
446. **Palatnik, J. *et al.*** The role of photosynthetic electron transport in the oxidative degradation of chloroplastic glutamine synthetase. *Plant Physiol.* 1999, *121*, 471–8.
447. **Ishida, H. *et al.*** Direct evidence for non-enzymatic fragmentation of chloroplastic glutamine synthetase by a reactive oxygen species. *Plant, Cell Environ.* 2002, *25*, 625–631.
448. **Castro-Rodríguez, V. *et al.*** Redundancy and metabolic function of the glutamine synthetase gene family in poplar. *BMC Plant Biol.* 2015, *15*, 1–14.
449. **Liao, J. *et al.*** Cloning, expression and antioxidant activity of a thioredoxin peroxidase from *Branchiostoma belcheri tsingtaunese*. *PLoS One* 2017, *12*, e0175162.
450. **Rahlfs, S. & Becker, K.** Thioredoxin peroxidases of the malarial parasite *Plasmodium falciparum*. *Eur. J. Biochem.* 2001, *268*, 1404–1409.
451. **Jeon, S.J. & Ishikawa, K.** Characterization of novel hexadecameric thioredoxin peroxidase from *Aeropyrum pernix* K1. *J. Biol. Chem.* 2003, *278*, 24174–24180.
452. **Cheong, N.E. *et al.*** Molecular cloning, expression, and functional characterization of a 2Cys-peroxiredoxin in Chinese cabbage. *Plant Mol. Biol.* 1999, *40*, 825–834.
453. **Hodges, M. *et al.*** Perspectives for a better understanding of the metabolic integration of photorespiration within a complex plant primary metabolism network. *J. Exp. Bot.* 2016, *67*, 3015–3026.
454. **Coschigano, K.T. *et al.*** Arabidopsis *gls* mutants and distinct Fd-GOGAT genes: Implications for photorespiration and primary nitrogen assimilation. *Plant Cell* 1998, *10*, 741–752.
455. **Taniguchi, M. *et al.*** Identifying and characterizing plastidic 2-oxoglutarate/malate and dicarboxylate transporters in *Arabidopsis thaliana*. *Plant Cell Physiol.* 2002, *43*, 706–717.
456. **Weber, A. & Flügge, U.I.** Interaction of cytosolic and plastidic nitrogen metabolism in plants. *J. Exp. Bot.* 2002, *53*, 865–874.
457. **Kaiser, W.M. *et al.*** Discrepancy between nitrate reduction rates in intact leaves and nitrate reductase activity in leaf extracts: what limits nitrate reduction in situ? *Planta* 2000, *210*, 801–807.
458. **Kaiser, W.M. *et al.*** What limits nitrate reduction in leaves? In *Photosynthetic Nitrogen Assimilation and Associated Carbon and Respiratory Metabolism. Advances in Photosynthesis and Respiration*; Foyer C.H., N.G. (eds), Ed.; Springer, Dordrecht, 2002; pp. 63–70.
459. **Hashida, S. *et al.*** Ferredoxin/thioredoxin system plays an important role in the chloroplastic NADP status of *Arabidopsis*. *Plant J.* 2018.
460. **Kaiser, W.M. & Huber, S.C.** Post-translational regulation of nitrate reductase: mechanism, physiological relevance and environmental triggers. *J. Exp. Bot.* 2001, *52*, 1981–1989.
461. **Quick, W.P. *et al.*** The impact of decreased Rubisco on photosynthesis, growth, allocation and storage in tobacco plants which have been transformed with antisense rbcS. *Plant J.* 1991, *1*, 51–58.
462. **Fritz, C. *et al.*** Regulation of secondary metabolism by the carbon-nitrogen status in tobacco: nitrate inhibits large sectors of phenylpropanoid metabolism. *Plant J.* 2006, *46*, 533–548.
463. **Dixon, R.A. & Paiva, N.L.** Stress-induced phenylpropanoid metabolism. *Plant Cell* 1995, *7*, 1085–1097.

464. **Vogt, T.** Phenylpropanoid biosynthesis. *Mol. Plant* 2010, *3*, 2–20.
465. **Shi, J. *et al.*** Phosphoenolpyruvate carboxylase in Arabidopsis leaves plays a crucial role in carbon and nitrogen metabolism. *Plant Physiol.* 2015, *167*, 671–681.
466. **Yamaryo, Y. *et al.*** In vitro reconstitution of monogalactosyldiacylglycerol (MGDG) synthase regulation by thioredoxin. *FEBS Lett.* 2006, *580*, 4086–4090.
467. **Bartsch, S. *et al.*** Three thioredoxin targets in the inner envelope membrane of chloroplasts function in protein import and chlorophyll metabolism. *Proc. Natl. Acad. Sci.* 2008, *105*, 4933–4938.
468. **Schwarz, C. *et al.*** An intermolecular disulfide-based light switch for chloroplast *psbD* gene expression in *Chlamydomonas reinhardtii*. *Plant J.* 2012, *72*, 378–389.
469. **Balmer, Y. *et al.*** Thioredoxin target proteins in chloroplast thylakoid membranes. *Antioxid. Redox Signal.* 2006, *8*, 1829–1834.
470. **Yano, H. & Kuroda, M.** Disulfide proteome yields a detailed understanding of redox regulations: A model study of thioredoxin-linked reactions in seed germination. *Proteomics* 2006, *6*, 294–300.
471. **Hägglund, P. *et al.*** Identification of thioredoxin target disulfides using isotope-coded affinity tags. In *Plant Proteomics. Methods in Molecular Biology (Methods and Protocols)*; Jorrin-Novo J., Komatsu S., Weckwerth W., W.S. (eds), Ed.; Humana Press, Totowa, NJ, 2014; Vol. 1072, pp. 677–685 ISBN 9781627036306.
472. **Kallis, G.B. & Holmgren, A.** Differential reactivity of the functional sulfhydryl groups of cysteine-32 and cysteine-32 present in the reduced form of thioredoxin from Escherichia coli. *J. Biol. Chem.* 1980, *255*, 10261–10265.
473. **Hennegan, K.P. & Danna, K.J.** pBIN20: An improved binary vector for Agrobacterium-mediated transformation. *Plant Mol. Biol. Report.* 1998, *16*, 129–131.
474. **Shilov, I. V. *et al.*** The Paragon Algorithm, a Next Generation Search Engine That Uses Sequence Temperature Values and Feature Probabilities to Identify Peptides from Tandem Mass Spectra. *Mol. Cell. Proteomics* 2007, *6*, 1638–1655.
475. **Tang, W.H. *et al.*** Nonlinear fitting method for determining local false discovery rates from decoy database searches. *J. Proteome Res.* 2008, *7*, 3661–3667.
476. **Brandes, H.K. *et al.*** Direct identification of the primary nucleophile of thioredoxin *f*. *J. Biol. Chem.* 1993, *268*, 18411–18414.
477. **Holmgren, A.** Thioredoxin structure and mechanism: conformational changes on oxidation of the active-site sulfhydryls to a disulfide. *Structure* 1995, *3*, 239–243.
478. **Edwards, K.D. *et al.*** A reference genome for *Nicotiana tabacum* enables map-based cloning of homeologous loci implicated in nitrogen utilization efficiency. *BMC Genomics* 2017, *18*, 448.
479. **Berardini, T.Z. *et al.*** The arabidopsis information resource: Making and mining the "gold standard" annotated reference plant genome. *Genesis* 2015, *53*, 474–485.
480. **Bolger, M.E. *et al.*** Plant genome and transcriptome annotations: from misconceptions to simple solutions. *Brief. Bioinform.* 2018, *19*, 437–449.
481. **Altschul, S.F. *et al.*** Basic local alignment search tool. *J. Mol. Biol.* 1990, *215*, 403–410.
482. **Marsian, J. & Lomonossoff, G.P.** Molecular pharming-VLPs made in plants. *Curr. Opin. Biotechnol.* 2016, *37*, 201–206.
483. **Berggård, T. *et al.*** Methods for the detection and analysis of protein-protein interactions. *Proteomics* 2007, *7*, 2833–2842.
484. **Rouhier, N. *et al.*** Identification of plant glutaredoxin targets. *Antioxid. Redox Signal.* 2005, *7*, 919–929.
485. **Ojeda, V. *et al.*** The NADPH-dependent thioredoxin reductase C-2-Cys peroxiredoxin redox system modulates the activity of thioredoxin x in Arabidopsis chloroplasts. *Plant Cell Physiol.* 2018.
486. **Dietz, K.-J.** Peroxiredoxins in plants and cyanobacteria. *Antioxid. Redox Signal.* 2011, *15*, 1129–1159.
487. **Broin, M. *et al.*** The plastidic 2-cysteine peroxiredoxin is a target for a thioredoxin involved in the protection of the photosynthetic apparatus against oxidative damage. *Plant Cell* 2002, *14*, 1417–32.
488. **Gama, F. *et al.*** Functional analysis and expression characteristics of chloroplastic Prx IIE. *Physiol. Plant.* 2008, *133*, 599–610.
489. **Chibani, K. *et al.*** Atypical thioredoxins in Poplar: The glutathione-dependent thioredoxin-like 2.1 supports the activity of target enzymes possessing a single redox active cysteine. *Plant Physiol.* 2012, *159*, 592–605.
490. **Motohashi, K. *et al.*** Identification of thioredoxin targeted proteins using thioredoxin single-cysteine mutant-immobilized resin. In *Methods in molecular biology*; Humana Press, Totowa, NJ, 2009; Vol. 479.

491. **Romero, H.M. *et al.*** Investigations into the role of the plastidial peptide methionine sulfoxide reductase in response to oxidative stress in Arabidopsis. *Plant Physiol.* 2004, *136*, 3784–3794.
492. **Chang, C.C.C. *et al.*** Arabidopsis chloroplastic glutathione peroxidases play a role in cross talk between photooxidative stress and immune responses. *Plant Physiol.* 2009, *150*, 670–683.
493. **DalCorso, G. *et al.*** A complex containing PGRL1 and PGR5 is involved in the switch between linear and cyclic electron flow in *Arabidopsis*. *Cell* 2008, *132*, 273–285.
494. **Scheibe, R. *et al.*** Primary structure and analysis of the location of the regulatory disulfide bond of pea chloroplast NADP-malate dehydrogenase. *Biochim. Biophys. Acta - Protein Struct. Mol. Enzymol.* 1991, *1076*, 1–8.
495. **Baginsky, S. & Gruissem, W.** Endonucleolytic activation directs dark-induced chloroplast mRNA degradation. *Nucleic Acids Res.* 2002, *30*, 4527–4533.
496. **López-Calcagno, P.E. *et al.*** The CP12 protein family: a thioredoxin-mediated metabolic switch? *Front. Plant Sci.* 2014, *5*, 1–9.
497. **Islam, M.R. *et al.*** Functional characterization of a gene encoding a dual domain for uridine kinase and uracil phosphoribosyltransferase in Arabidopsis thaliana. *Plant Mol. Biol.* 2007, *63*, 465–477.
498. **Ito, T. *et al.*** Two amidophosphoribosyltransferase genes of *Arabidopsis thaliana* expressed in defferent organs. *Plant Mol. Biol.* 1994, *26*, 529–533.
499. **Sallaud, C. *et al.*** Characterization of two genes for the biosynthesis of the labdane diterpene Z-abienol in tobacco (*Nicotiana tabacum*) glandular trichomes. *Plant J.* 2012, *72*, 1–17.
500. **Setya, A. *et al.*** Sulfate reduction in higher plants: molecular evidence for a novel 5'-adenylylsulfate reductase. *Proc. Natl. Acad. Sci.* 1996, *93*, 13383–13388.
501. **Gutierrez-Marcos, J.F. *et al.*** Three members of a novel small gene-family from *Arabidopsis thaliana* able to complement functionally an *Escherichia coli* mutant defective in PAPS reductase activity encode proteins with a thioredoxin-like domain and "APS reductase"activity. *Proc. Natl. Acad. Sci.* 1996, *93*, 13377–13382.
502. **Kopriva, S. & Koprivova, A.** Plant adenosine 5′-phosphosulphate reductase: the past, the present, and the future. *J. Exp. Bot.* 2004, *55*, 1775–1783.
503. **Bick, J.A. *et al.*** *Regulation of the plant-type 5'-adenylyl sulfate reductase by oxidative stress*; 2001; Vol. 40;.
504. **Bernal-Bayard, P. *et al.*** Molecular recognition in the interaction of chloroplast 2-Cys peroxiredoxin with NADPH-thioredoxin reductase C (NTRC) and thioredoxin x. *FEBS Lett.* 2014, *588*, 4342–4347.
505. **Chew, O. *et al.*** Molecular definition of the ascorbate-glutathione cycle in *Arabidopsis* mitochondria reveals dual targeting of antioxidant defenses in plants. *J. Biol. Chem.* 2003, *278*, 46869–46877.
506. **Dixon, D.P. *et al.*** Functional divergence in the glutathione transferase superfamily in plants. *J. Biol. Chem.* 2002, *277*, 30859–30869.
507. **Cerveau, D. *et al.*** Characterization of the *Arabidopsis thaliana* 2-Cys peroxiredoxin interactome. *Plant Sci.* 2016, *252*, 30–41.
508. **Ok, S.H. *et al.*** CBSXs are sensor relay proteins sensing adenosine-containing ligands in Arabidopsis. *Plant Signal. Behav.* 2012, *7*, 664–667.
509. **Yoo, K.S. *et al.*** Single cystathionine β-synthase domain-containing proteins modulate development by regulating the thioredoxin system in *Arabidopsis*. *Plant Cell* 2011, *23*, 3577–3594.
510. **Lee, K. *et al.*** Defining the plant disulfide proteome. *Electrophoresis* 2004, *25*, 532–541.
511. **Curmi, P.M.G. *et al.*** Crystal structure of the unactivated form of ribulose- 1,5-bisphosphate carboxylase/oxygenase from tobacco refined at 2.0-A resolution. *J. Biol. Chem.* 1992, *267*, 16980–16989.
512. **López-Castillo, L.M. *et al.*** Structural basis for redox regulation of cytoplasmic and chloroplastic triosephosphate isomerases from *Arabidopsis thaliana*. *Front. Plant Sci.* 2016, *7*, 1817.
513. **Hisabori, T. *et al.*** Towards a functional dissection of thioredoxin networks in plant cells. *Photochem. Photobiol.* 2007, *83*, 145–151.
514. **Koumoto, Y. *et al.*** Chloroplasts have a novel Cpn10 in addition to Cpn20 as co-chaperonins in *Arabidopsis thaliana*. *J. Biol. Chem.* 2001, *276*, 29688–29694.
515. **Hill, J.E. & Hemmingsen, S.M.** Arabidopsis thaliana type I and II chaperonins. *Cell Stress Chaperones* 2001, *6*, 190–200.
516. **Rolland, N. *et al.*** Spinach chloroplast O-acetylserine (thiol)-lyase exhibits two catalytically non-equivalent pyridoxal-5'-phosphate-containing active sites. *Eur. J. Biochem.* 1996, *236*, 272–282.
517. **Armbruster, U. *et al.*** Arabidopsis CURVATURE THYLAKOID1 Proteins Modify Thylakoid

Architecture by Inducing Membrane Curvature. *Plant Cell* 2013, *25*, 2661–2678.
518. **Kirchhoff, H.** Structural changes of the thylakoid membrane network induced by high light stress in plant chloroplasts. *Philos. Trans. R. Soc. B Biol. Sci.* 2014, *369*, 20130225–20130225.
519. **Saze, H. *et al.*** Thioredoxin-mediated reductive activation of a protein kinase for the regulatory phosphorylation of C4-form phosphoenolpyruvate carboxylase from maize. *Plant Cell Physiol.* 2001, *42*, 1295–302.
520. **Grimaud, F. *et al.*** Proteome and phosphoproteome analysis of starch granule-associated proteins from normal maize and mutants affected in starch biosynthesis. *J. Exp. Bot.* 2008, *59*, 3395–3406.
521. **Dietz, K.-J. & Pfannschmidt, T.** Novel Regulators in Photosynthetic Redox Control of Plant Metabolism and Gene Expression. *Plant Physiol.* 2011, *155*, 1477–1485.
522. **Cook, K.M. *et al.*** Allosteric control of βiI-tryptase by a redox active disulfide bond. *J. Biol. Chem.* 2013, *288*, 34920–34929.
523. **Kang, Z.H. & Wang, G.X.** Redox regulation in the thylakoid lumen. *J. Plant Physiol.* 2016, *192*, 28–37.
1. **Horton, P. *et al.*** Regulation of light harvesting in green plants. *Annu. Rev. Plant Physiol. Plant Mol. Biol.* 1996, *47*, 655–684.
2. **Shi, L.X. & Schröder, W.P.** The low molecular mass subunits of the photosynthetic supracomplex, photosystem II. *Biochim. Biophys. Acta - Bioenerg.* 2004, *1608*, 75–96.
3. **Shi, L.X. *et al.*** Photosystem II, a growing complex: Updates on newly discovered components and low molecular mass proteins. *Biochim. Biophys. Acta - Bioenerg.* 2012, *1817*, 13–25.
4. **Bricker, T.M. *et al.*** The extrinsic proteins of Photosystem II. *Biochim. Biophys. Acta - Bioenerg.* 2012, *1817*, 121–142.
5. **Galka, P. *et al.*** Functional analyses of the plant photosystem I-light-harvesting complex II supercomplex reveal that light-harvesting complex II loosely bound to photosystem II is a very efficient antenna for photosystem I in state II. *Plant Cell* 2012, *24*, 2963–2978.
6. **Dekker, J.P. & Boekema, E.J.** Supramolecular organization of thylakoid membrane proteins in green plants. *Biochim. Biophys. Acta - Bioenerg.* 2005, *1706*, 12–39.
7. **Minagawa, J.** Dynamic reorganization of photosynthetic supercomplexes during environmental acclimation of photosynthesis. *Front. Plant Sci.* 2013, *4*, 513.
8. **Croce, R. & Van Amerongen, H.** Light-harvesting in photosystem i. *Photosynth. Res.* 2013, *116*, 153–166.
9. **Quick, W.P. & Neuhaus, H.** The regulation and control of photosynthetic carbon assimilation. In *A molecular approach to primary metabolism in higher plants*; 1997; pp. 39–61.
10. **Raines, C.A.** The Calvin cycle revisited. *Photosynth. Res.* 2003, *75*, 1–10.
11. **Flügge, U.-I.** Phosphate Translocators in Plastids. *Annu. Rev. Plant Physiol. Plant Mol. Biol.* 1999, *50*, 27–45.
12. **Buchanan, B.B.** The Path to Thioredoxin and Redox Regulation in Chloroplasts. *Annu. Rev. Plant Biol.* 2016, *67*, 1–24.
13. **Buchanan, B.B.** Role of Light in the Regulation of Chloroplast Enzymes. *Annu. Rev. Plant Physiol.* 1980, *31*, 341–374.
14. **Jacquot, J.P. *et al.*** Thioredoxins: structure and function in plant cells. *New Phytol.* 1997, *136*, 543–570.
15. **Schürmann, P. & Buchanan, B.B.** The ferredoxin/thioredoxin system of oxygenic photosynthesis. *Antioxid. Redox Signal.* 2008, *10*, 1235–1274.
16. **Pesaresi, P. *et al.*** Dynamics of reversible protein phosphorylation in thylakoids of flowering plants: The roles of STN7, STN8 and TAP38. *Biochim. Biophys. Acta - Bioenerg.* 2011, *1807*, 887–896.
17. **Anderson, J.M.** Photoregulation of the composition, function, and strucutre of thylakoid membranes. *Annu. Rev. Plant Physiol.* 1986, *37*, 93–136.
18. **Ruban, A. V. *et al.*** The photoprotective molecular switch in the photosystem II antenna. *Biochim. Biophys. Acta - Bioenerg.* 2012, *1817*, 167–181.
19. **Minagawa, J.** State transitions-The molecular remodeling of photosynthetic supercomplexes that controls energy flow in the chloroplast. *Biochim. Biophys. Acta - Bioenerg.* 2011, *1807*, 897–905.
20. **Lemeille, S. & Rochaix, J.-D.** State transitions at the crossroad of thylakoid signalling pathways. *Photosynth. Res.* 2010, *106*, 33–46.
21. **Tikkanen, M. *et al.*** Novel insights into plant light-harvesting complex II phosphorylation and "state transitions." *Trends Plant Sci.* 2011, *16*, 126–131.
22. **Allen, J.F.** Protein phosphorylation in regulation of photosynthesis. *Biochim. Biophys. Acta - Bioenerg.* 1992, *1098*, 275–335.

23. **Allen, K.D. & Staehelin, L.A.** Biochemical characterization of photosystem-II antenna polypeptides in grana and stroma membranes of spinach. *Plant Physiol.* 1992, *100*, 1517–1526.
24. **Bellafiore, S. *et al.*** State transitions and light adaptation require chloroplast thylakoid protein kinase STN7. *Nature* 2005, *433*, 892–895.
25. **Zito, F. *et al.*** The Qo site of cytochrome b_6f complexes controls the activation of the LHCII kinase. *EMBO J.* 1999, *18*, 2961–2969.
26. **Vener, A. V *et al.*** Plastoquinol at the quinol oxidation site of reduced cytochrome *bf* mediates signal transduction between light and protein phosphorylation: Thylakoid protein kinase deactivation by a single-turnover flash. *Proc. Natl. Acad. Sci.* 1997, *94*, 1585–1590.
27. **Shapiguzov, A. *et al.*** Activation of the Stt7/STN7 kinase through dynamic interactions with the cytochrome b_6f complex. *Plant Physiol.* 2016, *171*, 82–92.
28. **Rintamäki, E. *et al.*** Phosphorylation of light-harvesting complex II and photosystem II core proteins shows different irradiance-dependent regulation in vivo. *J. Biol. Chem.* 1997, *272*, 30476–30482.
29. **Rintamäki, E. *et al.*** Cooperative regulation of light-harvesting complex II phosphorylation via the plastoquinol and ferredoxin-thioredoxin system in chloroplasts. *Proc. Natl. Acad. Sci.* 2000, *97*, 11644–11649.
30. **Puthiyaveetil, S.** A mechanism for regulation of chloroplast LHC II kinase by plastoquinol and thioredoxin. *FEBS Lett.* 2011, *585*, 1717–1721.
31. **Martinsuo, P. *et al.*** Dithiol oxidant and disulfide reductant dynamically regulate the phosphorylation of light-harvesting complex II proteins in thylakoid membranes. *Plant Physiol.* 2003, *133*, 37–46.
32. **Baslam, M. *et al.*** Genetic and isotope ratio mass spectrometric evidence for the occurrence of starch degradation and cycling in illuminated Arabidopsis leaves. *PLoS One* 2017, *12*, e0171245.
33. **Fernandez, O. *et al.*** Leaf Starch Turnover Occurs in Long Days and in Falling Light at the End of the Day. *Plant Physiol.* 2017, *174*, 2199–2212.
34. **Valerio, C. *et al.*** Thioredoxin-regulated β-amylase (BAM1) triggers diurnal starch degradation in guard cells, and in mesophyll cells under osmotic stress. *J. Exp. Bot.* 2011, *62*, 545–555.
35. **Thalmann, M. *et al.*** Regulation of Leaf Starch Degradation by Abscisic Acid Is Important for Osmotic Stress Tolerance in Plants. *Plant Cell* 2016, *28*, 1860–1878.
36. **Zanella, M. *et al.*** β-amylase 1 (BAM1) degrades transitory starch to sustain proline biosynthesis during drought stress. *J. Exp. Bot.* 2016, *67*, 1819–1826.
37. **Santelia, D. *et al.*** New insights into redox control of starch degradation. *Curr. Opin. Plant Biol.* 2015, *25*, 1–9.
38. **Zeeman, S.C. *et al.*** Starch: its metabolism, evolution, and biotechnological modification in plants. *Annu. Rev. Plant Biol.* 2010, *61*, 209–234.
39. **Zeeman, S.C. *et al.*** The breakdown of starch in leaves. *New Phytol.* 2004, *163*, 247–261.
40. **Geigenberger, P.** Regulation of starch biosynthesis in response to a fluctuating environment. *Plant Physiol.* 2011, *155*, 1566–1577.
41. **Baroja-Fernandez, E. *et al.*** Most of ADP-glucose linked to starch biosynthesis occurs outside the chloroplast in source leaves. *Proc. Natl. Acad. Sci.* 2004, *101*, 13080–13085.
42. **Pozueta-Romero, J. *et al.*** ADP-Glucose Transport by the Chloroplast Adenylate Translocator Is Linked to Starch Biosynthesis. *Plant Physiol.* 1991, *97*, 1565–72.
43. **Nielsen, T.H. *et al.*** Intermediary glucan structures formed during starch granule biosynthesis are enriched in short side chains, a dynamic pulse labeling approach. *J. Biol. Chem.* 2002, *277*, 20249–20255.
44. **Recondo, E. & Leloir, L.F.** Adenosine diphosphate glucose and starch synthesis. *Biochem. Biophys. Res. Commun.* 1961, *6*, 85–88.
45. **Seung, D. *et al.*** Protein targeting to starch is required for localising granule-bound starch synthase to starch granules and for normal amylose synthesis in Arabidopsis. *PLoS Biol.* 2015, *13*, e1002080.
46. **Nakamura, T. *et al.*** Production of waxy (amylose-free) wheats. *Mol. Gen. Genet. MGG* 1995, *248*, 253–259.
47. **Jacobsen, E. *et al.*** Phenotypic and genotypic characterization of an amylose-free starch mutant of the potato. *Euphytica* 1989, *44*, 43–48.
48. **Skryhan, K. *et al.*** Redox Regulation of Starch Metabolism. *Front. Plant Sci.* 2018, *9*, 1–8.
49. **Nakamura, Y. *et al.*** Characterization of the reactions of starch branching enzymes from rice endosperm. *Plant Cell Physiol.* 2010, *51*, 776–794.
50. **Dumez, S. *et al.*** Mutants of Arabidopsis lacking starch branching enzyme II substitute plastidial starch synthesis by cytoplasmic maltose accumulation. *Plant Cell* 2006, *18*, 2694–

2709.
51. **Yan, H.B. *et al.*** Comparison of the starch synthesis genes between maize and rice: copies, chromosome location and expression divergence. *Theor. Appl. Genet.* 2009, *119*, 815–825.
52. **Han, Y. *et al.*** Three orthologs in rice, *Arabidopsis*, and *Populus* encoding starch branching enzymes (SBEs) are different from other *SBE* gene families in plants. *Gene* 2007, *401*, 123–130.
53. **Streb, S. *et al.*** Starch granule biosynthesis in *Arabidopsis* is abolished by removal of all debranching enzymes but restored by the subsequent removal of an endoamylase. *Plant Cell* 2008, *20*, 3448–3466.
54. **Hussain, H. *et al.*** Three isoforms of isoamylase contribute different catalytic properties for the debranching of potato glucans. *Plant Cell* 2003, *15*, 133–149.
55. **Delatte, T. *et al.*** Arabidopsis mutants *Atisa1* and *Atisa2* have identical phenotypes and lack the same multimeric isoamylase, which influences the branch point distribution of amylopectin during starch synthesis. *Plant J.* 2005, *41*, 815–830.
56. **Delatte, T. *et al.*** Evidence for distinct mechanisms of starch granule breakdown in plants. *J. Biol. Chem.* 2006, *281*, 12050–12059.
57. **Yun, M.S. *et al.*** Rice debranching enzyme isoamylase3 facilitates starch metabolism and affects plastid morphogenesis. *Plant Cell Physiol.* 2011, *52*, 1068–1082.
58. **Zhang, X. *et al.*** Overlapping functions of the starch synthases SSII and SSIII in amylopectin biosynthesis in *Arabidopsis*. *BMC Plant Biol.* 2008, *8*, 96.
59. **Pfister, B. *et al.*** Genetic evidence that chain length and branch point distributions are linked determinants of starch granule formation in Arabidopsis. *Plant Physiol.* 2014, *165*, 1457–1474.
60. **Hennen-Bierwagen, T.A. *et al.*** Starch biosynthetic enzymes from developing maize endosperm associate in multisubunit complexes. *Plant Physiol.* 2008, *146*, 1892–1908.
61. **Hennen-Bierwagen, T.A. *et al.*** Proteins from multiple metabolic pathways associate with starch biosynthetic enzymes in high molecular weight complexes: A model for regulation of carbon allocation in maize amyloplasts. *Plant Physiol.* 2009, *149*, 1541–1559.
62. **Tetlow, I.J. *et al.*** Analysis of protein complexes in wheat amyloplasts reveals functional interactions among starch biosynthetic enzymes. *Plant Physiol.* 2008, *146*, 1878–1891.
63. **Ahmed, Z. *et al.*** Protein-protein interactions among enzymes of starch biosynthesis in high-amylose barley genotypes reveal differential roles of heteromeric enzyme complexes in the synthesis of A and B granules. *Plant Sci.* 2015, *233*, 95–106.
64. **Crofts, N. *et al.*** Amylopectin biosynthetic enzymes from developing rice seed form enzymatically active protein complexes. *J. Exp. Bot.* 2015, *66*, 4469–4482.
65. **Niittylä, T. *et al.*** A previously unknown maltose transporter essential for starch degradation in leaves. *Science (80-.).* 2004, *303*, 87–89.
66. **Cho, M.H. *et al.*** Role of the plastidic glucose translocator in the export of starch degradation products from the chloroplasts in *Arabidopsis thaliana*. *New Phytol.* 2011, *190*, 101–112.
67. **Edner, C. *et al.*** Glucan, water dikinase activity stimulates breakdown of starch granules by plastidial β-amylases. *Plant Physiol.* 2007, *145*, 17–28.
68. **Baunsgaard, L. *et al.*** A novel isoform of glucan, water dikinase phosphorylates pre-phosphorylated α-glucans and is involved in starch degradation in Arabidopsis. *Plant J.* 2005, *41*, 595–605.
69. **Kötting, O. *et al.*** Identification of a novel enzyme required for starch metabolism in Arabidopsis leaves. The Phosphoglucan, water dikinase. *Plant Physiol.* 2004, *137*, 242–252.
70. **Ritte, G. *et al.*** Phosphorylation of C6- and C3-positions of glucosyl residues in starch is catalysed by distinct dikinases. *FEBS Lett.* 2006, *580*, 4872–4876.
71. **Hejazi, M. *et al.*** Glucan, water dikinase phosphorylates crystalline maltodextrins and thereby initiates solubilization. *Plant J.* 2008, *55*, 323–334.
72. **Kotting, O. *et al.*** STARCH-EXCESS4 Is a Laforin-Like Phosphoglucan Phosphatase Required for Starch Degradation in Arabidopsis thaliana. *Plant Cell Online* 2009, *21*, 334–346.
73. **Santelia, D. *et al.*** The phosphoglucan phosphatase like sex four2 dephosphorylates starch at the C3-position in *Arabidopsis*. *Plant Cell* 2011, *23*, 4096–4111.
74. **Meekins, D.A. *et al.*** Phosphoglucan-bound structure of starch phosphatase Starch Excess4 reveals the mechanism for C6 specificity. *Proc. Natl. Acad. Sci.* 2014, *111*, 7272–7277.
75. **Fulton, D.C. *et al.*** β-AMYLASE4, a noncatalytic protein required for starch breakdown, acts upstream of three active β-Amylases in *Arabidopsis* chloroplasts. *Plant Cell* 2008, *20*, 1040–1058.
76. **Stanley, D. *et al.*** Characterisation of putative α-amylases from apple (*Malus domestica*) and Arabidopsis thaliana. *Biologia (Bratisl).* 2002, *57*, 137–148.
77. **Streb, S. & Zeeman, S.C.** *Starch metabolism in Arabidopsis*; 2012;
78. **Stitt, M. & Zeeman, S.C.** Starch turnover: Pathways, regulation and role in growth. *Curr. Opin.*

Plant Biol. 2012, *15*, 282–292.
79. **Krapp, A.** Plant nitrogen assimilation and its regulation: A complex puzzle with missing pieces. *Curr. Opin. Plant Biol.* 2015, *25*, 115–122.
80. **Meyer, C. & Stitt, M.** Nitrate reduction and signalling. In *Plant Nitrogen*; Lea, P.J., Morot-Gaudry, J.-F., Eds.; Springer Berlin Heidelberg: Berlin, Heidelberg, 2001; pp. 37–59 ISBN 978-3-662-04064-5.
81. **Lea, P.J. & Miflin, B.J.** Nitrogen Assimilation and its Relevance to Crop Improvement. In *Nitrogen Metabolism in Plants in the Post-genomic Era*; 2010; Vol. 42, pp. 1–40 ISBN 9781444328608.
82. **Keys, A.J. *et al.*** Photorespiratory nitrogen cycle. *Nature* 1978, *2758*, 741–743.
83. **Bittsánszky, A. *et al.*** Overcoming ammonium toxicity. *Plant Sci.* 2015, *231*, 184–190.
84. **Kimata-Ariga, Y. & Hase, T.** Multiple complexes of nitrogen assimilatory enzymes in spinach chloroplasts: Possible mechanisms for the regulation of enzyme function. *PLoS One* 2014, *9*, e108965.
85. **Seabra, A.R. *et al.*** Novel aspects of glutamine synthetase (GS) regulation revealed by a detailed expression analysis of the entire GS gene family of *Medicago truncatula* under different physiological conditions. *BMC Plant Biol.* 2013, *13*, 137.
86. **Taniguchi, M. & Miyake, H.** Redox-shuttling between chloroplast and cytosol: Integration of intra-chloroplast and extra-chloroplast metabolism. *Curr. Opin. Plant Biol.* 2012, *15*, 252–260.
87. **Diaz, C. *et al.*** Nitrogen recycling and remobilization are differentially controlled by leaf senescence and development stage in Arabidopsis under low nitrogen nutrition. *Plant Physiol.* 2008, *147*, 1437–1449.
88. **Masclaux-Daubresse, C. *et al.*** Leaf nitrogen remobilisation for plant development and grain filling. *Plant Biol.* 2008, *10*, 23–36.
89. **Tercé-Laforgue, T. *et al.*** New insights towards the function of glutamate dehydrogenase revealed during source-sink transition of tobacco (*Nicotiana tabacum*) plants grown under different nitrogen regimes. *Physiol. Plant.* 2004, *120*, 220–228.
90. **Kojima, S. *et al.*** NADH-dependent glutamate synthase participated in ammonium assimilation in Arabidopsis root. *Plant Signal. Behav.* 2014, *9*, e29402.
91. **Weber, A. & Flügge, U.-I.** Interaction of cytosolic and plastidic nitrogen metabolism in plants. *J. Exp. Bot.* 2002, *53*, 865–874.
92. **Woo, K.C. *et al.*** A two-translocator model for the transport of 2-oxoglutarate and glutamate in chloroplasts during ammonia assimilation in the light. *Plant Physiol.* 1987, *84*, 624–632.
93. **Schneidereit, J. *et al.*** Antisense repression reveals a crucial role of the plastidic 2-oxoglutarate/malate translocator DiT1 at the interface between carbon and nitrogen metabolism. *Plant J.* 2006, *45*, 206–224.
94. **Kinoshita, H. *et al.*** The chloroplastic 2-oxoglutarate/malate transporter has dual function as the malate valve and in carbon/nitrogen metabolism. *Plant J.* 2011, *65*, 15–26.
95. **Renné, P. *et al.*** The *Arabidopsis* mutant *dct* is deficient in the plastidic glutamate/malate translocator DiT2. *Plant J.* 2003, *35*, 316–331.
96. **Coruzzi, G. & Bush, D.R.** Nitrogen and carbon nutrient and metabolite signaling in plants. *Plant Physiol.* 2001, *125*, 61–64.
97. **Gutiérrez, R.A. *et al.*** Qualitative network models and genome-wide expression data define carbon/nitrogen-responsive molecular machines in *Arabidopsis*. *Genome Biol.* 2007, *8*, 1–13.
98. **Vincentz, M. *et al.*** Regulation of nitrate and nitrite reductase expression in *Nicotiana plumbaginifolia* leaves by nitrogen and carbon metabolites. *Plant J.* 1993, *3*, 315–324.
99. **Kaiser, W.M. & Huber, S.C.** Posttranslational regulation of nitrate reductase in higher plants. *Plant Physiol.* 1994, *106*, 817–821.
100. **Scheible, W.-R. *et al.*** Nitrate acts as a signal to induce organic acid metabolism and repress starch metabolism in tobacco. *Plant Cell* 1997, *9*, 783–798.
101. **Stitt, M. *et al.*** Steps towards an integrated view of nitrogen metabolism. *J. Exp. Bot.* 2002, *53*, 959–970.
102. **Foyer, C.H. *et al.*** Photosynthetic carbon–nitrogen interactions: Modelling inter-pathway control and signalling. In *Annual Plant Reviews: Control of Primary Metabolism in Plants*; Wiley Online Books; 2006; pp. 325–347 ISBN 9780470988640.
103. **Zhu, X.G. *et al.*** What is the maximum efficiency with which photosynthesis can convert solar energy into biomass? *Curr. Opin. Biotechnol.* 2008, *19*, 153–159.
104. **Oaks, A. & Hirel, B.** Nitrogen metabolism in roots. *Annu. Rev. Plant Physiol.* 1985, *36*, 345–365.
105. **Matt, P. *et al.*** The immediate cause of the diurnal changes of nitrogen metabolism in leaves of nitrate-replete tobacco: a major imbalance between the rate of nitrate reduction and the rates of nitrate uptake and ammonium metabolism during the first part of the light peri. *Plant, Cell*

Environ. 2001, *24*, 177–190.
106. **Matt, P. *et al.*** Elevated carbon dioxide increases nitrate uptake and nitrate reductase activity when tobacco is growing on nitrate, but increases ammonium uptake and inhibits nitrate reductase activity when tobacco is growing on ammonium nitrate. *Plant, Cell Environ.* 2001, *24*, 1119–1137.
107. **Lillo, C.** Signalling cascades integrating light-enhanced nitrate metabolism. *Biochem. J.* 2008, *415*, 11–19.
108. **Keys, A.J.** The re-assimilation of ammonia produced by photorespiration and the nitrogen economy of C3 higher plants. *Photosynth. Res.* 2006, *87*, 165–175.
109. **Bauwe, H. & Kolukisaoglu, Ü.** Genetic manipulation of glycine decarboxylation. *J. Exp. Bot.* 2003, *54*, 1523–1535.
110. **Hirel, B. & Lea, P.J.** Ammonia assimilation. In *Plant Nitrogen*; Lea, P.J., Morot-Gaudry, J.-F., Eds.; Springer Berlin Heidelberg: Berlin, Heidelberg, 2001; pp. 79–99 ISBN 978-3-662-04064-5.
111. **Wingler, A. *et al.*** Photorespiration: metabolic pathways and their role in stress protection. *Philos. Trans. R. Soc. B* 2000, *355*, 1517–1529.
112. **Nunes-Nesi, A. *et al.*** Metabolic and signaling aspects underpinning the regulation of plant carbon nitrogen interactions. *Mol. Plant* 2010, *3*, 973–996.
113. **Hodges, M. *et al.*** Higher plant $NADP^+$-dependent isocitrate dehydrogenases, ammonium assimilation and NADPH production. *Plant Physiol. Biochem.* 2003, *41*, 577–585.
114. **Lancien, M. *et al.*** Enzyme redundancy and the importance of 2-oxoglutarate in higher plant ammonium assimilation. *Plant Physiol.* 2000, *123*, 817–824.
115. **Lemaitre, T. *et al.*** NAD-dependent isocitrate dehydrogenase mutants of Arabidopsis suggest the enzyme is not limiting for nitrogen assimilation. *Plant Physiol.* 2007, *144*, 1546–1558.
116. **Nunes-Nesi, A. *et al.*** Operation and function of the tricarboxylic acid cycle in the illuminated leaf. *Physiol. Plant.* 2007, *129*, 45–56.
117. **Huppe, H.C. & Turpin, D.H.** Integration of carbon and nitrogen metabolism in plant and algal cells. *Annu. Rev. Plant Physiol. Plant Mol. Biol.* 1994, *45*, 577–607.
118. **Voll, L.M. *et al.*** Antisense inhibition of enolase strongly limits the metabolism of aromatic amino acids, but has only minor effects on respiration in leaves of transgenic tobacco plants. *New Phytol.* 2009, *184*, 607–618.
119. **Henkes, S. *et al.*** A small decrease of plastid transketolase activity in antisense tobacco transformants has dramatic effects on photosynthesis and phenylpropanoid metabolism. *Plant Cell* 2001, *13*, 535–551.
120. **Forde, B.G.** Local and long-range signaling pathways regulating plant responses to nitrate. *Annu. Rev. Plant Biol.* 2002, *53*, 203–224.
121. **Foyer, C.H. *et al.*** Markers and signals associated with nitrogen assimilation in higher plants. *J. Exp. Bot.* 2003, *54*, 585–593.
122. **Stitt, M.** Nitrate regulation of metabolism and growth. *Curr. Opin. Plant Biol.* 1999, *2*, 178–186.
123. **Dutilleul, C. *et al.*** Mitochondria-driven changes in leaf NAD status exert a crucial influence on the control of nitrate assimilation and the integration of carbon and nitrogen metabolism. *Plant Physiol.* 2005, *139*, 64–78.
124. **Zaffagnini, M. *et al.*** Redox Homeostasis in Photosynthetic Organisms: Novel and Established Thiol-Based Molecular Mechanisms. *Antioxid. Redox Signal.* 2018, *17*, ars.2018.7617.
125. **Meyer, Y. *et al.*** Thioredoxins and glutaredoxins: unifying elements in redox biology. *Annu. Rev. Genet.* 2009, *43*, 335–367.
126. **Holmgren, A.** Thioredoxin. *Annu. Rev. Biochem.* 1985, *54*, 237–271.
127. **Katti, S.K. *et al.*** Crystal structure of thioredoxin from *Escherichia coli* at 1.68 Å resolution. *J. Mol. Biol.* 1990, *212*, 167–184.
128. **Eklund, H. *et al.*** Conformational and functional similarities between glutaredoxin and thioredoxins. *EMBO J.* 1984, *3*, 1443–1449.
129. **Balmer, Y. *et al.*** Oxidation-reduction and activation properties of chloroplast fructose 1,6-bisphosphatase with mutated regulatory site. *Biochemistry* 2001, *40*, 15444–15450.
130. **Hara, S. *et al.*** Thioredoxin-*h*1 reduces and reactivates the oxidized cytosolic malate dehydrogenase dimer in higher plants. *J. Biol. Chem.* 2006, *281*, 32065–32071.
131. **Berndt, C. *et al.*** Thioredoxins and glutaredoxins as facilitators of protein folding. *Biochim. Biophys. Acta - Mol. Cell Res.* 2008, *1783*, 641–650.
132. **Sanz-Barrio, R. *et al.*** Chaperone-like properties of tobacco plastid thioredoxins f and m. *J. Exp. Bot.* 2012, *63*, 365–379.
133. **Chae, H.B. *et al.*** Thioredoxin reductase type C (NTRC) orchestrates enhanced thermotolerance to *Arabidopsis* by its redox-dependent holdase chaperone function. *Mol. Plant* 2013, *6*, 323–336.

134. **Hölscher, C. *et al.*** Dual-targeting of *Arabidopsis* 6-phosphogluconolactonase 3 (PGL3) to chloroplasts and peroxisomes involves interaction with Trx *m2* in the cytosol. *Mol. Plant* 2014, *7*, 252–255.
135. **Buchanan, B.B. *et al.*** Fifty years in the thioredoxin field and a bountiful harvest. *Biochim. Biophys. Acta - Gen. Subj.* 2012, *1820*, 1822–1829.
136. **Laurent, C.T. *et al.*** Enzymatic synthesis of deoxyribonucleotides. *J. Biol. Chem.* 1964, *239*, 3436–3444.
137. **Buchanan, B.B. *et al.*** Ferredoxin-activated fructose diphosphatase in isolated chloroplasts. *Biochem. Biophys. Res. Commun.* 1967, *29*, 74–79.
138. **Buchanan, B.B. & Wolosiuk, R.A.** Photosynthetic regulatory protein found in animal and bacterial cells. *Nature* 1976, *264*, 669–670.
139. **Holmgren, A. *et al.*** Photosynthetic regulatory protein from rabbit liver is identical with thioredoxin. *FEBS Lett.* 1977, *82*, 351–354.
140. **Wolosiuk, R.A. & Buchanan, B.B.** Thioredoxin and glutathione regulate photosynthesis in chloroplasts. *Nature* 1977, *266*, 565–567.
141. **Jacquot, J.P. *et al.*** Evidence for the existence of several enzyme-specific thioredoxins in plants. *FEBS Lett.* 1978, *96*, 243–246.
142. **Meyer, Y. *et al.*** Thioredoxin and glutaredoxin systems in plants: molecular mechanisms, crosstalks, and functional significance. *Antioxid. Redox Signal.* 2012, *17*, 1124–60.
143. **Meyer, Y. *et al.*** Thioredoxins in Arabidopsis and other plants. *Photosynth. Res.* 2005, *86*, 419–433.
144. **Rivera-Madrid, R. *et al.*** Evidence for five divergent thioredoxin *h* sequences in *Arabidopsis thaliana*. *Proc. Natl. Acad. Sci.* 1995, *92*, 5620–5624.
145. **Gelhaye, E. *et al.*** The thioredoxin h system of higher plants. *Plant Physiol. Biochem.* 2004, *42*, 265–271.
146. **Traverso, J.A. *et al.*** Roles of N-terminal fatty acid acylations in membrane compartment partitioning: *Arabidopsis* h-type thioredoxins as a case study. *Plant Cell* 2013, *25*, 1056–1077.
147. **Meng, L. *et al.*** A membrane-associated thioredoxin required for plant growth moves from cell to cell, suggestive of a role in intercellular communication. *Proc. Natl. Acad. Sci.* 2010, *107*, 3900–3905.
148. **Reichheld, J.-P. *et al.*** Inactivation of thioredoxin reductases reveals a complex interplay between thioredoxin and glutathione pathways in *Arabidopsis* development. *Plant Cell* 2007, *19*, 1851–1865.
149. **Kobrehel, K. *et al.*** Specific reduction of wheat storage proteins by thioredoxin *h*. *Plant Physiol.* 1992, *99*, 919–924.
150. **Kneeshaw, S. *et al.*** Selective protein denitrosylation activity of thioredoxin-h5 modulates plant immunity. *Mol. Cell* 2014, *56*, 153–162.
151. **Sweat, T.A. & Wolpert, T.J.** Thioredoxin *h5* is required for victorin sensitivity mediated by a CC-NBS-LRR gene in *Arabidopsis*. *Plant Cell* 2007, *19*, 673–687.
152. **Pulido, P. *et al.*** An antioxidant redox system in the nucleus of wheat seed cells suffering oxidative stress. *Plant J.* 2009, *57*, 132–145.
153. **Park, S.K. *et al.*** Heat-shock and redox-dependent functional switching of an h-type Arabidopsis thioredoxin from a disulfide reductase to a molecular chaperone. *Plant Physiol.* 2009, *150*, 552–561.
154. **Laloi, C. *et al.*** Identification and characterization of a mitochondrial thioredoxin system in plants. *Proc. Natl. Acad. Sci.* 2001, *98*, 14144–14149.
155. **Martí, M.C. *et al.*** Mitochondrial and nuclear localization of a novel pea thioredoxin: Identification of its mitochondrial target proteins. *Plant Physiol.* 2009, *150*, 646–657.
156. **Barranco-Medina, S. *et al.*** Hexameric oligomerization of mitochondrial peroxiredoxin PrxIIF and formation of an ultrahigh affinity complex with its electron donor thioredoxin Trx-o. *J. Exp. Bot.* 2008, *59*, 3259–3269.
157. **Yoshida, K. *et al.*** Systematic exploration of thioredoxin target proteins in plant mitochondria. *Plant Cell Physiol.* 2013, *54*, 875–892.
158. **Daloso, D.M. *et al.*** Thioredoxin, a master regulator of the tricarboxylic acid cycle in plant mitochondria. *Proc. Natl. Acad. Sci.* 2015, *112*, E1392–E1400.
159. **Ortiz-Espín, A. *et al.*** Mitochondrial *AtTrxo1* is transcriptionally regulated by AtbZIP9 and AtAZF2 and affects seed germination under saline conditions. *J. Exp. Bot.* 2017, *68*, 1025–1038.
160. **Fonseca-Pereira, P. da *et al.*** The mitochondrial thioredoxin system contributes to the metabolic responses under drought episodes in Arabidopsis. *Plant Cell Physiol.* 2018.
161. **Laughner, B.J. *et al.*** A novel nuclear member of the thioredoxin superfamily. *Plant Physiol.* 1998, *118*, 987–996.

162. **Marchal, C. *et al.*** NTR/NRX define a new thioredoxin system in the nucleus of Arabidopsis thaliana cells. *Mol. Plant* 2014, *7*, 30–44.
163. **Vignols, F. *et al.*** Redox control of Hsp70-co-chaperone interaction revealed by expression of a thioredoxin-like *Arabidopsis* protein. *J. Biol. Chem.* 2003, *278*, 4516–4523.
164. **Serrato, A.J. *et al.*** AtCXXS: Atypical members of the *Arabidopsis thaliana* thioredoxin h family with a remarkably high disulfide isomerase activity. *Physiol. Plant.* 2008, *133*, 611–622.
165. **Liu, Q. *et al.*** An Atypical Thioredoxin Imparts Early Resistance to *Sugarcane Mosaic Virus* in Maize. *Mol. Plant* 2017, *10*, 483–497.
166. **Alkhalfioui, F. *et al.*** A novel type of thioredoxin dedicated to symbiosis in legumes. *Plant Physiol.* 2008, *148*, 424–435.
167. **Lemaire, S.D. *et al.*** Characterization of thioredoxin y, a new type of thioredoxin identified in the genome of *Chlamydomonas reinhardtii*. *FEBS Lett.* 2003, *543*, 87–92.
168. **Mestres-Ortega, D. & Meyer, Y.** The *Arabidopsis thaliana* genome encodes at least four thioredoxins *m* and a new prokaryotic-like thioredoxin. *Gene* 1999, *240*, 307–316.
169. **Arsova, B. *et al.*** Plastidial thioredoxin z interacts with two fructokinase-like proteins in a thiol-dependent manner: Evidence for an essential role in chloroplast development in Arabidopsis and Nicotiana benthamiana. *Plant Cell Online* 2010, *22*, 1498–1515.
170. **Bohrer, A.-S. *et al.*** New insights into the reduction systems of plastidial thioredoxins point out the unique properties of thioredoxin z from *Arabidopsis*. *J. Exp. Bot.* 2012, *63*, 6315–6323.
171. **Belin, C. *et al.*** A comprehensive study of thiol reduction gene expression under stress conditions in *Arabidopsis thaliana*. *Plant, Cell Environ.* 2015, *38*, 299–314.
172. **Hartman, H. *et al.*** Contrasting evolutionary histories of chloroplast thioredoxins *f* and *m*. *Mol. Biol. Evol.* 1990, 7, 247–254.
173. **Sahrawy, M. *et al.*** Intron position as an evolutionary marker of thioredoxins and thioredoxin domains. *J. Mol. Evol.* 1996, *42*, 422–431.
174. **Tsugita, A. *et al.*** Spinach chloroplast thioredoxins in evolutionary drift. *Biochem. Biophys. Res. Commun.* 1983, *115*, 1–7.
175. **Capitani, G. *et al.*** Crystal structures of two functionally different thioredoxins in spinach chloroplasts. *J. Mol. Biol.* 2000, *302*, 135–154.
176. **Lemaire, S.D. *et al.*** *Chlamydomonas reinhardtii*: a model organism for the study of the thioredoxin family. *Plant Physiol. Biochem.* 2003, *41*, 513–521.
177. **Collin, V. *et al.*** The Arabidopsis plastidial thioredoxins. *J. Biol. Chem.* 2003, *278*, 23747–23752.
178. **Geck, M.K. *et al.*** Identification of residues of spinach thioredoxin f that influence interactions with target enzymes. *J. Biol. Chem.* 1996, *271*, 24736–24740.
179. **Geigenberger, P. & Fernie, A.R.** Metabolic control of redox and redox control of metabolism in plants. *Antioxid. Redox Signal.* 2014, *21*, 1389–1421.
180. **Geigenberger, P. *et al.*** The unprecedented versatility of the plant thioredoxin system. *Trends Plant Sci.* 2017, *22*, 249–262.
181. **Lichter, A. & Häberlein, I.** A light-dependent redox signal participates in the regulation of ammonia fixation in chloroplasts of higher plants - ferredoxin: glutamate synthase is a thioredoxin-dependent enzyme. *J. Plant Physiol.* 1998, *153*, 83–90.
182. **Rey, P. *et al.*** Overexpression of plastidial thioredoxins f and m differentially alters photosynthetic activity and response to oxidative stress in tobacco plants. *Front. Plant Sci.* 2013, *4*, 390.
183. **Okegawa, Y. & Motohashi, K.** Chloroplastic thioredoxin *m* functions as a major regulator of Calvin cycle enzymes during photosynthesis *in vivo*. *Plant J.* 2015, *84*, 900–913.
184. **Benitez-Alfonso, Y. *et al.*** Control of *Arabidopsis* meristem development by thioredoxin-dependent regulation of intercellular transport. *Proc. Natl. Acad. Sci.* 2009, *106*, 3615–3620.
185. **Collin, V. *et al.*** Characterization of plastidial thioredoxins from Arabidopsis belonging to the new y-type. *Plant Physiol.* 2004, *136*, 4088–4095.
186. **Navrot, N. *et al.*** Plant glutathione peroxidases are functional peroxiredoxins distributed in several subcellular compartments and regulated during biotic and abiotic stresses. *Plant Physiol.* 2006, *142*, 1364–1379.
187. **Laugier, E. *et al.*** Involvement of thioredoxin y2 in the preservation of leaf methionine sulfoxide reductase capacity and growth under high light. *Plant, Cell Environ.* 2013, *36*, 670–682.
188. **Vieira Dos Santos, C. *et al.*** Specificity of thioredoxins and glutaredoxins as electron donors to two distinct classes of Arabidopsis plastidial methionine sulfoxide reductases B. *FEBS Lett.* 2007, *581*, 4371–4376.
189. **Diaz, M.G. *et al.*** Redox regulation of PEP activity during seedling establishment in Arabidopsis thaliana. *Nat. Commun.* 2018, *9*.
190. **Wimmelbacher, M. & Börnke, F.** Redox activity of thioredoxin z and fructokinase-like protein

1 is dispensable for autotrophic growth of *Arabidopsis thaliana*. *J. Exp. Bot.* 2014, *65*, 2405–2413.

191. **Serrato, A.J. *et al.*** A novel NADPH thioredoxin reductase, localised in the chloroplast, which deficiency causes hypersensitivity to abiotic stress in *Arabidopsis thaliana*. *J. Biol. Chem.* 2004, *279*, 43821–43827.
192. **Kirchsteiger, K. *et al.*** NADPH Thioredoxin Reductase C Is Localized in Plastids of Photosynthetic and Nonphotosynthetic Tissues and Is Involved in Lateral Root Formation in *Arabidopsis*. *Plant Cell* 2012, *24*, 1534–1548.
193. **Alkhalfioui, F. *et al.*** Unique properties of NADP-thioredoxin reductase C in legumes. *J. Exp. Bot.* 2007, *58*, 969–978.
194. **Moon, J.C. *et al.*** The C-type Arabidopsis thioredoxin reductase ANTR-C acts as an electron donor to 2-Cys peroxiredoxins in chloroplasts. *Biochem. Biophys. Res. Commun.* 2006, *348*, 478–484.
195. **Puerto-Galán, L. *et al.*** The contribution of NADPH thioredoxin reductase C (NTRC) and sulfiredoxin to 2-Cys peroxiredoxin overoxidation in *Arabidopsis thaliana* chloroplasts. *J. Exp. Bot.* 2015, *66*, 2957–2966.
196. **Toivola, J. *et al.*** Overexpression of chloroplast NADPH-dependent thioredoxin reductase in *Arabidopsis* enhances leaf growth and elucidates *in vivo* function of reductase and thioredoxin domains. *Front. Plant Sci.* 2013, *4*, 389.
197. **Michalska, J. *et al.*** NTRC links built-in thioredoxin to light and sucrose in regulating starch synthesis in chloroplasts and amyloplasts. *Proc. Natl. Acad. Sci.* 2009, *106*, 9908–13.
198. **Richter, A.S. & Grimm, B.** Thiol-based redox control of enzymes involved in the tetrapyrrole biosynthesis pathway in plants. *Front. Plant Sci.* 2013, *4*, 371.
199. **Pérez-Ruiz, J.M. *et al.*** NADPH thioredoxin reductase C is involved in redox regulation of the Mg-chelatase I subunit in *Arabidopsis thaliana* chloroplasts. *Mol. Plant* 2014, *7*, 1252–1255.
200. **Perez-Ruiz, J.M.** Rice NTRC Is a High-Efficiency Redox System for Chloroplast Protection against Oxidative Damage. *Plant Cell Online* 2006, *18*, 2356–2368.
201. **Pérez-Ruiz, J.M. *et al.*** NTRC-dependent redox balance of 2-Cys peroxiredoxins is needed for optimal function of the photosynthetic apparatus. *Proc. Natl. Acad. Sci.* 2017, *114*, 12069–12074.
202. **Ojeda, V. *et al.*** NADPH thioredoxin reductase C and thioredoxins act concertedly in seedling development. *Plant Physiol.* 2017, *174*, 1436–1448.
203. **Rey, P. *et al.*** A novel thioredoxin-like protein located in the chloroplast is induced by water deficit in *Solanum tuberosum* L. plants. *Plant J.* 1998, *13*, 97–107.
204. **Broin, M. *et al.*** Involvement of CDSP 32, a drought-induced thioredoxin, in the response to oxidative stress in potato plants. *FEBS Lett.* 2000, *467*, 245–248.
205. **Broin, M. & Rey, P.** Potato plants lacking the CDSP32 plastidic thioredoxin exhibit overoxidation of the BAS1 2-cysteine peroxiredoxin and increased lipid peroxidation in thylakoids under photooxidative stress. *Plant Physiol.* 2003, *132*, 1335–1343.
206. **Tarrago, L. *et al.*** Plant thioredoxin CDSP32 regenerates 1-Cys methionine sulfoxide reductase B activity through the direct reduction of sulfenic acid. *J. Biol. Chem.* 2010, *285*, 14964–14972.
207. **Martin, M.N. *et al.*** The role of 5′-adenylylsulfate reductase in controlling sulfate reduction in plants. *Photosynth. Res.* 2005, *86*, 309–323.
208. **Bick, J.A. *et al.*** Glutaredoxin function for the carboxyl-terminal domain of the plant-type 5'-adenylylsulfate reductase. *Proc. Natl. Acad. Sci.* 1998, *95*, 8404–8409.
209. **Dangoor, I. *et al.*** A small family of chloroplast atypical thioredoxins. *Plant Physiol.* 2009, *149*, 1240–1250.
210. **Yoshida, K. *et al.*** Thioredoxin-like2/2-Cys peroxiredoxin redox cascade supports oxidative thiol modulation in chloroplasts. *Proc. Natl. Acad. Sci.* 2018, *115*, E8296–E8304.
211. **Motohashi, K. & Hisabori, T.** HCF164 receives reducing equivalents from stromal thioredoxin across the thylakoid membrane and mediates reduction of target proteins in the thylakoid lumen. *J. Biol. Chem.* 2006, *281*, 35039–35047.
212. **Motohashi, K. & Hisabori, T.** CcdA is a thylakoid membrane protein required for the transfer of reducing equivalents from stroma to thylakoid lumen in the higher plant chloroplast. *Antioxid. Redox Signal.* 2010, *13*, 1169–1176.
213. **Brooks, M.D. *et al.*** A thioredoxin-like/β-propeller protein maintains the efficiency of light harvesting in *Arabidopsis*. *Proc. Natl. Acad. Sci.* 2013, *110*, E2733–E2740.
214. **Karamoko, M. *et al.*** Lumen thiol oxidoreductase1, a disulfide bond-forming catalyst, is required for the assembly of photosystem II in *Arabidopsis*. *Plant Cell* 2011, *23*, 4462–4475.
215. **Jacquot, J.P. *et al.*** Arabidopsis thaliana NAPHP thioredoxin reductase: cDNA characterization and expression of the recombinant protein in *Escherichia coli*. *J. Mol. Biol.*

1994, *235*, 1357–1363.
216. **Balmer, Y. *et al.*** A complete ferredoxin/thioredoxin system regulates fundamental processes in amyloplasts. *Proc. Natl. Acad. Sci.* 2006, *103*, 2988–2993.
217. **Barajas-López, J. de D. *et al.*** Localization in roots and flowers of pea chloroplastic thioredoxin *f* and thioredoxin *m* proteins reveals new roles in nonphotosynthetic organs. *Plant Physiol.* 2007, *145*, 946–960.
218. **Hanke, G.T. *et al.*** Fd:FNR electron transfer complexes: evolutionary refinement of structural interactions. *Photosynth. Res.* 2004, *81*, 317–327.
219. **Hanke, G.T. *et al.*** Multiple iso-proteins of FNR in *Arabidopsis*: evidence for different contributions to chloroplast function and nitrogen assimilation. *Plant, Cell Environ.* 2005, *28*, 1146–1157.
220. **Pérez-Ruiz, J.M. & Cejudo, F.J.** A proposed reaction mechanism for rice NADPH thioredoxin reductase C, an enzyme with protein disulfide reductase activity. *FEBS Lett.* 2009, *583*, 1399–1402.
221. **Nikkanen, L. *et al.*** Crosstalk between chloroplast thioredoxin systems in regulation of photosynthesis. *Plant Cell Environ.* 2016, *39*, 1691–1705.
222. **Yoshida, K. & Hisabori, T.** Two distinct redox cascades cooperatively regulate chloroplast functions and sustain plant viability. *Proc. Natl. Acad. Sci.* 2016, *113*, E3967–E3976.
223. **Thormählen, I. *et al.*** Thioredoxin *f1* and NADPH-dependent thioredoxin reductase C have overlapping functions in regulating photosynthetic metabolism and plant growth in response to varying light conditions. *Plant Physiol.* 2015, *169*, 1766–1786.
224. **Chibani, K. *et al.*** Biochemical properties of poplar thioredoxin z. *FEBS Lett.* 2011, *585*, 1077–1081.
225. **Buchanan, B.B. *et al.*** The ferredoxin/thioredoxin system: from discovery to molecular structures and beyond. *Photosynth. Res.* 2002, *73*, 215–222.
226. **Montrichard, F. *et al.*** Thioredoxin targets in plants: the first 30 years. *J. Proteomics* 2009, *72*, 452–74.
227. **Wolosiuk, R.A. *et al.*** Isolation of three thioredoxins from spinach leaves. *J. Biol. Chem.* 1979, *254*, 1627–1632.
228. **Yoshida, K. *et al.*** Thioredoxin selectivity for thiol-based redox regulation of target proteins in chloroplasts. *J. Biol. Chem.* 2015, *290*, 14278–14288.
229. **Wong, J.H. *et al.*** Thioredoxin targets of developing wheat seeds identified by complementary proteomic approaches. *Phytochemistry* 2004, *65*, 1629–1640.
230. **Marchand, C. *et al.*** Comparative proteomic approaches for the isolation of proteins interacting with thioredoxin. *Proteomics* 2006, *6*, 6528–6537.
231. **Alkhalfioui, F. *et al.*** Thioredoxin-linked proteins are reduced during germination of *Medicago truncatula* seeds. *Plant Physiol.* 2007, *144*, 1559–1579.
232. **Pérez-Pérez, M.E. *et al.*** The deep thioredoxome in *Chlamydomonas reinhardtii*: New insights into redox regulation. *Mol. Plant* 2017, *10*, 1107–1125.
233. **Yano, H. *et al.*** A strategy for the identification of proteins targeted by thioredoxin. *Proc. Natl. Acad. Sci.* 2001, *98*, 4794–4799.
234. **Kobrehel, K. *et al.*** Role of the NADP/thioredoxin system in the reduction of α-amylase and trypsin inhibitor proteins. *J. Biol. Chem.* 1991, *266*, 16135–16140.
235. **Wong, J.H. *et al.*** Unraveling thioredoxin-linked metabolic processes of cereal starchy endosperm using proteomics. *FEBS Lett.* 2003, *547*, 151–156.
236. **Marx, C. *et al.*** Thioredoxin and germinating barley: targets and protein redox changes. *Planta* 2003, *216*, 454–60.
237. **Maeda, K. *et al.*** Cy5 maleimide labelling for sensitive detection of free thiols in native protein extracts: identification of seed proteins targeted by barley thioredoxin h isoforms. *Biochem. J.* 2004, *378*, 497–507.
238. **Marchand, C. *et al.*** New targets of Arabidopsis thioredoxins revealed by proteomic analysis. *Proteomics* 2004, *4*, 2696–2706.
239. **Hägglund, P. *et al.*** Identification of thioredoxin disulfide targets using a quantitative proteomics approach based on isotope-coded affinity tags. *J. Proteome Res.* 2008, *7*, 5270–5276.
240. **Zhang, T. *et al.*** Identification of thioredoxin targets in guard cell enriched epidermal peels using cysTMT proteomics. *J. Proteomics* 2016, *133*, 48–53.
241. **Wynn, R. *et al.*** Mixed disulfide intermediates during the reduction of disulfides by *Escherichia coli* thioredoxin. *Biochemistry* 1995, *34*, 11807–11813.
242. **Qin, J. *et al.*** Solution structure of human thioredoxin in a mixed disulfide intermediate complex with its target peptide from the transcription factor NFκB. *Structure* 1995, *3*, 289–297.
243. **Verdoucq, L. *et al.*** *In vivo* characterization of a thioredoxin h target protein defines a new

peroxiredoxin family. *J. Biol. Chem.* 1999, *274*, 19714–19722.
244. **Motohashi, K. *et al.*** Comprehensive survey of proteins targeted by chloroplast thioredoxin. *Proc. Natl. Acad. Sci.* 2001, *98*, 11224–11229.
245. **Balmer, Y. *et al.*** Proteomics gives insight into the regulatory function of chloroplast thioredoxins. *Proc. Natl. Acad. Sci.* 2003, *100*, 370–375.
246. **Yamazaki, D. *et al.*** Target proteins of the cytosolic thioredoxins in *Arabidopsis thaliana*. *Plant Cell Physiol.* 2004, *45*, 18–27.
247. **Balmer, Y. *et al.*** Thioredoxin links redox to the regulation of fundamental processes of plant mitochondria. *Proc. Natl. Acad. Sci.* 2004, *101*, 2642–2647.
248. **Marchand, C.H. *et al.*** Thioredoxin targets in *Arabidopsis* roots. *Proteomics* 2010, *10*, 2418–2428.
249. **Rey, P. *et al.*** Analysis of the proteins targeted by CDSP32, a plastidic thioredoxin participating in oxidative stress responses. *Plant J.* 2005, *41*, 31–42.
250. **Pérez-Pérez, M.E. *et al.*** Selecting thioredoxins for disulphide proteomics: Target proteomes of three thioredoxins from the cyanobacterium Synechocystis sp. PCC 6803. *Proteomics* 2006, *6*, S186–S195.
251. **Lemaire, S.D. *et al.*** New thioredoxin targets in the unicellular photosynthetic eukaryote Chlamydomonas reinhardtii. *Proc. Natl. Acad. Sci.* 2004, *101*, 7475–7480.
252. **Sturm, N. *et al.*** Identification of proteins targeted by the thioredoxin superfamily in plasmodium falciparum. *PLoS Pathog.* 2009, *5*.
253. **Richter, A.S. *et al.*** Posttranslational influence of NADPH-dependent thioredoxin reductase C on enzymes in tetrapyrrole synthesis. *Plant Physiol.* 2013, *162*, 63–73.
254. **Courteille, A. *et al.*** Thioredoxin m4 controls photosynthetic alternative electron pathways in Arabidopsis. *Plant Physiol.* 2013, *161*, 508–520.
255. **Brzezowski, P. *et al.*** Regulation and function of tetrapyrrole biosynthesis in plants and algae. *Biochim. Biophys. Acta* 2015, *1847*, 968–985.
256. **Da, Q. *et al.*** M-type thioredoxins are involved in the xanthophyll cycle and proton motive force to alter NPQ under low-light conditions in Arabidopsis. *Plant Cell Rep.* 2017, *37*, 279–291.
257. **Ikegami, A. *et al.*** The CHLI1 subunit of *Arabidopsis thaliana* magnesium chelatase is a target protein of the chloroplast thioredoxin. *J. Biol. Chem.* 2007, *282*, 19282–19291.
258. **Luo, T. *et al.*** Thioredoxin redox regulates ATPase activity of magnesium chelatase CHLI subunit and modulates redox-mediated signaling in tetrapyrrole biosynthesis and homeostasis of reactive oxygen species in pea plants. *Plant Physiol.* 2012, *159*, 118–130.
259. **Wang, P. *et al.*** Evidence for a role of chloroplastic m-type thioredoxins in the biogenesis of photosystem II in Arabidopsis. *Plant Physiol.* 2013, *163*, 1710–1728.
260. **Trebitsh, T. *et al.*** Translation of chloroplast psbA mRNA is modulated in the light by counteracting oxidizing and reducing activities. *Mol. Cell. Biol.* 2000, *20*, 1116–23.
261. **Trebitsh, T. & Danon, A.** Translation of chloroplast psbA mRNA is regulated by signals initiated by both photosystems II and I. *Proc. Natl. Acad. Sci.* 2001, *98*, 12289–12294.
262. **Hisabori, T. *et al.*** The chloroplast ATP synthase features the characteristic redox regulation machinery. *Antioxid. Redox Signal.* 2013, *19*, 1846–1854.
263. **Ort, D.R. & Oxborough, K.** In situ regulation of chloroplast coupling factor activity. *Annu. Rev. Plant Physiol. Plant Mol. Biol.* 1992, *43*, 269–291.
264. **Nowak, K.F. & McCarty, R.E.** Regulatory role of the C-terminus of the ε subunit from the chloroplast ATP synthase. *Biochemistry* 2004, *43*, 3273–3279.
265. **Mills, J.D. *et al.*** Modulation of coupling factor ATPase activity in intact chloroplasts. *FEBS Lett.* 1980, *112*, 173–177.
266. **Schwarz, O. *et al.*** Kinetics and thioredoxin specificity of thiol modulation of the chloroplast H^+-ATPase. *J. Biol. Chem.* 1997, *272*, 16924–16927.
267. **Carrillo, L.R. *et al.*** Multi-level regulation of the chloroplast ATP synthase: the chloroplast NADPH thioredoxin reductase C (NTRC) is required for redox modulation specifically under low irradiance. *Plant J.* 2016, *87*, 654–663.
268. **Naranjo, B. *et al.*** The chloroplast NADPH thioredoxin reductase C, NTRC, controls non-photochemical quenching of light energy and photosynthetic electron transport in *Arabidopsis*. *Plant Cell Environ.* 2016, *39*, 804–822.
269. **Tikkanen, M. *et al.*** Light-harvesting mutants show differential gene expression upon shift to high light as a consequence of photosynthetic redox and reactive oxygen species metabolism. *Philos. Trans. R. Soc. B* 2014, *369*, 20130229.
270. **Hertle, A.P. *et al.*** PGRL1 is the elusive ferredoxin-plastoquinone reductase in photosynthetic cyclic electron flow. *Mol. Cell* 2013, *49*, 511–523.
271. **Nikkanen, L. *et al.*** Regulation of cyclic electron flow by chloroplast NADPH-dependent thioredoxin system. *Plant Direct* 2018, 1–24.

272. **Dunford, R.P. *et al.*** Location of the redox-active cysteines in chloroplast sedoheptulose-1,7-bisphosphatase indicates that its allosteric regulation is similar but not identical to that of fructose-1,6-bisphosphatase. *Photosynth. Res.* 1998, *58*, 221–230.
273. **Sparla, F. *et al.*** Regulation of photosynthetic GAPDH dissected by mutants. *Plant Physiol.* 2005, *138*, 2210–2219.
274. **Geck, M.K. & Hartman, F.C.** Kinetic and mutational analyses of the regulation of phosphoribulokinase by thioredoxins. *J. Biol. Chem.* 2000, *275*, 18034–18039.
275. **Porter, M.A. *et al.*** Characterization of the regulatory thioredoxin site of phosphoribulokinase. *J. Biol. Chem.* 1988, *263*, 123–129.
276. **Wedel, N. *et al.*** CP12 provides a new mode of light regulation of Calvin cycle activity in higher plants. *Proc. Natl. Acad. Sci.* 1997, *94*, 10479–10484.
277. **Marri, L. *et al.*** Prompt and easy activation by specific thioredoxins of calvin cycle enzymes of arabidopsis thaliana associated in the GAPDH/CP12/PRK supramolecular complex. *Mol. Plant* 2009, *2*, 259–269.
278. **Naranjo, B. *et al.*** Type-*f* thioredoxins have a role in the short-term activation of carbon metabolism and their loss affects growth under short-day conditions in *Arabidopsis thaliana*. *J. Exp. Bot.* 2016, *67*, 1951–1964.
279. **Eliyahu, E. *et al.*** ACHT4-driven oxidation of APS1 attenuates starch synthesis under low light intensity in *Arabidopsis* plants. *Proc. Natl. Acad. Sci.* 2015, *112*, 12876–12881.
280. **Pulido, P. *et al.*** Functional analysis of the pathways for 2-Cys peroxiredoxin reduction in *Arabidopsis thaliana* chloroplasts. *J. Exp. Bot.* 2010, *61*, 4043–4054.
281. **Portis, A.R.** Rubisco activase - Rubisco's catalytic chaperone. *Photosynth. Res.* 2003, *75*, 11–27.
282. **Zhang, N. & Portis, A.R.** Mechanism of light regulation of Rubisco: a specific role for the larger Rubisco activase isoform involving reductive activation by thioredoxin-f. *Proc. Natl. Acad. Sci. U. S. A.* 1999, *96*, 9438–43.
283. **Zhang, N. *et al.*** Light modulation of Rubisco in Arabidopsis requires a capacity for redox regulation of the larger Rubisco activase isoform. *Proc. Natl. Acad. Sci.* 2002, *99*, 3330–3334.
284. **Heo, J. & Holbrook, G.P.** Regulation of 2-carboxy-D-arabinitol 1-phosphate phosphatase: activation by glutathione and interaction with thiol reagents. *Biochem. J.* 1999, *338*, 409–416.
285. **Thormählen, I. *et al.*** Thioredoxins play a crucial role in dynamic acclimation of photosynthesis in fluctuating light. *Mol. Plant* 2017, *10*, 168–182.
286. **Ojeda, V. *et al.*** 2-Cys peroxiredoxins participate in the oxidation of chloroplast enzymes in the dark. *Mol. Plant* 2018, 1–12.
287. **Hall, M. *et al.*** Thioredoxin targets of the plant chloroplast lumen and their implications for plastid function. *Proteomics* 2010, *10*, 987–1001.
288. **Karamoko, M. *et al.*** Operation of trans-thylakoid thiol-metabolizing pathways in photosynthesis. *Front. Plant Sci.* 2013, *4*, 476.
289. **Page, M.L.D. *et al.*** A homolog of prokaryotic thiol disulfide transporter CcdA is required for the assembly of the cytochrome b_6f complex in *Arabidopsis* chloroplasts. *J. Biol. Chem.* 2004, *279*, 32474–32482.
290. **Lennartz, K. *et al.*** HCF164 encodes a thioredoxin-like protein involved in the biogenesis of the cytochrome b_6f complex in Arabidopsis. *Plant Cell* 2001, *13*, 2539–2551.
291. **Onoa, B. *et al.*** Atomic force microscopy of photosystem II and its unit cell clustering quantitatively delineate the mesoscale variability in *Arabidopsis* thylakoids. *PLoS One* 2014, *9*, e101470.
292. **Lu, Y. *et al.*** Identification of potential targets for thylakoid oxidoreductase AtVKOR/LTO1 in chloroplasts. *Protein Pept. Lett.* 2015, *22*, 219–225.
293. **Gopalan, G. *et al.*** Structural analysis uncovers a role for redox in regulating FKBP13, an immunophilin of the chloroplast thylakoid lumen. *Proc. Natl. Acad. Sci.* 2004, *101*, 13945–13950.
294. **Buchanan, B.B. & Luan, S.** Redox regulation in the chloroplast thylakoid lumen: a new frontier in photosynthesis research. *J. Exp. Bot.* 2005, *56*, 1439–1447.
295. **Gollan, P.J. & Bhave, M.** A thylakoid-localised FK506-binding protein in wheat may be linked to chloroplast biogenesis. *Plant Physiol. Biochem.* 2010, *48*, 655–662.
296. **Lima, A. *et al.*** A redox-active FKBP-type immunophilin functions in accumulation of the photosystem II supercomplex in Arabidopsis thaliana. *Proc. Natl. Acad. Sci.* 2006, *103*, 12631–12636.
297. **Shapiguzov, A. *et al.*** Profound redox sensitivity of peptidyl-prolyl isomerase activity in Arabidopsis thylakoid lumen. *FEBS Lett.* 2006, *580*, 3671–3676.
298. **Kaiser, W.M. & Bassham, J.A.** Light-dark regulation of starch metabolism in chloroplasts: II. Effect of chloroplastic metabolite levels on the formation of ADP-Glucose by chloroplast

extracts. *Plant Physiol.* 1979, *63*, 109–113.
299. **Morell, M.K. *et al.*** Subunit structure of spinach leaf ADPglucose pyrophosphorylase. *Plant Physiol.* 1987, *85*, 182–187.
300. **Okita, T.W. *et al.*** The subunit structure of potato tuber ADPglucose pyrophosphorylase. *Plant Physiol.* 1990, *93*, 785–790.
301. **Fu, Y. *et al.*** Mechanism of reductive activation of potato tuber ADP-glucose pyrophosphorylase. *J. Biol. Chem.* 1998, *273*, 25045–25052.
302. **Ballicora, M.A. *et al.*** Activation of the potato tuber ADP-glucose pyrophosphorylase by thioredoxin. *J. Biol. Chem.* 2000, *275*, 1315–1320.
303. **Geigenberger, P. *et al.*** Redox regulation of carbon storage and partitioning in response to light and sugars. *J. Exp. Bot.* 2005, *56*, 1469–1479.
304. **Thormählen, I. *et al.*** Inactivation of thioredoxin *f1* leads to decreased light activation of ADP-glucose pyrophosphorylase and altered diurnal starch turnover in leaves of *Arabidopsis* plants. *Plant, Cell Environ.* 2013, *36*, 16–29.
305. **Sanz-Barrio, R. *et al.*** Overexpression of plastidial thioredoxin f leads to enhanced starch accumulation in tobacco leaves. *Plant Biotechnol. J.* 2013, *11*, 618–627.
306. **Lepistö, A. *et al.*** Deletion of chloroplast NADPH-dependent thioredoxin reductase results in inability to regulate starch synthesis and causes stunted growth under short-day photoperiods. *J. Exp. Bot.* 2013, *64*, 3843–3854.
307. **Glaring, M.A. *et al.*** Comprehensive survey of redox sensitive starch metabolising enzymes in *Arabidopsis thaliana*. *Plant Physiol. Biochem.* 2012, *58*, 89–97.
308. **Skryhan, K. *et al.*** The role of cysteine residues in redox regulation and protein stability of Arabidopsis thaliana starch synthase 1. *PLoS One* 2015, *10*, e0136997.
309. **Wang, F. *et al.*** The maize plastidic thioredoxin F-type gene *ZmTrxF* increases starch accumulation in transgenic *Arabidopsis*. *Sci. Hortic. (Amsterdam).* 2016, *210*, 205–212.
310. **Wang, F. *et al.*** Enhancement of starch content by constitutive expression of *GmTrxF* in transgenic *Arabidopsis*. *Plant Growth Regul.* 2018, *84*, 351–358.
311. **Balmer, Y. *et al.*** Proteome of amyloplasts isolated from developing wheat endosperm presents evidence of broad metabolic capability. *J. Exp. Bot.* 2006, *57*, 1591–1602.
312. **Kirchberger, S. *et al.*** Molecular and biochemical analysis of the plastidic ADP-glucose transporter (ZmBT1) from *Zea mays*. *J. Biol. Chem.* 2007, *282*, 22481–22491.
313. **Mikkelsen, R. *et al.*** α-glucan, water dikinase (GWD): a plastidic enzyme with redox-regulated and coordinated catalytic activity and binding affinity. *Proc. Natl. Acad. Sci.* 2005, *102*, 1785–90.
314. **Skeffington, A.W. *et al.*** Glucan, water dikinase exerts little control over starch degradation in Arabidopsis leaves at night. *Plant Physiol.* 2014, *165*, 866–879.
315. **Sokolov, L.N. *et al.*** A redox-regulated chloroplast protein phosphatase binds to starch diurnally and functions in its accumulation. *Proc. Natl. Acad. Sci.* 2006, *103*, 9732–9737.
316. **Silver, D.M. *et al.*** Insight into the redox regulation of the phosphoglucan phosphatase SEX4 involved in starch degradation. *FEBS J.* 2013, *280*, 538–548.
317. **Sparla, F. *et al.*** Redox regulation of a novel plastid-targeted β-Amylase. *Plant Physiol.* 2006, *141*, 840–850.
318. **Seung, D. *et al.*** *Arabidopsis thaliana* AMY3 is a unique redox-regulated chloroplastic α-amylase. *J. Biol. Chem.* 2013, *288*, 33620–33633.
319. **Schindler, I. *et al.*** Activation of spinach pullulanase by reduction results in a decrease in the number of isomeric forms. *Biochim. Biophys. Acta - Protein Struct. Mol. Enzymol.* 2001, *1548*, 175–186.
320. **Repellin, A. *et al.*** *In vitro* pullulanase activity of wheat (*Triticum aestivum* L.) limit-dextrinase type starch debranching enzyme is modulated by redox conditions. *J. Cereal Sci.* 2008, *47*, 302–309.
321. **Hase, T. *et al.*** The Interaction of Ferredoxin with Ferredoxin-Dependent Enzymes Photosystem I: The Light-Driven Plastocyanin:Ferredoxin Oxidoreductase. In *Photosystem I: Advances in Photosynthesis and Respiration*; Golbeck, J.H., Ed.; Springer Netherlands: Dordrecht, 2006; pp. 477–498 ISBN 978-1-4020-4256-0.
322. **Florencio, F.J. *et al.*** Thioredoxin-linked activation of the chloroplast and cytosolic forms of *Chlamydomonas reinhardtii* glutamine synthetase. *Plant Physiol. Biochem.* 1993, *31*, 649–655.
323. **Tischner, R. & Schmidt, A.** A thioredoxin-mediated activation of glutamine synthetase and glutamate synthase in Synchronous *Chlorella sorokiniana*. *Plant Physiol.* 1982, *70*, 113–116.
324. **Schmidt, A.** A Thioredoxin Activated Glutamine Synthetase in Chlorella. *Zeitschrift fur Naturforsch. - Sect. C J. Biosci.* 1981, *36*, 396–399.
325. **Papen, H. & Bothe, H.** The activation of glutamine synthetase from the cyanobacterium *Anabaena cylindrica* by thioredoxin. *FEMS Microbiol. Lett.* 1984, *23*, 41–46.

326. **Choi, Y.A. *et al.*** The plastidic glutamine synthetase activity is directly modulated by means of redox change at two unique cysteine residues. *Plant Sci.* 1999, *149*, 175–182.
327. **Taira, M. *et al.*** *Arabidopsis thaliana GLN2*-Encoded Glutamine Synthetase Is Dual Targeted to Leaf Mitochondria and Chloroplasts. *Plant Cell* 2004, *16*, 2048–2058.
328. **Kolbe, A. *et al.*** Combined transcript and metabolite profiling of Arabidopsis leaves reveals fundamental effects of the thiol-disulfide status on plant metabolism. *Plant Physiol.* 2006, *141*, 412–422.
329. **Entus, R. *et al.*** Redox regulation of Arabidopsis 3-deoxy- D -arabino- heptulosonate 7-phosphate synthase. *Plant Physiol.* 2002, *129*, 1866–1871.
330. **Nishizawa, A.N. *et al.*** Chloroplast phenylalanine ammonia-lyase from spinach leaves. *Planta* 1979, *145*, 7–12.
331. **Nikkanen, L. & Rintamäki, E.** Thioredoxin-dependent regulatory networks in chloroplasts under fluctuating light conditions. *Philos. Trans. R. Soc. B Biol. Sci.* 2014, *369*, 1–7.
332. **Allen, J.F.** State Transitions - a Question of Balance. *Science (80-.).* 2003, *299*, 1530–1532.
333. **Wientjes, E. *et al.*** During state 1 to state 2 transition in *Arabidopsis thaliana*, the photosystem II supercomplex gets phosphorylated but does not disassemble. *J. Biol. Chem.* 2013, *288*, 32821–32826.
334. **Crepin, A. & Caffarri, S.** The specific localizations of phosphorylated Lhcb1 and Lhcb2 isoforms reveal the role of Lhcb2 in the formation of the PSI-LHCII supercomplex in *Arabidopsis* during state transitions. *Biochim. Biophys. Acta - Bioenerg.* 2015, *1847*, 1539–1548.
335. **Wientjes, E. *et al.*** LHCII is an antenna of both photosystems after long-term acclimation. *Biochim. Biophys. Acta - Bioenerg.* 2013, *1827*, 420–426.
336. **Bonardi, V. *et al.*** Photosystem II core phosphorylation and photosynthetic acclimation require two different protein kinases. *Nature* 2005, *437*, 1179–1182.
337. **Depège, N. *et al.*** Role of chloroplast protein kinase Stt7 in LHCII phosphorylation and state transition in *Chlamydomonas*. *Science (80-.).* 2003, *299*, 1572–1575.
338. **Lemeille, S. *et al.*** Analysis of the chloroplast protein kinase Stt7 during state transitions. *PLoS Biol.* 2009, *7*, e1000045.
339. **Wunder, T. *et al.*** Control of *STN7* transcript abundance and transient STN7 dimerisation are involved in the regulation of STN7 activity. *Planta* 2013, *237*, 541–558.
340. **Bennett, J. *et al.*** Cytochrome b_6f complex is required for phosphorylation of light-harvesting chlorophyll a/b complex II in chloroplast photosynthetic membranes. *Eur. J. Biochem.* 1988, *171*, 95–100.
341. **Gal, A. *et al.*** Role of the Cytochrome b_6f complex in the redox-controlled activity of *Acetabularia* thylakoid protein kinase. *J. Biol. Chem.* 1988, *263*, 7785–7791.
342. **Gal, A. *et al.*** Interaction between light harvesting chlorophyll-*a/b* protein (LHCII) kinase and cytochrome b_6/f complex. *J. Biol. Chem.* 1990, *265*, 19742–19749.
343. **Schuster, G. *et al.*** Transient inactivation of the thylakoid photosystem II light-harvesting protein kinase system and concomitant changes in intramembrane particle size during photoinhibition of *Chlamydomonas reinhardtii*. *J. Cell Biol.* 1986, *103*, 71–80.
344. **Dietzel, L. *et al.*** Photosynthetic acclimation: State transitions and adjustment of photosystem stoichiometry - Functional relationships between short-term and long-term light quality acclimation in plants. *FEBS J.* 2008, *275*, 1080–1088.
345. **Wunder, T. *et al.*** The major thylakoid protein kinases STN7 and STN8 revisited: effects of altered STN8 levels and regulatory specificities of the STN kinases. *Front. Plant Sci.* 2013, *4*, 417.
346. **Sanz-Barrio, R. *et al.*** Tobacco plastidial thioredoxins as modulators of recombinant protein production in transgenic chloroplasts. *Plant Biotechnol. J.* 2011, *9*, 639–50.
347. **Genty, B. *et al.*** The relationship between the quantum yield of photosynthetic electron transport and quenching of chlorophyll fluorescence. *Biochim. Biophys. Acta - Gen. Subj.* 1989, *990*, 87–92.
348. **Kramer, D.M. *et al.*** New fluorescence parameters for the determination of Q_A redox state and excitation energy fluxes. *Photosynth. Res.* 2004, *79*, 209–218.
349. **von Caemmerer, S. & Farquhar, G.D.** Some relationships between the biochemistry of photosynthesis and the gas exchange of leaves. *Planta* 1981, *153*, 376–387.
350. **Sharkey, T.D. *et al.*** Fitting photosynthetic carbon dioxide response curves for C_3 leaves. *Plant, Cell Environ.* 2007, *30*, 1035–1040.
351. **Cornic, G. & Briantais, J.-M.** Partitioning of photosynthetic electron flow between CO_2 and O_2 reduction in a C3 leaf (*Phaseolus vulgaris* L.) at different CO_2 concentrations and during drought stress. *Planta* 1991, *183*, 178–184.
352. **Kral, J.P. & Edwards, G.E.** Relationship between photosystem II activity and CO_2 fixation in

leaves. *Physiol. Plant.* 1992, *86*, 180–187.
353. **Morales, F. *et al.*** Chlorophyll fluorescence and photon yield of oxygen evolution in iron-deficient sugar beet (*Beta vulgaris* L.) leaves. *Plant Physiol.* 1991, *97*, 886–893.
354. **Lichtenthaler, H.K.** Chlorophylls and carotenoids: Pigments of photosynthetic biomembranes. *Methods Enzymol.* 1987, *148*, 350–382.
355. **Rintamäki, E. *et al.*** Differential D1 dephosphorylation in functional and photodamaged photosystem II centers. *J. Biol. Chem.* 1996, *271*, 14870–14875.
356. **Järvi, S. *et al.*** Optimized native gel systems for separation of thylakoid protein complexes: novel super- and mega-complexes. *Biochem. J.* 2011, *439*, 207–214.
357. **Fernández-San Millán, A. *et al.*** Physiological performance of transplastomic tobacco plants overexpressing aquaporin AQP1 in chloroplast membranes. *J. Exp. Bot.* 2018, *69*, 3661–3673.
358. **Perez-Ruiz, J.M. *et al.*** Rice NTRC is a high-efficiency redox system for chloroplast protection against oxidative damage. *Plant Cell* 2006, *18*, 2356–2368.
359. **Vainonen, J.P. *et al.*** STN8 protein kinase in *Arabidopsis thaliana* is specific in phosphorylation of photosystem II core proteins. *J. Biol. Chem.* 2005, *280*, 33679–33686.
360. **Strasserf, R.J. *et al.*** POLYPHASIC CHLOROPHYLL a FLUORESCENCE TRANSIENT IN PLANTS AND CYANOBACTERIA. *Photochem. Photobiol.* 1995, *61*, 32–42.
361. **Tóth, S.Z. *et al.*** In intact leaves, the maximum fluorescence level (F_M) is independent of the redox state of the plastoquinone pool: A DCMU-inhibition study. *Biochim. Biophys. Acta - Bioenerg.* 2005, *1708*, 275–282.
362. **Belkhodja, R. *et al.*** Iron deficiency causes changes in chlorophyll fluorescence due to the reduciton in the dark of the Photosystem II acceptor side. *Photosynth. Res.* 1998, *56*, 265–276.
363. **Rumak, I. *et al.*** Correlation between spatial (3D) structure of pea and bean thylakoid membranes and arrangement of chlorophyll-protein complexes. *BMC Plant Biol.* 2012, *12*, 1–18.
364. **König, J. *et al.*** The plant-specific function of 2-Cys peroxiredoxin-mediated detoxification of peroxides in the redox-hierarchy of photosynthetic electron flux. *Proc. Natl. Acad. Sci.* 2002, *99*, 5738–5743.
365. **Hou, C.X. *et al.*** Environmental and metabolic control of LHCII protein phosphorylation: revealing the mechanisms for dual regulation of the LHCII kinase. *Plant, Cell Environ.* 2002, *25*, 1515–1525.
366. **Tikkanen, M. *et al.*** Thylakoid protein phosphorylation in higher plant chloroplasts optimizes electron transfer under fluctuating light. *Plant Physiol.* 2010, *152*, 723–735.
367. **Corneille, S. *et al.*** Reduction of the plastoquinone pool by exogenous NADH and NADPH in higher plant chloroplasts characterization of a NAD(P)H-plastoquinone oxidoreductase activity. *Biochim. Biophys. Acta - Bioenerg.* 1998, *1363*, 59–69.
368. **Pietrzykowska, M. *et al.*** The light-harvesting chlorophyll a/b binding proteins Lhcb1 and Lhcb2 play complementary roles during state transitions in *Arabidopsis*. *Plant Cell* 2014, *26*, 3646–3660.
369. **Wollman, F.-A. & Lemaire, C.** Studies on kinase-controlled state transitions in Photosystem II and b_6f mutants *Chlamydomonas reinhardtii* from which lack quinone-binding proteins. *Biochim. Biophys. Acta - Bioenerg.* 1988, *933*, 85–94.
370. **Breyton, C.** Conformational changes in the cytochrome b_6f complex induced by inhibitor binding. *J. Biol. Chem.* 2000, *275*, 13195–13201.
371. **Friso, G. *et al.*** In-depth analysis of the thylakoid membrane proteome of *Arabidopsis thaliana* chloroplasts: New proteins, new functions, and a plastid proteome database. *Plant Cell* 2004, *16*, 478–499.
372. **Kouřil, R. *et al.*** Structural characterization of a complex of photosystem I and light-harvesting complex II of *Arabidopsis thaliana*. *Biochemistry* 2005, *44*, 10935–10940.
373. **Pesaresi, P. *et al.*** *Arabidopsis* STN7 kinase provides a link between short- and long-term photosynthetic acclimation. *Plant Cell* 2009, *21*, 2402–2423.
374. **Allen, J.F.** Why we need to know the structure of phosphorylated chloroplast light-harvesting complex II. *Physiol. Plant.* 2017, *161*, 28–44.
375. **Chuartzman, S.G. *et al.*** Thylakoid membrane remodeling during state transitions in Arabidopsis. *Plant Cell* 2008, *20*, 1029–1039.
376. **Herbstová, M. *et al.*** Architectural switch in plant photosynthetic membranes induced by light stress. *Proc. Natl. Acad. Sci.* 2012, *109*, 20130–20135.
377. **Tikkanen, M. *et al.*** Phosphorylation-dependent regulation of excitation energy distribution between the two photosystems in higher plants. *Biochim. Biophys. Acta - Bioenerg.* 2008, *1777*, 425–432.
378. **Pribil, M. *et al.*** Structure and dynamics of thylakoids in land plants. *J. Exp. Bot.* 2014, *65*,

1955–1972.
379. **Lindahl, M. *et al.*** Regulatory proteolysis of the major light-harvesting chlorophyll a/b protein of photosystem II by a light-induced membrane-associated enzymic system. *Eur. J. Biochem.* 1995, *231*, 503–509.
380. **Yang, D.-H. *et al.*** Induction of acclimative proteolysis of the light-harvesting chlorophyll a/b protein of photosystem II in response to elevated light intensities. *Plant Physiol.* 1998, *118*, 827–834.
381. **Zelisko, A. *et al.*** AtFtsH6 is involved in the degradation of the light-harvesting complex II during high-light acclimation and senescence. *Proc. Natl. Acad. Sci.* 2005, *102*, 13699–13704.
382. **Luciński, R. & Jackowski, G.** AtFtsH heterocomplex-mediated degradation of apoproteins of the major light harvesting complex of photosystem II (LHCII) in response to stresses. *J. Plant Physiol.* 2013, *170*, 1082–1089.
383. **Wang, F. *et al.*** The high light response and redox control of thylakoid FtsH orotease in *Chlamydomonas reinhardtii*. *Mol. Plant* 2017, *10*, 99–114.
384. **Escoubas, J.M. *et al.*** Light intensity regulation of *cab* gene transcription is signaled by the redox state of the plastoquinone pool. *Proc. Natl. Acad. Sci.* 1995, *92*, 10237–10241.
385. **Yang, D.H. *et al.*** The redox state of the plastoquinone pool controls the level of the light-harvesting chlorophyll *a/b* binding protein complex II (LHC II) during photoacclimation. *Photosynth. Res.* 2001, *68*, 163–174.
386. **Finazzi, G. *et al.*** Involvement of state transitions in the switch between linear and cyclic electron flow in *Chlamydomonas reinhardtii*. *EMBO Rep.* 2002, *3*, 280–285.
387. **Wood, W.H.J. *et al.*** Dynamic thylakoid stacking regulates the balance between linear and cyclic photosynthetic electron transfer. *Nat. Plants* 2018, *4*, 116–127.
388. **Johnson, M.P.** Metabolic regulation of photosynthetic membrane structure tunes electron transfer function. *Biochem. J.* 2018, *475*, 1225–1233.
389. **Frenkel, M. *et al.*** Hierarchy amongst photosynthetic acclimation responses for plant fitness. *Physiol. Plant.* 2007, *129*, 455–459.
390. **Queval, G. & Noctor, G.** A plate reader method for the measurement of NAD, NADP, glutathione, and ascorbate in tissue extracts: Application to redox profiling during *Arabidopsis* rosette development. *Anal. Biochem.* 2007, *363*, 58–69.
391. **Lu, Y. *et al.*** A Small Zinc Finger Thylakoid Protein Plays a Role in Maintenance of Photosystem II in *Arabidopsis thaliana*. *Plant Cell* 2011, *23*, 1861–1875.
392. **Holmgren, A.** Thioredoxin catalyzes the reduction of insulin disulfides by dithiothreitol and dihydrolipoamide. *J. Biol. Chem.* 1979, *254*, 9627–9632.
393. **Chibani, K. *et al.*** Comparative genomic study of the thioredoxin family in photosynthetic organisms with emphasis on Populus trichocarpa. *Mol. Plant* 2009, *2*, 308–322.
394. **Spínola, M.C. *et al.*** NTRC new ways of using NADPH in the chloroplast. *Physiol. Plant.* 2008, *133*, 516–524.
395. **Stitt, M. *et al.*** Arabidopsis and primary photosynthetic metabolism - More than the icing on the cake. *Plant J.* 2010, *61*, 1067–1091.
396. **Pfister, B. & Zeeman, S.C.** Formation of starch in plant cells. *Cell. Mol. Life Sci.* 2016, *73*, 2781–2807.
397. **Kötting, O. *et al.*** Regulation of starch metabolism: the age of enlightenment? *Curr. Opin. Plant Biol.* 2010, *13*, 321–329.
398. **Hendriks, J.H.M. *et al.*** ADP-glucose pyrophosphorylase is activated by posttranslational redox-modification in response to light and to sugars in leaves of Arabidopsis and other plant species. *Plant Physiol.* 2003, *133*, 838–849.
399. **Hädrich, N. *et al.*** Mutagenesis of cysteine 81 prevents dimerization of the APS1 subunit of ADP-glucose pyrophosphorylase and alters diurnal starch turnover in *Arabidopsis thaliana* leaves. *Plant J.* 2012, *70*, 231–242.
400. **Li, J. *et al.*** Post-translational redox modification of ADP-glucose pyrophosphorylase in response to light is not a major determinant of fine regulation of transitory starch accumulation in Arabidopsis leaves. *Plant Cell Physiol.* 2012, *53*, 433–444.
401. **Lunn, J.E. *et al.*** Trehalose metabolism in plants. *Plant J.* 2014, *79*, 544–567.
402. **Bahaji, A. *et al.*** Starch biosynthesis, its regulation and biotechnological approaches to improve crop yields. *Biotechnol. Adv.* 2014, *32*, 87–106.
403. **Fernández-San Millán, A. *et al.*** Human papillomavirus L1 protein expressed in tobacco chloroplasts self-assembles into virus-like particles that are highly immunogenic. *Plant Biotechnol. J.* 2008, *6*, 427–441.
404. **Burch-Smith, T.M. *et al.*** Applications and advantages of virus-induced gene silencing for gene function studies in plants. *Plant J.* 2004, *39*, 734–746.
405. **Liu, Y.L. *et al.*** Virus-induced gene silencing in tomato. *Plant J.* 2002, *31*, 777–786.

406. **Liu, Y. *et al.*** Virus induced gene silencing of a *DEFICIENS* ortholog in *Nicotiana benthamiana*. *Plant Mol. Biol.* 2004, *54*, 701–711.
407. **Wu, C. *et al.*** The reliability of virus-induced gene silencing experiments using tobacco rattle virus in tomato is influenced by the size of the vector control. *Mol. Plant Pathol.* 2011, *12*, 299–305.
408. **Ganusova, E.E. *et al.*** Altered Expression of a Chloroplast Protein Affects the Outcome of Virus and Nematode Infection. *Mol. Plant-Microbe Interact.* 2017, *30*, 478–488.
409. **Pfaffl, M.W.** A new mathematical model for relative quantification in real-time RT-PCR. *Nucleic Acids Res.* 2001, *29*, 45e–45.
410. **Nakamura, Y. *et al.*** Carbohydrate metabolism in the developing endosperm of rice grains. *Plant Cell Physiol.* 1989, *30*, 833–839.
411. **Bock, R.** Engineering Plastid Genomes: Methods, Tools, and Applications in Basic Research and Biotechnology. *Annu. Rev. Plant Biol.* 2015, *66*, 211–241.
412. **Liu, Y. *et al.*** Tobacco Rar1, EDS1 and NPR1/NIM1 like genes are required for N-mediated resistance to tobacco mosaic virus. *Plant J.* 2002, *30*, 415–429.
413. **Häusler, R.E. *et al.*** Control of carbon partitioning and photosynthesis by the triose phosphate/phosphate translocator in transgenic tobacco plants (*Nicotiana tabacum* L.). I. Comparative physiological analysis of tobacco plants with antisense repression and overexpressi. *Planta* 2000, *210*, 371–382.
414. **Martins, M.C.M. *et al.*** Feedback inhibition of starch degradation in Arabidopsis leaves mediated by trehalose 6-phosphate. *Plant Physiol.* 2013, *163*, 1142–1163.
415. **Née, G. *et al.*** Redox regulation of chloroplastic glucose-6-phosphate dehydrogenase: A new role for f-type thioredoxin. *FEBS Lett.* 2009, *583*, 2827–2832.
416. **Née, G. *et al.*** Redox regulation of chloroplastic G6PDH activity by thioredoxin occurs through structural changes modifying substrate accessibility and cofactor binding. *Biochem. J.* 2014, *457*, 117–125.
417. **Wattebled, F. *et al.*** Mutants of Arabidopsis lacking a chloroplastic isoamylase accumulate phytoglycogen and an abnormal form of amylopectin. *Plant Physiol.* 2005, *138*, 184–195.
418. **Farran, I. *et al.*** Increased bioethanol production from commercial tobacco cultivars overexpressing thioredoxin f grown under field conditions. *Mol. Breed.* 2014, *34*, 457–469.
419. **Aranjuelo, I. *et al.*** Alteration by thioredoxin f over-expression of primary carbon metabolism and its response to elevated CO_2 in tobacco (*Nicotiana tabacum* L.). *Environ. Exp. Bot.* 2015, *118*, 40–48.
420. **Delvallé, D. *et al.*** Soluble starch synthase I: a major determinant for the synthesis of amylopectin in *Arabidopsis thaliana* leaves. *Plant J.* 2005, *43*, 398–412.
421. **Cuesta-Seijo, J.A. *et al.*** Structure of starch synthase I from barley: insight into regulatory mechanisms of starch synthase activity. *Acta Crystallogr. Sect. D Biol. Crystallogr.* 2013, *69*, 1013–1025.
422. **Wang, F.B. *et al.*** Constitutive expression of *SlTrxF* increases starch content in transgenic *Arabidopsis*. *Biol. Plant.* 2017, *61*, 494–500.
423. **Hendriks, J. *et al.*** ADP-glucose pyrophosphorylase is activated by posttranslational redox-modification in response to light and to sugars in leaves of Arabidopsis and other plant. *Plant …* 2003, *133*, 838–849.
424. **Nikkanen, L. *et al.*** Chloroplast thioredoxin systems: prospects for improving photosynthesis. *Philos. Trans. R. Soc. B* 2017, *372*, 20160474.
425. **Tischner, R. & Schmidt, A.** A Thioredoxin-Mediated Activation of Glutamine. *Plant Physiol.* 1982, *70*, 113–116.
426. **Lindahl, M. & Florencio, F.J.** Thioredoxin-linked processes in cyanobacteria are as numerous as in chloroplasts, but targets are different. *Proc. Natl. Acad. Sci.* 2003, *100*, 16107–16112.
427. **Geiger, M. *et al.*** The nitrate and ammonium nitrate supply have a major influence on the response of photosynthesis, carbon metabolism, nitrogen metabolism and growth to elevated carbon dioxide in tobacco. *Plant, Cell Environ.* 1999, *22*, 1177–1199.
428. **Loiret, F.G. *et al.*** Inoculation of sugarcane with *Pantoea* sp. increases amino acid contents in shoot tissues; serine, alanine, glutamine and asparagine permit concomitantly ammonium excretion and nitrogenase activity of the bacterium. *J. Plant Physiol.* 2009, *166*, 1152–1161.
429. **Lisec, J. *et al.*** Gas chromatography mass spectrometry–based metabolite profiling in plants. *Nat. Protoc.* 2006, *1*, 387–396.
430. **Kopka, J. *et al.*** GMD@CSB.DB: the Golm metabolome database. *Bioinformatics* 2005, *21*, 1635–1638.
431. **Schauer, N. *et al.*** GC-MS libraries for the rapid identification of metabolites in complex biological samples. *FEBS Lett.* 2005, *579*, 1332–1337.
432. **Luedemann, A. *et al.*** TagFinder: preprocessing software for the fingerprinting and the profiling

of gas chromatography–mass spectrometry based metabolome analyses. In *Plant Metabolomics. Methods in Molecular Biology (Methods and Protocols), vol 860*; Hardy, N.W., Hall, R.D., Eds.; Humana Press: Totowa, NJ, 2012; pp. 255–286 ISBN 978-1-61779-594-7.

433. **Gibon, Y. *et al.*** A robot-based platform to measure multiple enzyme activities in Arabidopsis using a set of cycling assays: Comparison of changes of enzyme activities and transcript levels during diurnal cycles and in prolonged darkness. *Plant Cell* 2004, *16*, 3304–3325.
434. **Biais, B. *et al.*** Remarkable reproducibility of enzyme activity profiles in tomato fruits grown under contrasting environments provides a roadmap for studies of fruit metabolism. *Plant Physiol.* 2014, *164*, 1204–1221.
435. **Bénard, C. & Gibon, Y.** Measurement of enzyme activities and optimization of continuous and discontinuous assays. *Curr. Protoc. Plant Biol.* 2016, *1*, 247–262.
436. **Cataldo, D.A. *et al.*** Rapid colorimetric determination of nitrate in plant tissue by nitration of salicylic acid. *Commun. Soil Sci. Plant Anal.* 1975, *6*, 71–80.
437. **Sarasketa, A. *et al.*** Exploring ammonium tolerance in a large panel of *Arabidopsis thaliana* natural accessions. *J. Exp. Bot.* 2014, *65*, 6023–6033.
438. **Miyake, C. & Yokota, A.** Determination of the rate of photoreduction of O_2 in the water-water cycle in watermelon leaves and enhancement of the rate by limitation of photosynthesis. *Plant Cell Physiol.* 2000, *41*, 335–343.
439. **Krall, J.P. & Edwards, G.E.** Relationship between photosystem II activity and CO_2 fixation in leaves. *Physiol. Plant.* 1992, *86*, 180–187.
440. **Walter, M. *et al.*** Visualization of protein interactions in living plant cells using bimolecular fluorescence complementation. *Plant J.* 2004, *40*, 428–438.
441. **Liu, L. *et al.*** An efficient system to detect protein ubiquitination by agroinfiltration in *Nicotiana benthamiana*. *Plant J.* 2010, *61*, 893–903.
442. **Unno, H. *et al.*** Atomic structure of plant glutamine synthetase: A key enzyme for plant productivity. *J. Biol. Chem.* 2006, *281*, 29287–29296.
443. **Ancín, M. *et al.*** Thioredoxin m overexpression in tobacco chloroplasts inhibits the protein kinase STN7 and alters photosynthetic performance. *J. Exp. Bot.* 2018.
444. **Fontaine, J.-X. *et al.*** Characterization of a NADH-Dependent Glutamate Dehydrogenase Mutant of *Arabidopsis* Demonstrates the Key Role of this Enzyme in Root Carbon and Nitrogen Metabolism. *Plant Cell* 2012, *24*, 4044–4065.
445. **Betti, M. *et al.*** Molecular analysis of two mutants from *Lotus japonicus* deficient in plastidic glutamine synthetase: Functional properties of purified GLN2 enzymes. *Planta* 2006, *224*, 1068–1079.
446. **Palatnik, J. *et al.*** The role of photosynthetic electron transport in the oxidative degradation of chloroplastic glutamine synthetase. *Plant Physiol.* 1999, *121*, 471–8.
447. **Ishida, H. *et al.*** Direct evidence for non-enzymatic fragmentation of chloroplastic glutamine synthetase by a reactive oxygen species. *Plant, Cell Environ.* 2002, *25*, 625–631.
448. **Castro-Rodríguez, V. *et al.*** Redundancy and metabolic function of the glutamine synthetase gene family in poplar. *BMC Plant Biol.* 2015, *15*, 1–14.
449. **Liao, J. *et al.*** Cloning, expression and antioxidant activity of a thioredoxin peroxidase from *Branchiostoma belcheri tsingtaunese*. *PLoS One* 2017, *12*, e0175162.
450. **Rahlfs, S. & Becker, K.** Thioredoxin peroxidases of the malarial parasite *Plasmodium falciparum*. *Eur. J. Biochem.* 2001, *268*, 1404–1409.
451. **Jeon, S.J. & Ishikawa, K.** Characterization of novel hexadecameric thioredoxin peroxidase from *Aeropyrum pernix* K1. *J. Biol. Chem.* 2003, *278*, 24174–24180.
452. **Cheong, N.E. *et al.*** Molecular cloning, expression, and functional characterization of a 2Cys-peroxiredoxin in Chinese cabbage. *Plant Mol. Biol.* 1999, *40*, 825–834.
453. **Hodges, M. *et al.*** Perspectives for a better understanding of the metabolic integration of photorespiration within a complex plant primary metabolism network. *J. Exp. Bot.* 2016, *67*, 3015–3026.
454. **Coschigano, K.T. *et al.*** Arabidopsis *gls* mutants and distinct Fd-GOGAT genes: Implications for photorespiration and primary nitrogen assimilation. *Plant Cell* 1998, *10*, 741–752.
455. **Taniguchi, M. *et al.*** Identifying and characterizing plastidic 2-oxoglutarate/malate and dicarboxylate transporters in *Arabidopsis thaliana*. *Plant Cell Physiol.* 2002, *43*, 706–717.
456. **Weber, A. & Flügge, U.I.** Interaction of cytosolic and plastidic nitrogen metabolism in plants. *J. Exp. Bot.* 2002, *53*, 865–874.
457. **Kaiser, W.M. *et al.*** Discrepancy between nitrate reduction rates in intact leaves and nitrate reductase activity in leaf extracts: what limits nitrate reduction in situ? *Planta* 2000, *210*, 801–807.
458. **Kaiser, W.M. *et al.*** What limits nitrate reduction in leaves? In *Photosynthetic Nitrogen Assimilation and Associated Carbon and Respiratory Metabolism. Advances in Photosynthesis*

and Respiration; Foyer C.H., N.G. (eds), Ed.; Springer, Dordrecht, 2002; pp. 63–70.
459. **Hashida, S. *et al.*** Ferredoxin/thioredoxin system plays an important role in the chloroplastic NADP status of *Arabidopsis*. *Plant J.* 2018.
460. **Kaiser, W.M. & Huber, S.C.** Post-translational regulation of nitrate reductase: mechanism, physiological relevance and environmental triggers. *J. Exp. Bot.* 2001, *52*, 1981–1989.
461. **Quick, W.P. *et al.*** The impact of decreased Rubisco on photosynthesis, growth, allocation and storage in tobacco plants which have been transformed with antisense rbcS. *Plant J.* 1991, *1*, 51–58.
462. **Fritz, C. *et al.*** Regulation of secondary metabolism by the carbon-nitrogen status in tobacco: nitrate inhibits large sectors of phenylpropanoid metabolism. *Plant J.* 2006, *46*, 533–548.
463. **Dixon, R.A. & Paiva, N.L.** Stress-induced phenylpropanoid metabolism. *Plant Cell* 1995, *7*, 1085–1097.
464. **Deng, Y. & Lu, S.** Biosynthesis and Regulation of Phenylpropanoids in Plants. *CRC. Crit. Rev. Plant Sci.* 2017, *36*, 257–290.
465. **Vogt, T.** Phenylpropanoid biosynthesis. *Mol. Plant* 2010, *3*, 2–20.
466. **Shi, J. *et al.*** Phosphoenolpyruvate carboxylase in Arabidopsis leaves plays a crucial role in carbon and nitrogen metabolism. *Plant Physiol.* 2015, *167*, 671–681.
467. **Yamaryo, Y. *et al.*** In vitro reconstitution of monogalactosyldiacylglycerol (MGDG) synthase regulation by thioredoxin. *FEBS Lett.* 2006, *580*, 4086–4090.
468. **Bartsch, S. *et al.*** Three thioredoxin targets in the inner envelope membrane of chloroplasts function in protein import and chlorophyll metabolism. *Proc. Natl. Acad. Sci.* 2008, *105*, 4933–4938.
469. **Schwarz, C. *et al.*** An intermolecular disulfide-based light switch for chloroplast *psbD* gene expression in *Chlamydomonas reinhardtii*. *Plant J.* 2012, *72*, 378–389.
470. **Balmer, Y. *et al.*** Thioredoxin target proteins in chloroplast thylakoid membranes. *Antioxid. Redox Signal.* 2006, *8*, 1829–1834.
471. **Yano, H. & Kuroda, M.** Disulfide proteome yields a detailed understanding of redox regulations: A model study of thioredoxin-linked reactions in seed germination. *Proteomics* 2006, *6*, 294–300.
472. **Hägglund, P. *et al.*** Identification of thioredoxin target disulfides using isotope-coded affinity tags. In *Plant Proteomics. Methods in Molecular Biology (Methods and Protocols)*; Jorrin-Novo J., Komatsu S., Weckwerth W., W.S. (eds), Ed.; Humana Press, Totowa, NJ, 2014; Vol. 1072, pp. 677–685 ISBN 9781627036306.
473. **Kallis, G.B. & Holmgren, A.** Differential reactivity of the functional sulfhydryl groups of cysteine-32 and cysteine-32 present in the reduced form of thioredoxin from Escherichia coli. *J. Biol. Chem.* 1980, *255*, 10261–10265.
474. **Hennegan, K.P. & Danna, K.J.** pBIN20: An improved binary vector for Agrobacterium-mediated transformation. *Plant Mol. Biol. Report.* 1998, *16*, 129–131.
475. **Shilov, I. V. *et al.*** The Paragon Algorithm, a Next Generation Search Engine That Uses Sequence Temperature Values and Feature Probabilities to Identify Peptides from Tandem Mass Spectra. *Mol. Cell. Proteomics* 2007, *6*, 1638–1655.
476. **Tang, W.H. *et al.*** Nonlinear fitting method for determining local false discovery rates from decoy database searches. *J. Proteome Res.* 2008, *7*, 3661–3667.
477. **Brandes, H.K. *et al.*** Direct identification of the primary nucleophile of thioredoxin *f*. *J. Biol. Chem.* 1993, *268*, 18411–18414.
478. **Holmgren, A.** Thioredoxin structure and mechanism: conformational changes on oxidation of the active-site sulfhydryls to a disulfide. *Structure* 1995, *3*, 239–243.
479. **Edwards, K.D. *et al.*** A reference genome for *Nicotiana tabacum* enables map-based cloning of homeologous loci implicated in nitrogen utilization efficiency. *BMC Genomics* 2017, *18*, 448.
480. **Berardini, T.Z. *et al.*** The arabidopsis information resource: Making and mining the “gold standard” annotated reference plant genome. *Genesis* 2015, *53*, 474–485.
481. **Bolger, M.E. *et al.*** Plant genome and transcriptome annotations: from misconceptions to simple solutions. *Brief. Bioinform.* 2018, *19*, 437–449.
482. **Altschul, S.F. *et al.*** Basic local alignment search tool. *J. Mol. Biol.* 1990, *215*, 403–410.
483. **Marsian, J. & Lomonossoff, G.P.** Molecular pharming-VLPs made in plants. *Curr. Opin. Biotechnol.* 2016, *37*, 201–206.
484. **Berggård, T. *et al.*** Methods for the detection and analysis of protein-protein interactions. *Proteomics* 2007, *7*, 2833–2842.
485. **Rouhier, N. *et al.*** Identification of plant glutaredoxin targets. *Antioxid. Redox Signal.* 2005, *7*, 919–929.
486. **Ojeda, V. *et al.*** The NADPH-dependent thioredoxin reductase C-2-Cys peroxiredoxin redox system modulates the activity of thioredoxin x in Arabidopsis chloroplasts. *Plant Cell Physiol.*

2018.
487. **Dietz, K.-J.** Peroxiredoxins in plants and cyanobacteria. *Antioxid. Redox Signal.* 2011, *15*, 1129–1159.
488. **Broin, M. *et al.*** The plastidic 2-cysteine peroxiredoxin is a target for a thioredoxin involved in the protection of the photosynthetic apparatus against oxidative damage. *Plant Cell* 2002, *14*, 1417–32.
489. **Gama, F. *et al.*** Functional analysis and expression characteristics of chloroplastic Prx IIE. *Physiol. Plant.* 2008, *133*, 599–610.
490. **Chibani, K. *et al.*** Atypical thioredoxins in Poplar: The glutathione-dependent thioredoxin-like 2.1 supports the activity of target enzymes possessing a single redox active cysteine. *Plant Physiol.* 2012, *159*, 592–605.
491. **Motohashi, K. *et al.*** Identification of thioredoxin targeted proteins using thioredoxin single-cysteine mutant-immobilized resin. In *Methods in molecular biology*; Humana Press, Totowa, NJ, 2009; Vol. 479.
492. **Romero, H.M. *et al.*** Investigations into the role of the plastidial peptide methionine sulfoxide reductase in response to oxidative stress in Arabidopsis. *Plant Physiol.* 2004, *136*, 3784–3794.
493. **Chang, C.C.C. *et al.*** Arabidopsis chloroplastic glutathione peroxidases play a role in cross talk between photooxidative stress and immune responses. *Plant Physiol.* 2009, *150*, 670–683.
494. **DalCorso, G. *et al.*** A complex containing PGRL1 and PGR5 is involved in the switch between linear and cyclic electron flow in *Arabidopsis*. *Cell* 2008, *132*, 273–285.
495. **Scheibe, R. *et al.*** Primary structure and analysis of the location of the regulatory disulfide bond of pea chloroplast NADP-malate dehydrogenase. *Biochim. Biophys. Acta - Protein Struct. Mol. Enzymol.* 1991, *1076*, 1–8.
496. **Baginsky, S. & Gruissem, W.** Endonucleolytic activation directs dark-induced chloroplast mRNA degradation. *Nucleic Acids Res.* 2002, *30*, 4527–4533.
497. **López-Calcagno, P.E. *et al.*** The CP12 protein family: a thioredoxin-mediated metabolic switch? *Front. Plant Sci.* 2014, *5*, 1–9.
498. **Islam, M.R. *et al.*** Functional characterization of a gene encoding a dual domain for uridine kinase and uracil phosphoribosyltransferase in Arabidopsis thaliana. *Plant Mol. Biol.* 2007, *63*, 465–477.
499. **Ito, T. *et al.*** Two amidophosphoribosyltransferase genes of *Arabidopsis thaliana* expressed in defferent organs. *Plant Mol. Biol.* 1994, *26*, 529–533.
500. **Sallaud, C. *et al.*** Characterization of two genes for the biosynthesis of the labdane diterpene Z-abienol in tobacco (*Nicotiana tabacum*) glandular trichomes. *Plant J.* 2012, *72*, 1–17.
501. **Setya, A. *et al.*** Sulfate reduction in higher plants: molecular evidence for a novel 5'-adenylylsulfate reductase. *Proc. Natl. Acad. Sci.* 1996, *93*, 13383–13388.
502. **Gutierrez-Marcos, J.F. *et al.*** Three members of a novel small gene-family from *Arabidopsis thaliana* able to complement functionally an *Escherichia coli* mutant defective in PAPS reductase activity encode proteins with a thioredoxin-like domain and "APS reductase"activity. *Proc. Natl. Acad. Sci.* 1996, *93*, 13377–13382.
503. **Kopriva, S. & Koprivova, A.** Plant adenosine 5′-phosphosulphate reductase: the past, the present, and the future. *J. Exp. Bot.* 2004, *55*, 1775–1783.
504. **Bick, J.A. *et al.*** *Regulation of the plant-type 5′-adenylyl sulfate reductase by oxidative stress*; 2001; Vol. 40;.
505. **Bernal-Bayard, P. *et al.*** Molecular recognition in the interaction of chloroplast 2-Cys peroxiredoxin with NADPH-thioredoxin reductase C (NTRC) and thioredoxin x. *FEBS Lett.* 2014, *588*, 4342–4347.
506. **Chew, O. *et al.*** Molecular definition of the ascorbate-glutathione cycle in *Arabidopsis* mitochondria reveals dual targeting of antioxidant defenses in plants. *J. Biol. Chem.* 2003, *278*, 46869–46877.
507. **Dixon, D.P. *et al.*** Functional divergence in the glutathione transferase superfamily in plants. *J. Biol. Chem.* 2002, *277*, 30859–30869.
508. **Cerveau, D. *et al.*** Characterization of the *Arabidopsis thaliana* 2-Cys peroxiredoxin interactome. *Plant Sci.* 2016, *252*, 30–41.
509. **Ok, S.H. *et al.*** CBSXs are sensor relay proteins sensing adenosine-containing ligands in Arabidopsis. *Plant Signal. Behav.* 2012, *7*, 664–667.
510. **Yoo, K.S. *et al.*** Single cystathionine β-synthase domain-containing proteins modulate development by regulating the thioredoxin system in *Arabidopsis*. *Plant Cell* 2011, *23*, 3577–3594.
511. **Lee, K. *et al.*** Defining the plant disulfide proteome. *Electrophoresis* 2004, *25*, 532–541.
512. **Curmi, P.M.G. *et al.*** Crystal structure of the unactivated form of ribulose- 1,5-bisphosphate carboxylase/oxygenase from tobacco refined at 2.0-A resolution. *J. Biol. Chem.* 1992, *267*,

16980–16989.
513. **López-Castillo, L.M. *et al.*** Structural basis for redox regulation of cytoplasmic and chloroplastic triosephosphate isomerases from *Arabidopsis thaliana*. *Front. Plant Sci.* 2016, *7*, 1817.
514. **Hisabori, T. *et al.*** Towards a functional dissection of thioredoxin networks in plant cells. *Photochem. Photobiol.* 2007, *83*, 145–151.
515. **Koumoto, Y. *et al.*** Chloroplasts have a novel Cpn10 in addition to Cpn20 as co-chaperonins in *Arabidopsis thaliana*. *J. Biol. Chem.* 2001, *276*, 29688–29694.
516. **Hill, J.E. & Hemmingsen, S.M.** Arabidopsis thaliana type I and II chaperonins. *Cell Stress Chaperones* 2001, *6*, 190–200.
517. **Rolland, N. *et al.*** Spinach chloroplast O-acetylserine (thiol)-lyase exhibits two catalytically non-equivalent pyridoxal-5'-phosphate-containing active sites. *Eur. J. Biochem.* 1996, *236*, 272–282.
518. **Armbruster, U. *et al.*** Arabidopsis CURVATURE THYLAKOID1 Proteins Modify Thylakoid Architecture by Inducing Membrane Curvature. *Plant Cell* 2013, *25*, 2661–2678.
519. **Kirchhoff, H.** Structural changes of the thylakoid membrane network induced by high light stress in plant chloroplasts. *Philos. Trans. R. Soc. B Biol. Sci.* 2014, *369*, 20130225–20130225.
520. **Saze, H. *et al.*** Thioredoxin-mediated reductive activation of a protein kinase for the regulatory phosphorylation of C4-form phosphoenolpyruvate carboxylase from maize. *Plant Cell Physiol.* 2001, *42*, 1295–302.
521. **Grimaud, F. *et al.*** Proteome and phosphoproteome analysis of starch granule-associated proteins from normal maize and mutants affected in starch biosynthesis. *J. Exp. Bot.* 2008, *59*, 3395–3406.
522. **Dietz, K.-J. & Pfannschmidt, T.** Novel Regulators in Photosynthetic Redox Control of Plant Metabolism and Gene Expression. *Plant Physiol.* 2011, *155*, 1477–1485.
523. **Cook, K.M. *et al.*** Allosteric control of βil-tryptase by a redox active disulfide bond. *J. Biol. Chem.* 2013, *288*, 34920–34929.
524. **Kang, Z.H. & Wang, G.X.** Redox regulation in the thylakoid lumen. *J. Plant Physiol.* 2016, *192*, 28–37.
525. **Howard,T.P. *et al*.** Thioredoxin-mediated reversible dissociation of a stromal multiprotein complex in response to changes in light availability. *Proc. Natl. Acad. Sci.* 2008, *105*, 4056–4061.
526. **Wolosiuk, R.A. & Buchanan, B.B.** Activation of chloroplast NADP-linked glyceraldehyde 3-phosphate dehydro- genase by the ferredoxin/thioredoxin system. *Plant Physiol.* 1978, *61*, 669–671
527. **Baalmann, E. *et al*.** Reductive modification and nonreductive activation of purified spinach chloroplast NADP-dependent glyceraldehyde-3-phosphate dehydrogenase. *Arch Biochem Biophys.* 1995, *324*, 201-208.
528. **Wolosiuk, R.A. and Buchanan, B.B.** Regulation of chlo- roplast phosphoribulokinase by the ferredoxin/thioredoxin system. *Arch. Biochem. Biophys*. 1978, *189*, 97–101.
529. **Breazeale, V.D. *et al.*** Chloroplast sedoheptulose 1,7- bisphosphatase: evidence for regulation by the ferredoxin/thioredoxin system *Z. Naturforsch* 1978, *33c*, 521–528.
530. **Wolosiuk, R.A. *et al.*** Enzyme regulation in C4 photosynthesis: Role of Ca^{2+} in thioredoxin-linked activation of sedoheptulose bisphosphatase from corn leaves. *FEBS Lett*. 1982, *140*, 31-35.
531. **Tsukamoto, Y. *et al*.** Redox control of the activity of phosphoglycerate kinase in Synechocystis sp. PCC6803. *Plant Cell Physiol*. 2013; *54*, 484-491.
532. **McKinney, D.W. *et al.*** Activation of chloroplast ATPase by reduced thioredoxin. *Phytochemistry*. 1978, *17*, 794–795.
533. **Wolosiuk, R.A. *et al.*** Regulation of NADP-malate dehydrogenase by the light-actuated ferredoxin/thioredoxin system of chloroplasts. *FEBS Lett*. 1977, *81*, 253–258.
534. **Scheibe, R. & Anderson, L.E.** Dark modulation of NADP-dependent malate dehydrogenase and glucose-6-phos- phate dehydrogenase in the chloroplast. *Biochim. Biophys. Acta*. 1981, *636*, 58–64.
535. **Sasaki, Y. *et al*.** Link between light and fatty acid synthesis: thioredoxin-linked reductive activation of plastidic acetyl-CoA carboxylase. *Proc. Natl. Acad. Sci.* 1997, *94*, 11096–11101.
536. **Nee, G. *et al*.** Redox regulation of chloroplastic glucose-6-phosphate dehydrogenase: a new role for f-type thioredoxin. *FEBS Lett*. 2009, 583, 2827–2832.
537. **Cardi, M. *et al.*** Plastidic P2 glucose-6P dehydrogenase from poplar is modulated by thioredoxin m-type: Distinct roles of cysteine residues in redox regulation and NADPH inhibition. *Plant Sci.* 2016, *252*, 257-266.

538. **Balsera, M. *et al*.** Characterization of Tic110, a channel-forming protein at the inner envelope membrane of chloroplasts, unveils a response to Ca^{2+} and a stromal regulatory disulfide bridge. *J. Biol. Chem*. 2009, *284*, 2603–2616.

539. **Kim, J & Mayfield, S.P.** The active site of the thioredoxin-like domain of chloroplast protein disulfide isomerase, RB60, catalyzes the redox-regulated binding of chloroplast poly(A)-binding protein, RB47, to the 5' untranslated region of psbA mRNA. *Plant Cell Phy*siol. 2002, *43*,1238-1243.

540. **Motohashi, K. *et al.*** Chloroplast cyclophilin is a target protein of thioredoxin. Thiol modulation of the peptidyl-prolyl cis-trans isomerase activity. *J Biol Chem*. 2003, *278*, 31848-31852.